

DOE/RA/50294--T4  
DE 86005740

6101803 For Geo. and Resources Council  
1985

THREE-DIMENSIONAL P-VELOCITY STRUCTURE OF THE SUMMIT CALDERA OF NEWBERRY VOLCANO, OREGON

Douglas A. Stauber<sup>1</sup>, H. M. Iyer, Walter D. Mooney, and Phillip B. Dawson

AI01-79 RA50294  
U. S. Geological Survey, Menlo Park, CA 94025

<sup>1</sup>Present address: Sohio Petroleum Co., Dallas, TX 75240

ABSTRACT

A three-dimensional high-resolution seismic study of the summit caldera of Newberry Volcano, Oregon, was conducted by the U.S. Geological Survey using an adaptation of the method applied by Mercassian et al., (1984). Preliminary interpretation of the traveltime residuals reveals a ring of high P-velocity material coinciding with the inner ring fault system of the caldera in the upper 2 km. A zone of lower P velocities extends deeper than 2 km in the center of the caldera.

INTRODUCTION

Newberry Volcano is a young shield volcano located in central Oregon about 50 km east of the axis of the Cascade volcanic chain (Figure 1). MacLeod and Sammel (1982) describe the geology of Newberry Volcano. The flanks of the shield are veneered with basalt and basaltic-andesite cinder cones and flows, the youngest having 0-14 ages of 5800 years. A 6-km diameter caldera is present at the summit and has been the locus of recurring rhyolitic volcanism during the last 6000 years. The youngest rhyolite is 1350 years old and vented near the southern edge of the caldera. The continuing rhyolitic volcanism in the summit caldera has made it an attractive target for geothermal exploration and suggests that silicic magma may be present in the shallow crust beneath the caldera.

Two geothermal wells drilled in the caldera encountered high temperatures at shallow depths. A 930-m well drilled by the U.S. Geological Survey (USGS) had a bottom hole temperature of 265°C (Sammel, 1981). A 424-m well drilled nearer the caldera ring faults by Sandia National Laboratories encountered a similar but slightly hotter temperature profile. This pattern led Black et al. (1984) to suggest that thermal waters were flowing away from the caldera ring fault system. The locations of magmatic intrusions, and the likely heat source for the thermal water, are poorly understood. They may be near the ring faults, or deeper, with the ring faults serving as conduits for the water.

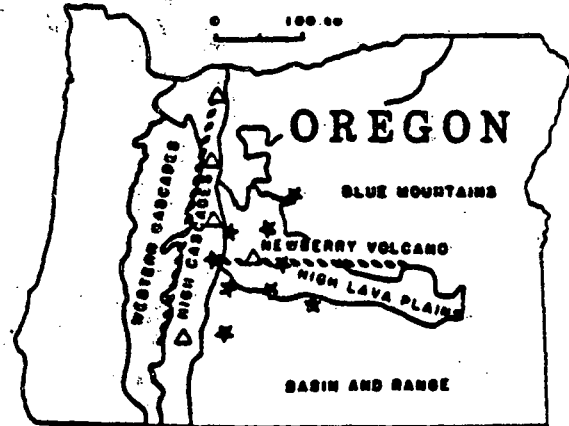


Figure 1. Location of Newberry Volcano and major Cascade Range volcanoes: volcanoes (open triangles), previous seismic refraction lines (dashed lines), and shotpoints used in the current study (stars).

The USGS has conducted several seismic studies of Newberry Volcano to elucidate its structure and to locate magma chambers. Stauber et al., (1985) did a teleseismic P-residual study to examine the crust beneath the volcano to a depth of 40 km with a spatial resolution of 5-10 km. Figure 2 is a northwest-southeast cross section of the P-velocity model obtained. The main feature is the zone of high P-velocities beneath the caldera extending from within 10 km of the surface to 25 km depth. Stauber et al. (1985) show that these high velocities severely limit the fraction of magma present in this volume to less than a few percent. They interpret the high P-velocities to be caused by numerous subsolidus mafic intrusions, lodged in the crust as the volcano grew.

Next, to examine the shallow structure of the volcano, the USGS conducted an east-west seismic refraction experiment across the volcano. A preliminary interpretation of the seismic refraction profile (Stauber and Berge, 1984) is shown in Figure 3. This interpretation

NOTICE

THIS REPORT IS ILLEGIBLE TO A DEGREE  
THAT PRECLUDES SATISFACTORY REPRODUCTION

MASTER

REPRODUCTION OF THIS DOCUMENT IS PROHIBITED

Jsw

where  $T_{ij}$  is the observed traveltime at the  $i$ th station for the  $j$ th shot,  $S$  is a constant for the  $j$ th shot,  $S$  is the slowness, and  $D_{ij}$  is the distance between the  $i$ th shot and the  $j$ th station, and  $R_{ij}$  is the travel-time residual due to velocity deviations from

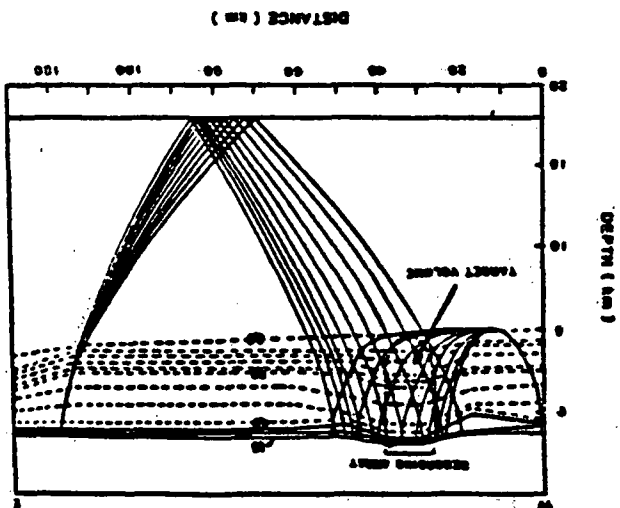
$$T_{ij} = T_j + S \cdot D_{ij} + R_{ij}$$

We compute the traveltime residuals with respect to a laterally homogeneous earth structure. Over the array dimension, the expected traveltime versus distance curve for the  $j$ th phase departs from a straight line by less than a hundredth of a second. Consequently, we computed residuals by fitting lines of the following form to the measured  $T_{ij}$  arrival times:

Arrival-times were measured for both phases by filtering the seismic traces with a narrow-band filter (centered on the dominant frequency of the desired phase) and then measuring the time of a peak or trough in the first cycle. An example of 21 narrow-band filtered  $T_{ij}$  traces from one shot are shown in Figure 4. Uncertainties in the arrival-time measurements are less than a few hundredths of a second.

80 to 90 km away, produced a strong wide-angle reflection from the mid-crust (east shotpoint in Figure 3).

Figure 3. Preliminary P-velocity model for the western part of the east-west seismic refraction profile through Newberry Volcano (Stauber and Bergs, 1984). The low-velocity contours are at uniform intervals between the labeled contours. Data are km/s. Newberry Volcano spans the section under the title "RECORDING ARRAY". Examples of the raypaths used in the present study are shown—Pg raypaths on the left and the wide-angle mid-crustal reflection on the right.



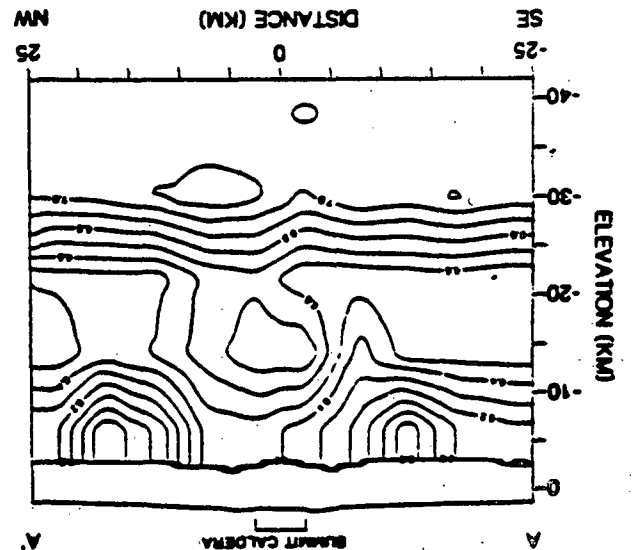
To examine the three-dimensional structure of the upper 5 km beneath the caldera, we used a technique similar to that applied at the Mont Dore volcano, France, by Heccestein et al. (1984). In this technique, a two-dimensional array of seismic recorders is deployed over the target volume. Explosions are detonated in several directions at a distance selected to give strong reflected or refracted phases traveling upward through the target volume toward the array (Figure 3). By illuminating the target volume in this manner from many different directions and measuring the travel-times, the three-dimensional velocity structure of the volume can be found.

We deployed 120 portable seismographs in an array 12 km in diameter centered on the caldera of Newberry Volcano (Figures 3 and 5). We placed a spatial resolution of about 1 km, and we expect a spatial resolution of about 1 km. The average station spacing was about 1 km and we placed shotpoints at two distances from the array in an azimuthal distribution as possible (Figure 1). Raypaths for the Pg phase from the closest shot, 30 to 40 km from the array, penetrate to a depth of about 6 km (east shotpoint in Figure 3). The more distant shots,

EXPERIMENT DESCRIPTION

Figure 2. P-velocity cross-section through Newberry Volcano from teleseismic P-residual study of Stauber et al. (1985). P-velocity in km/s.

downward from this shallow high-velocity feature, detected in the teleseismic experiment contains the same elevation. The high P-velocity zone beneath the volcano than in adjacent areas at Volcano so that the velocity is about 10% higher contours in the upper 6 km rise beneath Newberry



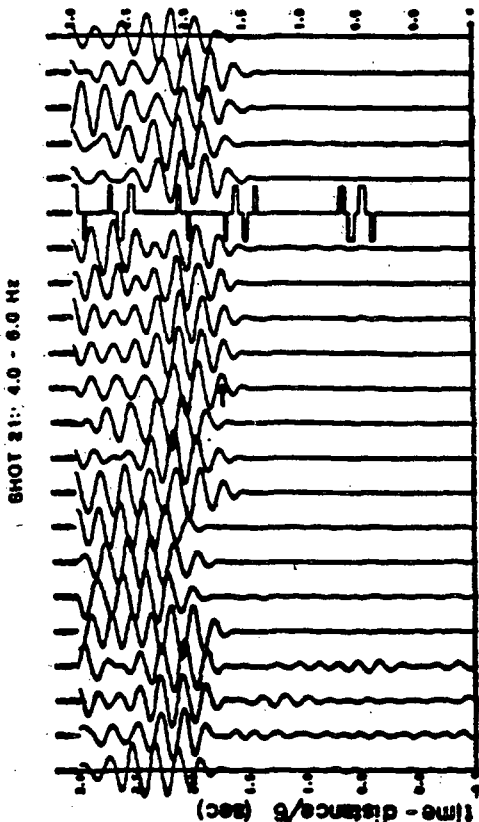


Figure 4. Reduced time plot of 21 narrow-band filtered seismograms for Fig. The first large trough, indicated by the arrow near the center trace, was timed in this case.

This pattern of late arrivals on the opposite side of the caldera from the source and a ring of early arrivals around the rest of the caldera can be interpreted in the following way. A ring of high-velocity material exists in the upper 2 km all the way around the inner ring fault system of the caldera producing the early arrivals observed there. In the center of the caldera and extending to a depth of greater than 2 km is a zone of low-velocity material which casts a "shadow" of late arrivals on the side of the caldera opposite the shot. The widths of these early and late arrival zones are on the order of 2 to 3 km and the magnitude of the residual variation is 0.15 to 0.25 s. These dimensions require P-velocity variations of 20 to 40%.

The presence of a ring of high-velocity rock in the upper 2 km around the ring fault system is consistent with an interpretation of gravity data made by Grissom and Roberts (1963). They suggest that a ring of short-wavelength gravity highs around the ring faults are the result of a ring of high density intrusive rocks in the upper

Generally homogeneous structure.  $T_0$  (intercept time) and  $S$  (slope of traveltime linear fit) were computed by a least-squares algorithm using all of the measured  $T_0$  times from the six closer shots. Residuals,  $R_i$ , were then computed by subtracting the predicted arrival times,  $T_0 + S \cdot D_i$ , from the observed times.

The residuals have a simple geometric interpretation. If the raypath for a particular observation passes through a region with lower than average velocity for that depth, the arrival-time will be later than predicted and the residual will be positive. Conversely, higher than normal velocities produce negative residuals. As the direction to the shot is varied, rays passing through the anomalous region reach the surface at varying positions. The deeper the anomalous region, the greater the change in position of the traveltime anomaly. By observing how the residual pattern varies with direction of approach of the seismic waves one can qualitatively infer the location of anomalous regions. The process can be made quantitative by using a linear inversion technique.

DATA AND QUALITATIVE INTERPRETATION

Fig residuals for four shots are plotted in map view in Figure 5. The first feature to note is the large magnitude of the residual variations, up to several tenths of seconds—much larger than the uncertainties of the measurements. The north and south sides of the array are relatively late (positive residuals) and the central and western parts of the array are relatively early. This pattern indicates that the average velocities beneath the northern and southern parts of the array are lower than beneath the central and western areas.

Within the caldera, the anomaly pattern varies systematically with azimuth. In Figure 5a (for a shot from the west) a partial ring of negative residuals occurs near the inner ring fault system on the north, west, and south edges of the caldera; extending from the center of the caldera toward the east is a zone of positive residuals. In Figure 5b (for a shot to the southwest) this pattern has rotated such that the later arrivals are in the northeastern part of the caldera with the early arrivals near the ring faults completely surrounding them. As the direction to the source rotates further, to just east of south (Figure 5c), the residual pattern in the caldera again rotates with it. The late arrivals now extend away from the caldera to the north-northwest. The early arrivals near the ring faults now extend from the west through the south, east, and northeast part of the caldera. Finally, in Figure 5d (shot to the east) the late arrivals are located along the northwest edge of the caldera with the early arrivals in the south and east.

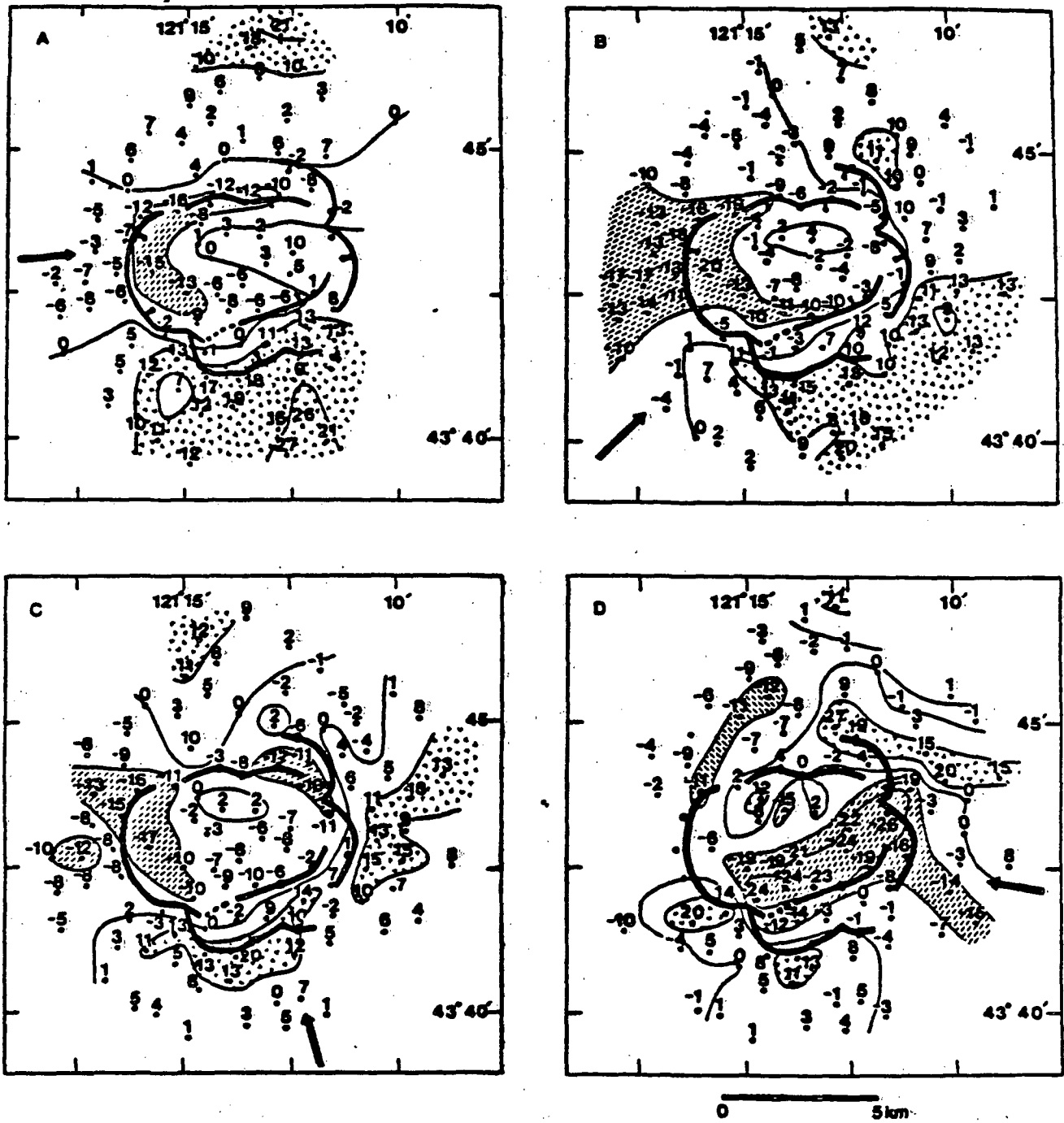


Figure 5. Pg residuals for 4 shots recorded at the Newberry caldera array. The values are in units of hundredths of seconds and are contoured at 0.1 s intervals. Areas with residuals greater than 0.1 s and less than -0.1 s are indicated by the shading. The heavy dark lines show the caldera ring-fault system. Dark arrows show the direction of wave propagation across the array.

few km. Higher density and higher P-velocity are expected in crystalline intrusive bodies due to lower porosity and lower glass content than the surrounding extrusive rocks. This effect is clearly demonstrated for the rift zones of Kilauea volcano by Ellsworth and Koyanagi (1977) and Broyles et al. (1979). A zone of frequent small intrusions in the upper few km around the ring fault system at Newberry Volcano is an attractive candidate for the heat source of the hot well water found in the caldera.

The source of the rhyolitic magmas erupted in the caldera is not addressed with this ring-intrusion model. The teleseismic P-residual experiment ruled out the presence of a magma chamber below 5 km depth with dimensions of 5 km or greater. However, the deeper portion of the low-velocity zone located in the center of the caldera by the present study is a possible candidate for a small silicic magma chamber. A formal inversion of the present Pg and wide-angle reflection data is needed to evaluate this hypothesis (and is underway).

#### CONCLUSIONS

Qualitative analysis of the traveltime residual patterns obtained by a three-dimensional seismic imaging experiment at Newberry Volcano indicates that P-velocity anomalies on the order of 30%, are present in the upper 5 km of the volcano. In particular, a ring of high-velocity material in the upper 2 km around the caldera ring fault system is inferred to exist and coincide with a density anomaly inferred by Griscom and Roberts (1983). A low-velocity zone in the center of the caldera is inferred to extend somewhat deeper than the high-velocity ring and is a possible source region for the high-silica rhyolitic magmas which have erupted in the caldera several times in the last 6000 years.

#### ACKNOWLEDGEMENTS

The authors gratefully acknowledge the efforts of the 40 people who performed the field work that made this study possible. This work was supported by the U.S. Geological Survey and the U.S. Department of Energy, Geothermal and Hydropower Technologies Division.

#### REFERENCES

- Black, G.L., Priest, G.R., and Voller, W.M., 1984, Temperature data and drilling history of the Sandia National Laboratories well at Newberry caldera, Oregon, *Oregon Geology*, v. 46, p. 7-9.
- Broyles, M.L., Suyanaga, W., and Furumoto, A.S., 1979, Structure of the lower east rift zone of Kilauea volcano, Hawaii, from seismic and gravity data, *Jour. Volcanol. Geotherm. Res.*, v. 5, p. 317-336.
- Ellsworth, W.L., and Koyanagi, R.Y., 1977, Three-dimensional crust and mantle structure of Kilauea volcano, Hawaii, *Jour. Geophys. Res.*, v. 82, p. 5379-5394.
- Griscom, A., and Roberts, C.W., 1983, Gravity and magnetic interpretation of Newberry Volcano, State of Oregon Department of Mineral Industries, Open-File Report O-83-3, p. 68-81.
- MacLeod, W.S. and Sammel, E.A., 1982, Newberry Volcano, Oregon, a Cascade Range geothermal prospect, *California Geology*, v. 35, p. 235-244.
- Mercession, Al., Hirn, Al., and Tarantola, Al., 1984, Three-dimensional seismic transmission prospecting of the Mont Dore volcano, France, *Geophys. Jour. Roy. Astr. Soc.*, v. 76, p. 307-315.
- Sammel, E.A., 1981, Results of test drilling at Newberry Volcano, Oregon, and some implications for geothermal prospects in the Cascades, *Geothermal Resources Council Bull.*, v. 10, p. 3-8.
- Stauber, D.A., and Berge, P.A., 1984, P-velocity structure of Mt. Shasta, CA, and Newberry Volcano, (abstract), *EOS, Trans. Am. Geophys. Un.*, v. 66, p. 25.
- Stauber, D.A., Green, S.M., and Iyer, H.M., Three-dimensional P-velocity structure of the crust below Newberry Volcano, Oregon, submitted to *Jour. Geophys. Res.*

#### DISCLAIMER

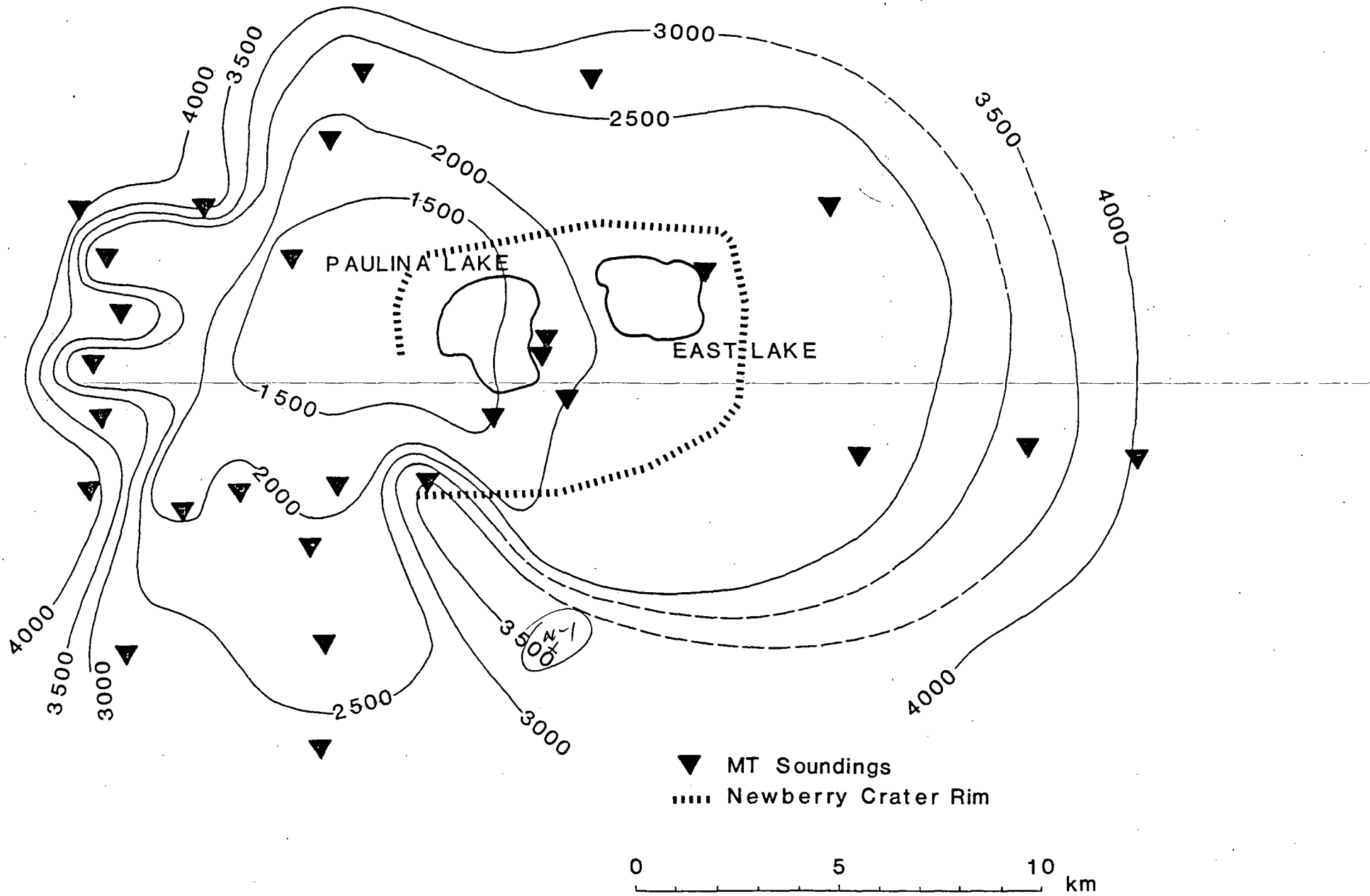
This report was prepared as an account of work sponsored by an agency of the United States Government. Neither the United States Government nor any agency thereof, nor any of their employees, makes any warranty, express or implied, or assumes any legal liability or responsibility for the accuracy, completeness, or usefulness of any information, apparatus, product, or process disclosed, or represents that its use would not infringe privately owned rights. Reference herein to any specific commercial product, process, or service by trade name, trademark, manufacturer, or otherwise does not necessarily constitute or imply its endorsement, recommendation, or favoring by the United States Government or any agency thereof. The views and opinions of authors expressed herein do not necessarily state or reflect those of the United States Government or any agency thereof.

## **LEGIBILITY NOTICE**

A major purpose of the Technical Information Center is to provide the broadest possible dissemination of information contained in DOE's Research and Development Reports to business, industry, the academic community, and federal, state, and local governments. Non-DOE originated information is also disseminated by the Technical Information Center to support ongoing DOE programs.

Although large portions of this report are not reproducible, it is being made available only in paper copy form to facilitate the availability of those parts of the document which are legible. Copies may be obtained from the National Technical Information Service. Authorized recipients may obtain a copy directly from the Department of Energy's Technical Information Center.

# DEPTH TO ELECTRICAL BASEMENT



5

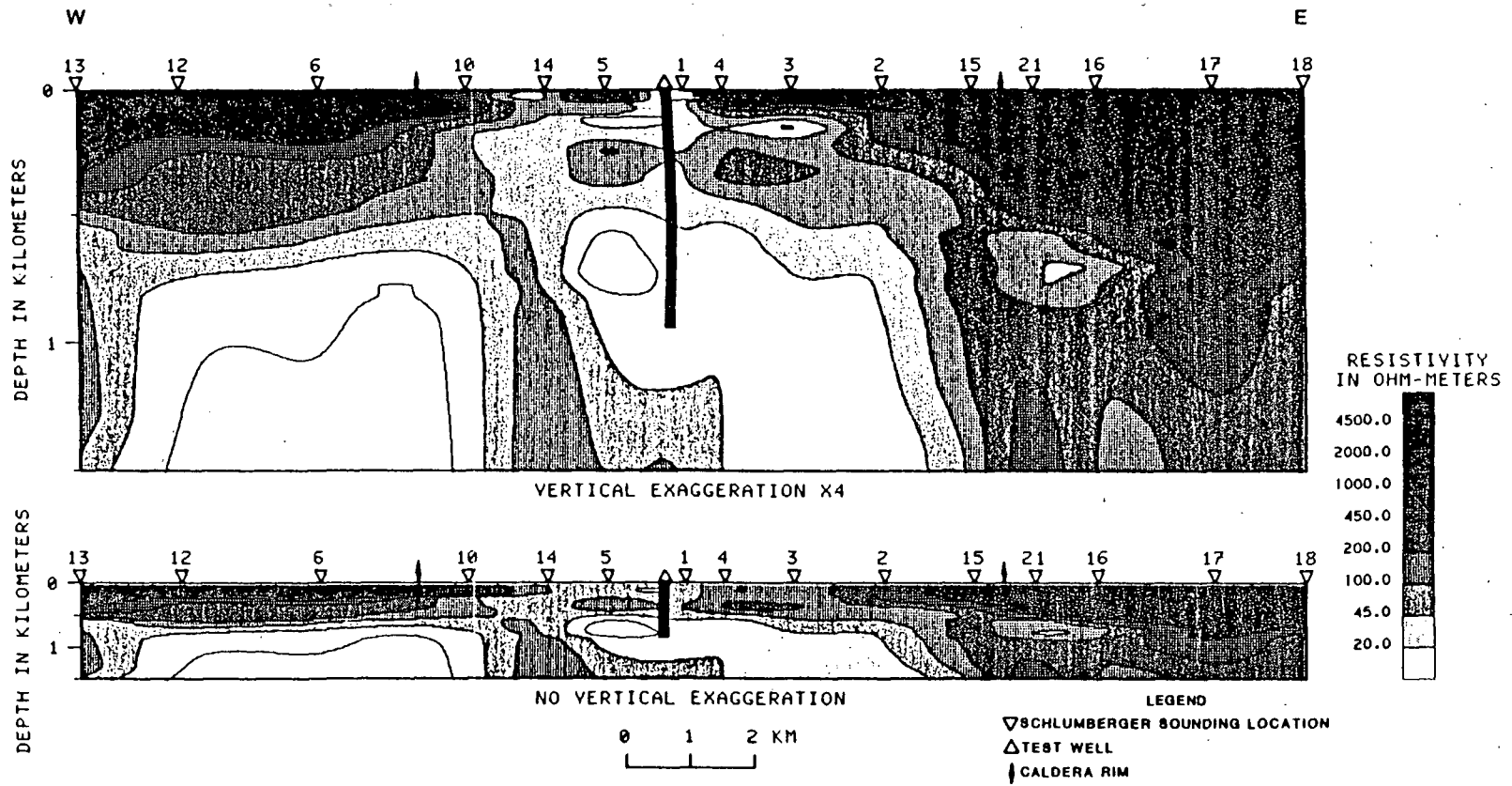
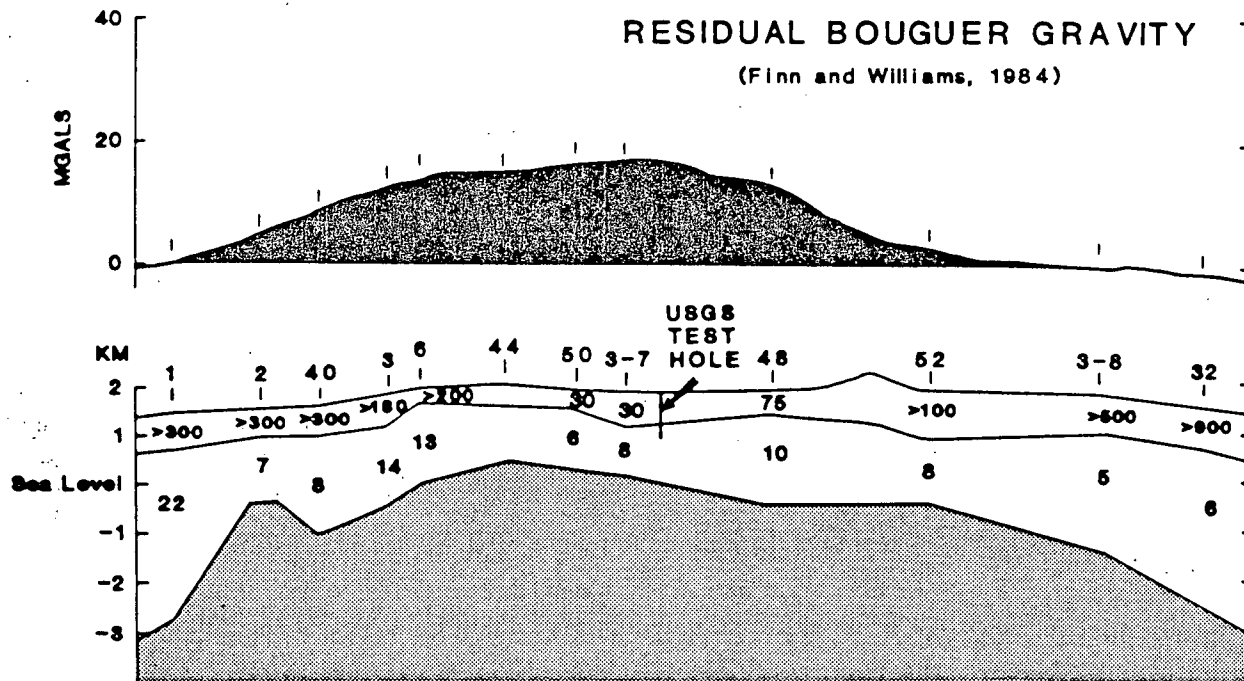


FIGURE 2. Computer-generated geoelectric cross section. Top and bottom parts are vertically exaggerated 4 and 1 times respectively.



# RESIDUAL BOUGUER GRAVITY

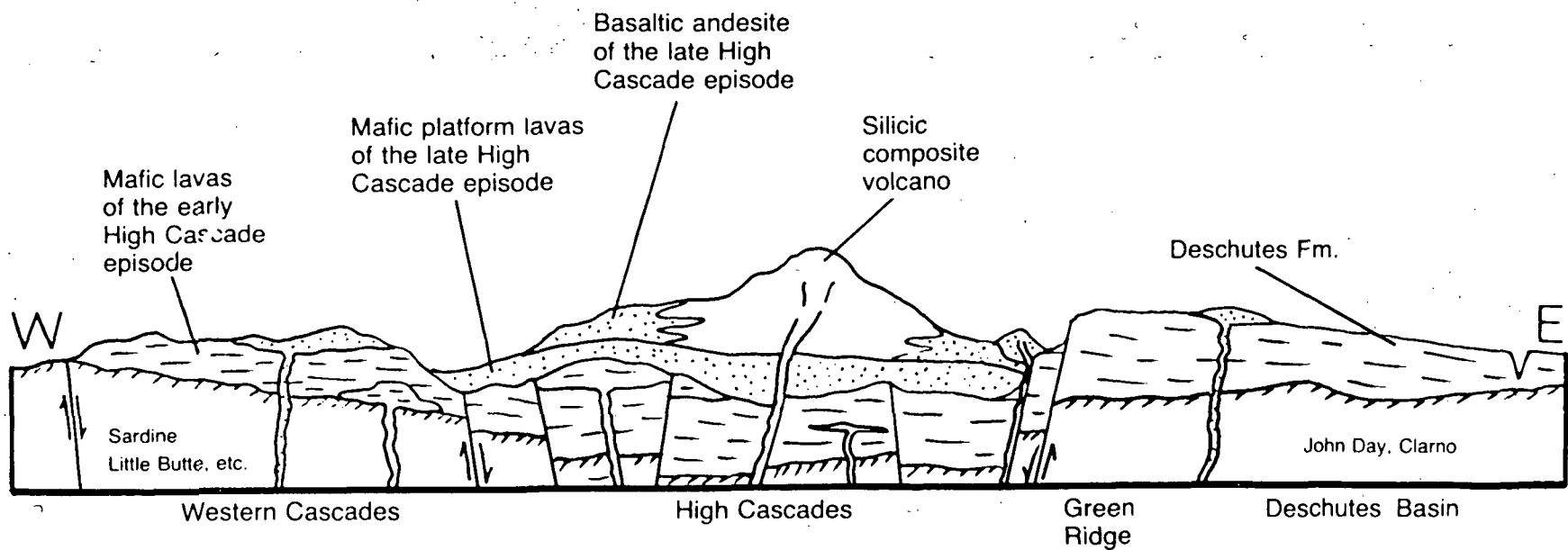
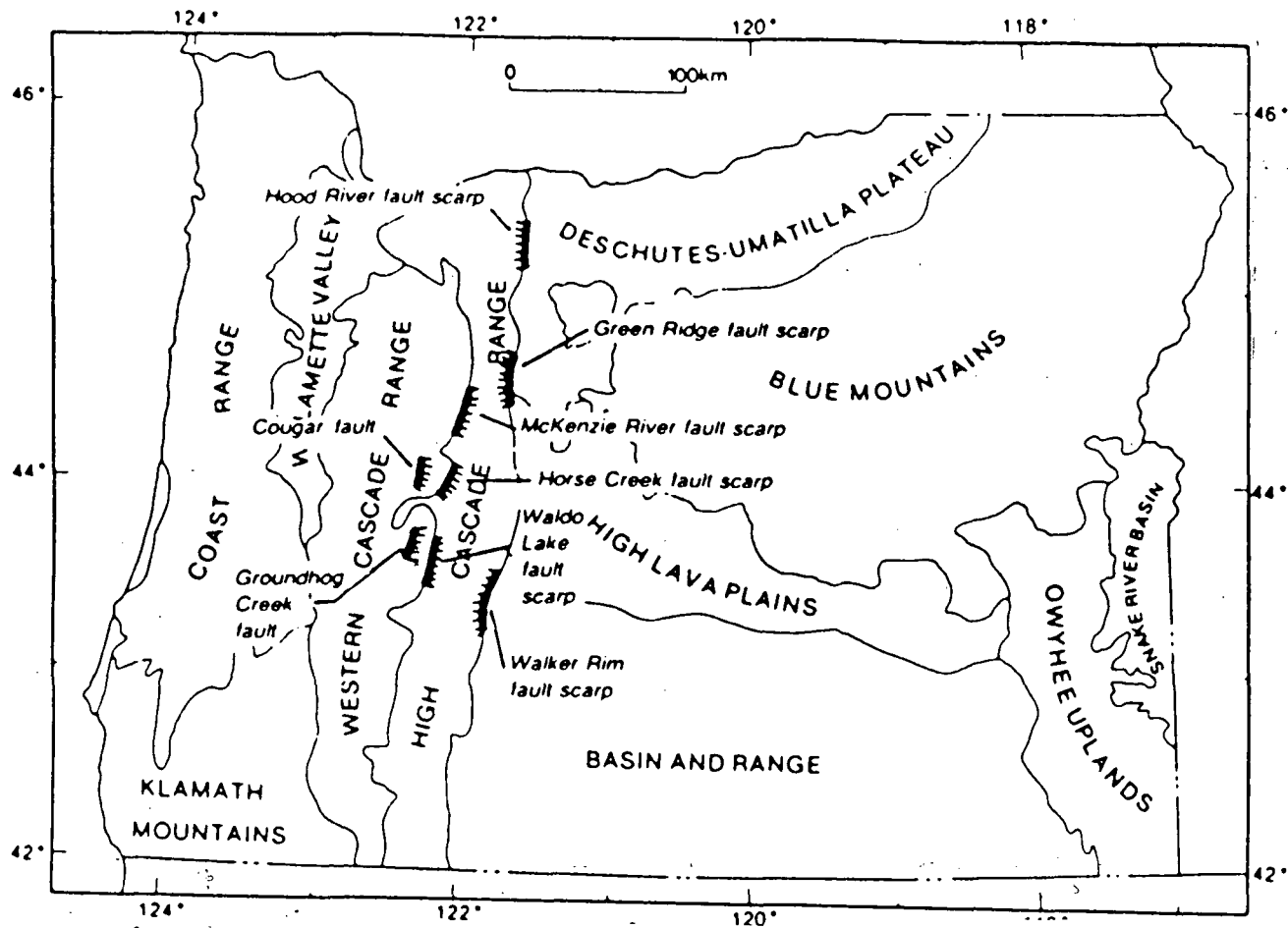
(Finn and Williams, 1984)



OHM-m

- 1000  QUATERNARY VOLCANIC FLOWS
- 200  LAKE SEDIMENTS AND FLOWS
- 30  ALTERED TERTIARY SEDIMENTS AND VOLCANIC FLOWS
- 5

- 500  PRE-TERTIARY BASEMENT ROCK, POSSIBLY LARGELY INTRUSIVE IN NATURE
- 100



## GENERAL GEOLOGY OF THE CASCADES<sup>2,1</sup>

The central Oregon Cascade Range is separable into two physiographic provinces: (1) the Western Cascade Range—a deeply dissected, uplifted block of Miocene and older tuffs and lavas, and (2) the High Cascade Range—a relatively undissected pile of chiefly post-Miocene volcanic rocks (Figure 2.1). Whereas great thicknesses of volcanic rock were accumulating in the area during Oligocene to Miocene time, the Cascade Range was not high enough until the Pliocene to deplete the prevailing westerly winds of their moisture and thereby to create semiarid conditions in eastern Oregon (Chaney, 1938; Williams, 1942). In the early Pliocene (5 to 4 m.y. B.P.), rapid uplift and erosion of the central Western Cascades relative to the area now occupied by the High Cascades created an elevated mountain range in the western part of the province, thereby causing an effective rain shadow (e.g., Chaney, 1938; Williams, 1942, 1953; Taylor, 1980; Flaherty, 1981). Deep valleys were rapidly cut into the elevated western part of the range, and by about 4 to 3 m.y. B.P., most of the relief and the drainage patterns which characterize the present-day Western Cascade physiographic province were well established (e.g., Thayer, 1936, 1939; Williams, 1942, 1953; Flaherty, 1981). Most of the present relief on the High Cascade Range did not exist until the Quaternary, when the majority of the High Cascade composite cones were built on a platform of voluminous mafic Pliocene lavas (e.g., Williams, 1953; Taylor, 1980).

These changes in the physiography of the central Cascades were accompanied by changes in the style of tectonic deformation and the overall composition of the volcanic rocks. During latest Eocene to earliest Miocene time, voluminous silicic ash flows and lesser amounts of black tholeiitic lava and calc-alkaline andesite, dacite, and rhyolite covered all of the area now occupied by the Western Cascades (e.g., Callaghan, 1933; Thayer, 1937, 1939; Peck and others, 1964; White, 1980a,c). At about the same time, similar but more alkaline lavas and tuffs were erupted from the area just east of the High Cascade Range (e.g., see descriptions of the western facies of the John Day Formation by Robinson and Brem, 1981). During the middle Miocene, calc-alkaline andesite, basaltic andesite, and quartz-normative basalt flows were erupted (Thayer, 1936, 1939; Williams, 1953; Peck and others, 1964; Hammond, 1979; Hammond and others, 1980). Toward the end of the Miocene and beginning of the Pliocene, between about 9 to 4 m.y. B.P., eruption of olivine-normative basalt, basaltic andesite, and subordinate andesite and dacite from vents east of many of the earlier Cascade vents began. In the latter part of this episode, basaltic andesite to dacitic volcanism became more common. When the volcanism became increasingly mafic, about 9 m.y. B.P., the local minor folding which characterized the middle Miocene north-central Oregon Cascades was replaced by normal faulting along north to northwest trends, and numerous northwest-trending dikes were injected (e.g., Hammond and others, 1980; Avramenko, 1981; Priest and Woller, Chapters 3 and 4).

Uplift of the Western Cascade Range in early Pliocene time was accompanied by additional north- to northwest-trending normal faulting, especially at the present Western Cascade-High Cascade physiographic boundary. Major north-south faults form the eastern boundary of the uplifted Western Cascade block in the McKenzie River-Horse Creek area (Taylor, 1980; Flaherty, 1981; Avramenko, 1981) and in the Waldo Lake area (Chapter 6).

<sup>2,1</sup> See discussion of nomenclature in section on petrochemistry later in this chapter for a discussion of rock classification used here.

Lineaments in the topography (e.g., Allen, 1966) and regional gravity anomalies (Couch and others, 1982a,b) suggest that similar faults bound the Western Cascade Range in other localities as well. The uplift, faulting, and development of most of the resulting erosional relief on the McKenzie River-Horse Creek escarpment occurred over a very short interval between about 5 and 3.4 m.y. B.P., according to Flaherty's (1981) data. Taylor (1980) concluded that most of the faulting on the east-facing McKenzie River escarpment and west-facing Green Ridge escarpment (Figure 2.1) probably occurred between 5 and 4 m.y. B.P. He suggested that these faults bound a downfaulted block of the High Cascade province.

This major faulting event in the early Pliocene was followed by voluminous eruptions of basalt and basaltic andesite in the High Cascade Range. Highly fluid diktytaxitic basalt flows which dominated the earliest eruptions frequently poured into the Western Cascade drainages, whereas the more silicic lavas were constrained by their higher viscosity to the low shieldlike platform that was developing on the present site of the High Cascade Range (e.g., Taylor, 1980). By Quaternary time, basaltic andesite composite cones were developing as the result of explosive volcanic activity along the central and western parts of the High Cascade province at the same time that effusive eruptions of basalt and basaltic andesite were continuing on the platform (Williams, 1953; Taylor, 1980). Intermediate to silicic composite volcanoes were built in the latter part of the Quaternary at Mount Hood, Mount Jefferson, Mount Bachelor, South Sister, and Mount Mazama, but basaltic eruptions continued in the surrounding platform (e.g., Williams, 1953; Taylor, 1980). The youngest eruptions in the High Cascade Range have been chiefly dacite to rhyodacite (e.g., South Sister, Mount Hood, and Mount Mazama) and basalt to basaltic andesite (the Belknap Crater and Sand Mountain flows).

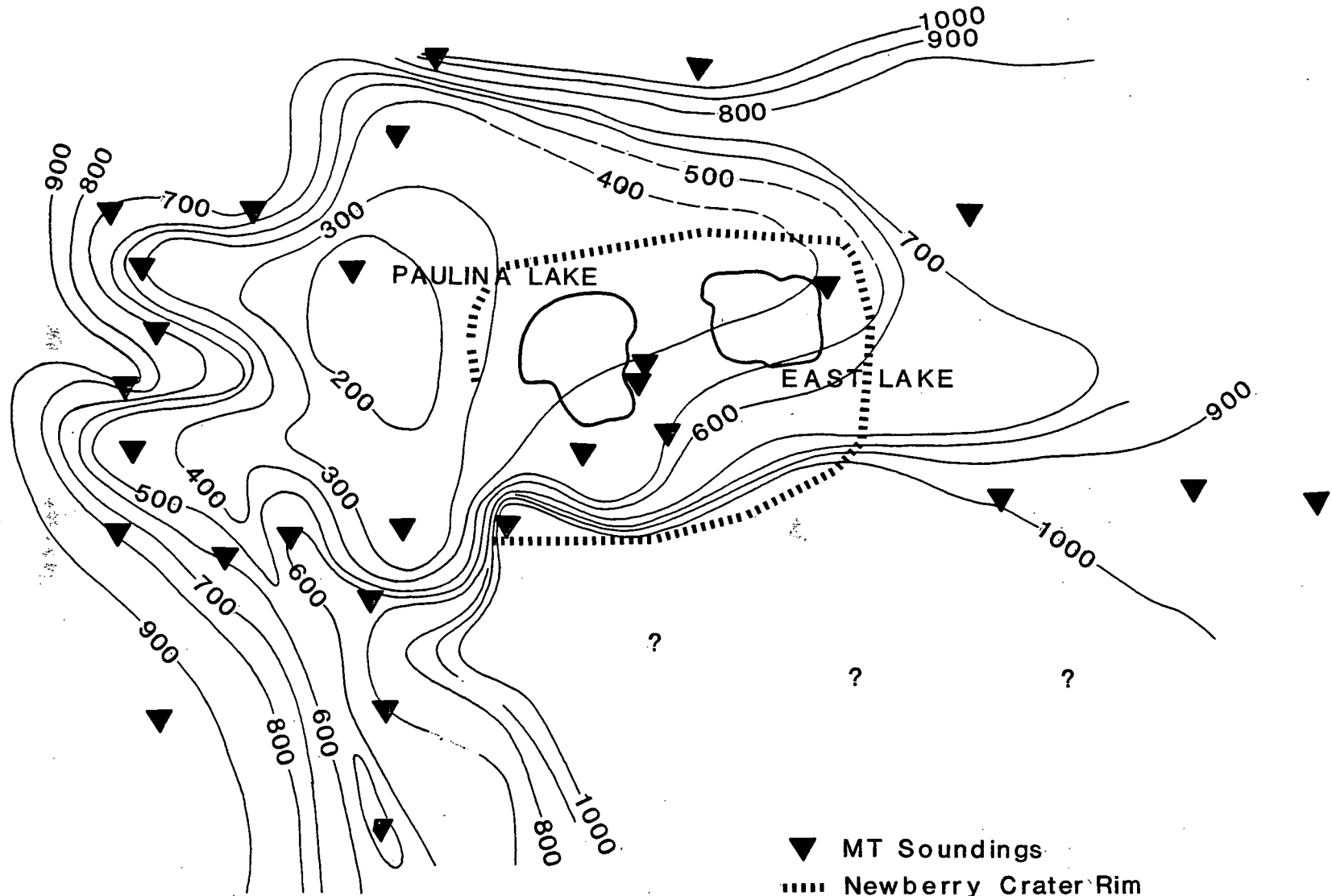
## VOLCANIC STRATIGRAPHY

### Introduction

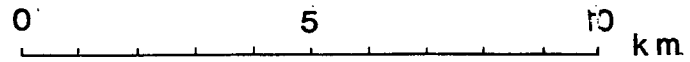
A combination of time- and rock-stratigraphic units has traditionally been used for regional stratigraphy in the Cascade Range (e.g., Wells and Peck, 1961; Peck and others, 1964). Because of regional changes in the composition of volcanic rocks along the Cascades through time, certain intervals of geologic time are characterized by distinctive rock-stratigraphic units. Ages of volcanic rock have been judged in the past by both radiometric dates and relative degree of alteration, as well as by the tacit assumption that distinctive compositional types of volcanic rock characterize certain geologic times. Radiometric and compositional data from the present study suggest that the latter assumption is often, though not invariably, justified.

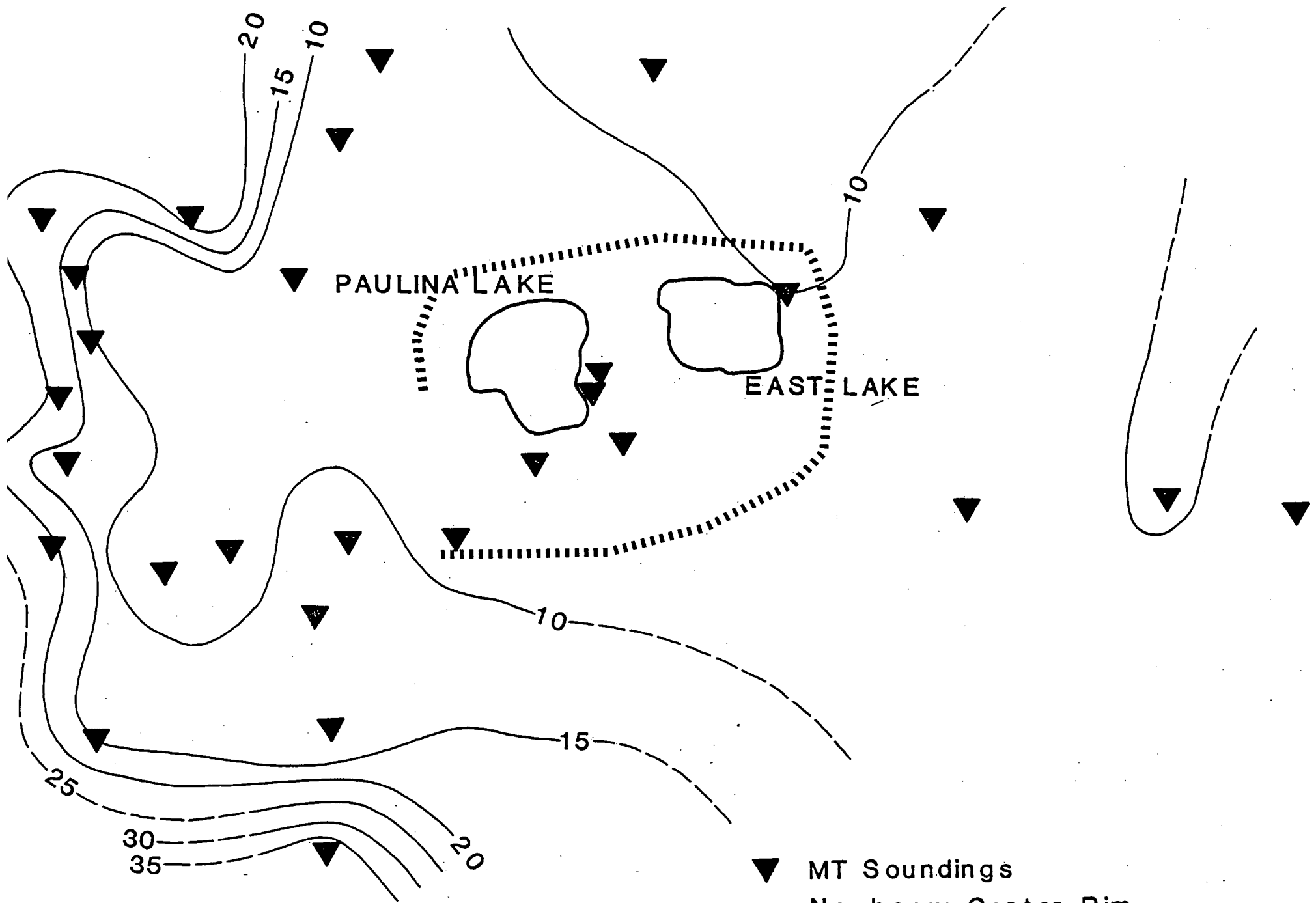
Figure 2.3 summarizes regional and local stratigraphic units defined by various workers in the north-central Cascades and compares them to an informal system of time categories used for this paper (Tables 2.1 and 2.2). The system used here provides a basis for discussion in this paper and is not intended to be used as formal usage or as a replacement for existing rock-stratigraphic nomenclature. It is based on breaks in time which, from mapping in the central Cascades, appear to correspond to broad changes in the overall composition of volcanic sequences. This system avoids some of the confusion generated by previous usage of regional rock-stratigraphic systems which sought to correlate particular type sections over unrealistically large distances along the Cascades. Terms such as "Sardine Formation," whose meaning, in terms of the age of the rocks concerned, is still debated (e.g.,

# DEPTH TO ALTERED LAYER



▼ MT Soundings  
----- Newberry Crater Rim  
Contour Interval 100 meters

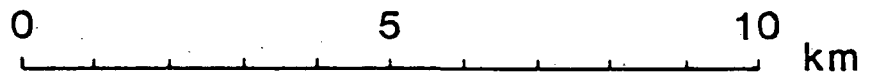




PAULINA LAKE

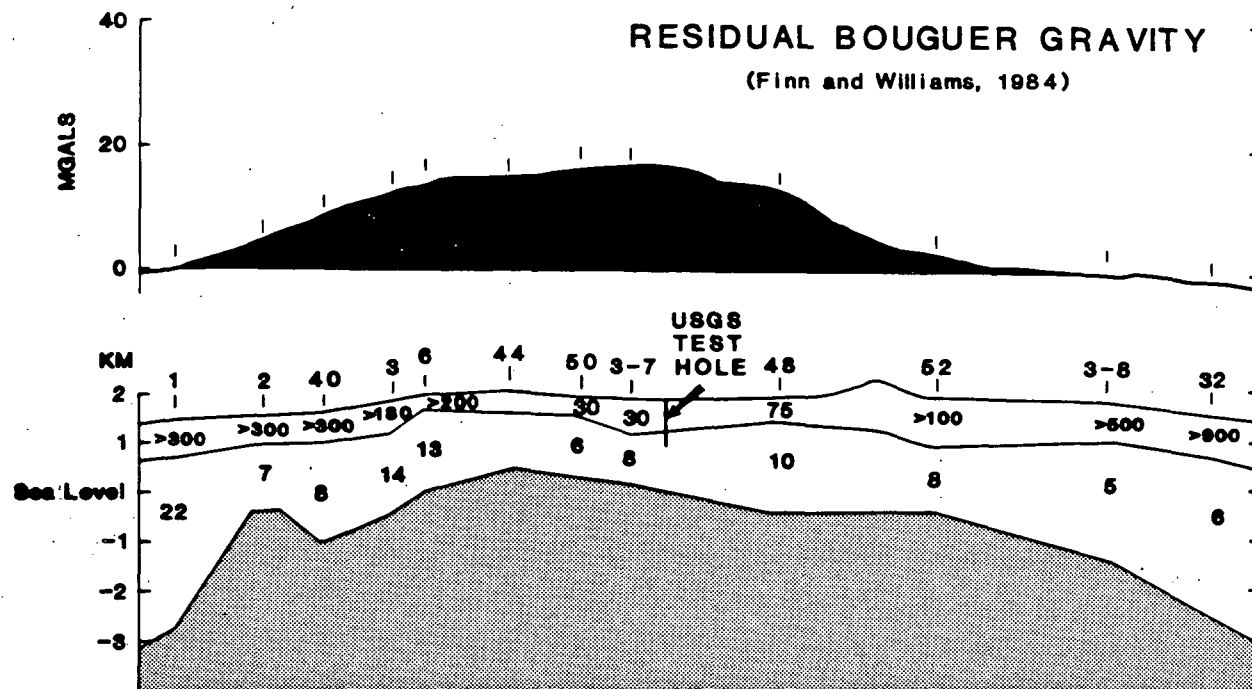
EAST LAKE

▼ MT Soundings  
..... Newberry Crater Rim  
Contour Interval 5  $\Omega$ M

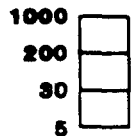


# RESIDUAL BOUGUER GRAVITY

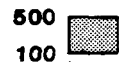
(Finn and Williams, 1984)



OHM-m

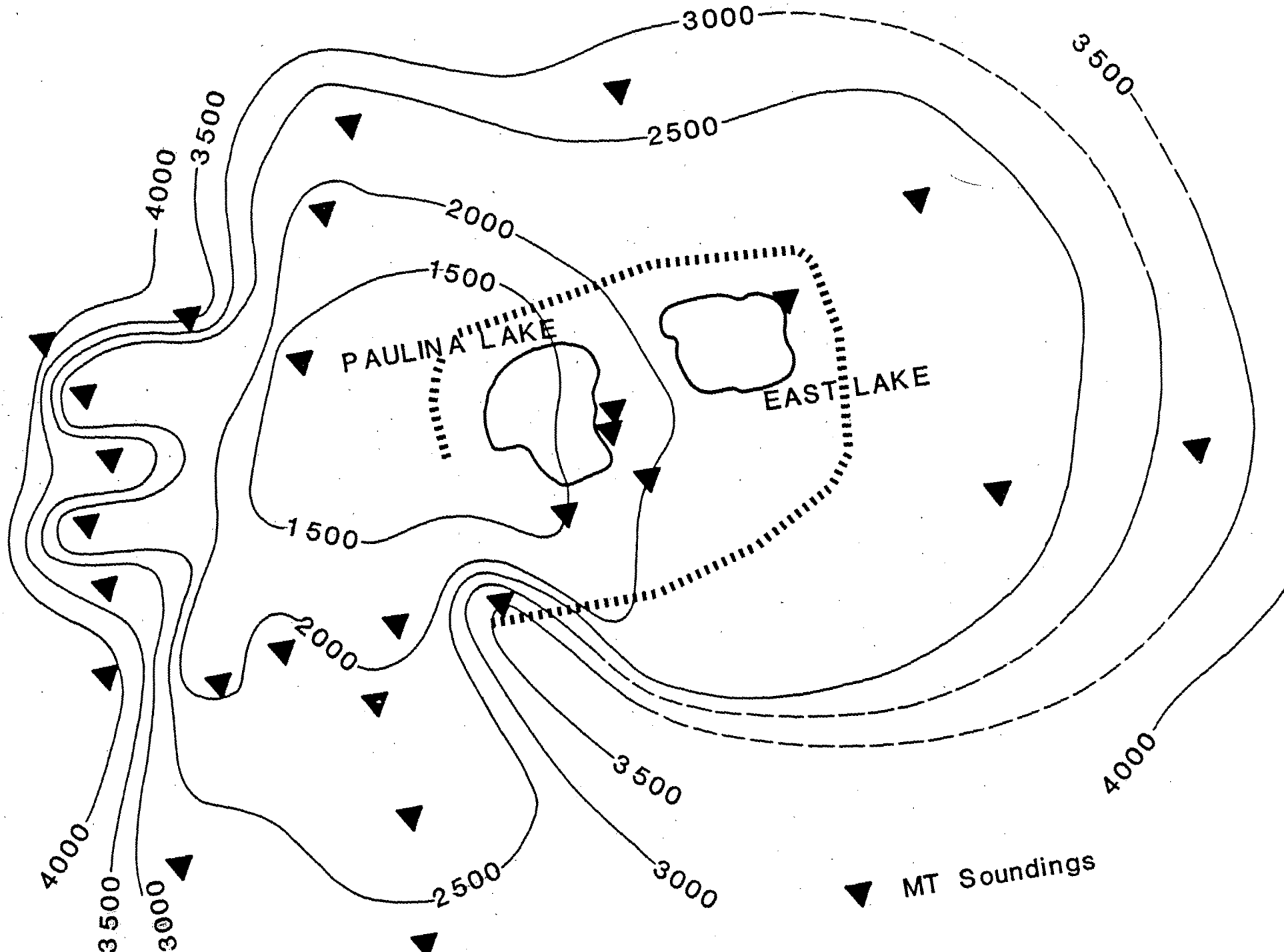


QUATERNARY VOLCANIC FLOWS  
 LAKE SEDIMENTS AND FLOWS  
 ALTERED TERTIARY SEDIMENTS AND VOLCANIC FLOWS



PRE-TERTIARY BASEMENT ROCK, POSSIBLY LARGELY INTRUSIVE IN NATURE

DEPTH TO ELECTRICAL BASE



# NEWBERRY CALDERA, OREGON

*Schlumberger Soundings*

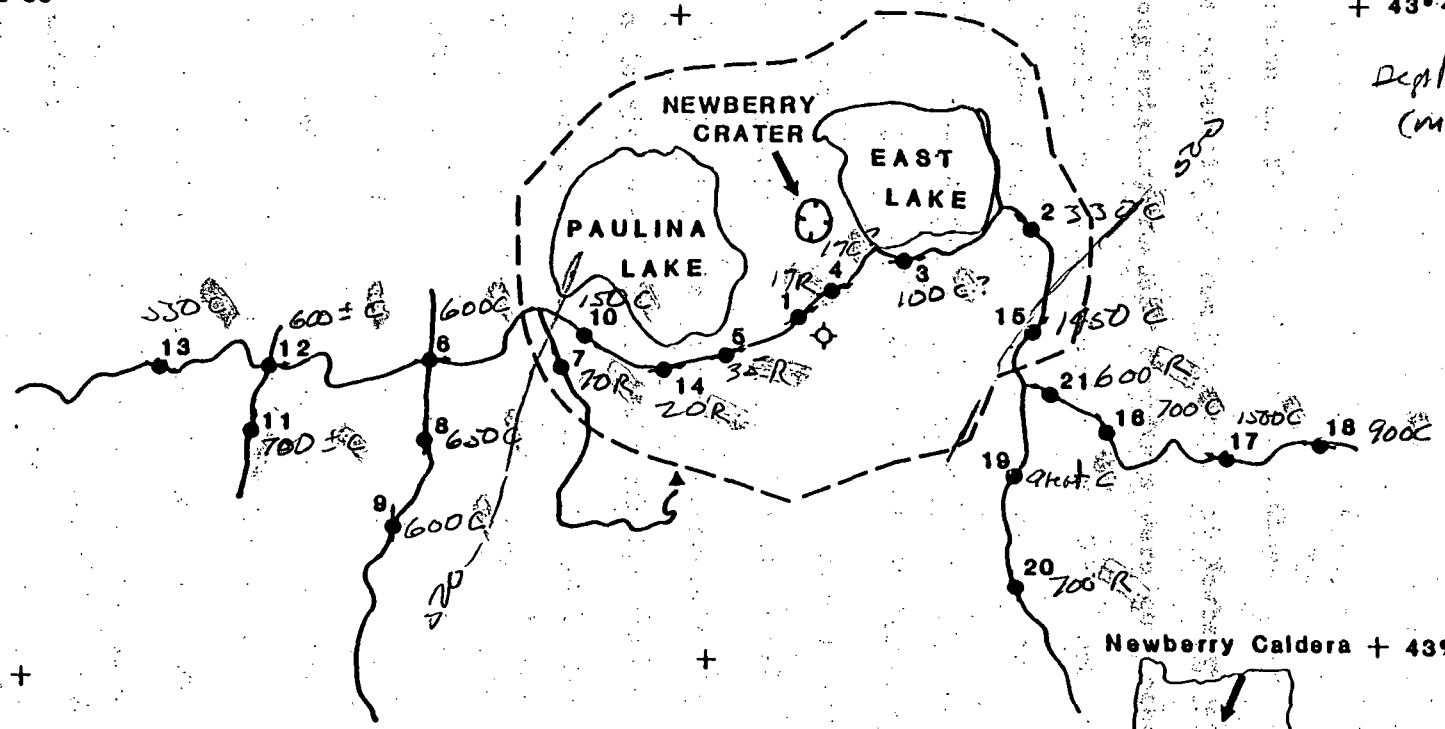
*Bischof 1983*

121°07'30"  
+ 43°45'

*Depth to  $\approx$  200 m  
(m)*

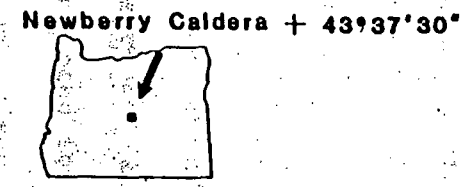
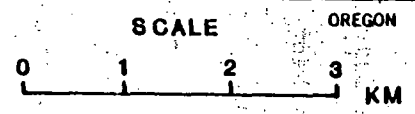
121°22'30"  
+

121°15'  
+



## LEGEND

- Station Location with Azimuth
- ▲ Paulina Peak Lookout
- ◇ U.S.G.S. Test Well
- - - Newberry Caldera Rim



MAP OF NEWBERRY AND VICINITY SHOWING SCHLUMBERGER SOUNDING LOCATIONS

FIGURE 1



# NEWBERRY CALDERA, OREGON

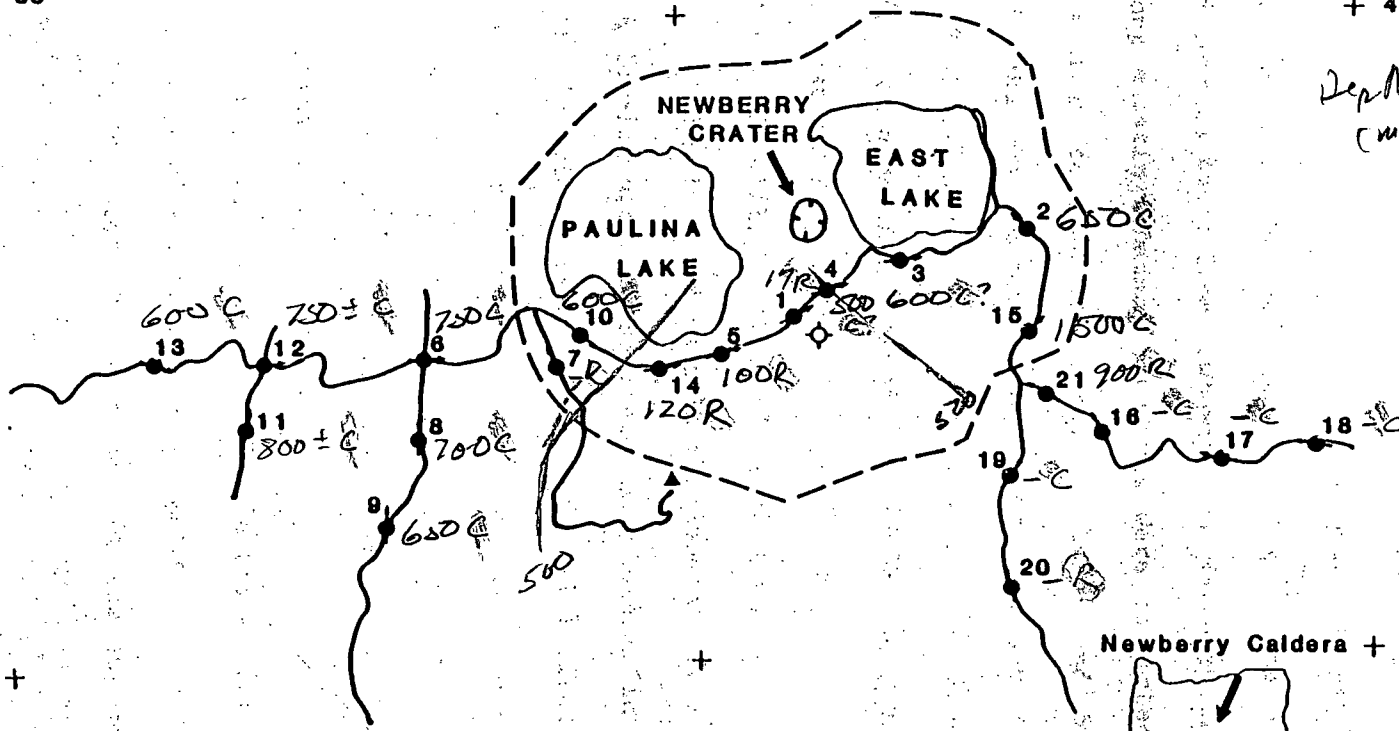
Schlumberger Soundings

121°07'30" Bas Jan 1983  
+ 43°45'

Depth to  $\leq 200$  ohm m  
(m)

121°22'30"  
+

121°15'  
+



2

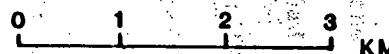
## LEGEND

- Station Location with Azimuth
- ▲ Paulina Peak Lookout
- ◆ U.S.G.S. Test Well
- Newberry Caldera Rim

Newberry Caldera + 43°37'30"



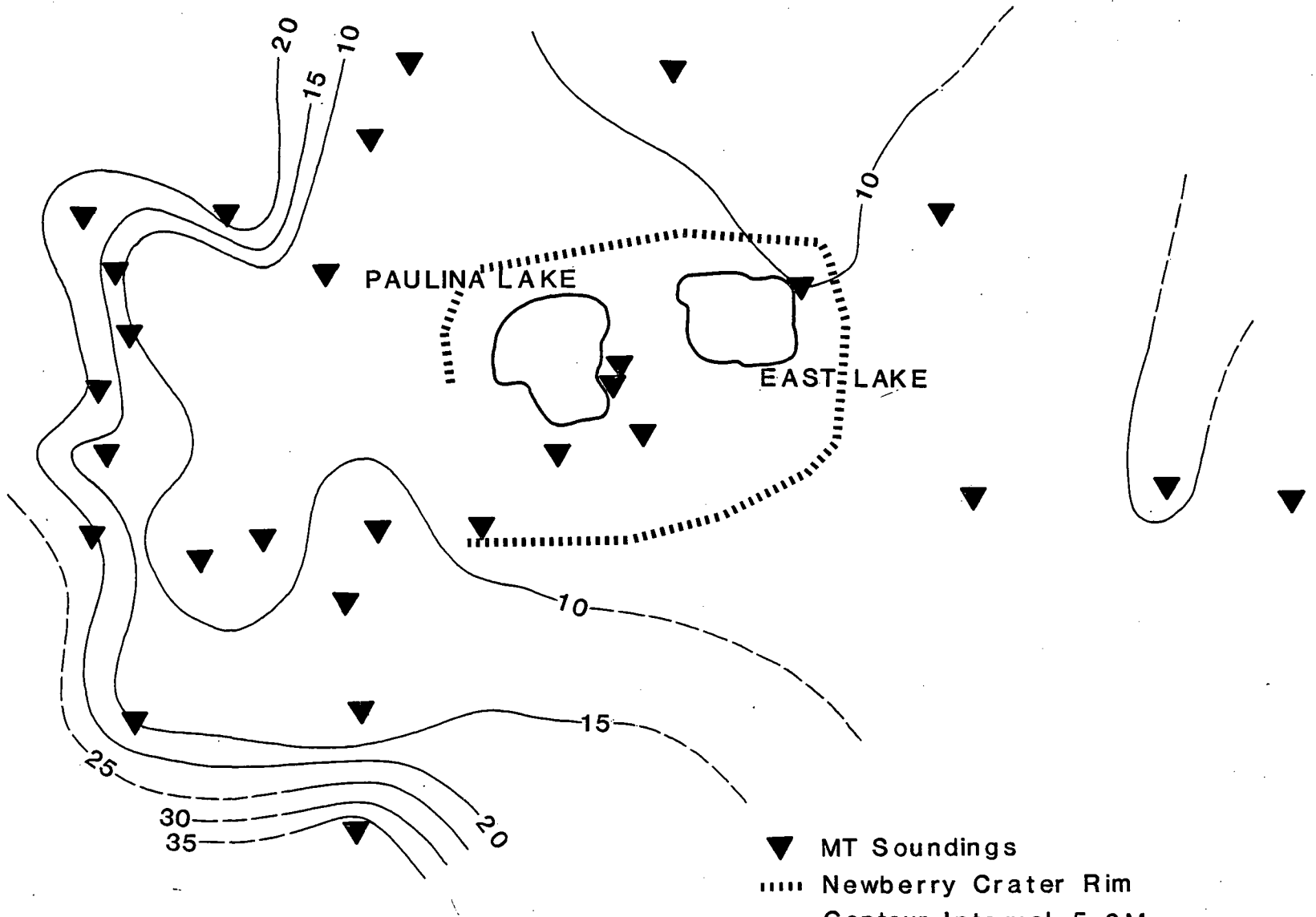
SCALE



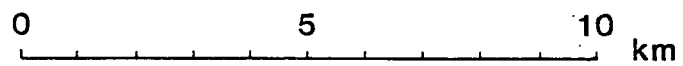
MAP OF NEWBERRY AND VICINITY SHOWING SCHLUMBERGER SOUNDING LOCATIONS

FIGURE 1

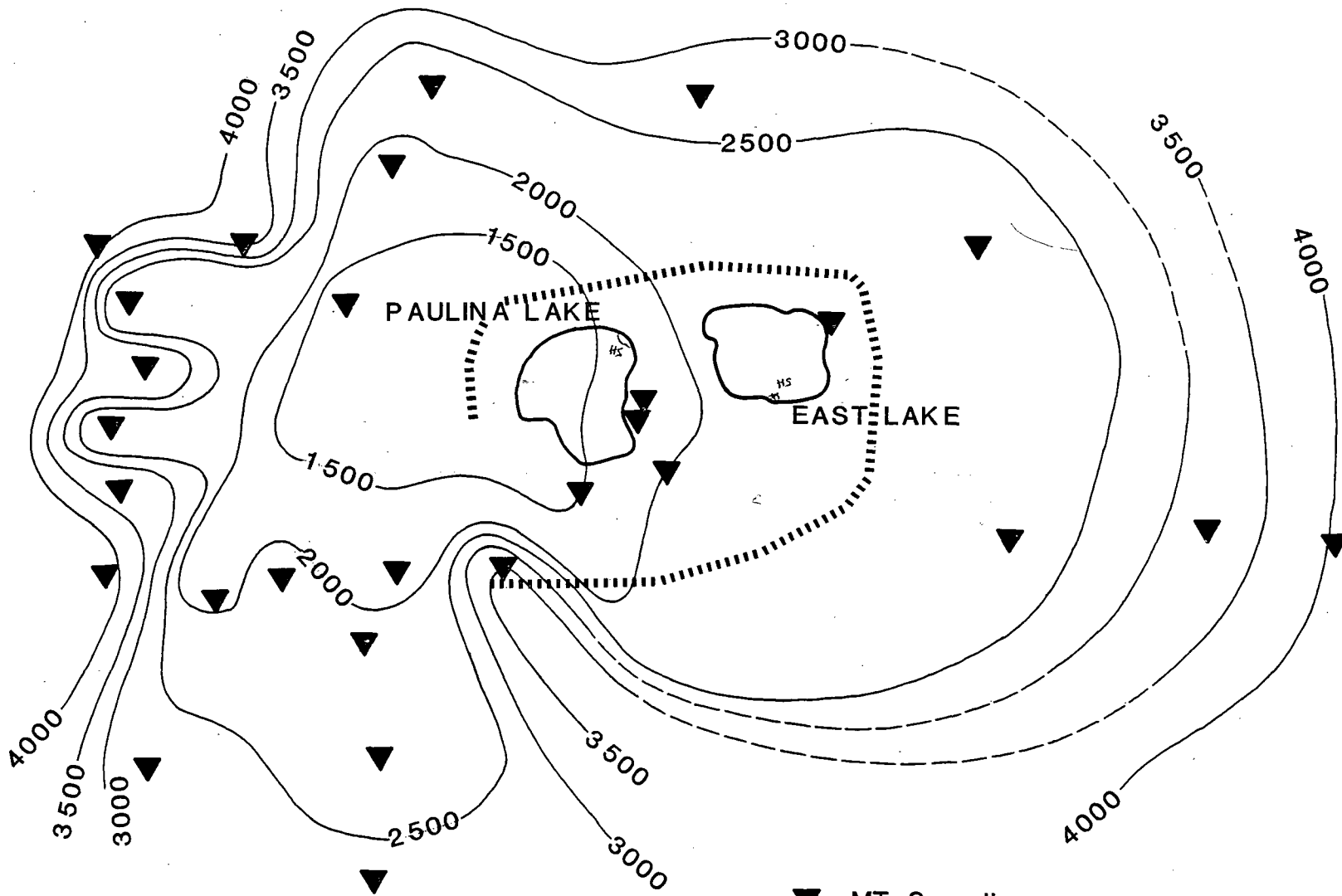
SECOND LAYER RESISTIVITY  
(ALTERED UNIT)



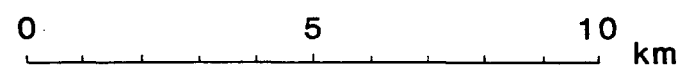
- ▼ MT Soundings
- ..... Newberry Crater Rim
- Contour Interval 5  $\Omega$ M

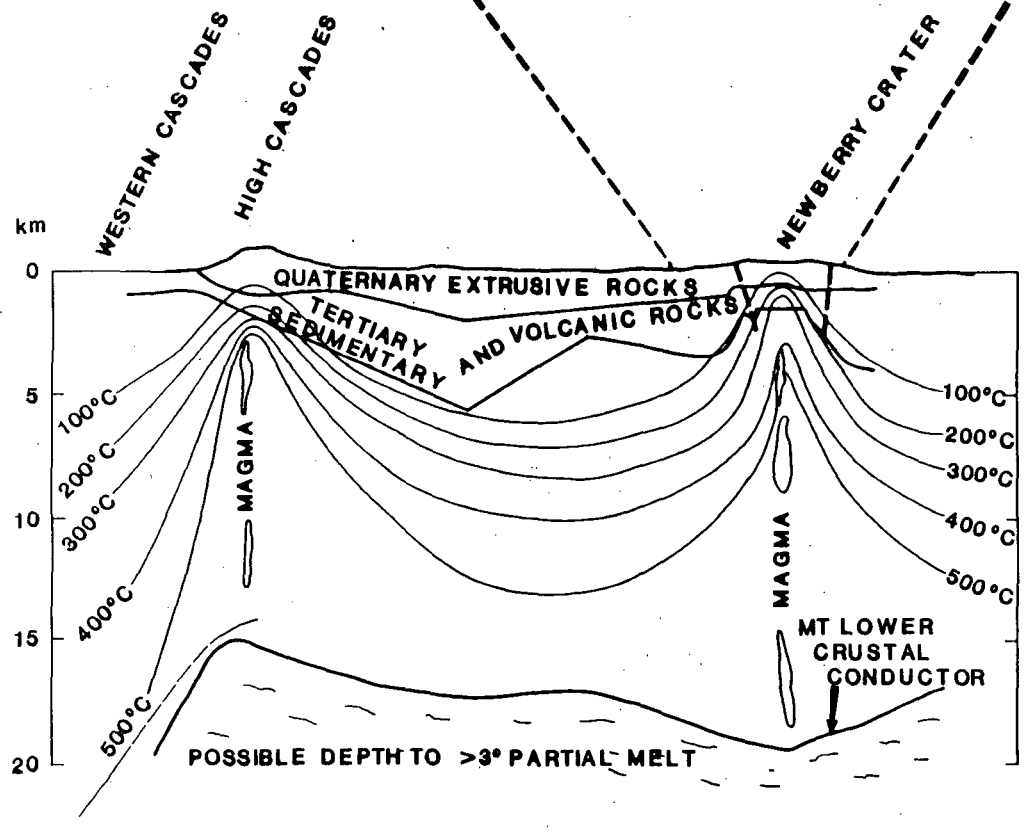
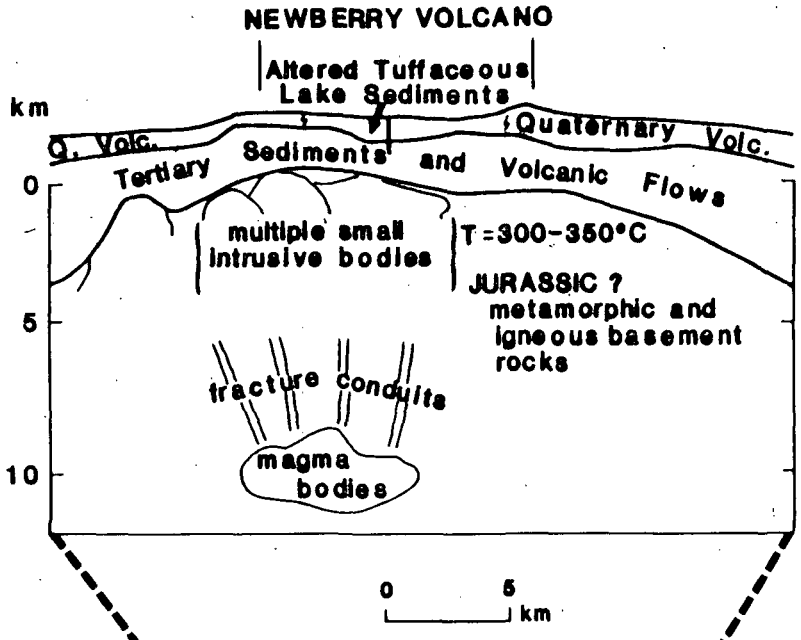


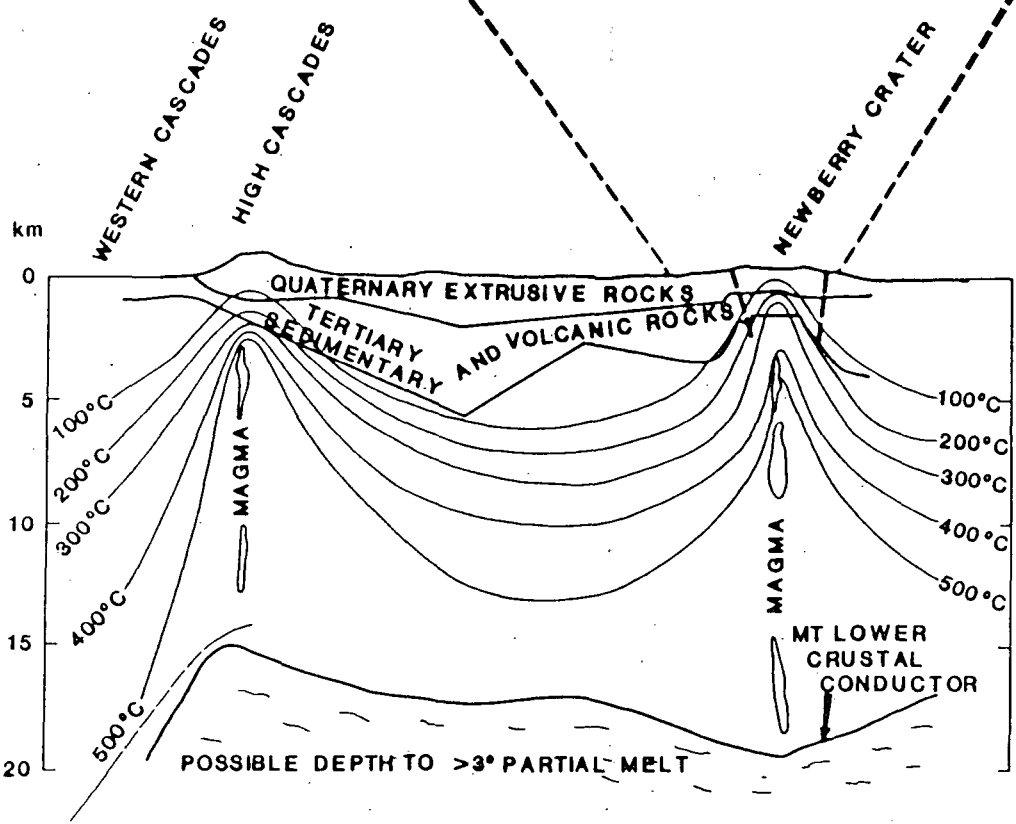
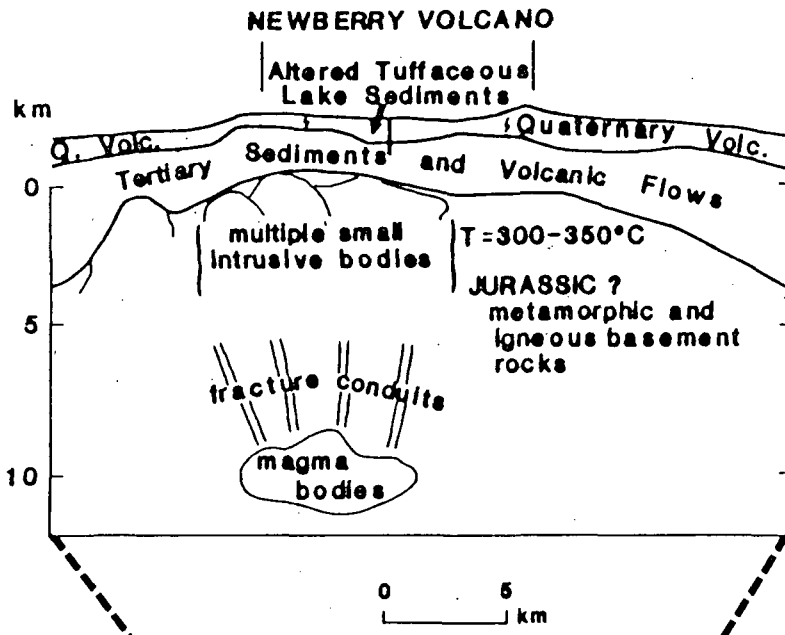
# DEPTH TO ELECTRICAL BASEMENT



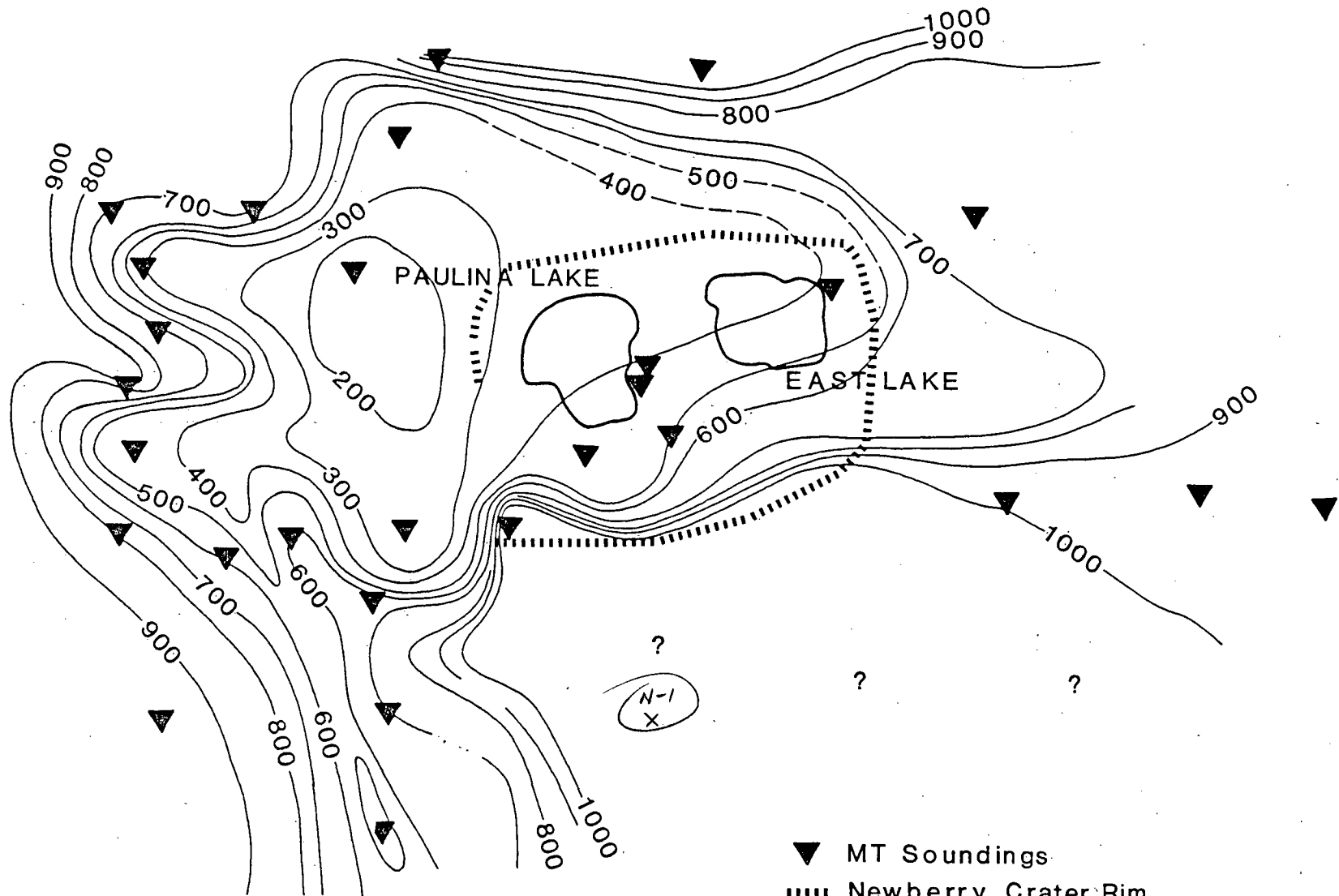
- ▼ MT Soundings
- Newberry Crater Rim



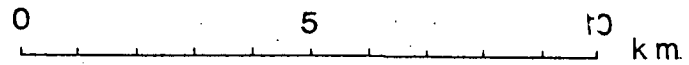




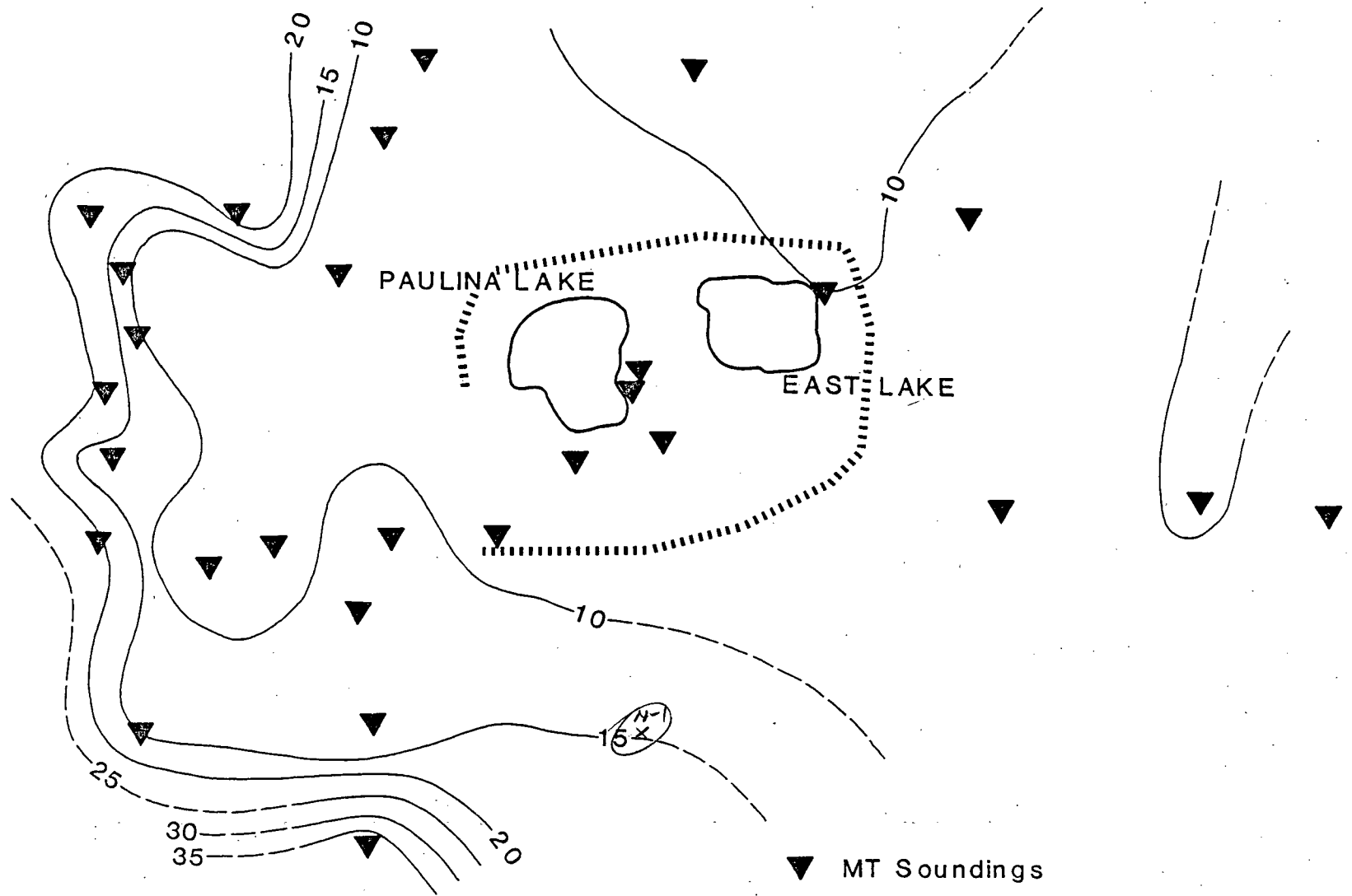
# DEPTH TO ALTERED LAYER



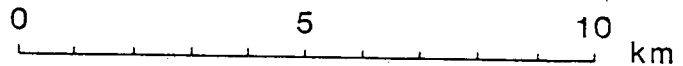
- ▼ MT Soundings
- Newberry Crater Rim
- Contour Interval 100 meters



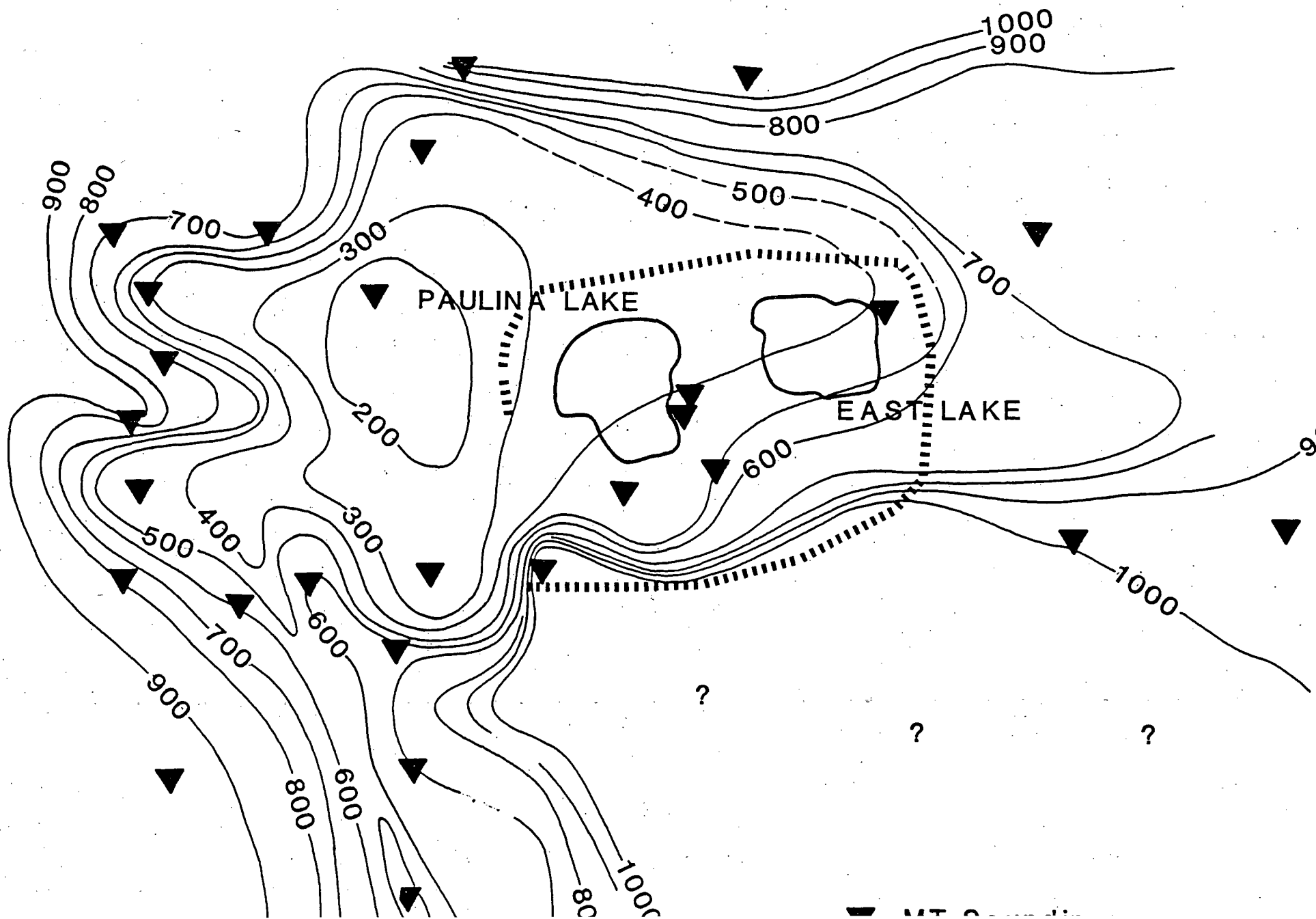
SECOND LAYER RESISTIVITY  
(ALTERED UNIT)



- ▼ MT Soundings
- ..... Newberry Crater Rim
- Contour Interval 5  $\Omega$ M

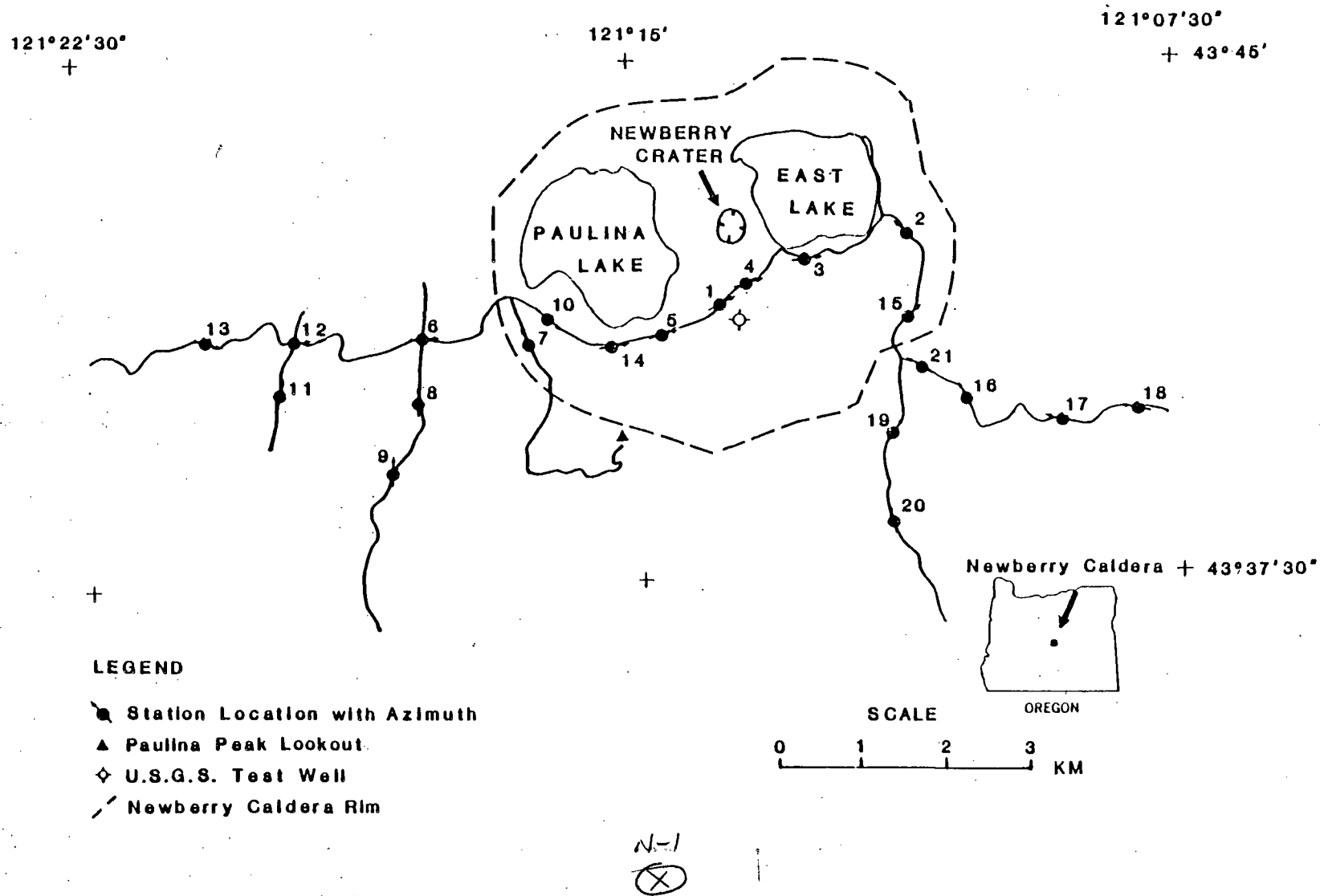


# DEPTH TO ALTERED LAYER





# NEWBERRY CALDERA, OREGON



MAP OF NEWBERRY AND VICINITY SHOWING SCHLUMBERGER SOUNDING LOCATIONS

FIGURE 1

UNITED STATES DEPARTMENT OF THE INTERIOR

GEOLOGICAL SURVEY

SCHLUMBERGER SOUNDINGS NEAR NEWBERRY CALDERA, OREGON

By

Robert J. Bisdorf

Open File Report 83-825

1983

This report is preliminary and has not been reviewed for conformity with U.S. Geological Survey editorial standards. Any use of trade names is for descriptive purposes only and does not constitute endorsement by the USGS.

# Schlumberger Soundings near Newberry Caldera, Oregon

by

Robert J. Bisdorf

## INTRODUCTION

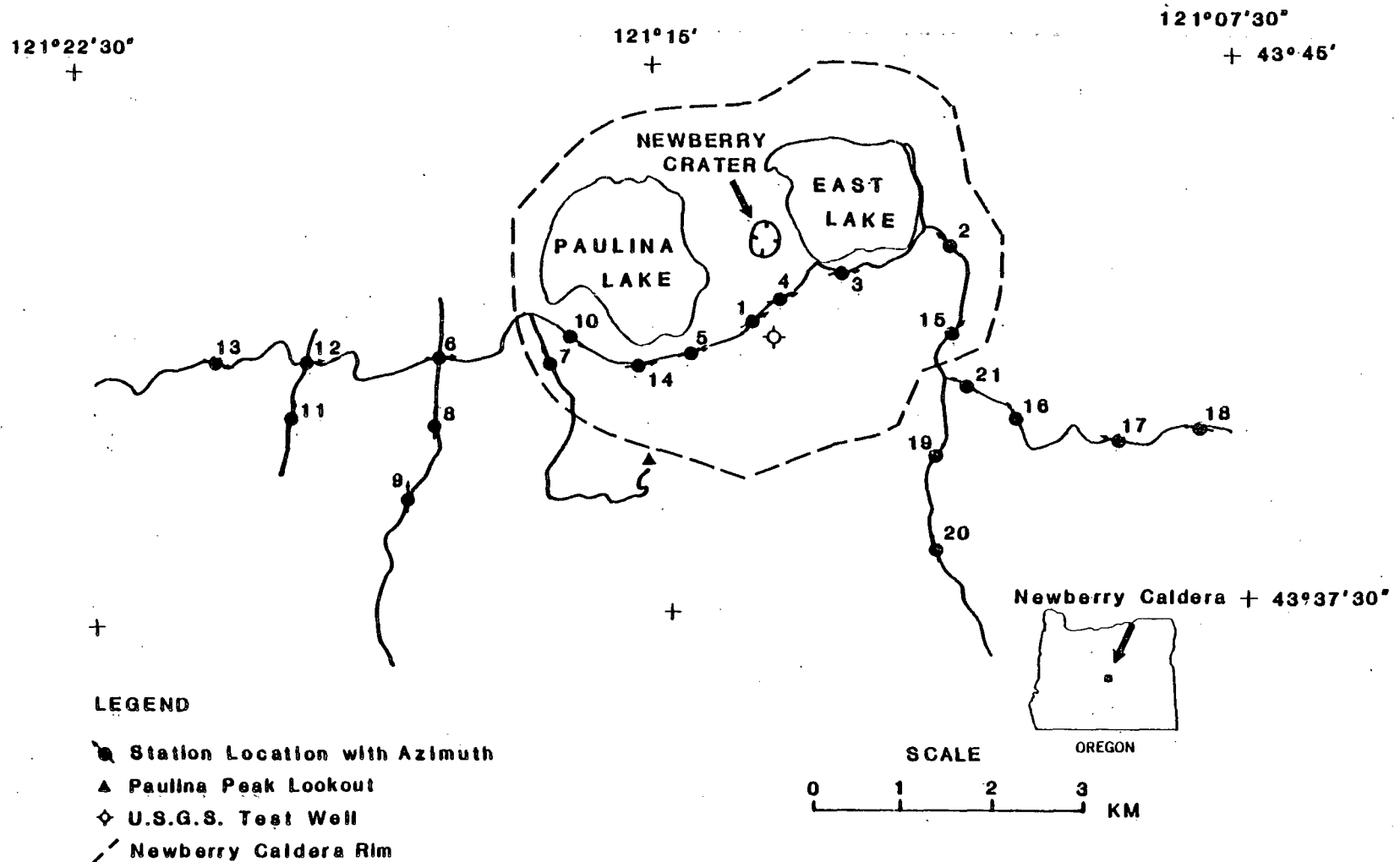
In 1982 the U.S. Geological Survey made 21 Schlumberger soundings in and near Newberry Caldera in Oregon (fig. 1). The soundings were made as part of the U.S.G.S.'s Geothermal program. The purpose of the soundings was to find areas of possible geothermal potential and to map zones of hot water which have been detected by drilling (Sammel, 1981).

Newberry Volcano, located about 40 km south of Bend, Oregon, is one of the largest Quaternary volcanoes in the conterminous United States. The volcano and its lava flows cover an area of greater than 1200 km<sup>2</sup>. Paulina Peak (elevation 2434 m) is the highest remnant of the former mountain. The floor rocks and ejecta that form the volcano range in composition from basaltic to rhyolitic (Sammel, 1981).

The Newberry caldera (fig. 1) covers an area of about 45 km<sup>2</sup>. All exposed rocks within the caldera are Quaternary in age. The present caldera floor is composed mainly of rhyolitic domes and flows of obsidian, basalt, and andesite (McLeod and others, 1981). Two lakes, Paulina and East, are located within the caldera. A line of hot springs occurs along the south shore of East Lake and a few springs occur on the north shore of Paulina Lake.

In 1981 the USGS drilled a geothermal test well in the caldera floor, to a depth of 930 m. Water temperature at the bottom of the hole was 256° C. The upper 610 m of the hole was described as very permeable and the lower 320 m as probably quite impermeable (Sammel, 1981).

# NEWBERRY CALDERA, OREGON



MAP OF NEWBERRY AND VICINITY SHOWING SCHLUMBERGER SOUNDING LOCATIONS

FIGURE 1

The purpose of this report is to release the Schlumberger sounding data. Automatic inversions and a geoelectric cross section are also given and discussed.

### SCHLUMBERGER SOUNDINGS

Figure 1 is a map showing the location, identifying number, and direction of expansion of the Schlumberger soundings. The Schlumberger soundings are numbered consecutively from Newberry 1 to Newberry 21. All the soundings were made along existing roads. Soundings were corrected for road curvature in a manner similar to that described by Zohdy and Bisdorf (1982). All the sounding data were automatically processed and interpreted (Zohdy, 1973; Zohdy, 1975) as shown in the graphs in the Appendix. The curves were interpreted on a Hewlett-Packard (HP) 9845B desk top computer using a program based on that of Zohdy (1973). The HP program was modified to use O'Neill coefficients (O'Neill, 1975) in place of Ghosh coefficients (Ghosh, 1971).

For each sounding, the data in the Appendix include:

- 1) A log-log plot of the field data points, in which the "O"'s represent the individual data points. The AB/2 electrode spacings, which were measured in feet, have been converted to meters. Each set of data points that was made with the same potential electrode spacing (MN) is connected with a solid line. Measurements were made at the fixed MN/2 spacings of 2, 6, 20, 60, 200, and 600 feet.
- 2) A tabulation of the AB/2 electrode spacings in meters and the corresponding apparent resistivities in ohm-m.
- 3) A log-log plot of the output of the automatic inversion program in which:
  - a) The continuous curve represents the shifted-digitized field curve (Bisdorf and Zohdy, 1979).

- b) The step-function curve represents the distribution of interpreted-true resistivity with depth.
  - c) The plus (+) signs represent points on the theoretical sounding curve for the given distribution of resistivity with depth. These points are given to show how well the interpreted model fits the shifted-digitized curve.
- 4) A tabulation of the interpreted depths in meters and the interpreted resistivities in ohm-m.

Soundings 1, 3, 18, and 19 had cusps that were obviously caused by cultural factors or current leakage. These cusps were manually smoothed before interpretation. Soundings 2, 4, 5, 12, 15, 16, 17, 20 and 21 had cusps and other features including rapid decreases of apparent resistivity from a maximum on the sounding curve. Such features were manually smoothed so that the inversion program could better fit the undistorted portions of the soundings. Smoothed soundings have "-S" designations after the title on the sounding interpretation plots in the appendix. Sounding 7 was not expanded to the originally planned AB/2 spacing due to the effects of a buried telephone cable.

#### GEOELECTRIC CROSS SECTION

Figure 2 shows a geoelectric cross section constructed from the interpretation of the Schlumberger sounding data. The figure consists of two parts, a nonvertically exaggerated cross section, and the same cross section vertically exaggerated four times. The cross sections were generated in a manner similar to that described by Bisdorf (1982, pages 5 to 7). On the right hand side of the figure a scale is presented which relates interpreted resistivities with shades of gray. Darker shades indicate higher resistivities and lighter shades indicate lower resistivities. Triangles at the top of the cross sec-

9

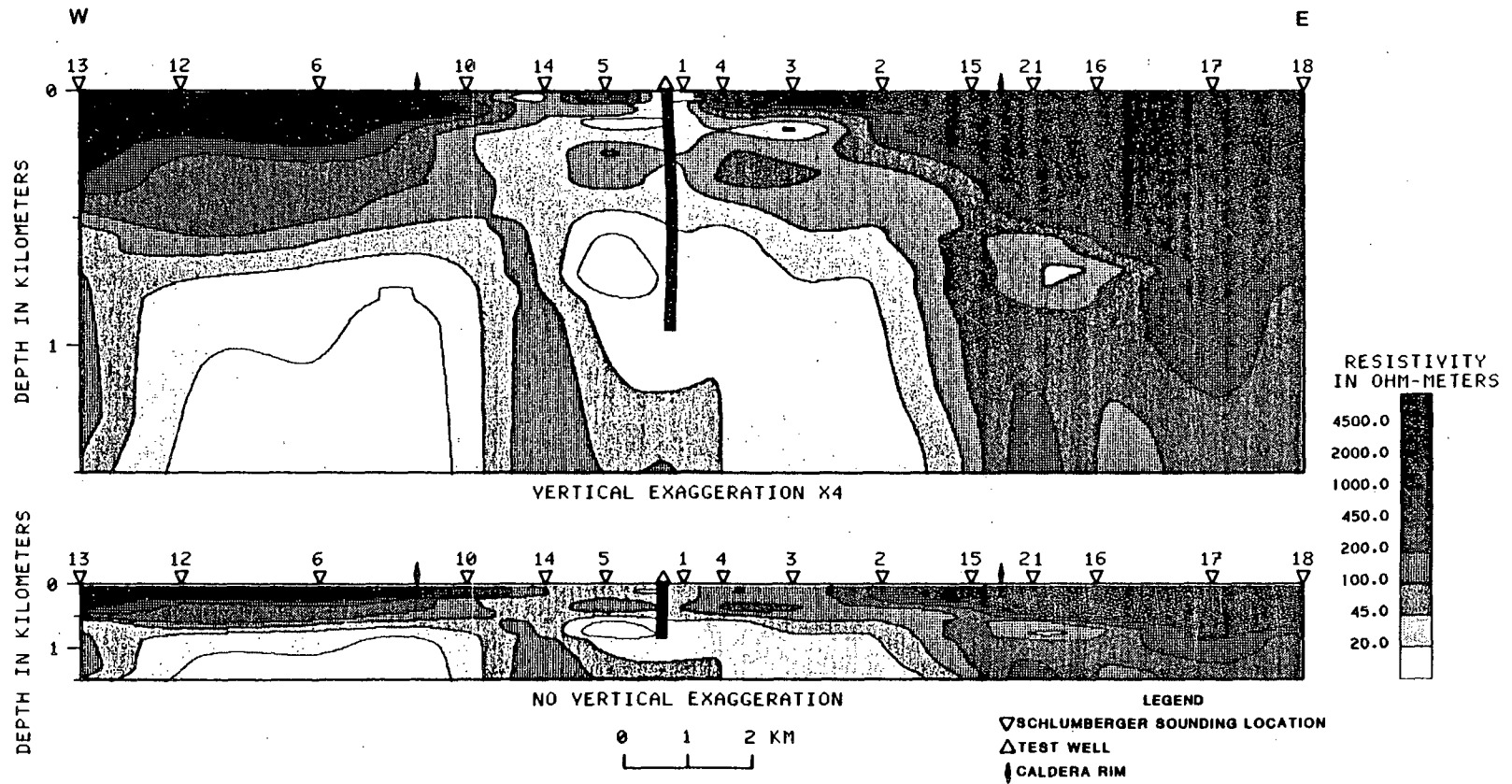


FIGURE 2. Computer-generated geoelectric cross section. Top and bottom parts are vertically exaggerated 4 and 1 times respectively.

tions indicate sounding locations and the numbers above the triangles are the sounding numbers.

Two factors need to be considered when interpreting the cross section. The first factor is that, due to the nature of the interpolation techniques used, anomalies not based on existing data may be generated between sounding locations. For example, between soundings 16 and 17 in the upper 100 m a lower resistivity area is shown. This area is very much lower than the resistivities under soundings 16 and 17 would dictate. The second factor is the limited resolution of the plotter which produced the original plots. Because of its fixed resolution the x1 and x4 cross sections were generated with a different number of vertical points. Therefore the x1 cross section is only presented to show the layered structure of the cross section and the x4 cross section is presented to show the detail.

On the top of the cross section the approximate location of the caldera rim is shown. The location of the USGS test well described by Sammel (1981) is shown where it projects onto the cross section. The well is located about 1/4 mile southeast of this location (fig. 1).

The generalized lithologic log of the test well (Sammel, 1981) indicates that the intermediate resistivity, 45 to 1000 ohm-m, materials could correspond to tuffs, breccias, rhyolite flows, and lacustrine or fluvial sediments. In the vicinity of sounding one, at a depth of about 600 m, the main rock type changes to dacite and basalt flows. Generally these rock types exhibit higher resistivities than the 45 ohm-m (or lower) value indicated by the interpretation of soundings 4, 5, and 1. The low resistivities could be indicative of a significant amount of alteration, large quantities of hot or saline water, or both. The temperature profile for the test well indicates an increase in temperature at about 680 m, thus the low resistivity zone seems to



correlate with the increasing temperature. A larger low resistivity zone at a depth of about 700 m is present under soundings 10, 6, and 12. The resistivity cross section does not indicate a hydrologic connection between the low resistivity areas in the upper 1.5 km, but this zone probably contains hot water.

High resistivity material ( $>1000$  ohm-m) is present in the upper 600 m along the flanks of the volcano, mostly outside the caldera. This material most likely consists of scoria and basalt or andesite flows. A thin ( $<100$  m) layer of this material extends into the caldera from the east.

#### SUMMARY

The USGS test well has shown the presence of hot water in the Newberry Caldera. Schlumberger sounding interpretations correlate well with the drill hole indications of elevated borehole temperatures. Low resistivity zones can be assumed to be related to the presence of hot water or alteration zones. Another low resistivity zone not necessarily hydrologically related to the zone near the test well is present to the west and could contain significant amounts of hot water.

High resistivity material up to 600 m thick was detected on the flanks of the volcano. High-resistivity materials do not occur in such large thicknesses inside the caldera. The high-resistivity unit either does not occur inside the caldera, or it has been altered.

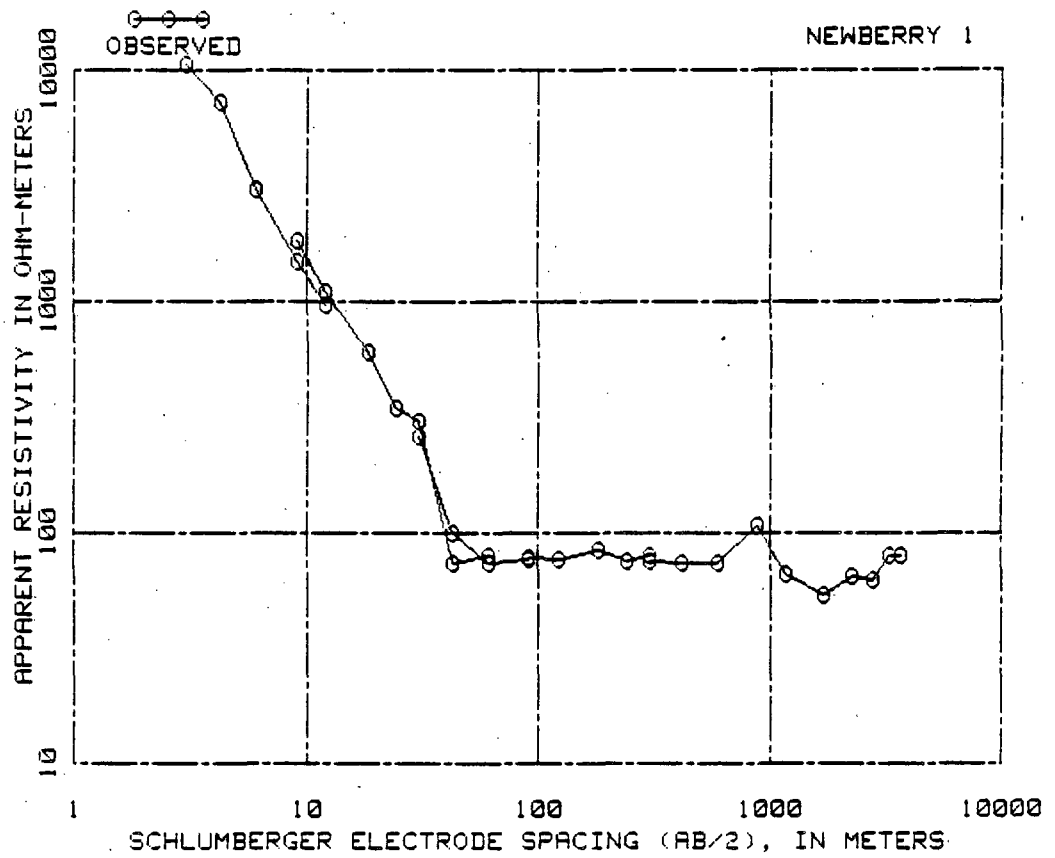
#### ACKNOWLEDGMENT

This work was funded in part by the Department of Energy under the Inter-agency Agreement DE-AI01-79RA50294. Permission to conduct the field work was granted by the Dept. of Agriculture, Forest Service, Deschutes National Forest, Bend, Oregon. The field work was accomplished with the help of Dean Schoenthaler, R. Grette, D. Piper, M. Seals and D. Churchill.

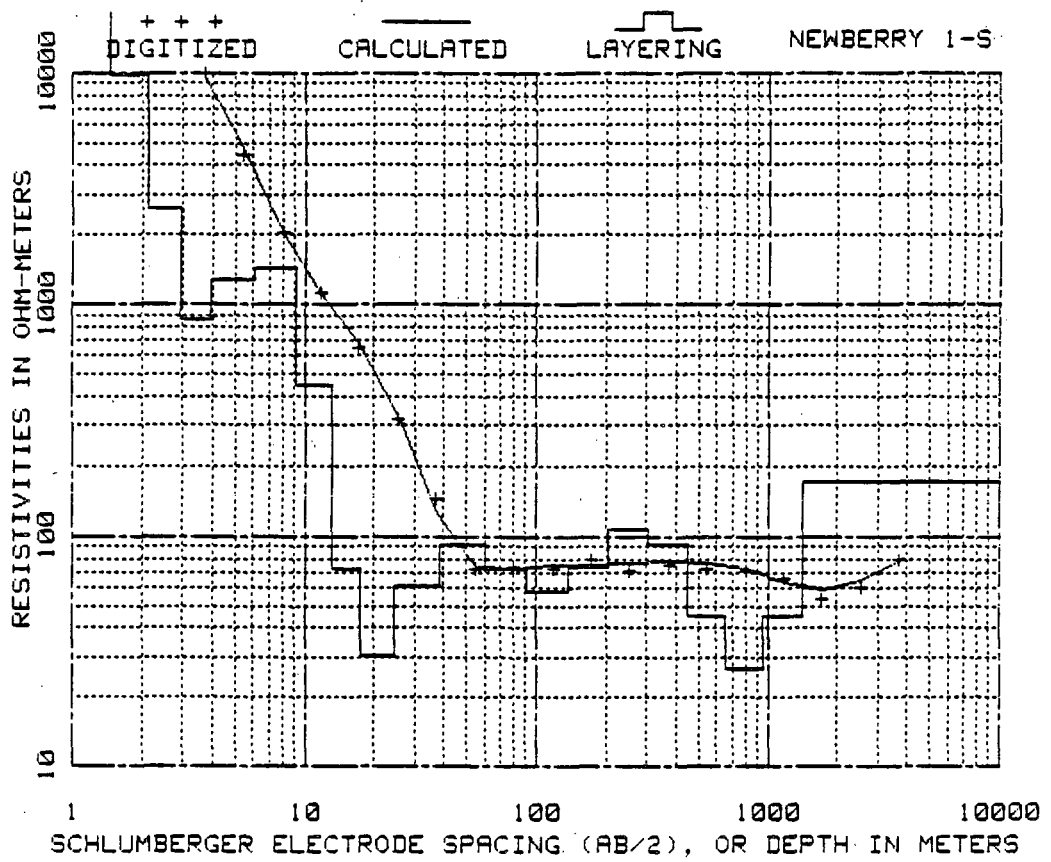
## REFERENCES

- Bisdorf, R. J., 1982, Schlumberger sounding investigations in the Date Creek Basin, Arizona: U.S. Geological Survey Open-File Report 82-953, 54 p.
- Bisdorf, R. J., and Zohdy, A. A. R., 1979, Geoelectric investigations with Schlumberger soundings near Brunswick, Georgia: U.S. Geological Survey Open-File Report 79-1551, 125 p.
- Ghosh, D. P., 1971, Inverse filter coefficients for the computation of apparent resistivity standard curves over horizontally stratified earth: Geophysical Prospecting [Netherlands], v. 19, no. 4, p. 769-775.
- McLeod, N. S., Sherrod, D. R., Chitwood, L. A., and McKee, E. H., 1981, Newberry Volcano, Oregon: Guide to some Volcanic Terranes in Washington, Idaho, Oregon and Northern California (D. A. Johnston and J. Donnelly-Nolan, eds), U.S. Geological Survey Circular 838, p. 85-103.
- O'Neill, D. J., 1975, Improved linear filter coefficients for application in apparent resistivity computations: Bulletin Australian Society Exploration Geophysics, v. 6, no. 4, p. 104-109.
- Sammel, E. A., 1981, Results of test drilling at Newberry Volcano, Oregon: Geothermal Resources Council Bull., Dec. 1981.
- Zohdy, A. A. R., 1973, A computer program for the automatic interpretation of Schlumberger sounding curves over horizontally stratified media: available only from U.S. Dept. of Commerce, Nat'l. Tech. Inf. Service, Springfield, Va. 22161, as U.S. Geological Survey Report USGS-GD-74-017, PB232 703.
- \_\_\_\_\_, 1975, Automatic interpretation of Schlumberger sounding curves using modified Dar Zarrouk functions: U.S. Geological Survey Bull. 1313-E, 39p.
- Zohdy, A. A. R., and Bisdorf, R. J., 1982, Schlumberger soundings in the Medicine Lake Area, California, U.S. Geological Survey Open-File Report 82-887, 162 p.

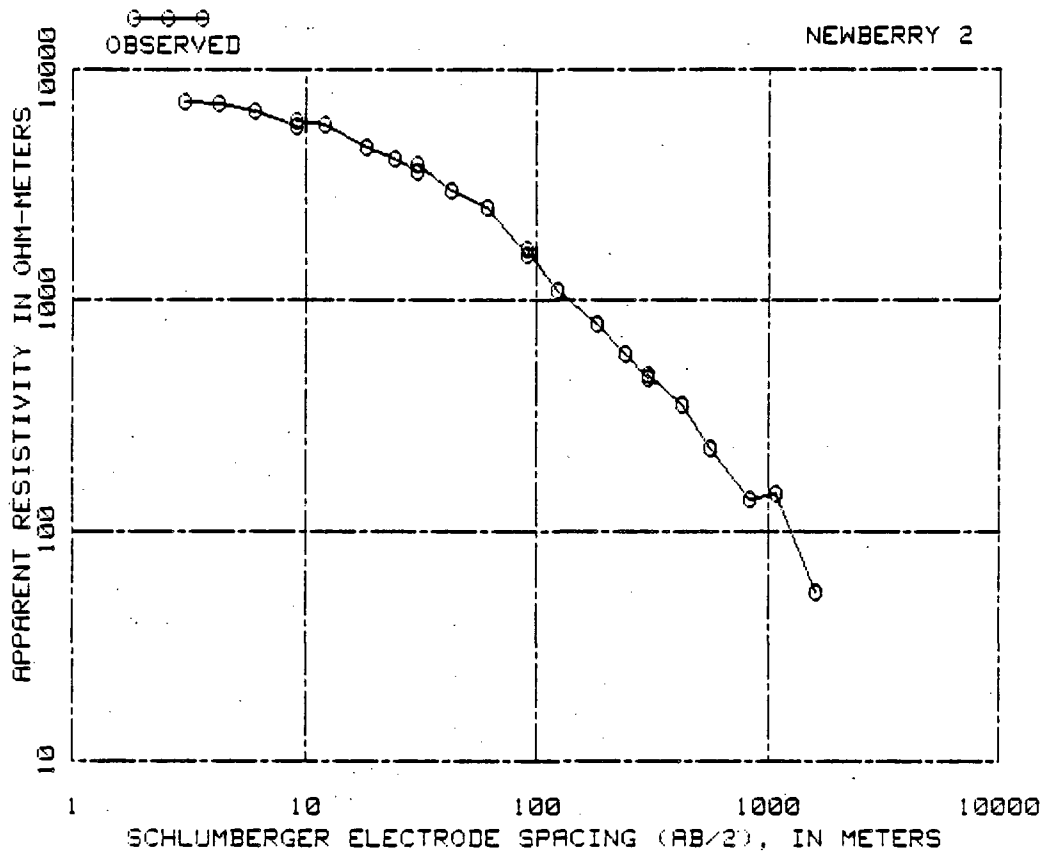
APPENDIX



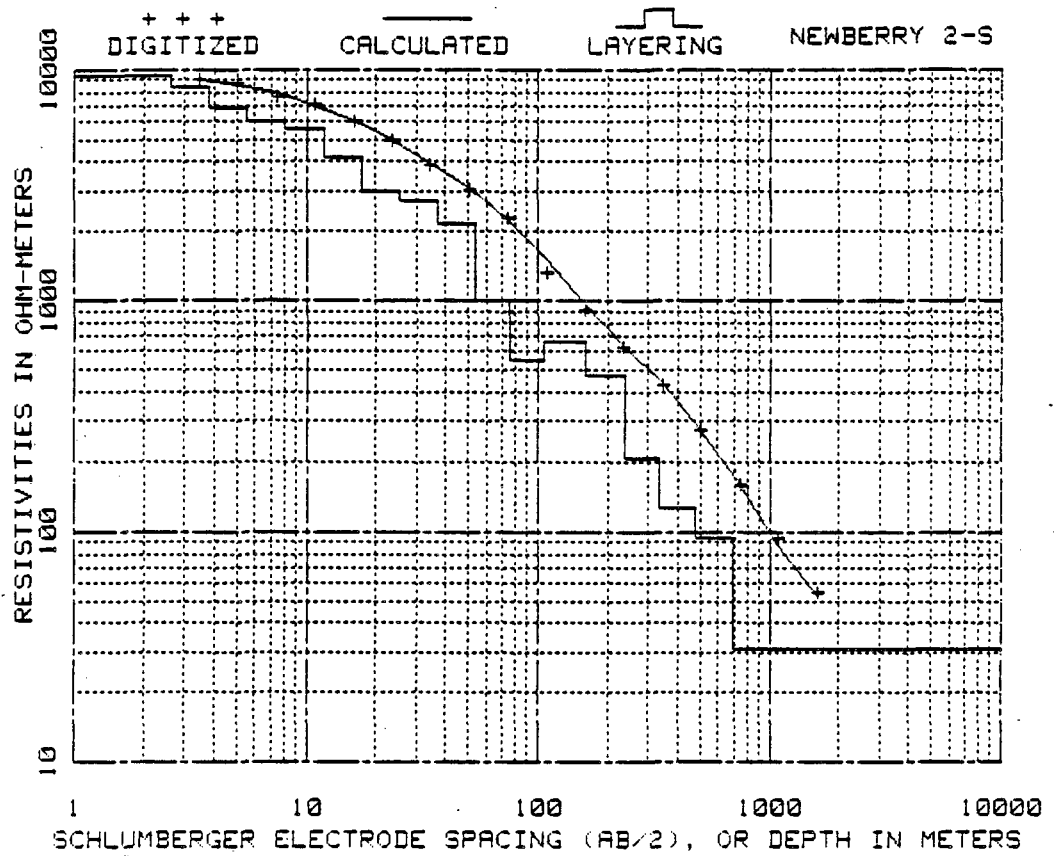
AB/2 IN METERS	OBSERVED RESISTIVITY IN OHM-METERS	AB/2 IN METERS	OBSERVED RESISTIVITY IN OHM-METERS
3.05	10500.00	91.44	79.00
4.27	7200.00	121.92	76.00
6.10	3040.00	182.88	84.00
9.14	1500.00	243.84	75.00
12.19	960.00	304.80	79.00
9.14	1840.00	304.80	75.00
12.19	1100.00	419.71	73.00
18.29	600.00	593.45	73.00
24.38	345.00	889.41	108.00
30.48	300.00	889.41	108.00
42.67	73.00	1181.71	66.00
60.96	80.00	1692.86	54.00
30.48	260.00	2267.71	65.00
42.67	100.00	2769.11	62.00
60.96	73.00	3297.63	79.00
91.44	76.00	3713.68	79.00



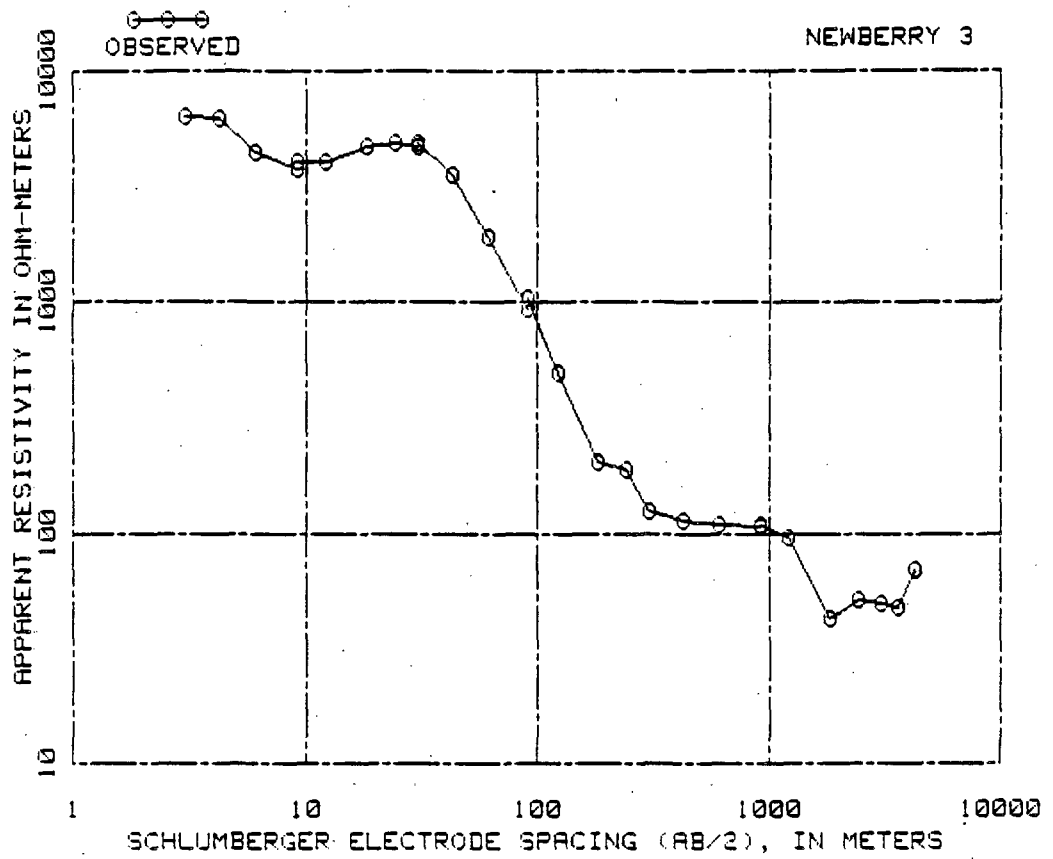
INTERPRETED DEPTH IN METERS	INTERPRETED RESISTIVITY IN OHM-METERS	INTERPRETED DEPTH IN METERS	INTERPRETED RESISTIVITY IN OHM-METERS
.21	20345.26	17.37	72.29
.31	19984.27	24.31	30.66
.46	19548.74	38.67	60.58
.68	20255.62	60.23	91.58
.99	22520.22	91.80	72.48
1.46	20299.58	137.85	57.61
2.11	9751.39	206.13	73.00
2.90	2634.53	301.62	106.31
3.97	858.50	447.97	92.63
6.03	1288.29	657.04	45.12
9.16	1422.66	953.39	26.55
13.18	448.61	1418.54	45.30
		1001417.54	171.69



AB/2 IN METERS	OBSERVED RESISTIVITY IN OHM-METERS	AB/2 IN METERS	OBSERVED RESISTIVITY IN OHM-METERS
3.05	7200.00	91.44	1580.00
4.27	7150.00	91.44	1660.00
6.10	6600.00	121.92	1100.00
9.14	5700.00	182.88	790.00
9.14	6000.00	243.84	580.00
12.19	5800.00	304.80	460.00
13.29	4600.00	304.80	473.00
24.38	4100.00	426.72	350.00
30.48	3590.00	565.40	228.00
30.48	3900.00	834.85	136.00
42.67	3000.00	834.85	138.00
60.96	2530.00	1087.53	146.00
		1600.50	55.00

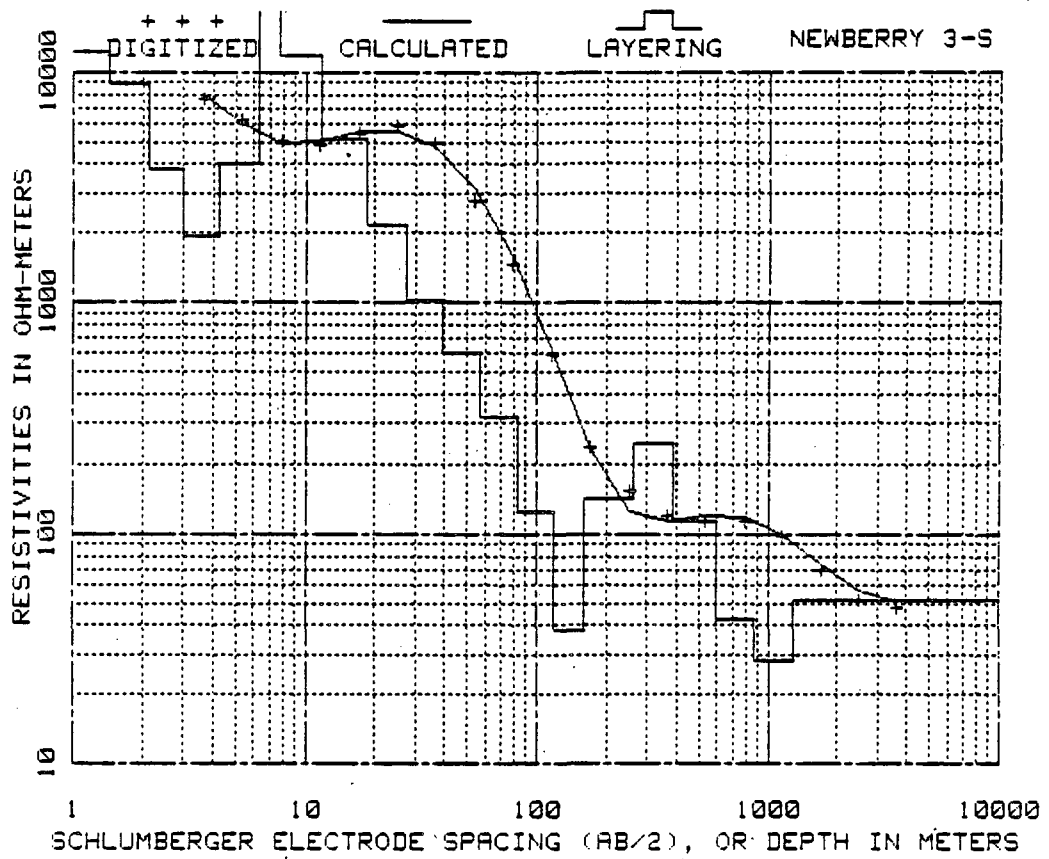


INTERPRETED DEPTH IN METERS	INTERPRETED RESISTIVITY IN OHM-METERS	INTERPRETED DEPTH IN METERS	INTERPRETED RESISTIVITY IN OHM-METERS
.25	9357.84	17.34	4165.31
.38	9355.97	25.13	3010.63
.56	9346.42	36.79	2716.00
.82	9339.19	53.80	2183.19
1.20	9379.98	75.76	1004.61
1.76	9493.39	106.16	548.20
2.59	9423.10	159.18	662.73
3.79	8433.89	235.46	471.35
5.55	6787.45	331.88	205.81
8.12	5974.26	473.57	126.80
11.90	5590.59	693.68	93.59
		1000	62.68
		1000	30.88

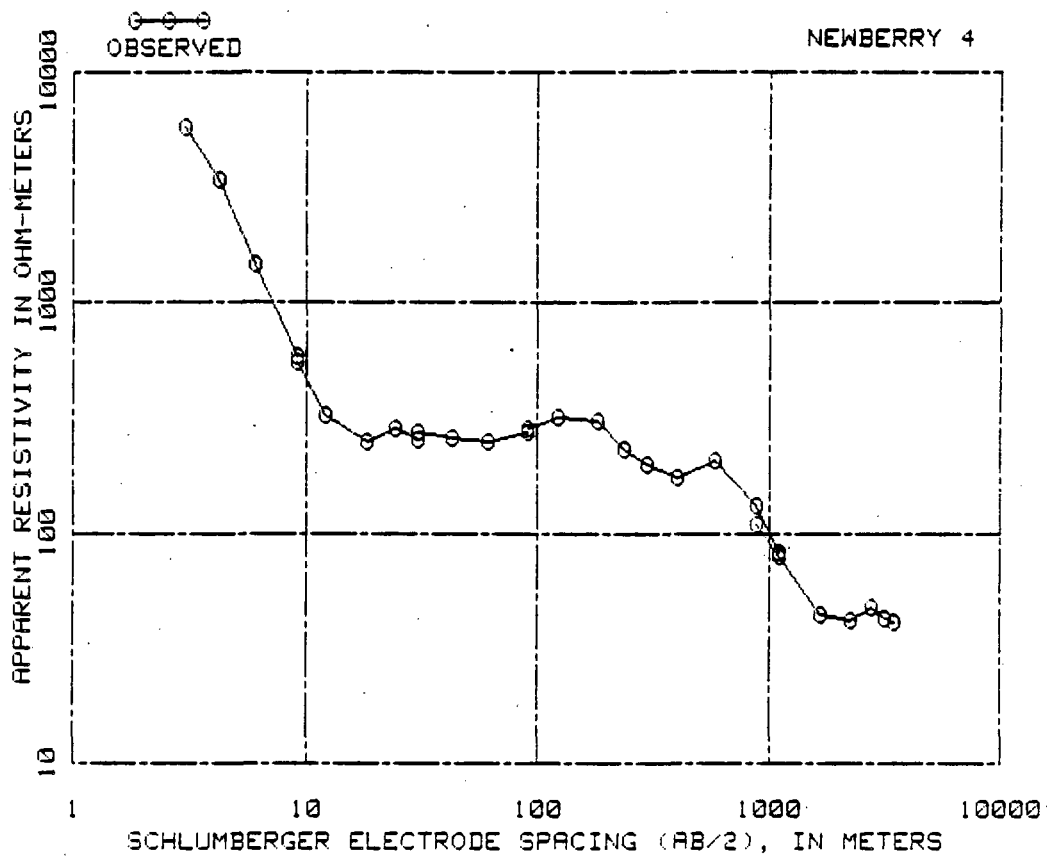


AB/2 IN METERS	OBSERVED RESISTIVITY IN OHM-METERS	AB/2 IN METERS	OBSERVED RESISTIVITY IN OHM-METERS
3.05	6350.00	121.92	492.00
4.27	6210.00	182.88	203.00
6.10	4400.00	243.34	187.00
9.14	3760.00	304.80	124.00
9.14	4050.00	304.30	125.00
12.19	4050.00	426.72	114.00
18.29	4650.00	609.60	110.00
24.38	4900.00	914.40	107.00
30.48	4700.00	914.40	110.00
30.48	4900.00	1219.20	95.00
42.67	3550.00	1828.80	43.00
60.96	1900.00	2438.40	52.00
91.44	940.00	3048.00	50.00
91.44	1050.00	3657.60	48.00
		4267.20	69.00

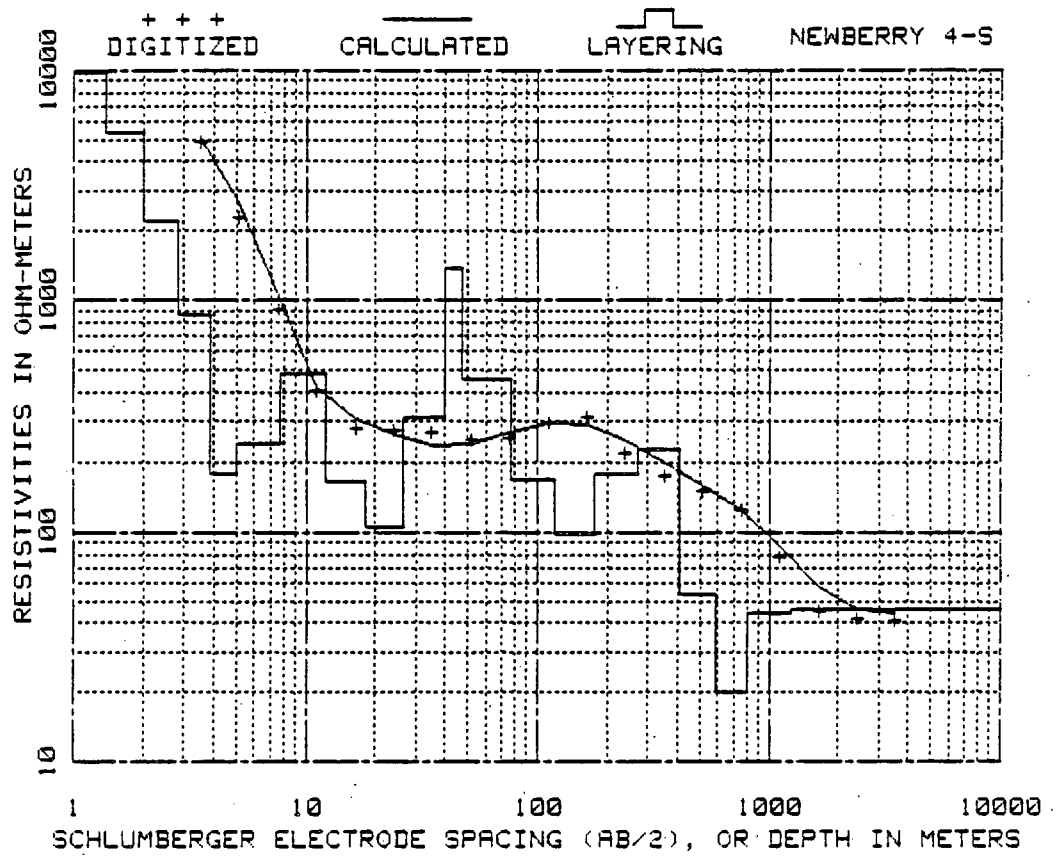




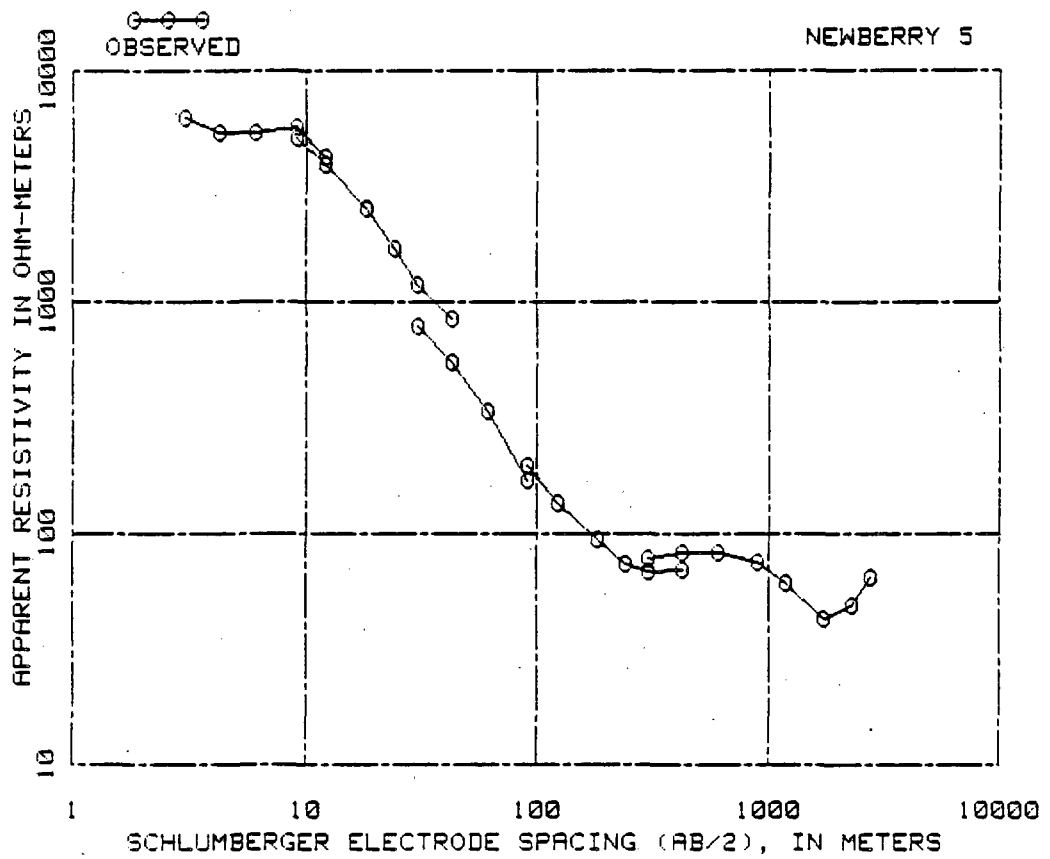
INTERPRETED DEPTH IN METERS	INTERPRETED RESISTIVITY IN OHM-METERS	INTERPRETED DEPTH IN METERS	INTERPRETED RESISTIVITY IN OHM-METERS
.21	11345.32	18.35	5174.14
.31	11539.13	27.20	2158.36
.45	11311.37	39.31	1026.42
.67	11008.44	57.26	604.16
.98	11500.12	83.07	319.99
1.44	12225.18	117.42	124.37
2.10	8960.33	161.40	38.46
3.00	3811.45	260.04	142.59
4.24	1927.99	389.28	247.52
6.37	4026.87	599.26	114.32
7.81	20462.32	871.61	42.31
11.70	11795.76	1277.30	28.27
		1001276.30	51.64



AB/2 IN METERS	OBSERVED RESISTIVITY IN OHM-METERS	AB/2 IN METERS	OBSERVED RESISTIVITY IN OHM-METERS
3.05	5790.00	182.88	310.00
4.27	3400.00	237.74	231.00
6.10	1475.00	295.05	198.00
9.14	580.00	295.05	199.00
9.14	555.00	404.16	174.00
12.19	326.00	589.48	208.00
18.29	252.00	881.79	133.00
24.38	285.00	1107.34	93.00
30.48	254.00	881.79	110.00
30.48	277.00	1107.34	79.00
42.67	260.00	1689.51	44.00
60.96	250.00	2246.99	42.00
91.44	275.00	2804.16	48.00
91.44	285.00	3197.05	43.00
121.92	320.00	3514.34	41.00

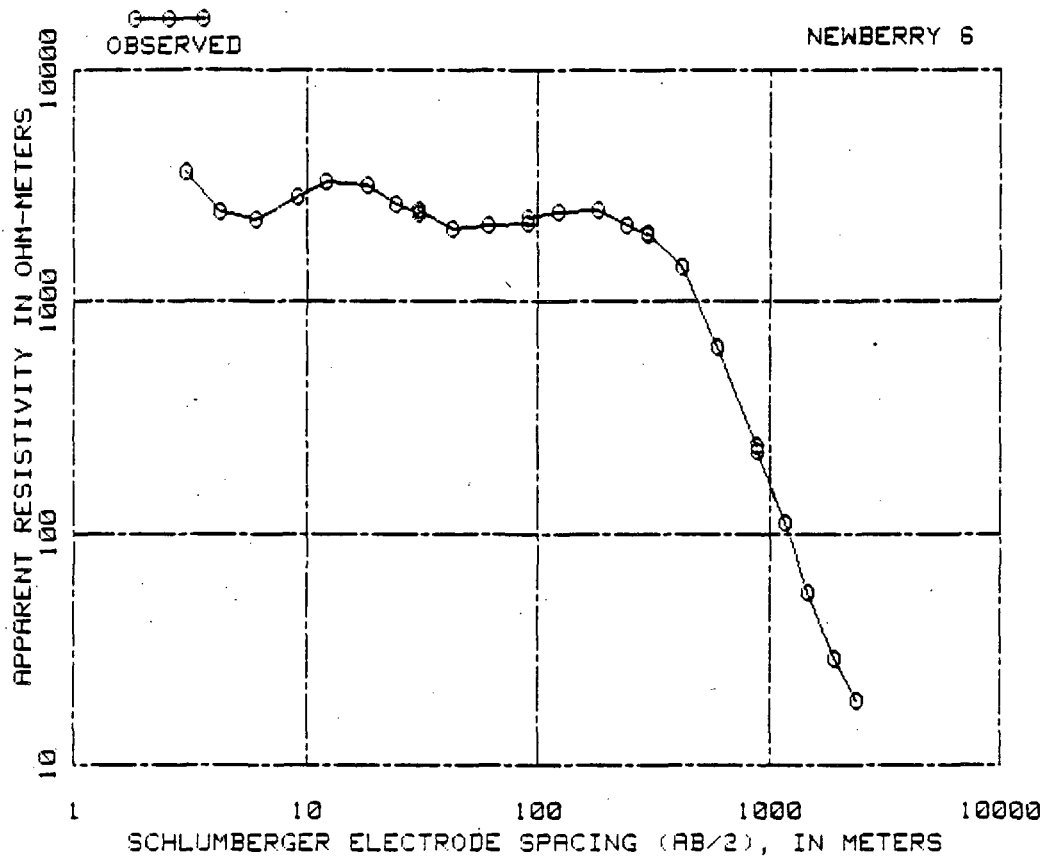


INTERPRETED DEPTH IN METERS	INTERPRETED RESISTIVITY IN OHM-METERS	INTERPRETED DEPTH IN METERS	INTERPRETED RESISTIVITY IN OHM-METERS
.20	9732.86	17.93	165.38
.30	9823.89	26.40	104.69
.44	9552.97	39.53	311.18
.64	9563.92	47.57	1384.02
.94	10468.45	76.60	453.74
1.38	9826.34	118.11	167.43
2.00	5385.53	176.66	97.44
2.82	2206.69	271.49	177.19
3.89	859.88	408.38	226.68
5.07	179.16	583.56	53.08
7.72	239.64	812.17	20.11
12.12	479.20	1250.22	44.30
		1001249.22	45.64

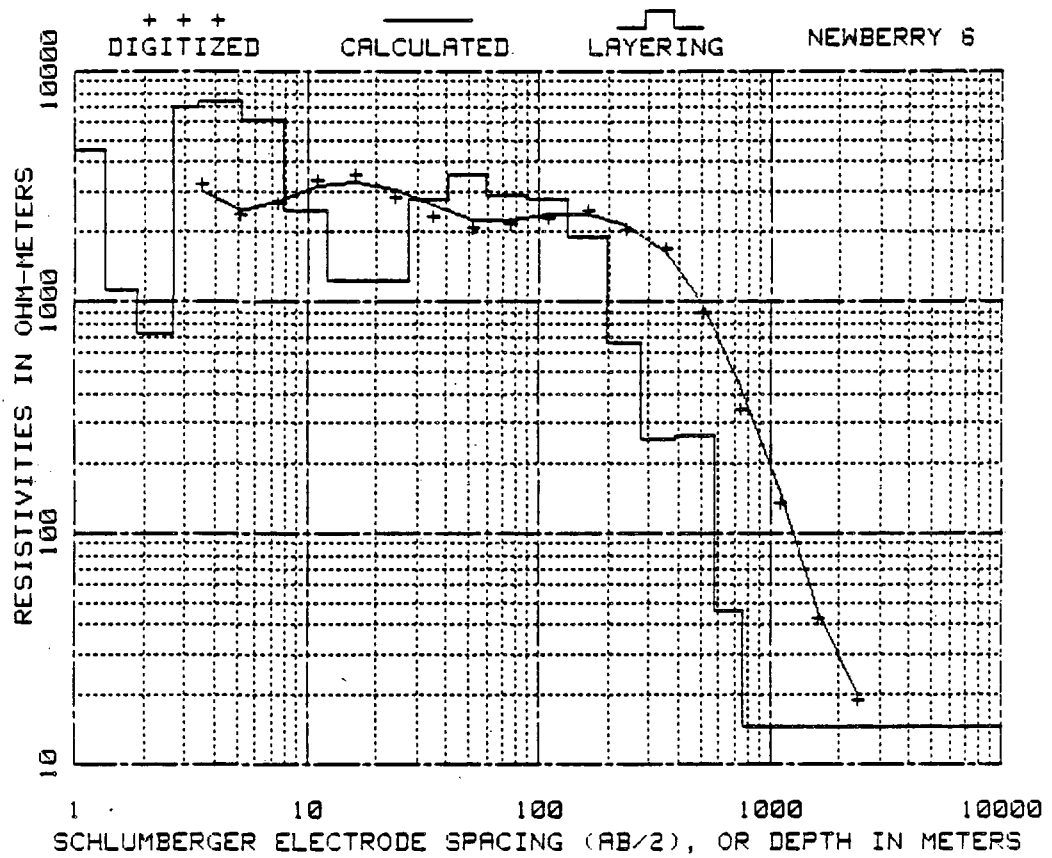


AB/2 IN METERS	OBSERVED RESISTIVITY IN OHM-METERS	AB/2 IN METERS	OBSERVED RESISTIVITY IN OHM-METERS
3.05	6100.00	91.44	170.00
4.27	5400.00	91.44	194.00
6.10	5400.00	121.92	135.00
9.14	5700.00	182.88	94.00
12.19	4100.00	243.84	74.00
9.14	5100.00	304.80	68.00
12.19	3920.00	426.72	70.00
18.29	2510.00	304.80	78.00
24.38	1700.00	426.72	82.00
30.48	1200.00	609.60	82.00
42.67	850.00	905.56	75.00
30.48	780.00	1196.95	61.00
42.67	550.00	1748.33	43.00
60.96	340.00	2305.20	49.00
		2803.86	65.00

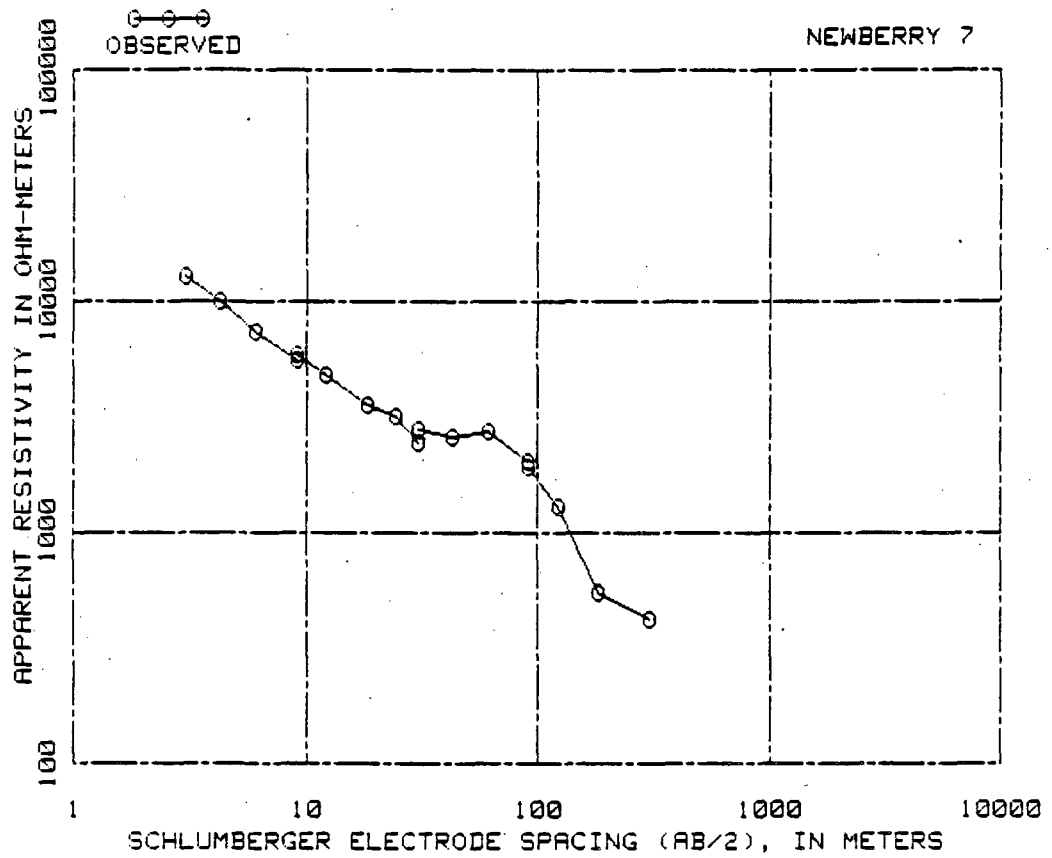




AB/2 IN METERS	OBSERVED RESISTIVITY IN OHM-METERS	AB/2 IN METERS	OBSERVED RESISTIVITY IN OHM-METERS
3.05	3600.00	91.44	2280.00
4.27	2450.00	121.92	2450.00
6.10	2250.00	182.88	2500.00
9.14	2850.00	239.88	2133.00
9.14	2850.00	300.23	1950.00
12.19	3280.00	300.23	1969.00
19.29	3150.00	418.80	1408.00
24.38	2600.00	599.54	638.00
30.48	2400.00	891.54	239.00
30.48	2500.00	891.54	229.00
42.67	2060.00	1177.75	112.00
60.96	2125.00	1473.71	56.00
91.44	2160.00	1908.96	29.00
		2383.54	19.00



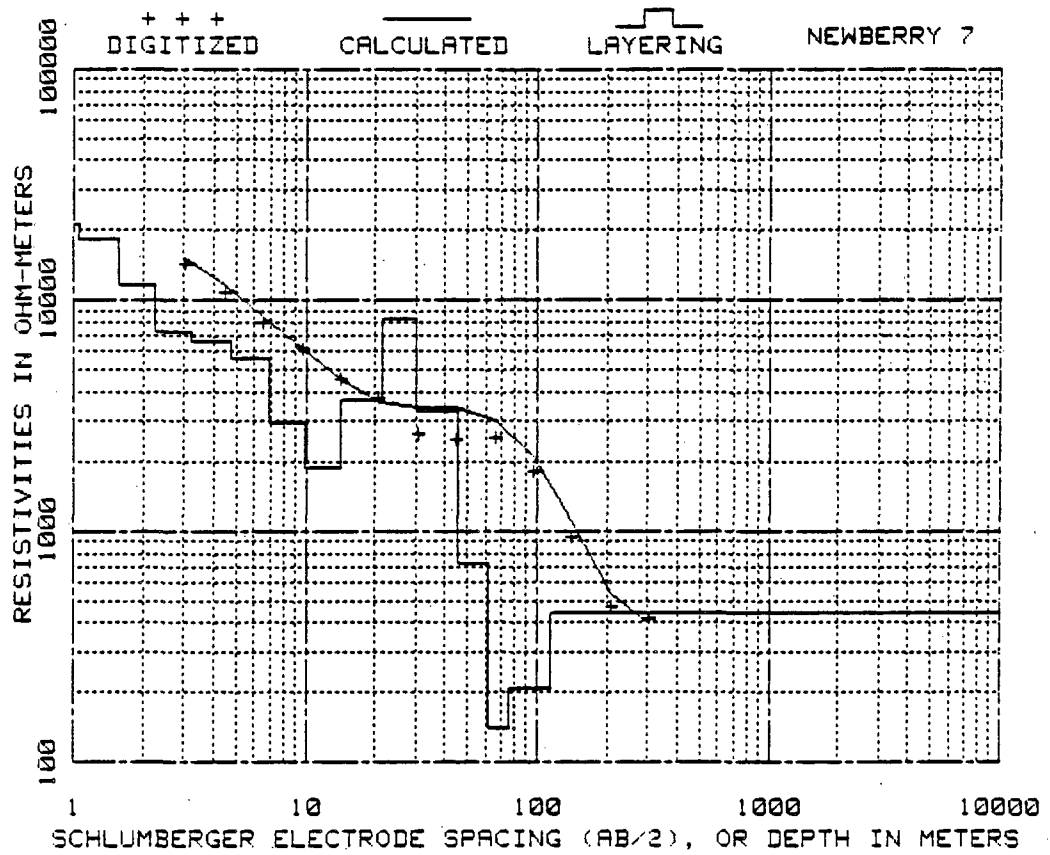
INTERPRETED DEPTH IN METERS	INTERPRETED RESISTIVITY IN OHM-METERS	INTERPRETED DEPTH IN METERS	INTERPRETED RESISTIVITY IN OHM-METERS
.20	6896.26	18.02	1228.46
.30	6822.86	27.10	1233.07
.43	6518.11	40.25	2753.92
.64	7112.00	58.76	3561.63
.93	8099.57	88.38	2863.13
1.36	4528.78	132.12	2790.28
1.86	1134.97	195.81	1916.86
2.65	727.81	277.14	659.77
3.39	6958.21	383.60	253.99
5.22	7391.98	570.56	266.98
7.97	6117.01	757.60	46.32
12.23	2487.04	1000756.60	14.61



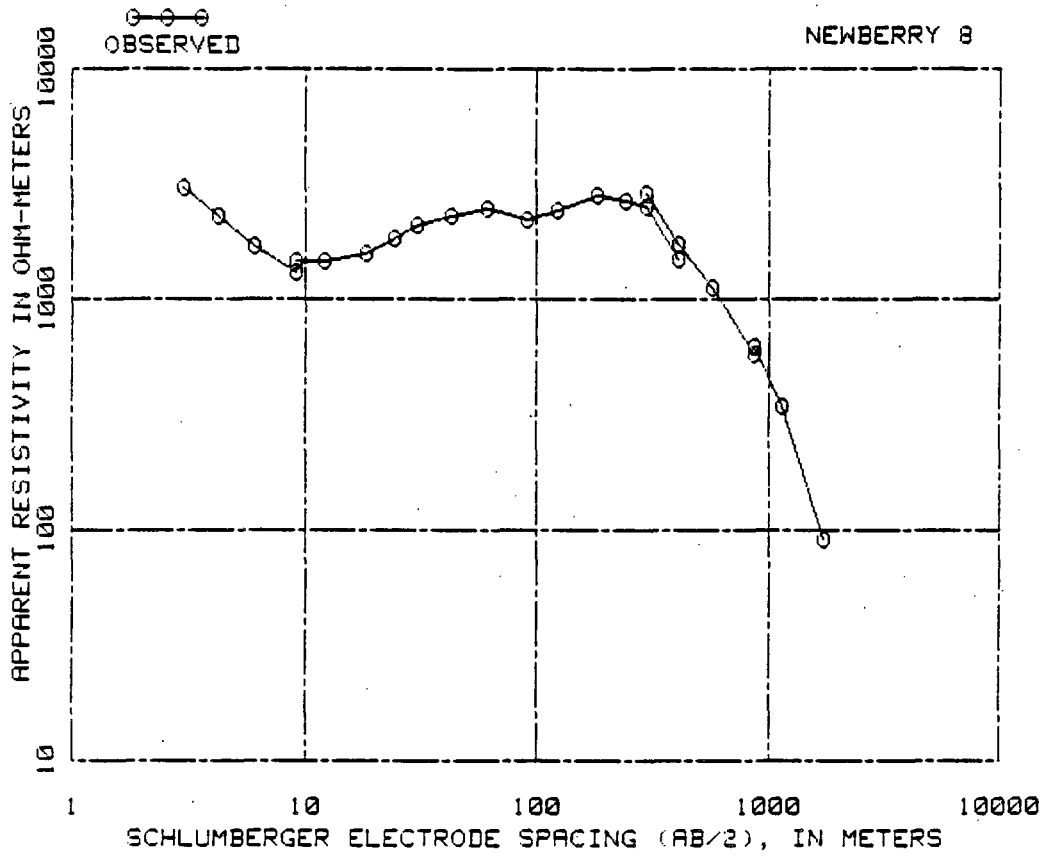
AB/2 IN METERS	OBSERVED RESISTIVITY IN OHM-METERS
----------------------	--

3.05	12000.00
4.27	10000.00
6.10	7450.00
9.14	5650.00
9.14	5900.00
12.19	4800.00
18.29	3600.00
24.38	3200.00
30.48	2450.00
30.48	2800.00
42.67	2600.00
60.96	2760.00
91.44	2020.00
91.44	1910.00
121.92	1300.00
182.88	550.00
304.80	416.00

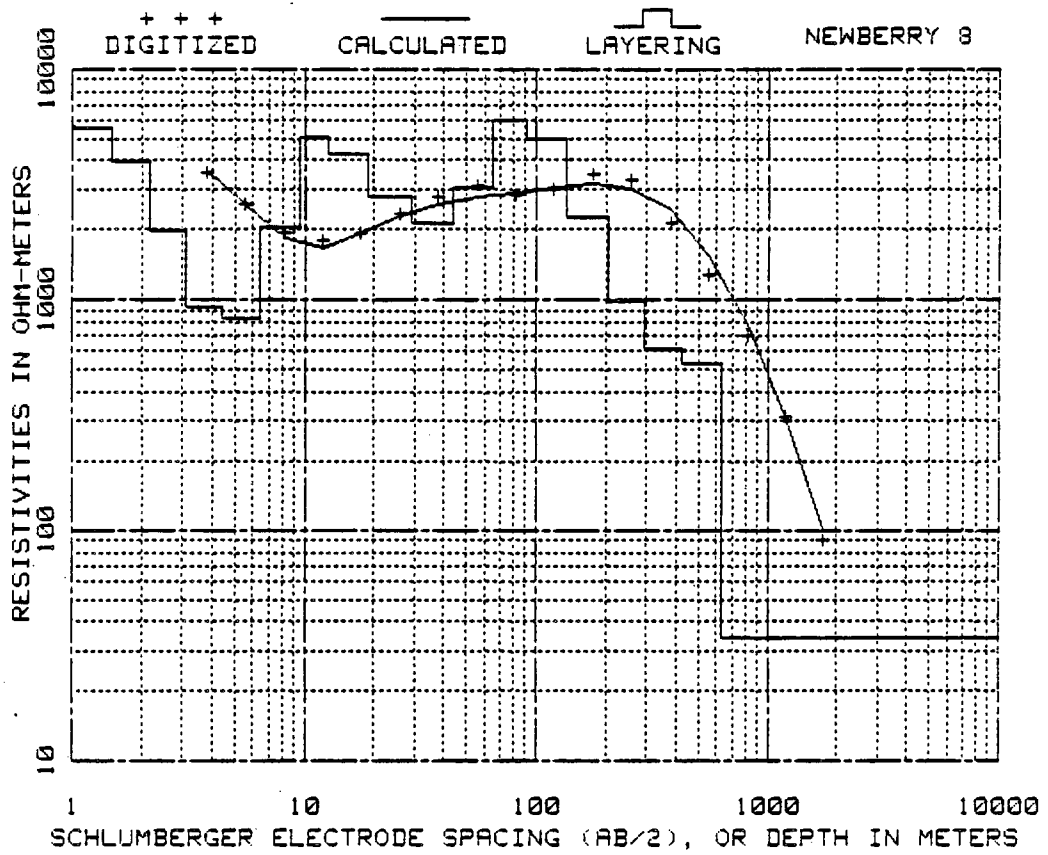




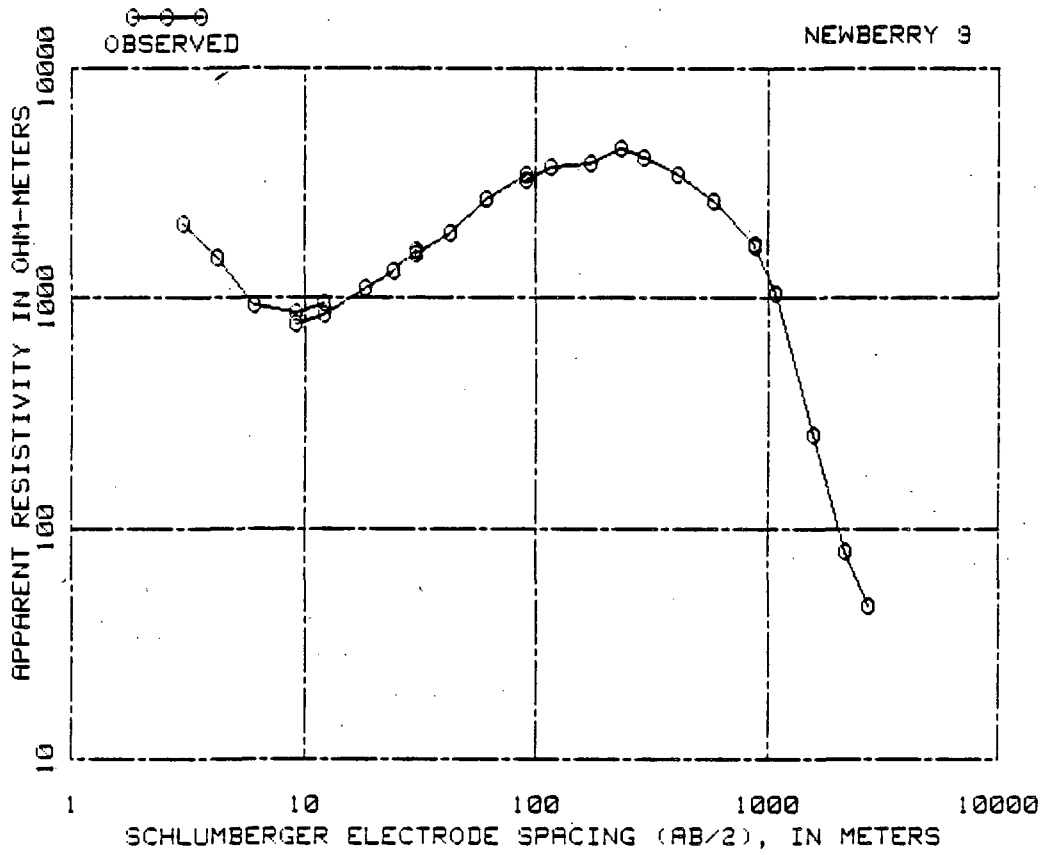
INTERPRETED DEPTH IN METERS	INTERPRETED RESISTIVITY IN OHM-METERS	INTERPRETED DEPTH IN METERS	INTERPRETED RESISTIVITY IN OHM-METERS
.23	20704.94	6.92	5632.57
.34	20646.29	9.88	2967.09
.49	20623.52	14.12	1898.79
.72	20943.78	21.41	3716.99
1.06	21191.04	30.04	8383.42
1.56	18199.41	45.47	3302.72
2.25	11577.78	61.02	721.28
3.23	7260.01	74.86	139.66
4.72	6609.55	114.07	209.08
		1000	113.07
			443.96



AB/2 IN METERS	OBSERVED RESISTIVITY IN OHM-METERS	AB/2 IN METERS	OBSERVED RESISTIVITY IN OHM-METERS
3.05	3050.00	91.44	2200.00
4.27	2200.00	121.92	2420.00
6.10	1710.00	182.88	2300.00
9.14	1300.00	241.71	2665.00
9.14	1460.00	295.66	2503.00
12.19	1450.00	406.91	1502.00
18.29	1500.00	295.66	2905.00
24.38	1820.00	406.91	1739.00
30.48	2100.00	579.42	1128.00
30.48	2110.00	865.02	587.00
42.67	2300.00	865.02	631.00
60.96	2500.00	1159.15	342.00
91.44	2200.00	1753.51	90.00

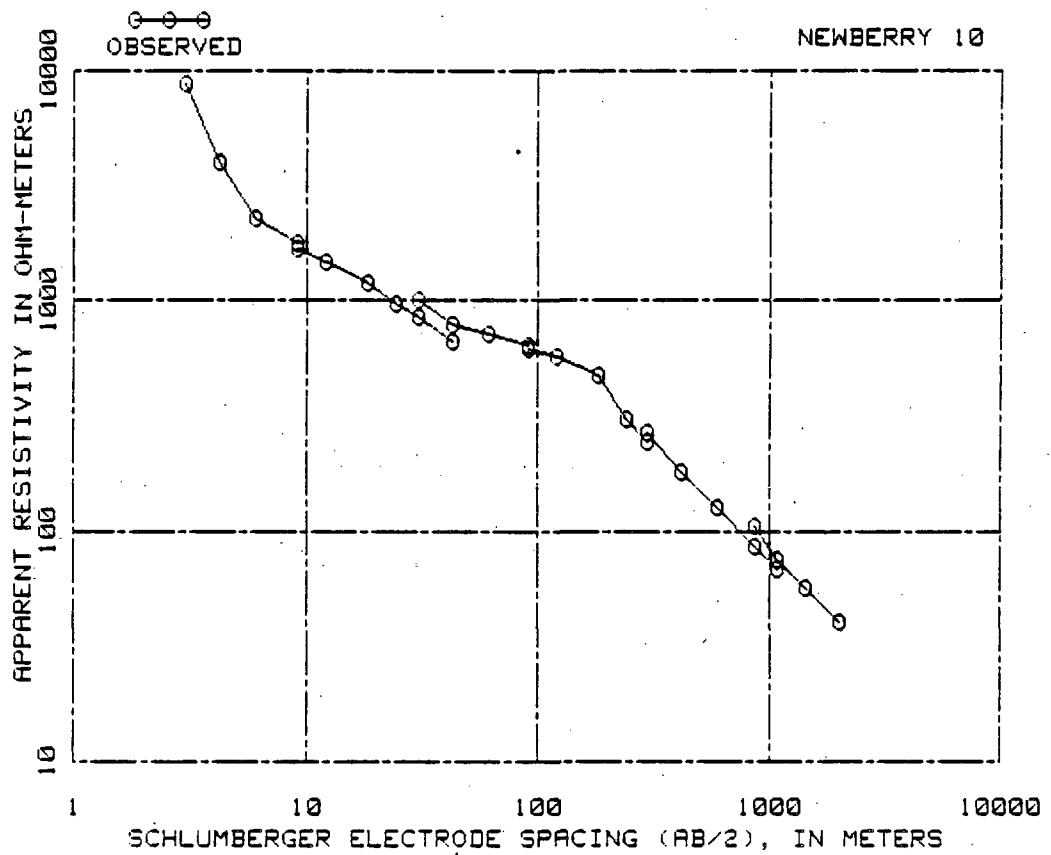


INTERPRETED DEPTH IN METERS	INTERPRETED RESISTIVITY IN OHM-METERS	INTERPRETED DEPTH IN METERS	INTERPRETED RESISTIVITY IN OHM-METERS
.22	5414.45	12.65	5047.45
.32	5295.18	18.61	4252.80
.47	5219.45	28.80	2758.16
.69	5321.27	43.69	2126.88
1.01	5664.49	65.31	3078.76
1.48	5560.87	91.12	6018.50
2.17	3979.84	136.03	4947.36
3.12	1992.99	203.78	2266.35
4.39	926.15	293.84	984.41
6.43	834.60	425.96	628.75
9.53	2061.11	531.10	533.60
		1000630.10	34.24

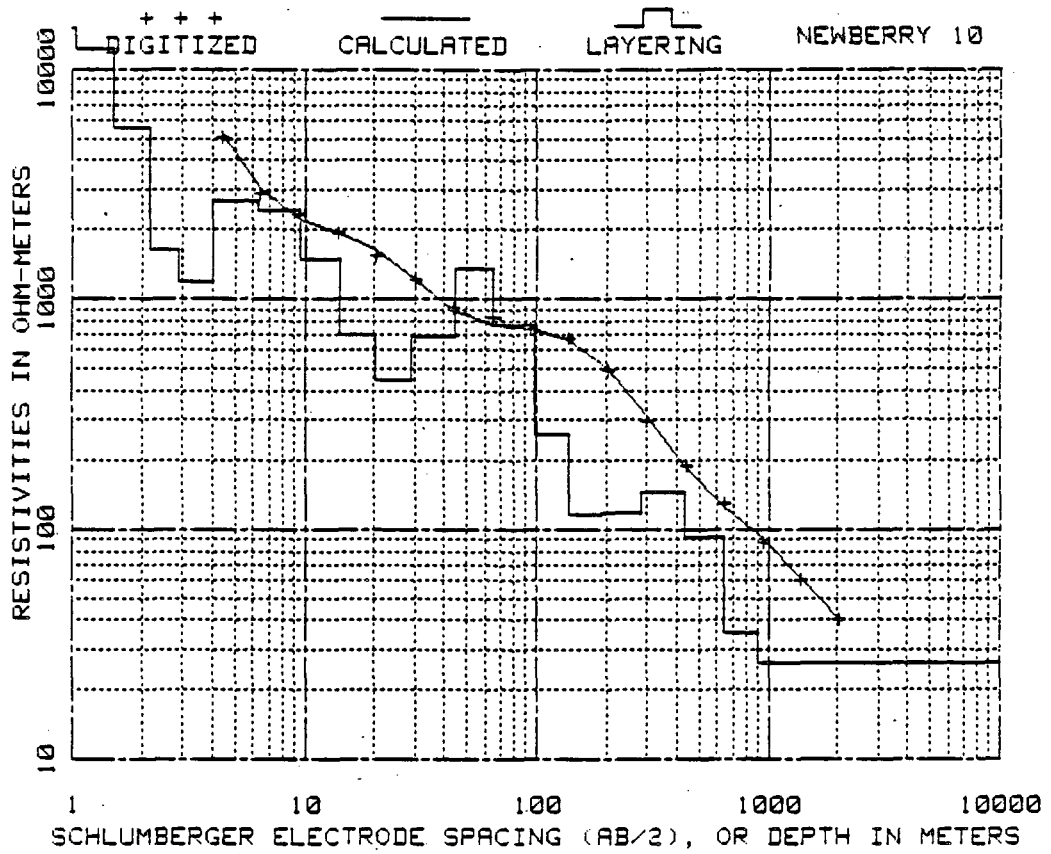


AB/2 IN METERS	OBSERVED RESISTIVITY IN OHM-METERS	AB/2 IN METERS	OBSERVED RESISTIVITY IN OHM-METERS
3.05	2000.00	91.44	3200.00
4.27	1500.00	115.21	3698.00
6.10	930.00	171.91	3847.00
9.14	860.00	233.78	4409.00
12.19	950.00	290.78	4059.00
9.14	770.00	290.78	4072.00
12.19	850.00	409.35	3415.00
18.29	1100.00	590.09	2645.00
24.38	1300.00	882.70	1692.00
30.48	1600.00	882.70	1682.00
30.48	1550.00	1088.14	1034.00
42.67	1900.00	1586.48	257.00
60.96	2650.00	2174.14	79.00
91.44	3400.00	2753.26	46.00

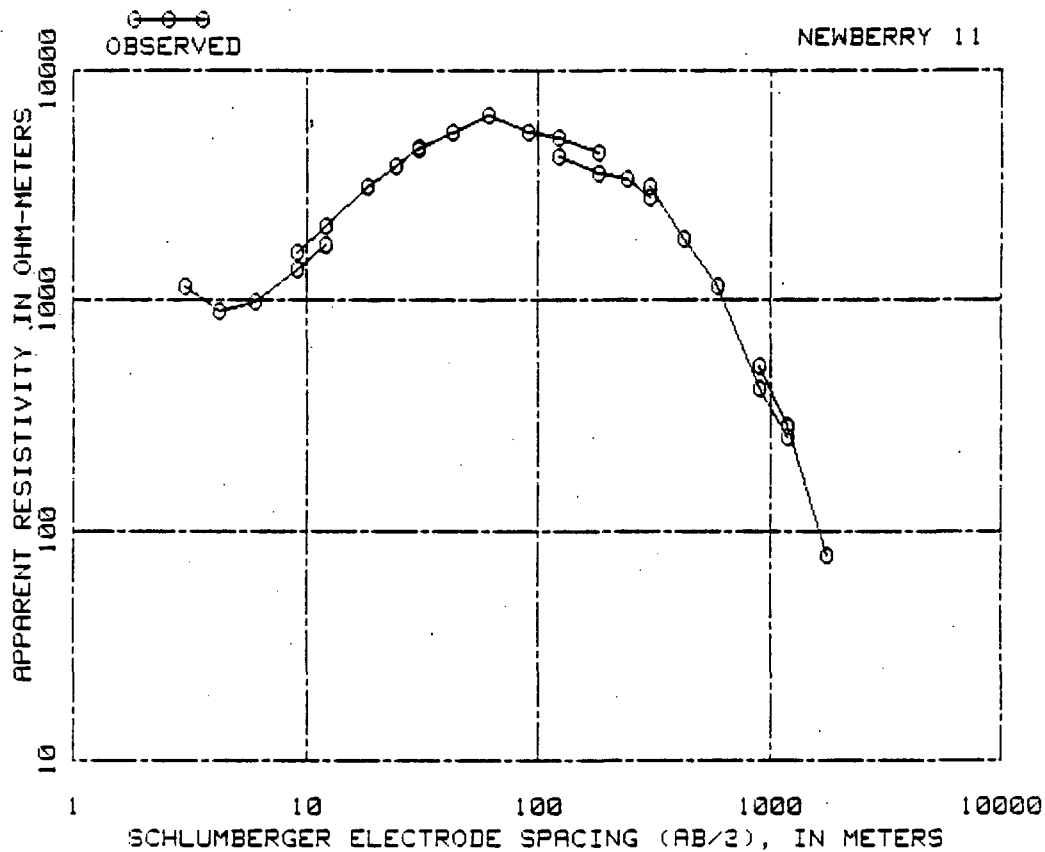




AB/2 IN METERS	OBSERVED RESISTIVITY IN OHM-METERS	AB/2 IN METERS	OBSERVED RESISTIVITY IN OHM-METERS
3.05	8780.00	91.44	620.00
4.27	3980.00	128.70	570.00
6.10	2260.00	181.97	478.00
9.14	1770.00	239.88	308.00
9.14	1680.00	296.88	244.00
12.19	1450.00	296.88	268.00
18.29	1200.00	416.05	181.00
24.38	970.00	594.97	128.00
30.48	845.00	875.08	85.00
42.67	660.00	1094.84	68.00
30.48	1000.00	875.08	106.00
42.67	790.00	1094.84	75.00
60.96	720.00	1448.41	57.00
91.44	640.00	2036.67	40.00

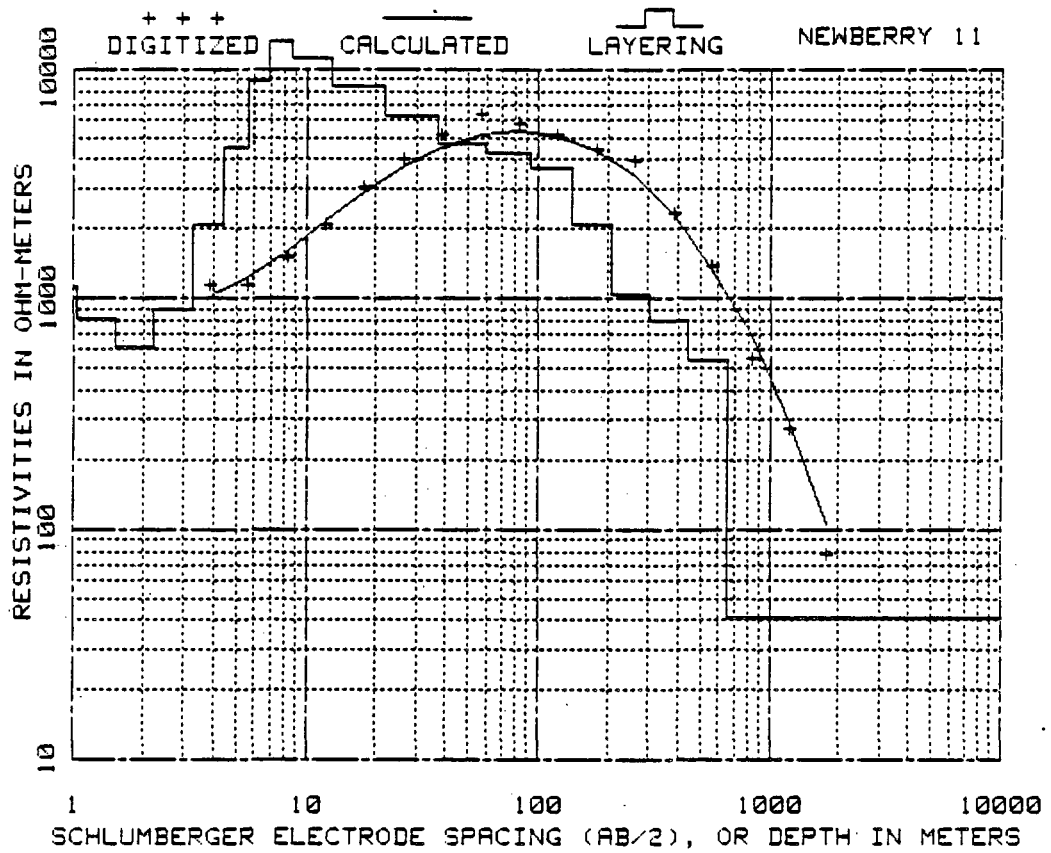


INTERPRETED DEPTH IN METERS	INTERPRETED RESISTIVITY IN OHM-METERS	INTERPRETED DEPTH IN METERS	INTERPRETED RESISTIVITY IN OHM-METERS
.33	14422.22	20.25	708.47
.48	14337.85	29.00	450.24
.71	14774.02	44.19	693.21
1.04	15112.94	65.19	1356.44
1.52	12142.13	98.07	766.12
2.16	5562.95	137.79	260.46
2.86	1650.62	189.18	115.03
4.04	1199.12	281.60	118.50
6.29	2650.42	431.79	144.36
9.59	2449.26	641.98	91.59
14.23	1497.62	896.51	35.25
		1000895.51	26.11

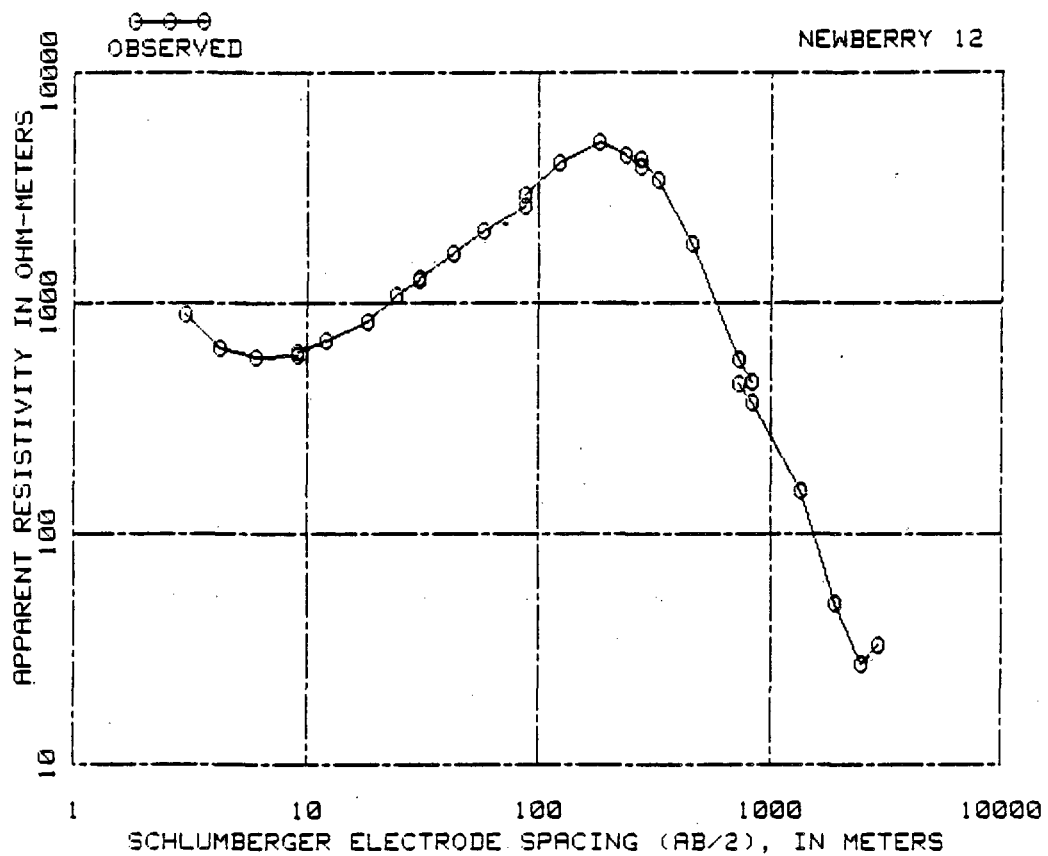


AB/2 IN METERS	OBSERVED RESISTIVITY IN OHM-METERS	AB/2 IN METERS	OBSERVED RESISTIVITY IN OHM-METERS
3.85	1150.00	121.92	5100.00
4.27	900.00	182.88	4350.00
5.10	900.00	121.92	4200.00
9.14	1350.00	182.88	3550.00
12.19	1720.00	242.01	3364.00
9.14	1600.00	302.06	2770.00
12.19	2100.00	302.06	3079.00
18.29	3000.00	422.15	1818.00
24.38	3800.00	595.58	1137.00
30.48	4600.00	898.25	416.00
30.48	4550.00	1195.43	256.00
42.67	5350.00	898.25	521.00
60.96	6350.00	1195.43	286.00
91.44	5400.00	1787.96	78.00

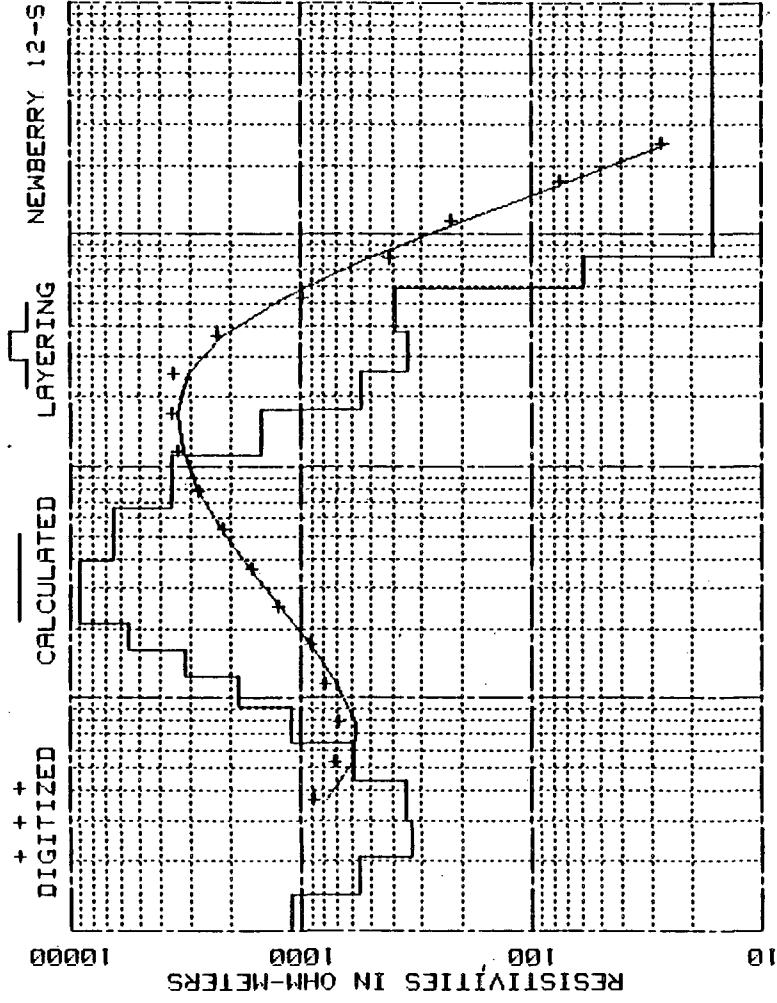




INTERPRETED DEPTH IN METERS	INTERPRETED RESISTIVITY IN OHM-METERS	INTERPRETED DEPTH IN METERS	INTERPRETED RESISTIVITY IN OHM-METERS
.22	1034.63	8.75	13297.78
.33	1021.98	12.92	11198.80
.48	1071.10	21.77	8406.87
.70	1159.34	36.85	6170.31
1.03	1117.14	59.28	4693.02
1.51	814.44	91.94	4275.32
2.21	621.98	139.91	3703.04
3.24	398.85	207.69	2189.63
4.42	2876.83	301.43	1048.29
5.61	4538.71	443.46	799.57
6.92	8834.58	651.75	544.83
		1000650.75	41.06

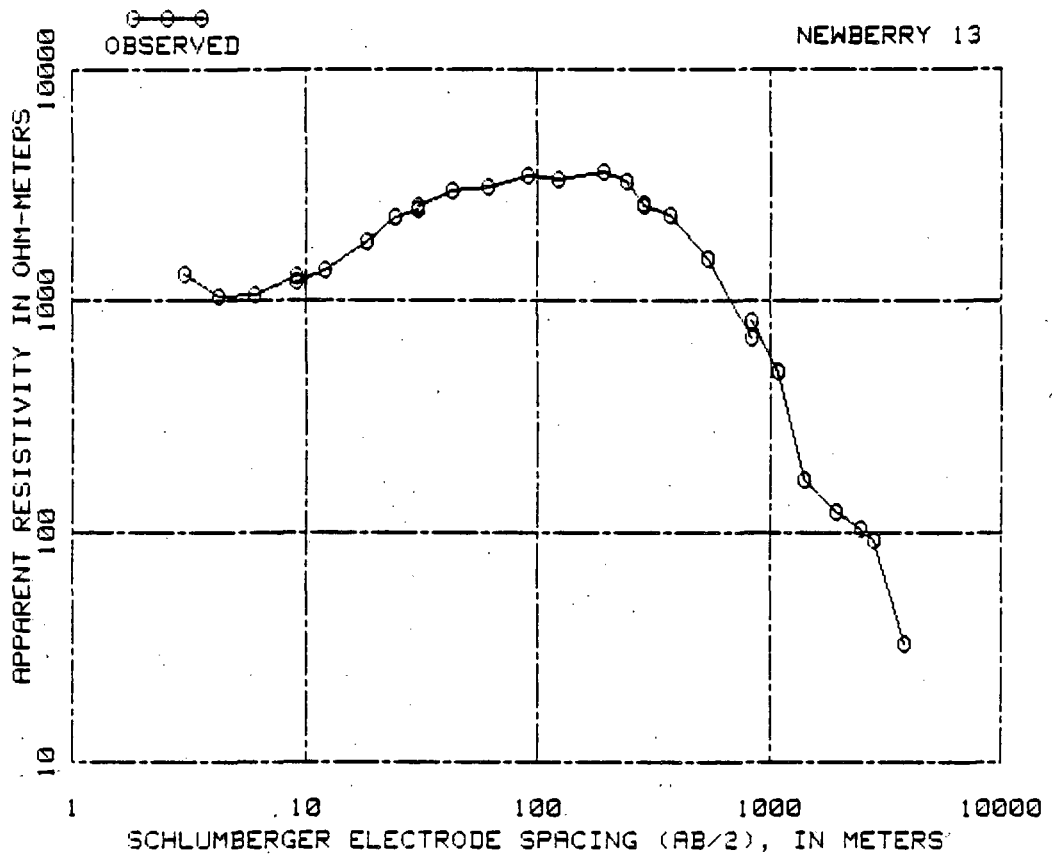


AB/2 IN METERS	OBSERVED RESISTIVITY IN OHM-METERS	AB/2 IN METERS	OBSERVED RESISTIVITY IN OHM-METERS
3.05	900.00	121.92	4037.00
4.27	645.00	183.79	4941.00
6.10	500.00	235.61	4361.00
9.14	590.00	277.67	3868.00
9.14	620.00	277.67	4208.00
12.19	695.00	327.96	3391.00
18.29	840.00	459.94	1783.00
24.38	1075.00	732.43	576.00
30.48	1250.00	843.69	455.00
30.48	1280.00	732.13	445.00
42.67	1650.00	843.69	372.00
58.52	2068.00	1357.58	153.00
87.78	2609.00	1924.51	50.00
87.78	2931.00	2491.74	27.00
		2970.28	33.00

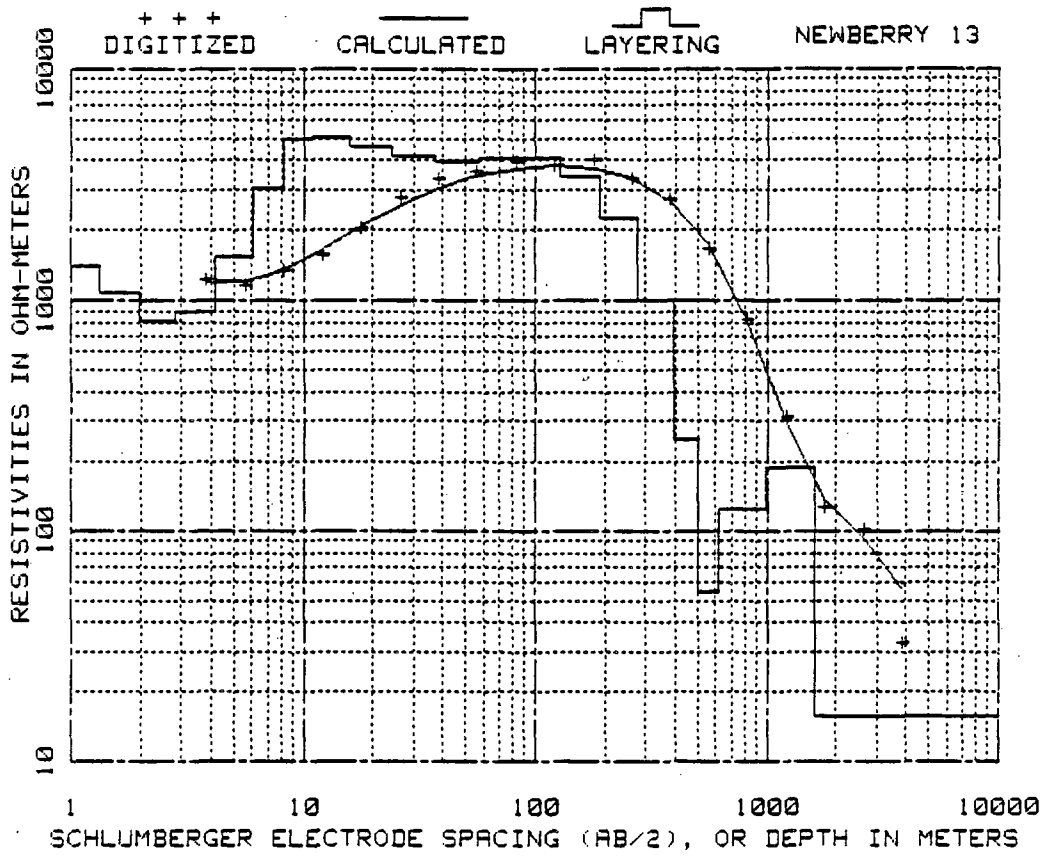


1 10 100 1000 10000  
SCHLUMBERGER ELECTRODE SPACING (AB/2), OR DEPTH IN METERS

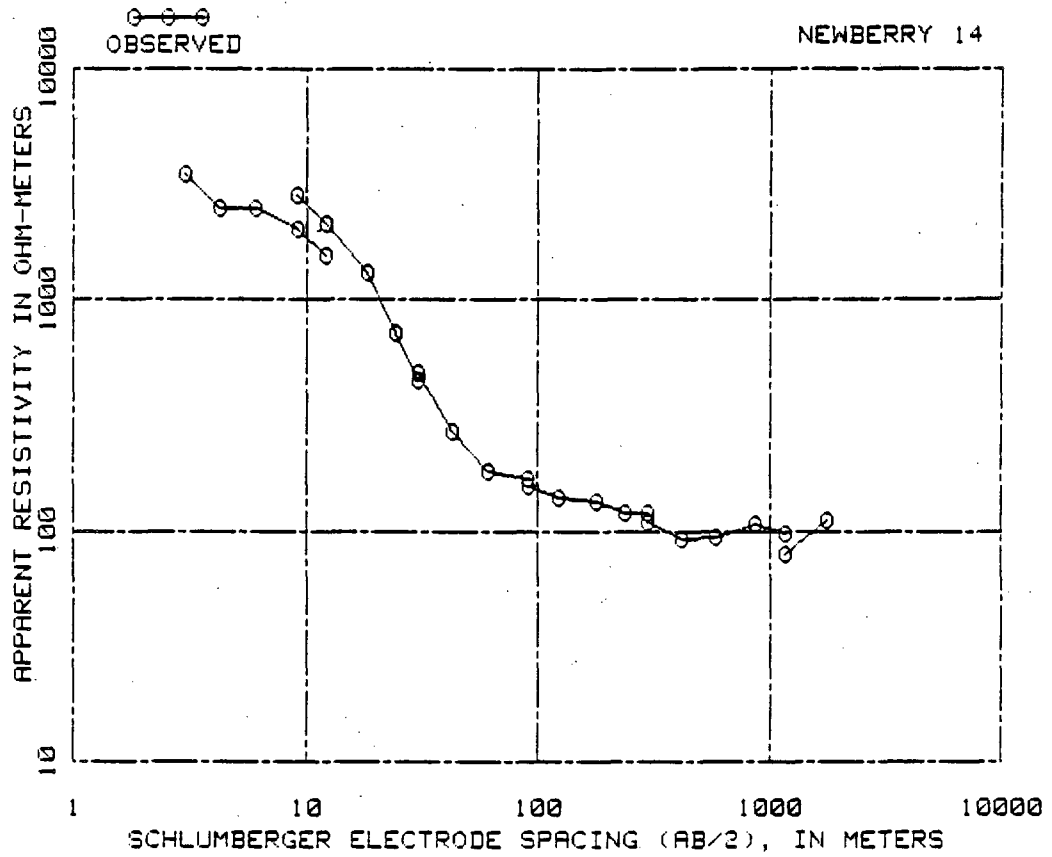
INTERPRETED DEPTH IN METERS	INTERPRETED RESISTIVITY IN OHM-METERS	INTERPRETED DEPTH IN METERS	INTERPRETED RESISTIVITY IN OHM-METERS
.21	1485.79	16.29	3149.66
.31	1427.79	21.01	5608.98
.45	1454.96	27.19	8976.98
.67	1569.82	39.26	9988.15
.98	1569.14	65.98	6428.37
1.43	1105.44	111.67	3577.47
2.07	563.32	174.47	1493.44
2.97	331.12	256.67	534.96
4.38	352.54	382.85	341.42
6.49	595.98	587.29	392.41
9.11	1103.71	800.54	59.24
12.32	1981.88	1000799.54	16.27



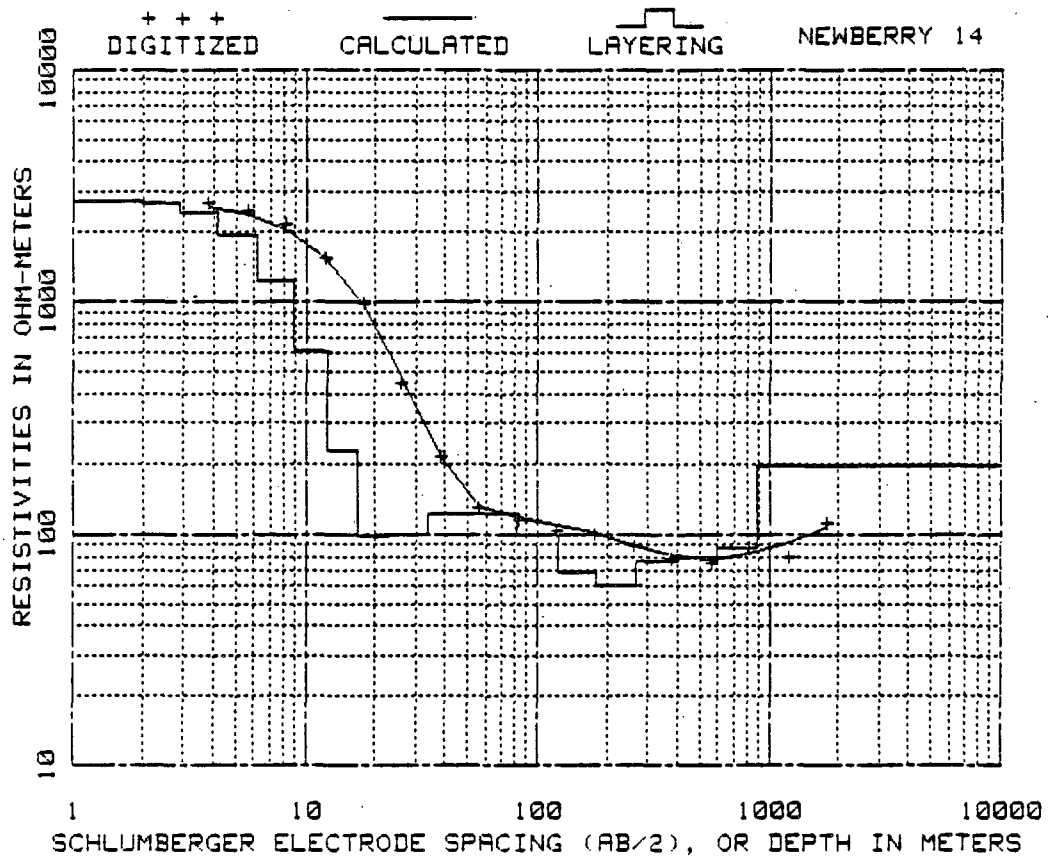
AB/2 IN METERS	OBSERVED RESISTIVITY IN OHM-METERS	AB/2 IN METERS	OBSERVED RESISTIVITY IN OHM-METERS
3.05	1300.00	121.92	3350.00
4.27	1050.00	191.41	3579.00
6.10	1070.00	240.49	3265.00
9.14	1275.00	285.90	2634.00
9.14	1210.00	285.90	2559.00
12.19	1350.00	375.51	2332.00
18.29	1800.00	541.63	1524.00
24.38	2280.00	837.29	691.00
30.48	2500.00	837.29	810.00
30.48	2550.00	1086.61	480.00
42.67	3000.00	1417.32	170.00
60.96	3125.00	1955.60	123.00
91.44	3450.00	2505.15	104.00
91.44	3500.00	2816.05	93.00
		3831.95	33.00



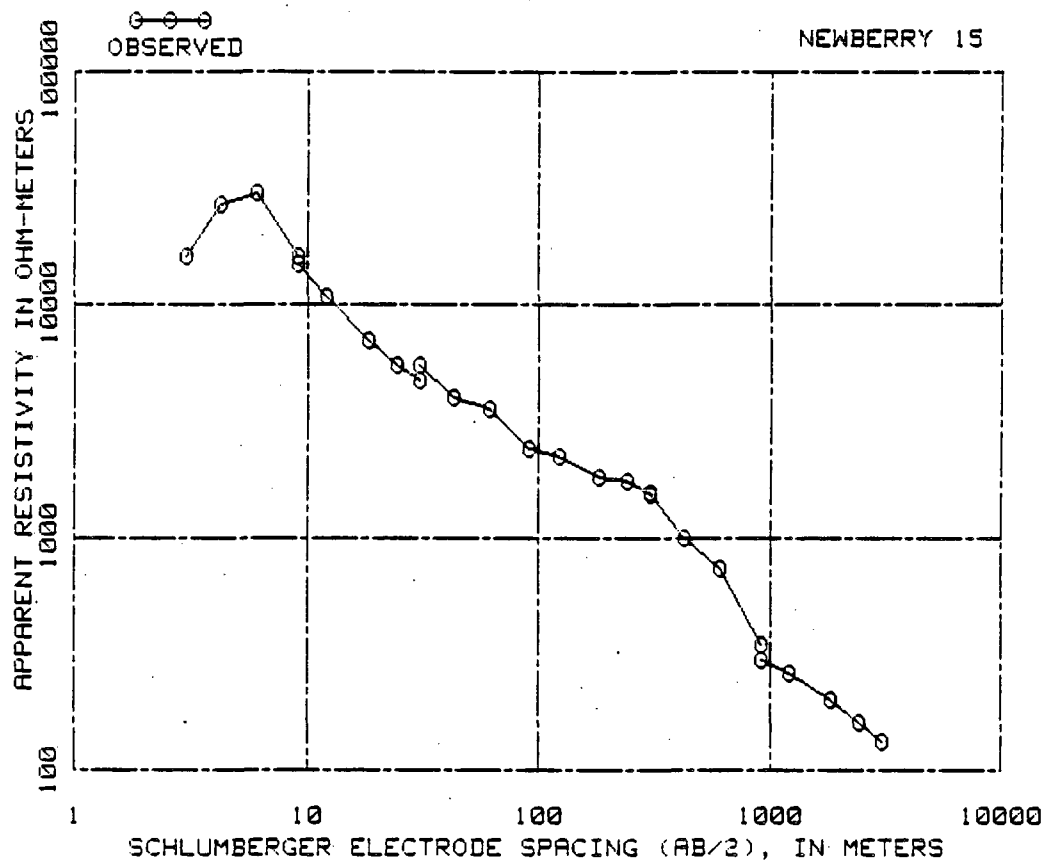
INTERPRETED DEPTH IN METERS	INTERPRETED RESISTIVITY IN OHM-METERS	INTERPRETED DEPTH IN METERS	INTERPRETED RESISTIVITY IN OHM-METERS
.29	1503.68	23.97	4565.09
.42	1514.21	37.02	4171.68
.62	1534.23	56.60	3968.99
.91	1537.29	85.39	4079.56
1.33	1410.12	127.77	4102.40
1.95	1080.63	190.03	3433.59
2.84	818.75	278.53	2251.55
4.17	901.58	391.98	1004.70
6.05	1543.99	506.20	252.30
8.21	3018.20	617.54	54.61
10.94	4949.15	989.80	124.15
15.71	5046.89	1510.13	190.30
		1001609.13	15.68



AB/2 IN METERS	OBSERVED RESISTIVITY IN OHM-METERS	AB/2 IN METERS	OBSERVED RESISTIVITY IN OHM-METERS
3.05	3450.00	91.44	170.00
4.27	2500.00	91.44	155.00
6.10	2490.00	121.92	140.00
9.14	2000.00	179.22	135.00
12.19	1550.00	237.44	120.00
9.14	2000.00	299.92	119.00
12.19	2150.00	299.92	109.00
18.29	1300.00	420.01	93.00
24.38	710.00	586.13	94.00
30.48	450.00	869.29	108.00
30.48	400.00	1165.56	98.00
42.67	270.00	1165.56	79.00
60.96	180.00	1771.50	111.00

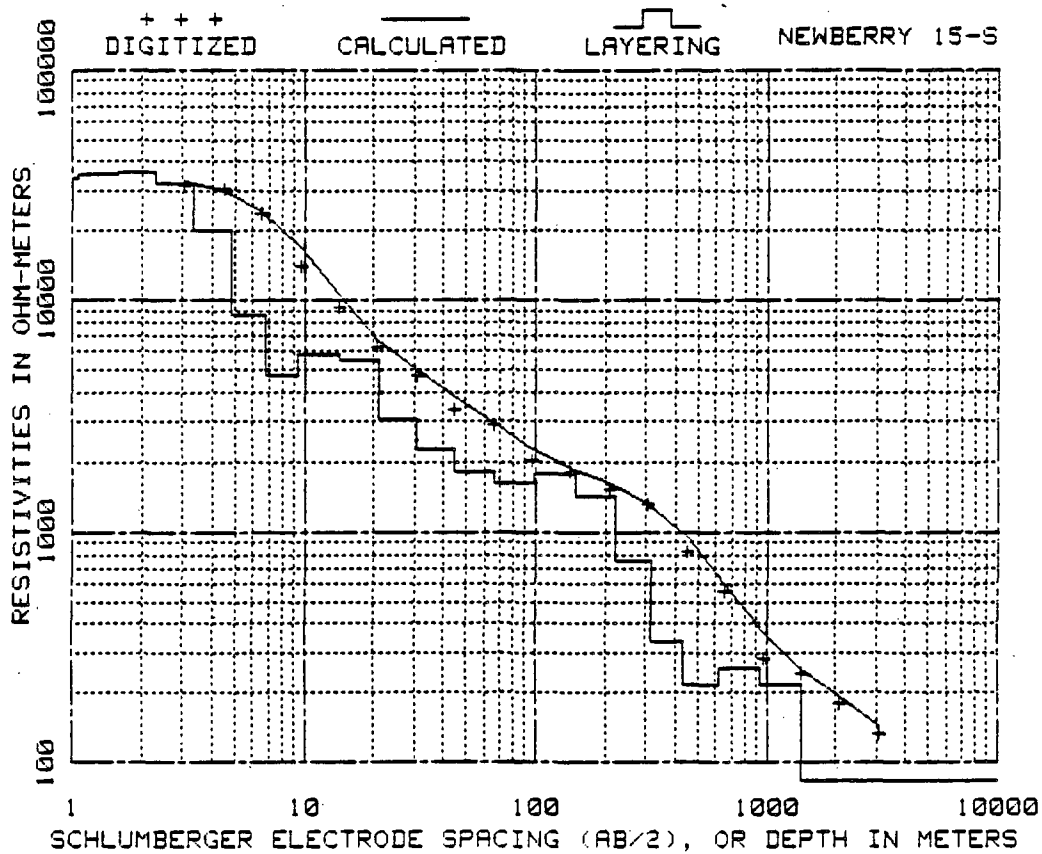


INTERPRETED DEPTH IN METERS	INTERPRETED RESISTIVITY IN OHM-METERS	INTERPRETED DEPTH IN METERS	INTERPRETED RESISTIVITY IN OHM-METERS
.29	2716.14	16.76	229.71
.42	2714.63	22.52	97.85
.62	2713.88	33.66	99.35
.91	2715.77	52.54	122.36
1.33	2720.69	80.89	121.68
1.95	2717.80	122.11	99.14
2.86	2663.67	180.55	67.91
4.20	2448.12	268.00	60.20
6.14	1932.96	401.50	75.79
8.86	1227.16	597.97	79.10
12.44	611.43	886.10	86.57
		1000885.10	197.31

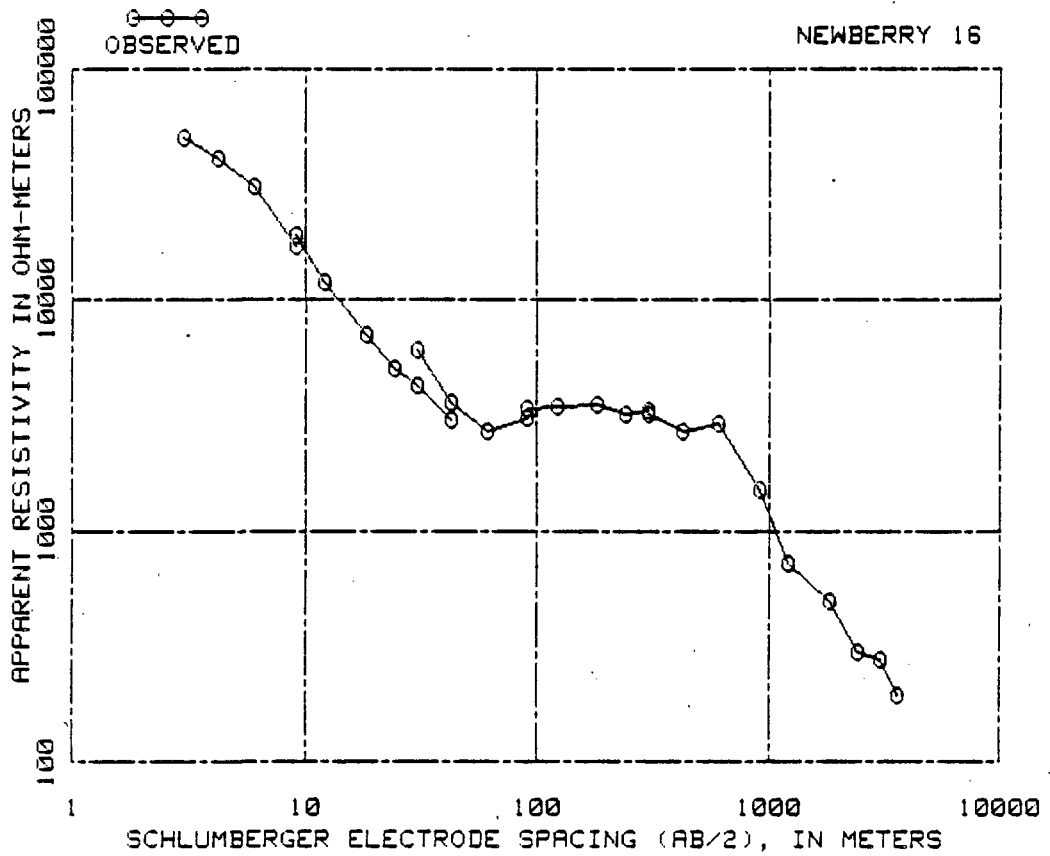


AB/2 IN METERS	OBSERVED RESISTIVITY IN OHM-METERS	AB/2 IN METERS	OBSERVED RESISTIVITY IN OHM-METERS
3.05	16200.00	91.44	2400.00
4.27	26800.00	121.92	2250.00
6.10	30000.00	182.80	1825.00
9.14	16000.00	243.84	1750.00
9.14	14800.00	304.80	1540.00
12.19	10800.00	304.80	1550.00
18.29	7000.00	426.72	1000.00
24.38	5500.00	609.60	740.00
30.48	4700.00	914.40	350.00
30.48	5500.00	914.40	300.00
42.67	4000.00	1219.20	260.00
60.96	3600.00	1828.80	200.00
91.44	2400.00	2438.40	160.00
		3048.00	133.00

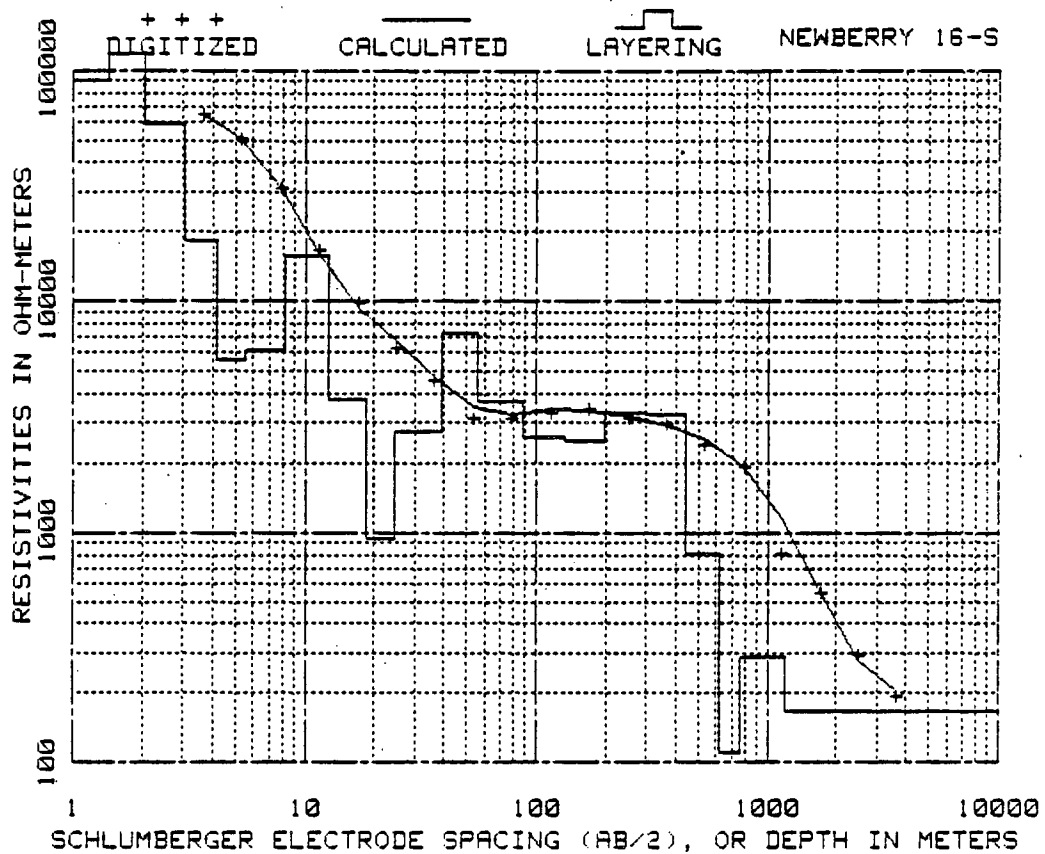




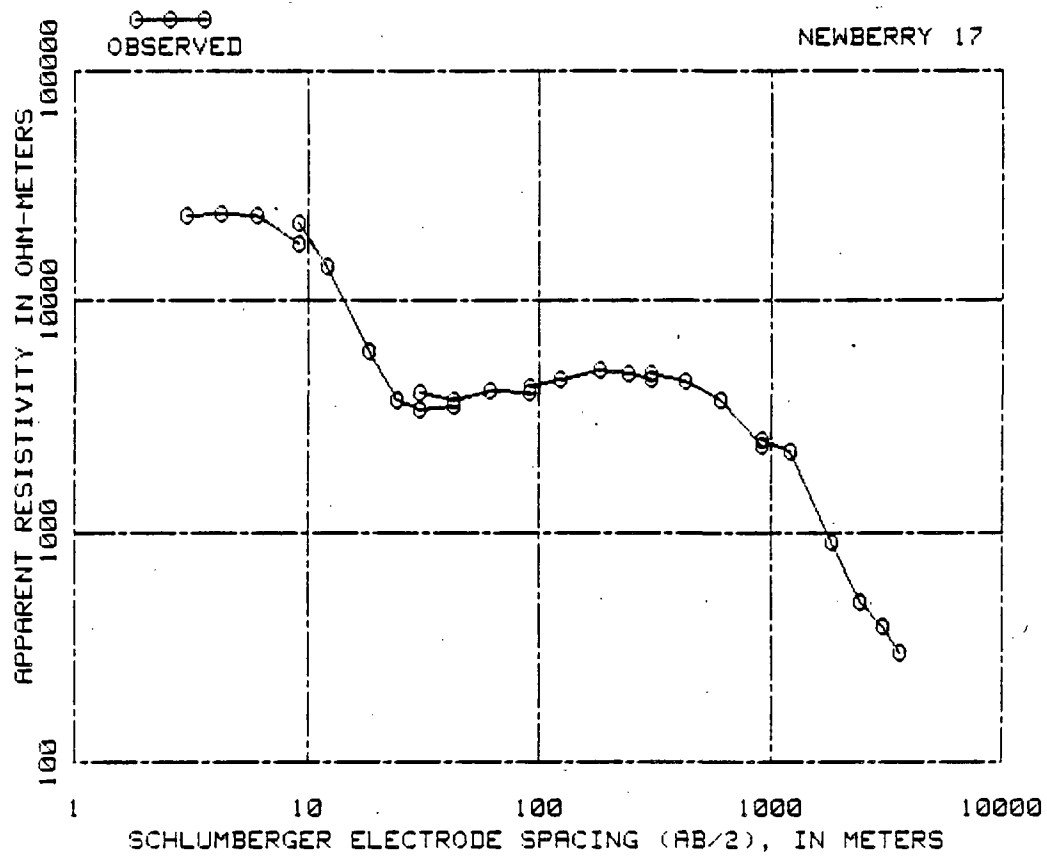
INTERPRETED DEPTH IN METERS	INTERPRETED RESISTIVITY IN OHM-METERS	INTERPRETED DEPTH IN METERS	INTERPRETED RESISTIVITY IN OHM-METERS
.23	34488.84	21.18	5584.81
.34	34395.33	30.78	3861.90
.49	34315.36	44.98	2285.26
.72	34287.83	66.19	1815.46
1.06	34388.11	98.24	1688.63
1.56	35256.77	147.29	1797.85
2.28	36387.46	218.36	1438.60
3.35	32445.85	313.61	745.16
4.86	28825.83	435.33	333.58
6.78	8719.28	619.01	215.36
9.44	4729.45	938.48	259.42
14.12	5886.73	1411.68	218.24
		1001410.60	83.58



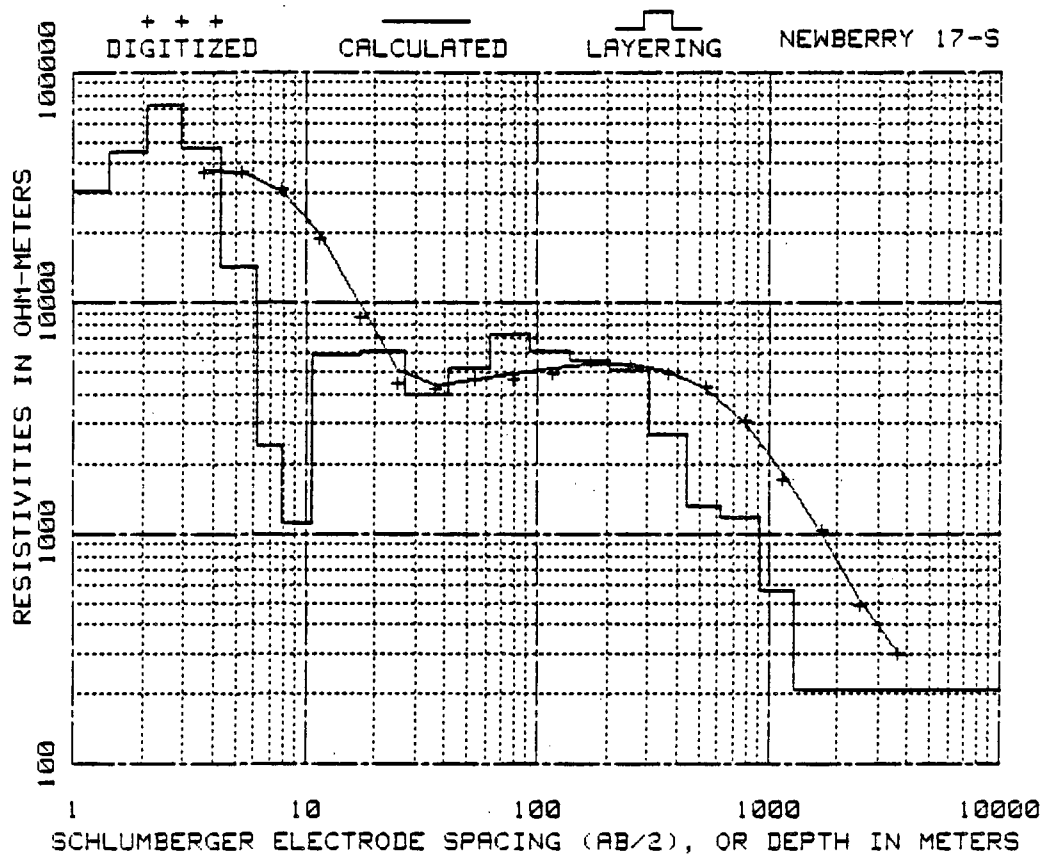
AB/2 IN METERS	OBSERVED RESISTIVITY IN OHM-METERS	AB/2 IN METERS	OBSERVED RESISTIVITY IN OHM-METERS
3.85	51000.00	91.44	3400.00
4.27	41500.00	121.92	3440.00
6.10	31000.00	182.88	3500.00
9.14	17000.00	243.84	3200.00
9.14	19000.00	304.80	3300.00
12.19	12000.00	304.80	3200.00
18.29	7000.00	426.72	2700.00
24.38	5000.00	609.60	2900.00
30.48	4250.00	914.40	1500.00
42.67	3000.00	914.40	1500.00
30.48	6000.00	1219.20	725.00
42.67	3600.00	1828.80	500.00
60.96	2700.00	2438.40	300.00
91.44	3100.00	3048.00	278.00
		3657.60	194.00



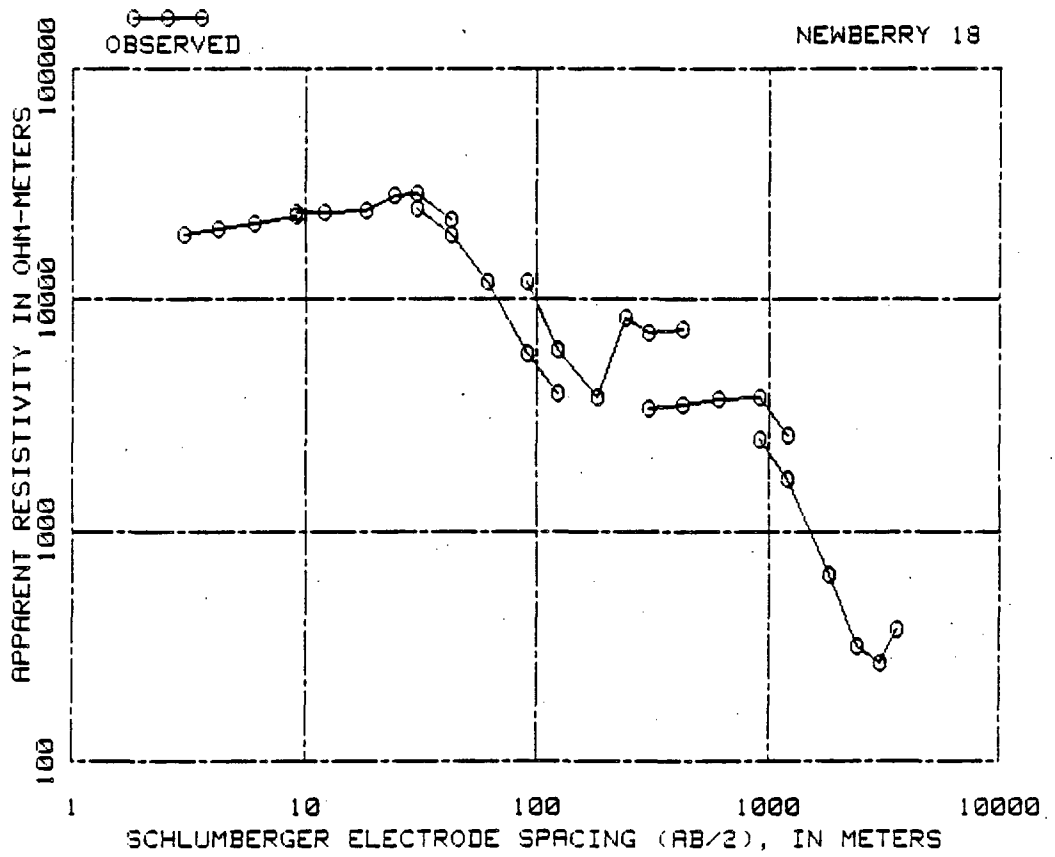
INTERPRETED DEPTH IN METERS	INTERPRETED RESISTIVITY IN OHM-METERS	INTERPRETED DEPTH IN METERS	INTERPRETED RESISTIVITY IN OHM-METERS
.21	64741.59	18.43	3788.67
.31	66219.35	24.50	938.82
.45	67026.74	38.92	2761.78
.67	61097.43	55.84	7302.57
.98	60864.37	87.02	3698.37
1.42	91331.97	131.94	2586.32
2.03	117798.06	198.46	2487.56
3.01	58902.91	296.91	3330.28
4.18	18324.11	441.77	3227.93
5.56	5621.55	615.25	806.77
8.27	6108.51	755.92	109.35
12.77	15642.24	1186.67	285.90
		1001185.67	166.76



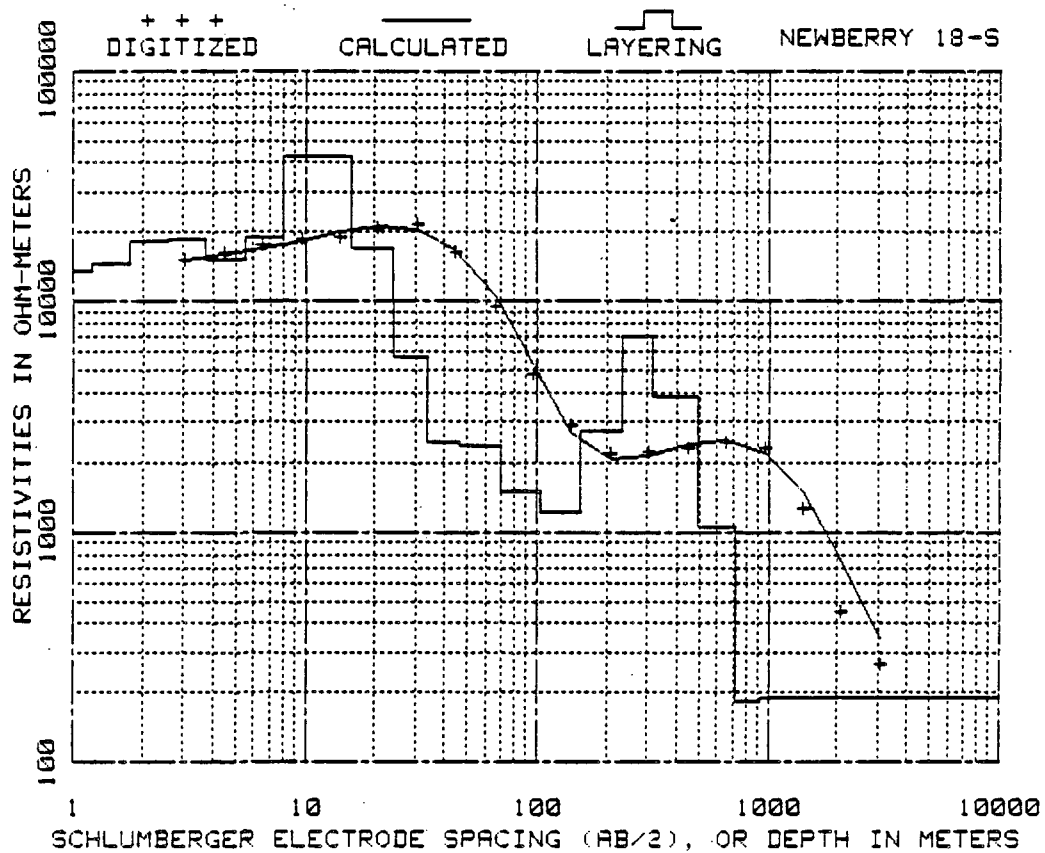
AB/2 IN METERS	OBSERVED RESISTIVITY IN OHM-METERS	AB/2 IN METERS	OBSERVED RESISTIVITY IN OHM-METERS
3.05	23500.00	91.44	4200.00
4.27	24000.00	121.92	4550.00
6.10	23600.00	182.98	5000.00
9.14	17500.00	243.84	4800.00
9.14	21800.00	304.80	4600.00
12.19	14000.00	304.80	4800.00
18.29	6000.00	426.72	4500.00
24.38	3700.00	609.60	3700.00
30.48	3400.00	914.40	2350.00
42.67	3500.00	914.40	2500.00
30.48	4000.00	1219.20	2250.00
42.67	3700.00	1828.80	900.00
60.96	4100.00	2438.40	500.00
91.44	4000.00	3048.00	390.00
		3657.60	300.00



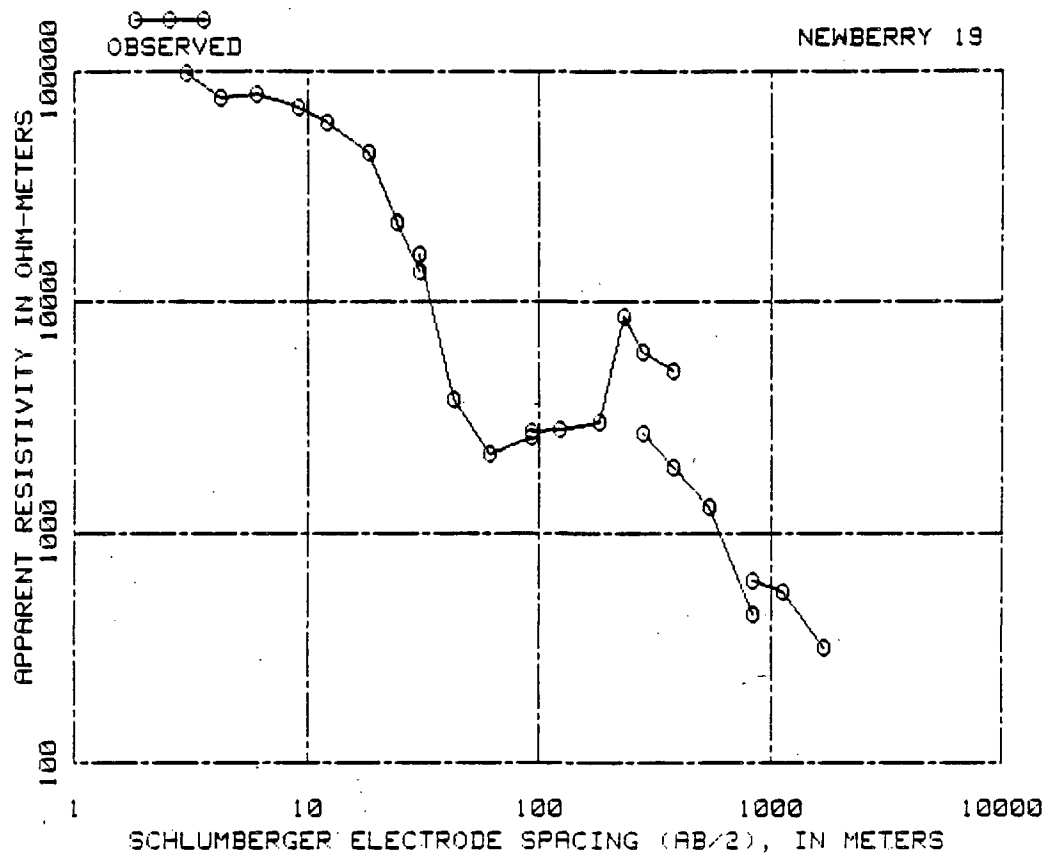
INTERPRETED DEPTH IN METERS	INTERPRETED RESISTIVITY IN OHM-METERS	INTERPRETED DEPTH IN METERS	INTERPRETED RESISTIVITY IN OHM-METERS
.21	33399.50	17.00	5924.39
.31	32992.74	26.71	6199.01
.45	34162.80	41.09	3996.90
.67	34647.37	62.28	5248.35
.98	31494.31	91.89	7254.29
1.44	30423.21	137.53	6144.44
2.08	44791.02	204.78	5631.37
2.92	71947.53	303.31	5098.46
4.37	46634.99	440.01	2693.02
6.21	14260.02	623.22	1325.26
7.89	2422.71	912.27	1186.54
10.59	1108.26	1297.26	567.95
		1001296.26	209.91



AB/2 IN METERS	OBSERVED RESISTIVITY IN OHM-METERS	AB/2 IN METERS	OBSERVED RESISTIVITY IN OHM-METERS
3.05	18900.00	121.92	6000.00
4.27	20000.00	182.88	3800.00
6.10	21250.00	243.84	8360.00
9.14	23000.00	304.80	7200.00
9.14	24000.00	426.72	7500.00
12.19	23950.00	304.80	3400.00
18.29	24300.00	426.72	3500.00
24.38	28000.00	609.60	3700.00
30.48	29000.00	914.40	3750.00
42.67	22000.00	1219.20	2600.00
30.48	25000.00	914.40	2500.00
42.67	19000.00	1219.20	1700.00
60.96	12000.00	1828.80	650.00
91.44	5800.00	2438.40	317.00
121.92	3950.00	3048.00	265.00
91.44	12000.00	3657.60	378.00

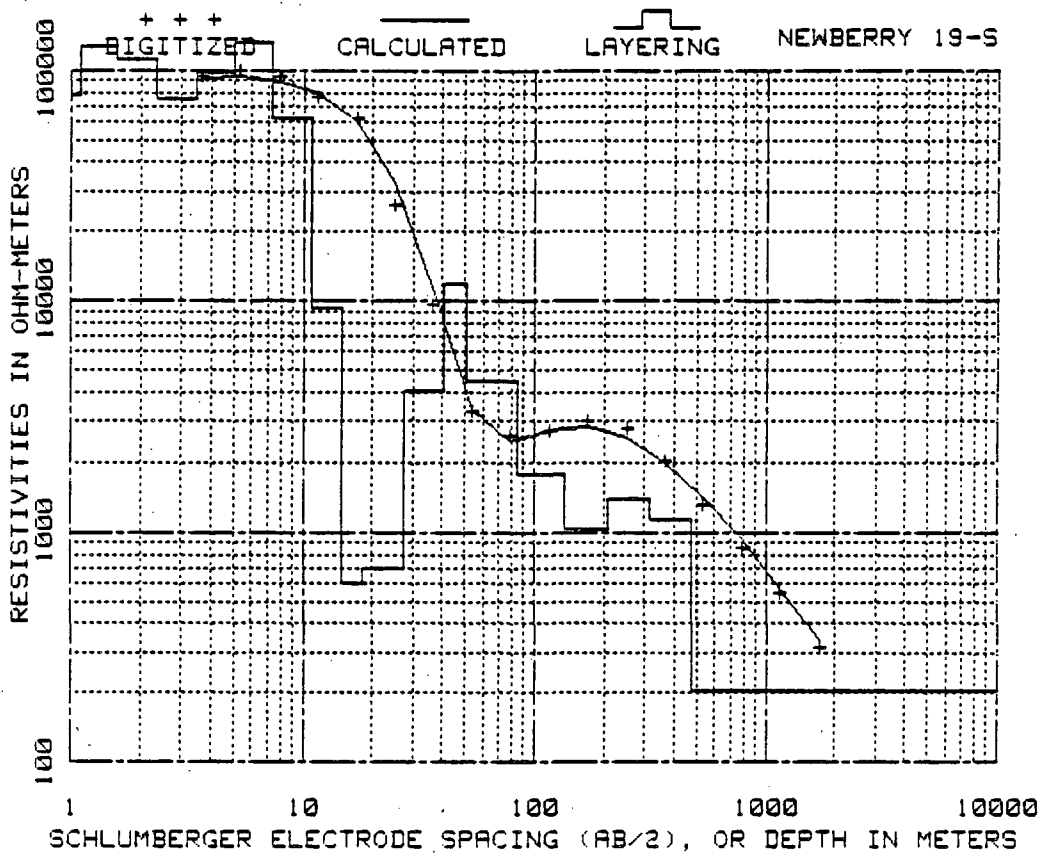


INTERPRETED DEPTH IN METERS	INTERPRETED RESISTIVITY IN OHM-METERS	INTERPRETED DEPTH IN METERS	INTERPRETED RESISTIVITY IN OHM-METERS
.18	14068.13	15.80	42427.81
.26	13976.51	23.85	17896.06
.38	14891.76	33.65	5699.64
.56	14271.37	46.78	2439.23
.82	14016.83	69.73	2372.63
1.20	13462.42	103.12	1514.37
1.76	14579.62	154.36	1223.85
2.56	18172.98	234.93	2751.76
3.75	18749.68	315.90	7854.45
5.52	15334.72	489.99	3887.11
8.10	18948.13	714.60	1047.69
10.98	42626.45	921.48	183.27
		1000920.48	191.71

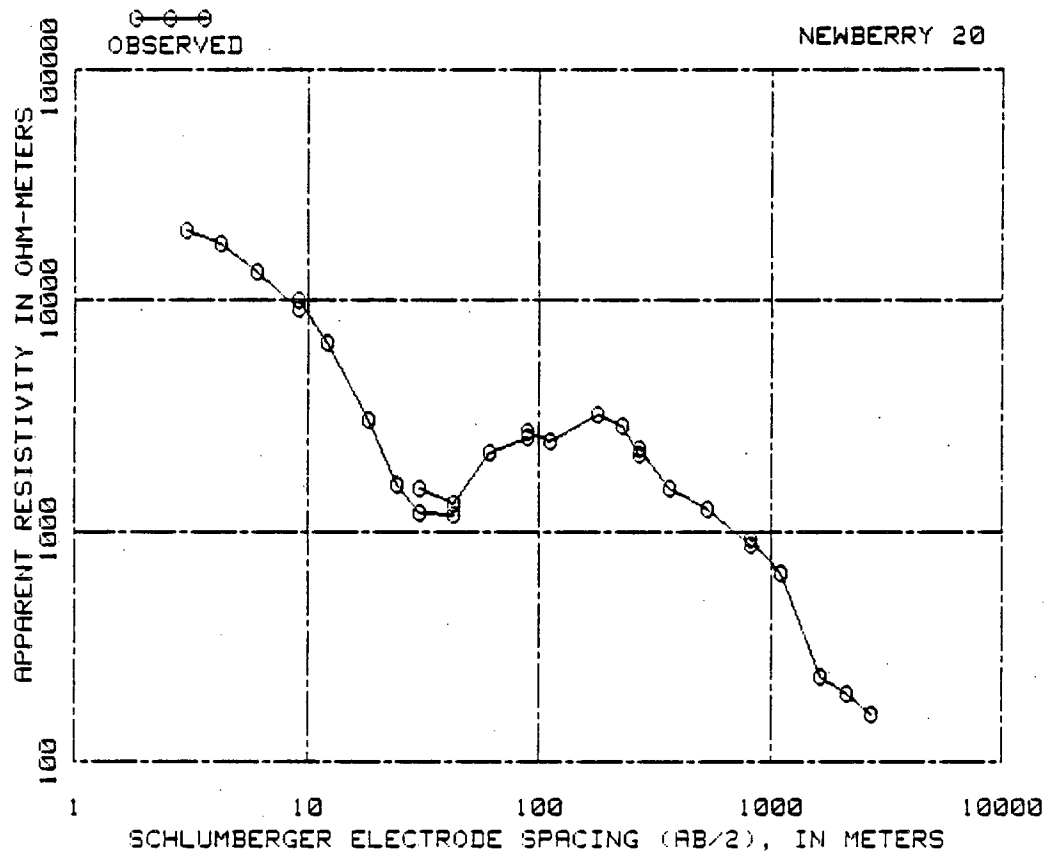


AB/2 IN METERS	OBSERVED RESISTIVITY IN OHM-METERS	AB/2 IN METERS	OBSERVED RESISTIVITY IN OHM-METERS
3.05	98000.00	93.57	2721.00
4.27	77000.00	123.14	2781.00
6.10	30000.00	184.10	3034.00
9.14	70000.00	231.95	8627.00
9.14	70000.00	281.94	5998.00
12.19	60000.00	380.70	4967.00
18.29	44000.00	281.94	2695.00
24.38	22000.00	380.70	1915.00
30.48	13500.00	542.24	1305.00
30.48	16000.00	835.15	445.00
42.67	3800.00	835.15	626.00
60.96	2200.00	1136.29	558.00
93.57	2579.00	1695.60	319.00

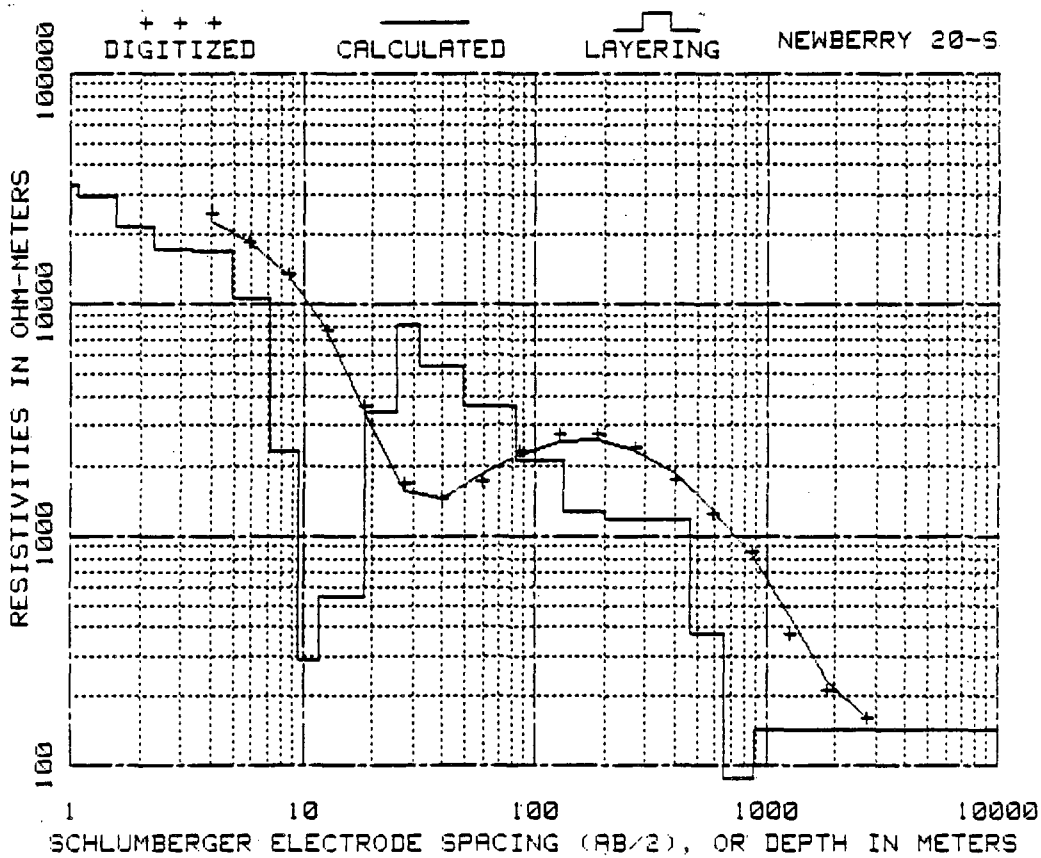




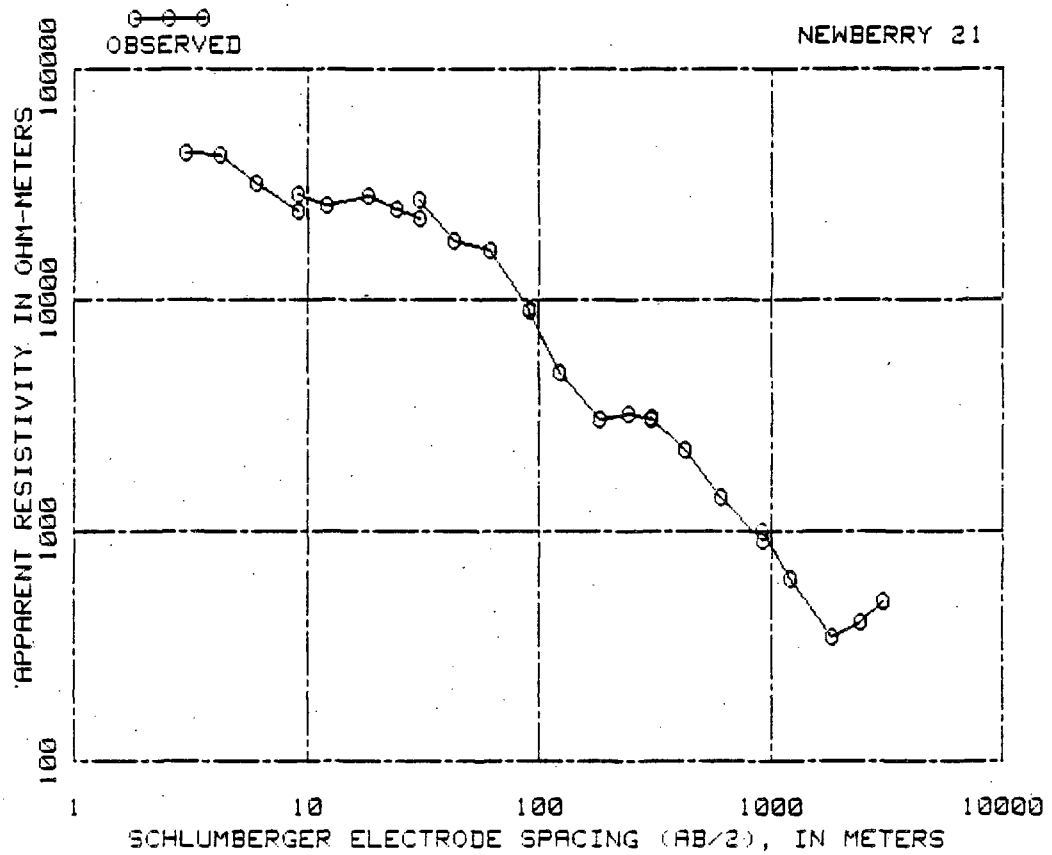
INTERPRETED DEPTH IN METERS	INTERPRETED RESISTIVITY IN OHM-METERS	INTERPRETED DEPTH IN METERS	INTERPRETED RESISTIVITY IN OHM-METERS
.16	80983.82	10.82	62273.88
.24	82316.62	14.66	9277.80
.35	93336.18	17.98	601.27
.51	85708.00	27.21	691.52
.75	67852.16	40.32	4060.63
1.10	78228.39	50.79	11903.71
1.58	127868.82	84.74	4436.66
2.33	111534.94	134.79	1775.16
3.44	75661.53	206.20	1039.60
5.06	98318.42	316.94	1406.38
7.36	132667.84	478.59	1130.99
		1000477.59	203.39



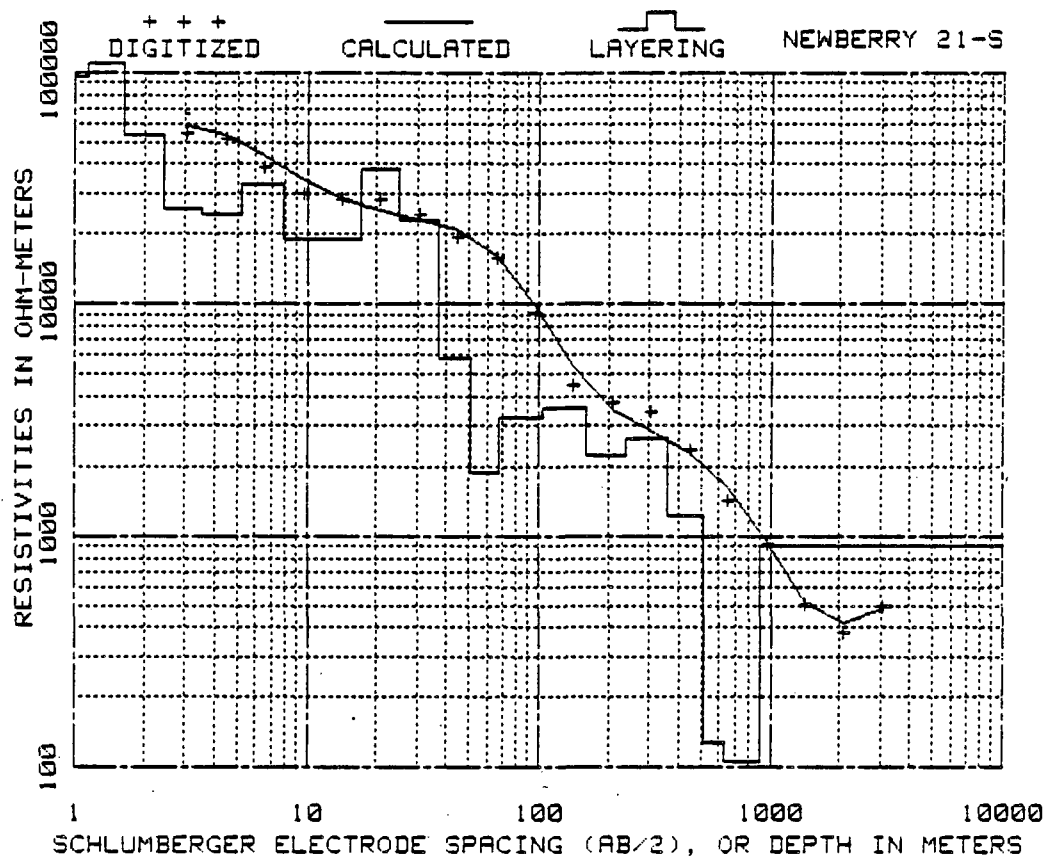
AB/2 IN METERS	OBSERVED RESISTIVITY IN OHM-METERS	AB/2 IN METERS	OBSERVED RESISTIVITY IN OHM-METERS
3.05	20200.00	88.70	2679.00
4.27	17500.00	111.25	2458.00
6.10	13200.00	179.83	3205.00
9.14	9200.00	228.90	2829.00
9.14	10000.00	270.97	2171.00
12.19	6500.00	270.97	2282.00
18.29	3000.00	366.06	1521.00
24.38	1600.00	535.23	1240.00
30.48	1200.00	822.05	872.00
42.67	1175.00	822.05	929.00
30.48	1540.00	1118.92	654.00
42.67	1325.00	1650.49	234.00
61.87	2195.00	2125.98	198.00
88.70	2524.00	2725.22	162.00



INTERPRETED DEPTH IN METERS	INTERPRETED RESISTIVITY IN OHM-METERS	INTERPRETED DEPTH IN METERS	INTERPRETED RESISTIVITY IN OHM-METERS
.23	30952.03	19.25	541.16
.34	30563.14	25.36	3419.90
.50	30476.69	31.95	8139.36
.73	31445.45	49.14	5415.32
1.07	32797.42	82.20	3655.99
1.57	29569.75	131.74	2097.05
2.30	21631.53	201.60	1262.91
3.36	17296.75	306.66	1177.43
4.93	16850.84	463.44	1188.35
7.15	10695.46	659.86	378.04
9.60	2308.09	878.87	97.71
11.76	286.09	1000877.87	142.97



AB/2 IN METERS	OBSERVED RESISTIVITY IN OHM-METERS	AB/2 IN METERS	OBSERVED RESISTIVITY IN OHM-METERS
3.05	43500.00	91.44	3900.00
4.27	43000.00	121.92	4800.00
6.10	32500.00	182.88	3000.00
9.14	24500.00	243.84	3200.00
9.14	28000.00	304.80	3000.00
12.19	25500.00	304.80	3100.00
18.29	28000.00	426.72	2250.00
24.38	25000.00	609.60	1400.00
30.48	22700.00	914.40	900.00
30.48	27400.00	914.40	1000.00
42.67	17900.00	1219.20	620.00
60.96	16500.00	1828.80	350.00
91.44	9200.00	2438.40	400.00
		3048.00	500.00



INTERPRETED DEPTH IN METERS	INTERPRETED RESISTIVITY IN OHM-METERS	INTERPRETED DEPTH IN METERS	INTERPRETED RESISTIVITY IN OHM-METERS
.18	46682.01	16.99	19031.63
.26	49037.91	24.69	38429.86
.38	45011.97	36.70	22808.75
.56	40410.61	50.59	5859.88
.81	50636.00	67.40	1886.10
1.13	96760.21	103.58	3235.07
1.62	108840.93	158.86	3544.59
2.44	53299.27	236.74	2232.90
3.54	25667.00	356.48	2650.88
5.23	24375.24	516.58	1219.00
7.83	32990.56	632.63	127.73
11.49	19001.27	894.36	105.99
		1000893.36	908.14

UNITED STATES DEPARTMENT OF THE INTERIOR

GEOLOGICAL SURVEY

Time-Domain Electromagnetic Soundings of Newberry Volcano,  
Deschutes County, Oregon

by

David V. Fitterman

Open-File Report 83-832

4 November 1983

This report is preliminary and has not been reviewed for conformity with U.S. Geological Survey editorial standards. Any use of trade names is for descriptive purposes only and does not imply endorsement by the U.S. Geological Survey.

## Introduction

A time-domain electromagnetic (TDEM) survey of Newberry Volcano, Oregon was carried out during July 1983 as part of a research project funded by Department of Energy in conjunction with the USGS Geothermal Program. Nineteen TDEM soundings were made using a central induction loop configuration at locations shown in Figure 1. This report describes the results of layered earth inversions.

Newberry Volcano is a large Quaternary volcano located about 40 km south of Bend, Oregon (MacLeod and Sammel, 1982). The flanks of the volcano are composed of basaltic flows, andesitic to rhyolitic tuffs, and alluvial sediments. The summit caldera, which contains Paulina and East Lakes, is interpreted as being a collapse feature formed after the eruption of large volumes of tephra.

In 1981 the USGS completed a 932 m deep drill hole in the caldera; temperatures as high as 265°C were encountered (Sammel, 1981; MacLeod and Sammel, 1982). The demonstrated occurrence of such high-temperature water has caused an increase in geothermal exploration activity in the vicinity of Newberry Volcano.

## Field Procedure and Equipment

TDEM measurements were made using a SIROTEM II system (Buselli and O'Neill, 1977). The SIROTEM system injects a bipolar, square-wave current into a transmitter loop. When the current is turned off, the voltage induced in a receiving coil located at the center of the transmitter loop is recorded. The SIROTEM system records and stacks the transients from a large number of current turn-offs, and reports the averaged voltage-current ratios.

Square transmitter loops 457 m, 229 m, and 152 m on a side were used. The receiver coil was an eight turn 38 m x 38 m loop (receiver coil moment  $M_r = 11,613 \text{ turn-m}^2$ ) situated at the center of the transmitter loop. Four to six runs, consisting of 2,048 transients per run, were made at each site. The polarity of the receiver coil was reversed on alternate runs to reduce instrumental noise.

At several locations, an external transmitter built by the USGS was used to increase transmitter current to about 12 amperes, which is about three times the current delivered by the SIROTEM transmitter. The higher current made it possible to record the transient with an acceptable signal-to-noise ratio at later times, thereby gathering information from greater depths.

## Data Preparation

The recorded voltage-current ratios were converted to late stage apparent resistivity (Kaufmann and Keller, 1983, p. 457) using the formula

$$\rho = \frac{\mu_o}{4\pi t} \left( \frac{2\mu_o L^2 M_r}{5t V/I} \right)^{2/3}$$

where  $\mu_0$  is the free space permeability, L is the length of a side of the transmitter loop,  $M_r$  is the receiver loop moment, t is time since current shutoff, and V/I is the voltage-current ratio (all in SI units). Data from several runs were averaged and converted to apparent resistivity. Data from the first two SIROTEM channels were not used because they appeared to be noisy. Late-time data were rejected when the data appeared to be noisy and the apparent resistivity curves no longer behaved smoothly. Data obtained using the external transmitter were combined with data from the internal transmitter to obtain longer data records with less noise.

### Inversion of Soundings

Initial models for the data were obtained by curve matching using a catalog of two-layer models (Kaufmann and Keller, 1983). These models served as starting points for a non-linear least squares inversion by computer (Anderson, 1982). Best-fit two and three layer models were found for each sounding. If the three layer model did not provide a significantly better fit than the two-layer model, then the three-layer model was rejected.

### Results

Results of the inversions are presented in Figures 2 through 19. Figures 2a through 19a contain the output from the inversion program. This consists of the sounding title, the effective transmitter loop radius ( $A = \pi^{-1/2}L$ ), and a list of the model parameters held fixed. For all models the SHIFT parameter, which is a scaling factor, has been set to 1.0. The next line of the output specifies the type of convergence criteria which terminated the inversion. See Dennis et al. (1979) for a discussion of the convergence criteria.

The first table contains the observed (OBS.Y(I)) and calculated (CAL) apparent resistivities, and the residual (RES), i.e. the difference between the observed and calculated apparent resistivity. The residual is also expressed as a percentage of the calculated resistivity. The last column (X(I,1)) gives the time. The line following this table gives the RMS error of the fit.

The next table is the parameter correlation matrix. This provides a measure of the interdependence of the model parameter estimates. A high correlation between parameters indicates that only their ratio can be determined, while a high inverse correlation between parameters means that only their product can be resolved. Only the lower half of the symmetric correlation matrix is shown. The column of integers to the left gives the parameter number. It corresponds to the columns of integers in the following two tables. As an example, if we consider the second entry in the first column of any given correlation matrix, this will be the correlation between the second and first unconstrained model parameters.

The third table gives the model parameter estimate (PARM\_SOL.), the standard deviation in the parameter estimate (STD\_ERROR), the relative error which is the standard deviation divided by the model parameter (REL\_ERROR), and the percentage relative error (% ERROR). The column of integers to the left gives the parameter number.



The last table gives the final model parameter estimates: parameter number and name, layer conductivities and resistivities, layer thicknesses, and depths to the bottom of each layer. All units are SI.

Figure 2b through 19b present the observed apparent resistivity (circles) and the computed model apparent resistivity (solid line) as a function of time. The actual model resistivities as a function of depth are given in Figures 2c through 19c.

The RMS error of the models ranges from 1 to 14% with most errors less than 10%. The percentage error of the layer thickness estimates is smaller than the percentage error of the conductivity estimates. The second layer conductivity is usually resolved to better than 5%. In a few cases, the first layer conductivity is not well resolved, most often when the first layer is very resistive.

Using the inversion results, three cross sections were constructed (AA', BB', and CC'; see Figure 1). The first (A-A', Figure 20) runs along an east-west line through the caldera. The second (B-B', Figure 21) goes north-south just west of the western edge of the caldera. The third (C-C', Figure 22) goes north-south just to the west of the eastern caldera wall.

### Discussion

The east-west profile A-A' (Figure 20) can be divided into three regions. The western boundary, which lies between stations 5 and 18, is slightly west of the caldera rim and a probable ring fracture (MacLeod and Sammel, 1982). The eastern boundary, lying between stations 17 and 16, corresponds to the inner caldera rim and the caldera rim fracture (MacLeod and Sammel, 1982).

The western region is characterized by a resistive (>300 ohm-m) near-surface zone with a thickness of 300 to 500 m, underlain by a conductive basement with resistivities in the range 16 to 61 ohm-m. The basement becomes more conductive in the direction of the caldera.

The eastern region, which is near or outside of the caldera, has a very resistive first layer (2,500 to 4,300 ohm-m). The resistive zone thickens from 440 m at station 16 on the west to 500 m at station 11 on the east. The second layer is a conductive zone with resistivities of 39-53 ohm-m; this zone is similar to the near-surface layer on the eastern edge of the caldera. The electrical basement below station 16 is even more conductive (10 ohm-m).

The central region, which roughly corresponds to the caldera, is composed of a first layer that has resistivities of 56 to 190 ohm-m and which varies in depth from 270 to 430 m. Station 17 was interpreted as a three-layer section, but the first two layers are comparable to the first layer at the other intra-caldera stations. A conductor having resistivities of 2 to 31 ohm-m underlies the caldera floor and bulges upward between stations 1 and 4. The first layer corresponds with the fragmental rocks seen to a depth of 500 m in USGS test hole Newberry 2; the deeper conductor corresponds to the flows and associated breccia below 500 m depth (MacLeod and Sammel, 1982).

The western profile B-B' (Figure 21) is similar to the western end of the east-west profile. A resistive surface layer (210 to 730 ohm-m) overlies a conductor (12 to 62 ohm-m). The depth of the conductor varies from 430 to 690 m. The conductor rises below station 2, which is near a hole being drilled by Union Oil Company.

The eastern profile C-C' (Figure 22) is more complicated. The interpreted section at station 12 resembles the intra-caldera sections shown in figure 20. Stations 16 and 13 show a very resistive first layer underlain by progressively more conductive material; a section similar to that of station 11 (Figure 20), which is located east of the caldera. The electrical section at station 10 is similar to the section to the west of the caldera (see Figure 20).

The TDEM soundings at Newberry Volcano indicate the presence of a conductor at depth which becomes shallowest within the caldera. The overlying material is more resistive, but falls into three categories: moderately conductive inside the caldera, moderately resistive to the west of the caldera, and very resistive to the east of the caldera.

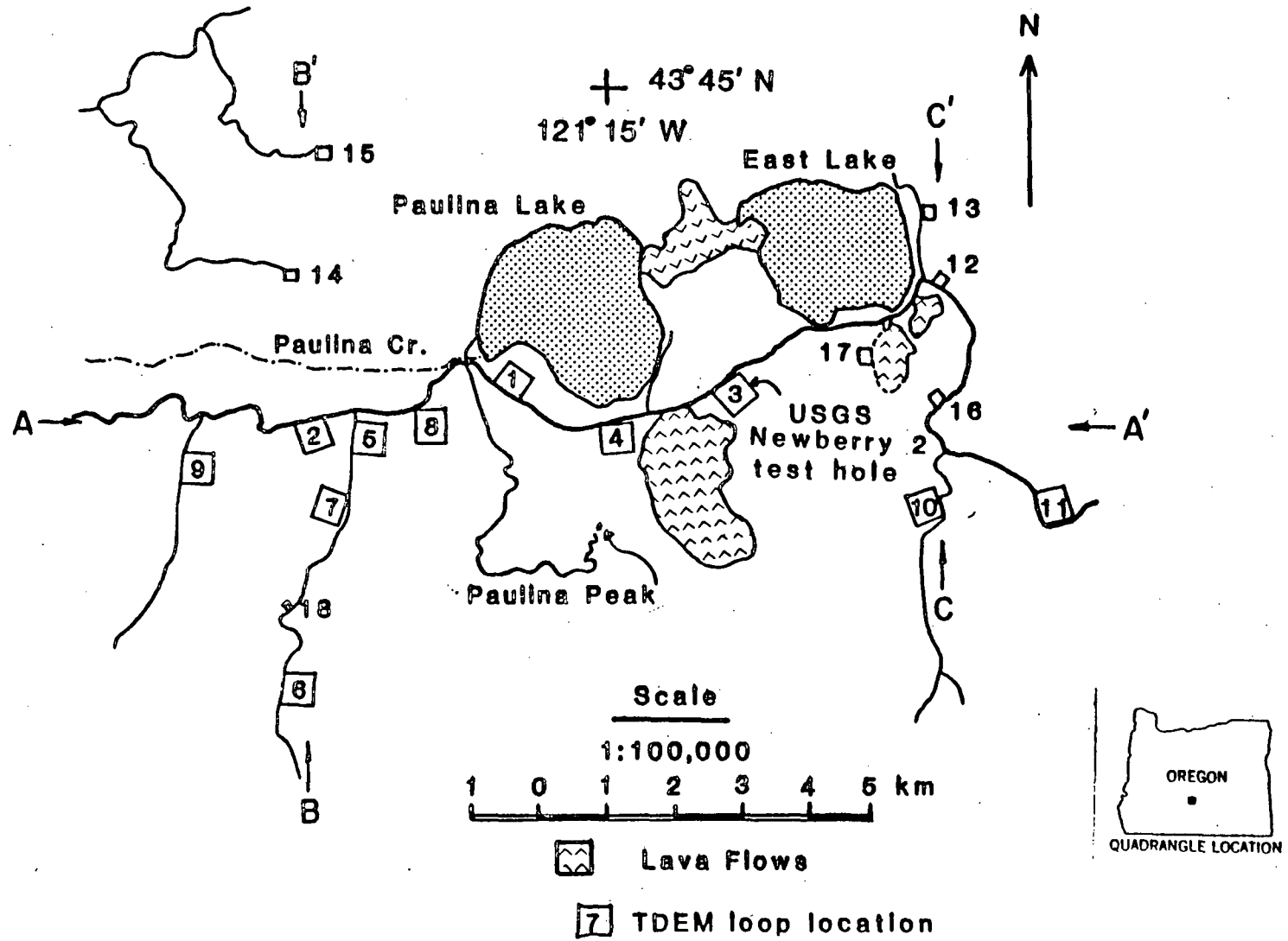
#### Acknowledgements

This work was funded by Department of Energy under Interagency Agreement DE-AI01-79RA50294. Permission to conduct the field work was granted by the Deschutes National Forest, Bend, Oregon. The field work was accomplished with the help of Jerry Bradley, Roger Grette, and Clark Grose. Discussions concerning data interpretation with Walter Anderson, Frank Frischknecht, and Alexander Kaufman are gratefully acknowledged.

## References

- Anderson, W. L., 1982, Nonlinear least-squares inversion of transient soundings for a central induction loop system (Program NLSTCI): U.S. Geological Survey Open-File Report 82-1129, 85 p.
- Buselli, G., and O'Neill, G., 1977, SIROTEM--a new portable instrument for multichannel electromagnetic measurements: Bull. Aust. Soc. Expl. Geophys., 8, 82-87.
- Dennis, J. E., Gay, D. M., and Welsch, R. E., 1979, An adaptive nonlinear least-squares algorithm: Univ. of Wisconsin MRC Tech. Sum. Rept. 2010 (also available as NTIS Rept. AD-A079-716), 40 p.
- Kaufman, A. A., and Keller, G. R., 1983, Frequency and Transient Sounding: Amsterdam, Elsevier, 687 p.
- MacLeod, N. S., and Sammel, E. A., 1982, Newberry Volcano, Oregon--a Cascade Range geothermal prospect: California Geology, 35, 235-244.
- Sammel, E. A., 1981, Results of test drilling at Newberry Volcano, Oregon, and some implications for geothermal prospects in the Cascades: Geothermal Resources Council Bulletin, 10 3-8.

# NEWBERRY CRATER



<NLSTCI2>: Newberry Crater NB-1 2 layer

A= 0.257900E+03

PARAMETERS HELD FIXED: IB= 4

\*\*\*\*\* X-CONVERGENCE \*\*\*\*\*

I	OBS.Y(I)	CAL	RES	%RES.ERR	X(I,1)
1	0.182000E+03	0.180539E+03	0.146E+01	0.809157E+00	0.120000E-02
2	0.159000E+03	0.159708E+03	-0.708E+00	-0.443076E+00	0.160000E-02
3	0.142000E+03	0.143564E+03	-0.156E+01	-0.108944E+01	0.200000E-02
4	0.124000E+03	0.124469E+03	-0.469E+00	-0.377156E+00	0.260000E-02
5	0.109000E+03	0.107754E+03	0.125E+01	0.115602E+01	0.340000E-02
6	0.983000E+02	0.969028E+02	0.140E+01	0.144185E+01	0.420000E-02
7	0.900000E+02	0.884078E+02	0.159E+01	0.180095E+01	0.500000E-02
8	0.788000E+02	0.821539E+02	-0.335E+01	-0.408248E+01	0.580000E-02
9	0.747000E+02	0.756246E+02	-0.925E+00	-0.122269E+01	0.700000E-02
10	0.698000E+02	0.690392E+02	0.761E+00	0.110199E+01	0.860000E-02
11	0.644000E+02	0.643324E+02	0.676E-01	0.105062E+00	0.102000E-01
12	0.605000E+02	0.608401E+02	-0.340E+00	-0.558980E+00	0.118000E-01
13	0.597000E+02	0.580973E+02	0.160E+01	0.275868E+01	0.134000E-01
14	0.543000E+02	0.548513E+02	-0.551E+00	-0.100503E+01	0.158000E-01

\*\* RMSERR= 0.15671540E+01

CORRELATION MATRIX

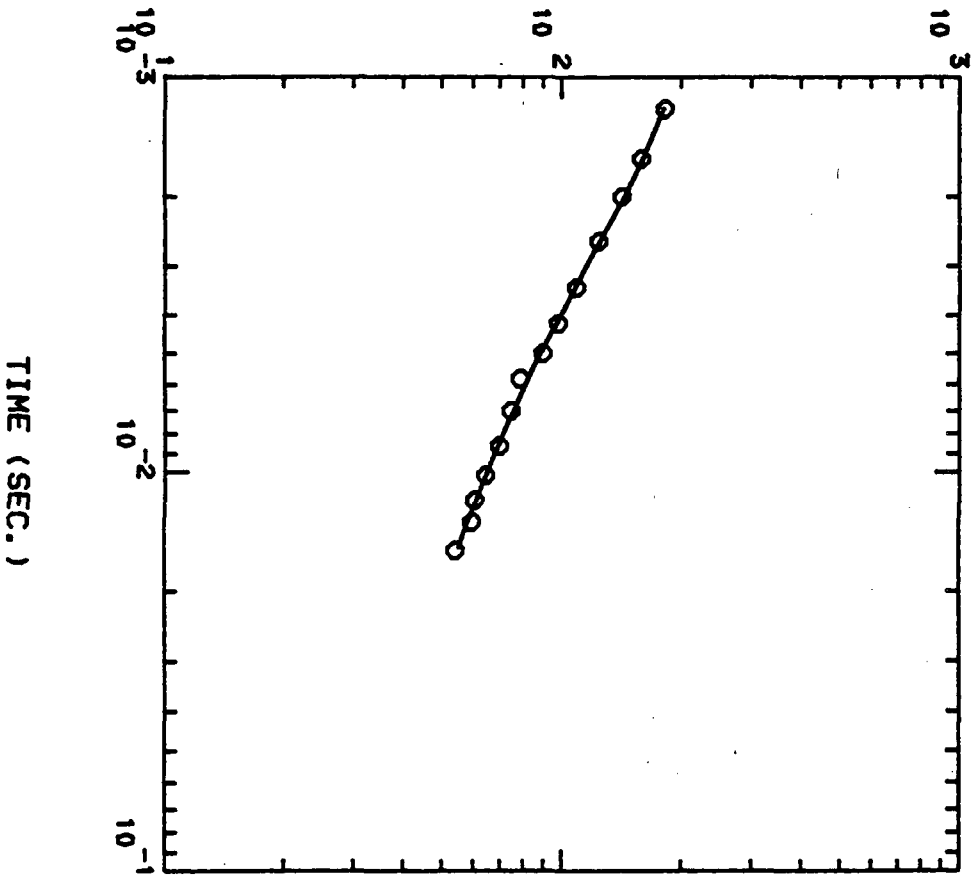
1	0.1000E+01		
2	0.3587E+00	0.1000E+01	
3	0.5697E+00	0.7172E+00	0.1000E+01

**PARAM_SOL.	STD_ERROR	REL_ERROR	% ERROR **	
1	0.5998E-02	0.1449E-03	0.2416E-01	0.2416E+01
2	0.3872E-01	0.6775E-03	0.1750E-01	0.1750E+01
3	0.3730E+03	0.2166E-02	0.5806E-05	0.5806E-03

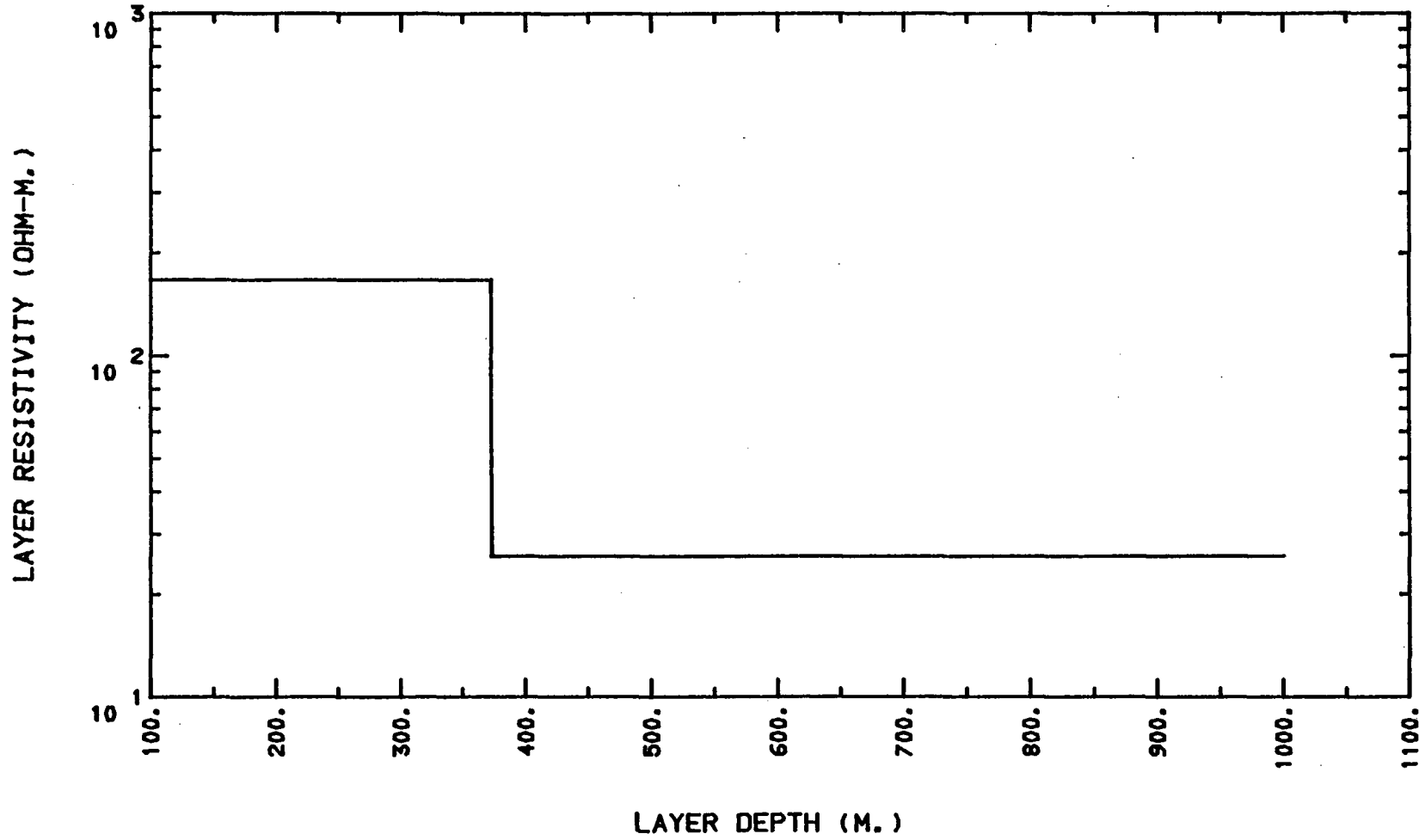
PARAMETER NAME	FINAL SOLUTION	RESISTIVITY	LAYER DEPTH
1 SIGMA( 1) =	0.59982953E-02	1 0.16671404E+03	
2 SIGMA( 2) =	0.38715161E-01	2 0.25829674E+02	
3 THICK( 1) =	0.37302838E+03		1 0.37302838E+03
4 SHIFT =	0.10000000E+01		

APPARENT RESISTIVITY (OHM-M.)

Newberry Crater NB-1 2 layer



Newberry Crater NB-1 2 LAYER



<NLSTCI2>: Newberry Crater NB-2 2 layer

A= 0.257900E+03

PARAMETERS HELD FIXED: IB= 4

\*\*\*\*\* X-CONVERGENCE \*\*\*\*\*

I	OBS.Y(I)	CAL	RES	%RES.ERR	X(I,1)
1	0.336000E+03	0.328380E+03	0.762E+01	0.232039E+01	0.120000E-02
2	0.270000E+03	0.279927E+03	-0.993E+01	-0.354645E+01	0.160000E-02
3	0.243000E+03	0.243790E+03	-0.790E+00	-0.323934E+00	0.200000E-02
4	0.205000E+03	0.202656E+03	0.234E+01	0.115665E+01	0.260000E-02
5	0.171000E+03	0.168195E+03	0.281E+01	0.166785E+01	0.340000E-02
6	0.147000E+03	0.146398E+03	0.602E+00	0.411096E+00	0.420000E-02
7	0.130000E+03	0.130043E+03	-0.430E-01	-0.330302E-01	0.500000E-02
8	0.119000E+03	0.118268E+03	0.732E+00	0.618799E+00	0.580000E-02
9	0.106000E+03	0.105851E+03	0.149E+00	0.140463E+00	0.700000E-02
10	0.954000E+02	0.938310E+02	0.157E+01	0.167216E+01	0.860000E-02
11	0.849000E+02	0.854220E+02	-0.522E+00	-0.611043E+00	0.102000E-01
12	0.799000E+02	0.792177E+02	0.682E+00	0.861254E+00	0.118000E-01
13	0.722000E+02	0.743712E+02	-0.217E+01	-0.291943E+01	0.134000E-01
14	0.669000E+02	0.687234E+02	-0.182E+01	-0.265319E+01	0.158000E-01

\*\* RMSERR= 0.40761223E+01

CORRELATION MATRIX

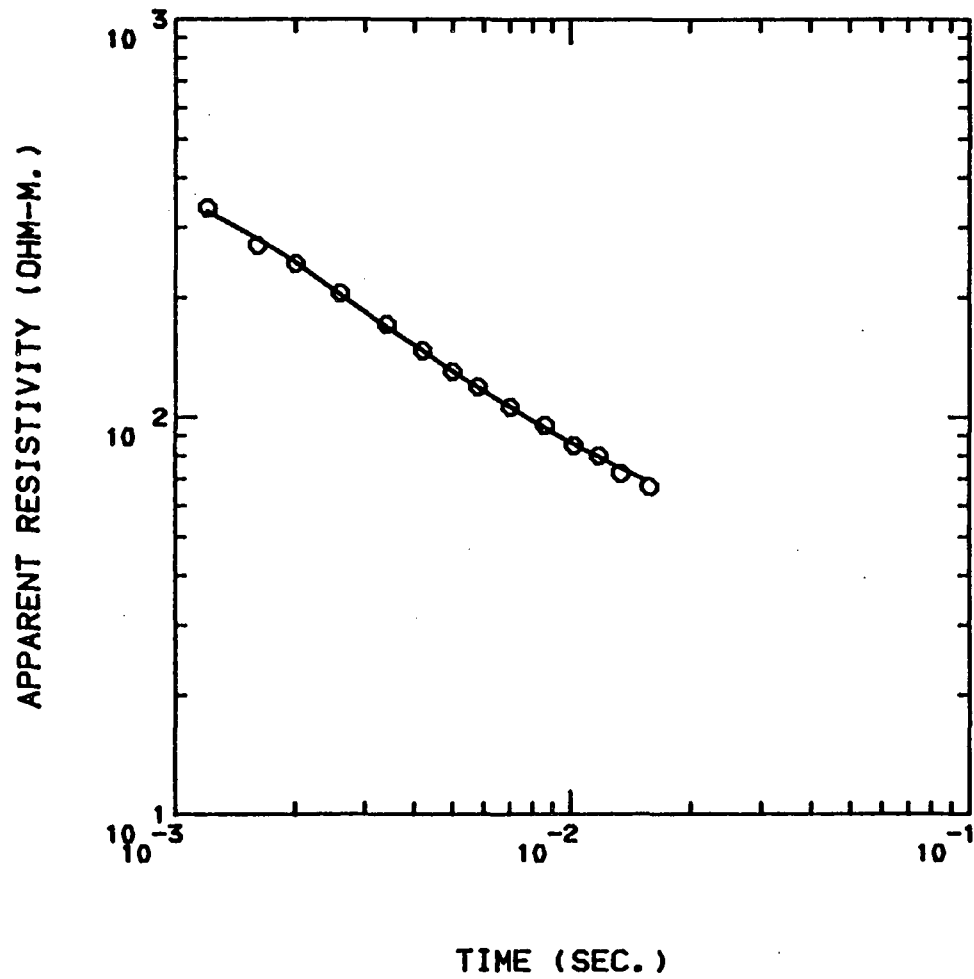
1	0.1000E+01		
2	-0.4530E-01	0.1000E+01	
3	0.4387E+00	0.3108E+00	0.1000E+01

**PARAM_SOL.	STD_ERROR	REL_ERROR	% ERROR **
1	0.3334E-02	0.1098E-03	0.3294E-01
2	0.4288E-01	0.1030E-02	0.2402E-01
3	0.4925E+03	0.1621E-02	0.3291E-03

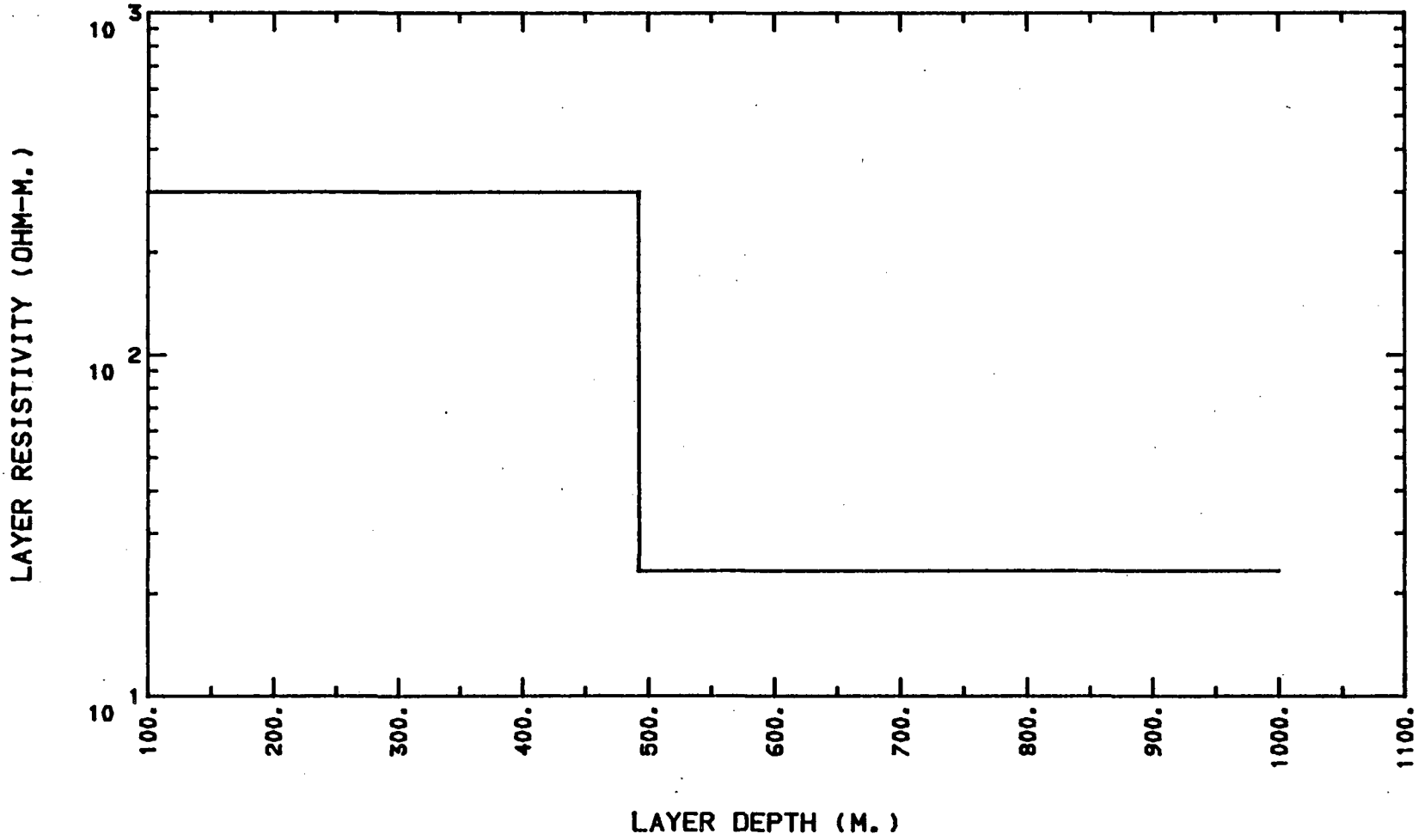
PARAMETER NAME	FINAL SOLUTION	RESISTIVITY	LAYER DEPTH
1 SIGMA( 1) =	0.33337125E-02	1 0.29996588E+03	
2 SIGMA( 2) =	0.42883433E-01	2 0.23319029E+02	
3 THICK( 1) =	0.49249362E+03		1 0.49249362E+03
4 SHIFT =	0.10000000E+01		



Newberry Crater NB-2 2 layer



Newberry Crater NB-2 2 layer



<NLSTCI2>: Newberry Crater NB-3 2 layer

A= 0.257900E+03

PARAMETERS HELD FIXED: IB= 4

\*\*\*\*\* VARIABILITY CONVERGENCE \*\*\*\*\*

I	OBS.Y(I)	CAL	RES	%RES.ERR	X(I,1)
1	0.671000E+02	0.660378E+02	0.106E+01	0.160854E+01	0.120000E-02
2	0.669000E+02	0.652104E+02	0.169E+01	0.259093E+01	0.160000E-02
3	0.663000E+02	0.647156E+02	0.158E+01	0.244823E+01	0.200000E-02
4	0.637000E+02	0.648072E+02	-0.111E+01	-0.170849E+01	0.260000E-02
5	0.620000E+02	0.636003E+02	-0.160E+01	-0.251615E+01	0.340000E-02
6	0.600000E+02	0.615260E+02	-0.153E+01	-0.248028E+01	0.420000E-02
7	0.575000E+02	0.593285E+02	-0.183E+01	-0.308201E+01	0.500000E-02
8	0.563000E+02	0.567574E+02	-0.457E+00	-0.805928E+00	0.580000E-02
9	0.530000E+02	0.528882E+02	0.112E+00	0.211305E+00	0.700000E-02
10	0.498000E+02	0.485370E+02	0.126E+01	0.260217E+01	0.860000E-02
11	0.462000E+02	0.452112E+02	0.989E+00	0.218714E+01	0.102000E-01
12	0.434000E+02	0.424898E+02	0.910E+00	0.214228E+01	0.118000E-01
13	0.412000E+02	0.400854E+02	0.111E+01	0.278051E+01	0.134000E-01
14	0.382000E+02	0.371044E+02	0.110E+01	0.295270E+01	0.158000E-01
15	0.351000E+02	0.344064E+02	0.694E+00	0.201581E+01	0.190000E-01
16	0.324000E+02	0.323341E+02	0.659E-01	0.203877E+00	0.222000E-01
17	0.299000E+02	0.305756E+02	-0.676E+00	-0.220949E+01	0.254000E-01
18	0.286000E+02	0.291289E+02	-0.529E+00	-0.181566E+01	0.286000E-01
19	0.265000E+02	0.275415E+02	-0.104E+01	-0.378153E+01	0.334000E-01
20	0.249000E+02	0.259293E+02	-0.103E+01	-0.396955E+01	0.398000E-01

\*\* RMSERR= 0.12219495E+01

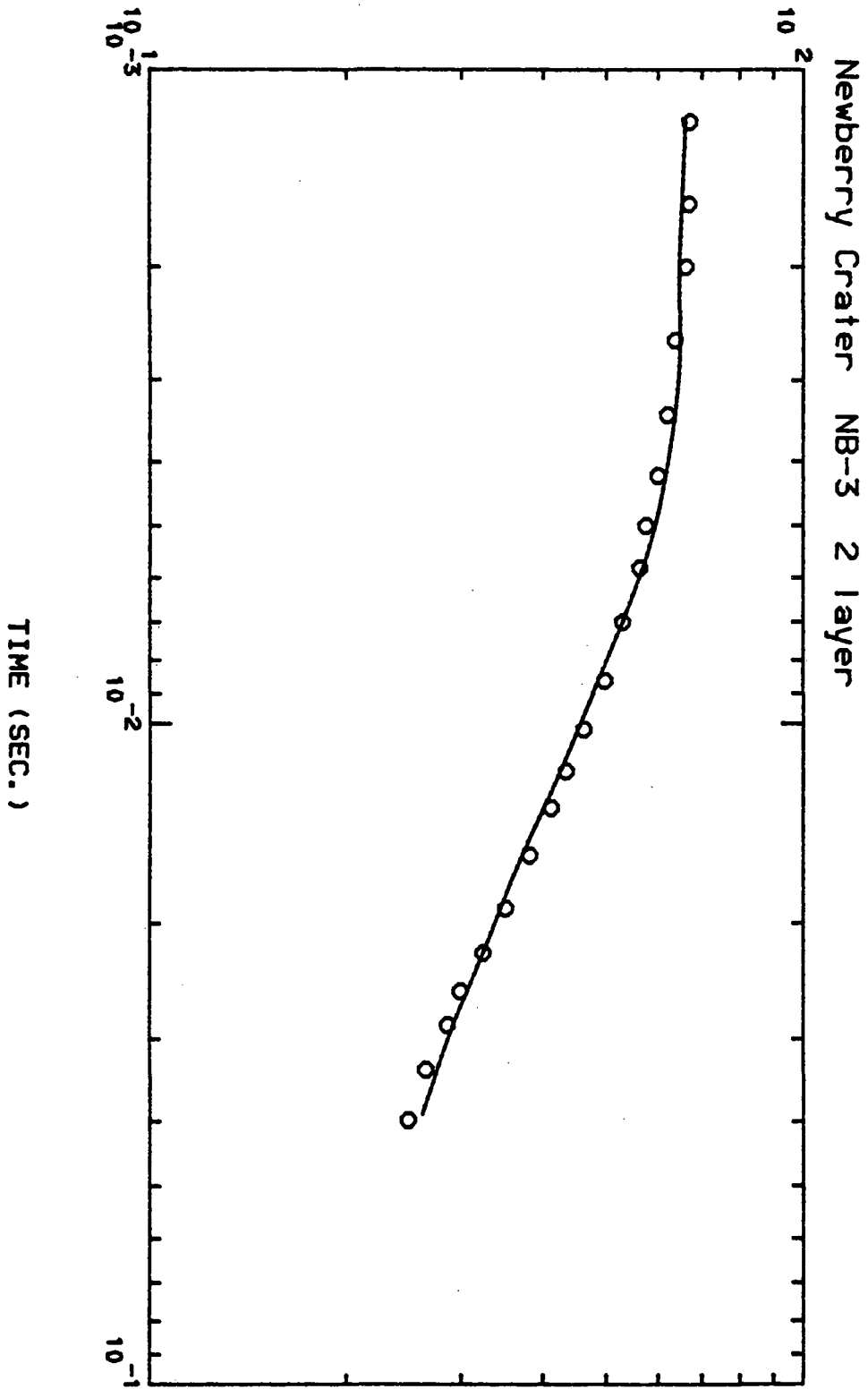
CORRELATION MATRIX

1	0.1000E+01		
2	0.2307E+00	0.1000E+01	
3	0.2442E+00	0.7058E+00	0.1000E+01

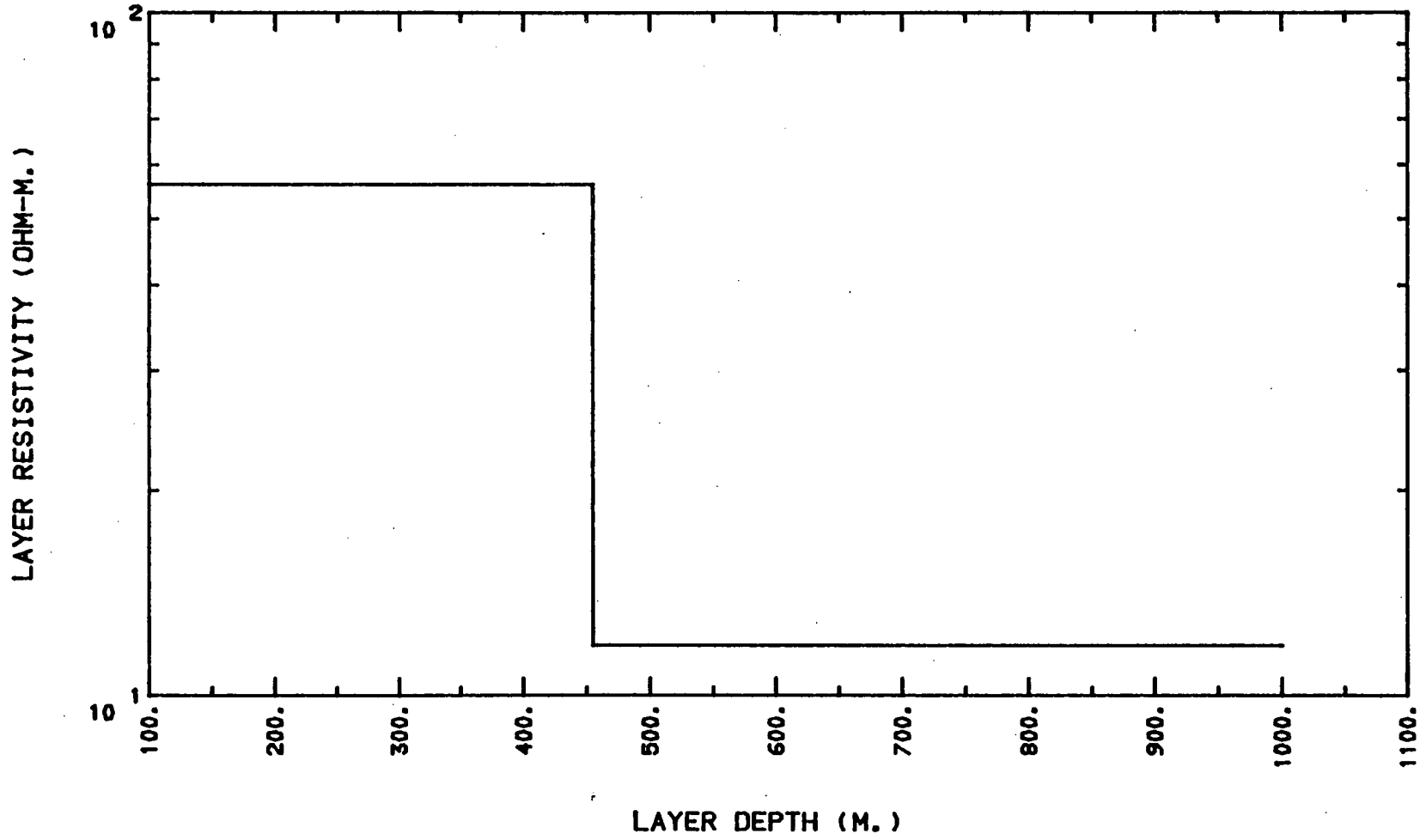
**	PARAM_SOL.	STD_ERROR	REL_ERROR	% ERROR **
1	0.1781E-01	0.1672E-03	0.9389E-02	0.9389E+00
2	0.8440E-01	0.1959E-02	0.2321E-01	0.2321E+01
3	0.4553E+03	0.3160E-02	0.6940E-05	0.6940E-03

PARAMETER NAME	FINAL SOLUTION	RESISTIVITY	LAYER DEPTH
1 SIGMA( 1) =	0.17807685E-01	1 0.56155533E+02	
2 SIGMA( 2) =	0.84403656E-01	2 0.11847828E+02	
3 THICK( 1) =	0.45531293E+03		1 0.45531293E+03
4 SHIFT =	0.10000000E+01		

APPARENT RESISTIVITY (OHM-M.)



Newberry Crater NB-3 2 layer



<NLSTCI2>: Newberry Crater NB-4 2 layer

A= 0.257900E+03

PARAMETERS HELD FIXED: IB= 4

\*\*\*\*\* VARIABILITY CONVERGENCE \*\*\*\*\*

I	OBS.Y(I)	CAL	RES	%RES.ERR	X(I,1)
1	0.124000E+03	0.123296E+03	0.704E+00	0.570923E+00	0.120000E-02
2	0.118000E+03	0.118845E+03	-0.845E+00	-0.711317E+00	0.160000E-02
3	0.111000E+03	0.111500E+03	-0.500E+00	-0.448676E+00	0.200000E-02
4	0.996000E+02	0.101860E+03	-0.226E+01	-0.221831E+01	0.260000E-02
5	0.905000E+02	0.909406E+02	-0.441E+00	-0.484514E+00	0.340000E-02
6	0.832000E+02	0.821203E+02	0.108E+01	0.131480E+01	0.420000E-02
7	0.769000E+02	0.755689E+02	0.133E+01	0.176144E+01	0.500000E-02
8	0.718000E+02	0.707651E+02	0.103E+01	0.146248E+01	0.580000E-02
9	0.647000E+02	0.650146E+02	-0.315E+00	-0.483853E+00	0.700000E-02
10	0.599000E+02	0.590745E+02	0.825E+00	0.139732E+01	0.860000E-02
11	0.562000E+02	0.551483E+02	0.105E+01	0.190713E+01	0.102000E-01
12	0.518000E+02	0.520977E+02	-0.298E+00	-0.571381E+00	0.118000E-01
13	0.488000E+02	0.495726E+02	-0.773E+00	-0.155859E+01	0.134000E-01
14	0.464000E+02	0.465781E+02	-0.178E+00	-0.382345E+00	0.158000E-01
15	0.421000E+02	0.437467E+02	-0.165E+01	-0.376413E+01	0.190000E-01

\*\* RMSERR= 0.11577367E+01

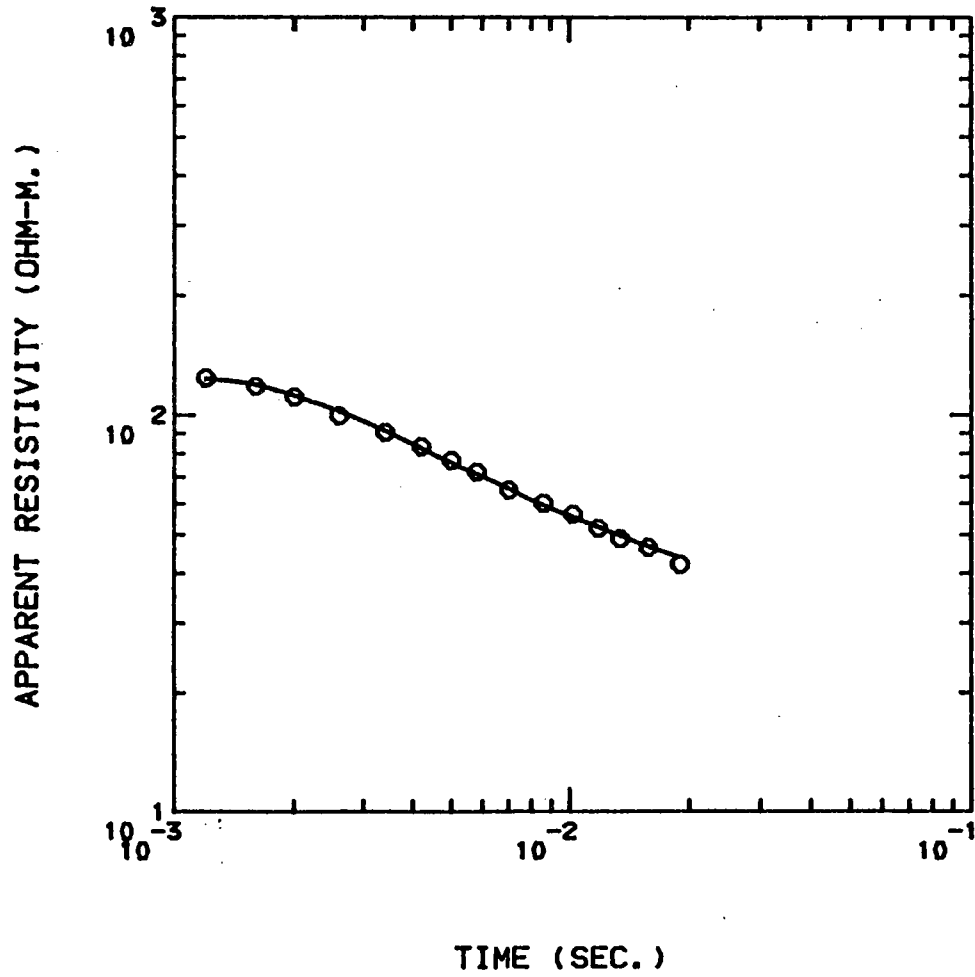
CORRELATION MATRIX

1	0.1000E+01		
2	0.7853E+00	0.1000E+01	
3	0.8616E+00	0.9171E+00	0.1000E+01

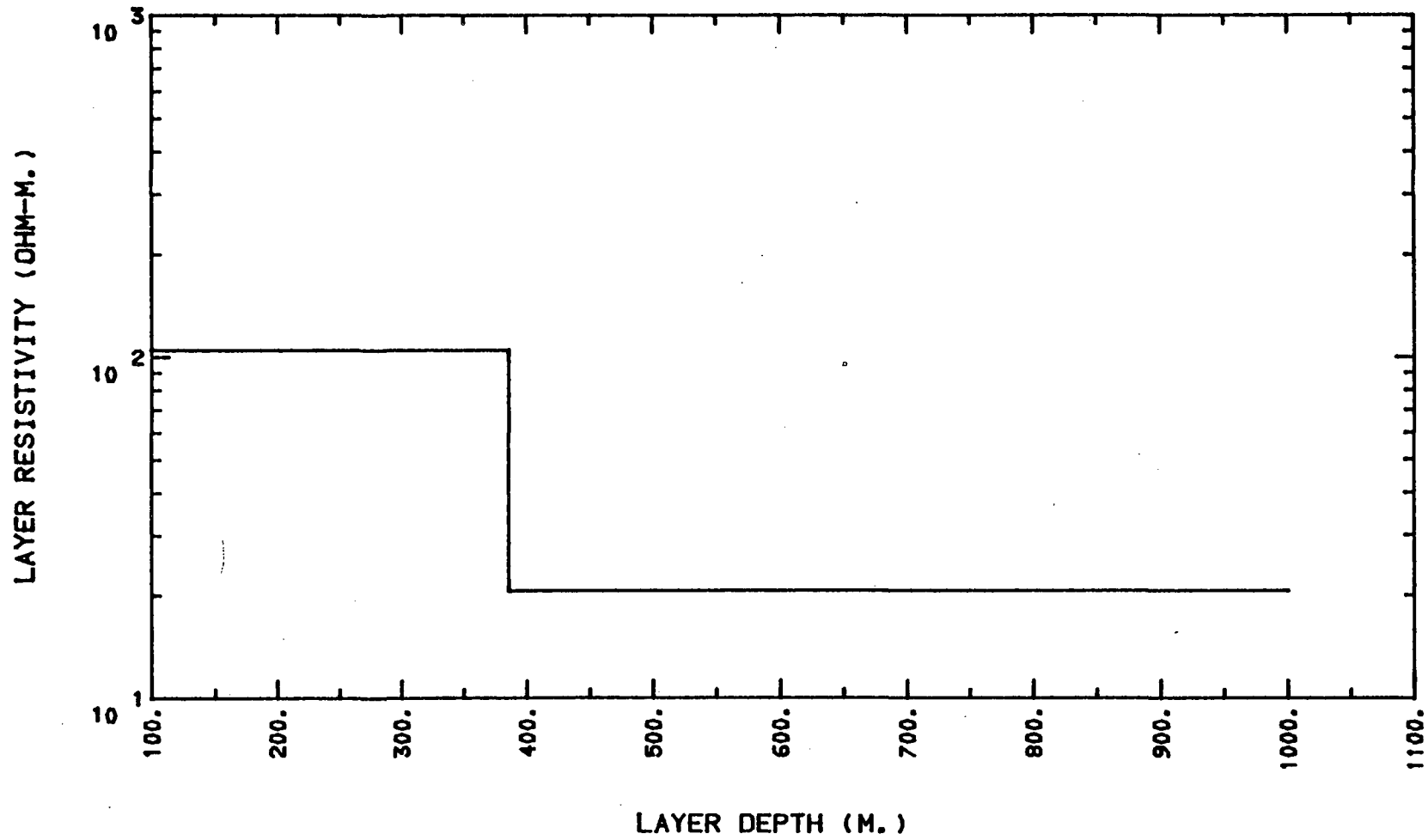
**PARM_SOL.	STD_ERROR	REL_ERROR	% ERROR **
1	0.9541E-02	0.2090E-03	0.2190E-01
2	0.4840E-01	0.1793E-02	0.3704E-01
3	0.3856E+03	0.4702E-02	0.1219E-04

PARAMETER NAME	FINAL SOLUTION	RESISTIVITY	LAYER DEPTH
1 SIGMA( 1) =	0.95408158E-02	1 0.10481284E+03	
2 SIGMA( 2) =	0.48400078E-01	2 0.20661123E+02	
3 THICK( 1) =	0.38564847E+03		1 0.38564847E+03
4 SHIFT =	0.10000000E+01		

Newberry Crater NB-4 2 layer



Newberry Crater NB-4 2 layer





<NLSTCI2>: Newberry Crater NB-5 3 layer

A= 0.257900E+03

PARAMETERS HELD FIXED: IB= 6

\*\*\*\*\* X-CONVERGENCE \*\*\*\*\*

I	OBS.Y(I)	CAL	RES	%RES.ERR	X(I,1)
1	0.298000E+03	0.284898E+03	0.131E+02	0.459875E+01	0.120000E-02
2	0.250000E+03	0.252716E+03	-0.272E+01	-0.107472E+01	0.160000E-02
3	0.222000E+03	0.228278E+03	-0.628E+01	-0.275008E+01	0.200000E-02
4	0.189000E+03	0.196463E+03	-0.746E+01	-0.379862E+01	0.260000E-02
5	0.163000E+03	0.165631E+03	-0.263E+01	-0.158869E+01	0.340000E-02
6	0.143000E+03	0.143776E+03	-0.776E+00	-0.540056E+00	0.420000E-02
7	0.128000E+03	0.127957E+03	0.430E-01	0.336045E-01	0.500000E-02
8	0.122000E+03	0.115827E+03	0.617E+01	0.532940E+01	0.580000E-02
9	0.107000E+03	0.102141E+03	0.486E+01	0.475761E+01	0.700000E-02
10	0.937000E+02	0.894113E+02	0.429E+01	0.479661E+01	0.860000E-02
11	0.839000E+02	0.805051E+02	0.339E+01	0.421696E+01	0.102000E-01
12	0.758000E+02	0.737343E+02	0.207E+01	0.280159E+01	0.118000E-01
13	0.693000E+02	0.684333E+02	0.867E+00	0.126654E+01	0.134000E-01
14	0.621000E+02	0.623905E+02	-0.291E+00	-0.465641E+00	0.158000E-01
15	0.564000E+02	0.566014E+02	-0.201E+00	-0.355823E+00	0.190000E-01
16	0.523000E+02	0.523013E+02	-0.132E-02	-0.251632E-02	0.222000E-01
17	0.475000E+02	0.490090E+02	-0.151E+01	-0.307902E+01	0.254000E-01
18	0.434000E+02	0.463933E+02	-0.299E+01	-0.645197E+01	0.286000E-01
19	0.418000E+02	0.433341E+02	-0.153E+01	-0.354024E+01	0.334000E-01
20	0.401000E+02	0.403164E+02	-0.216E+00	-0.536726E+00	0.398000E-01
21	0.366000E+02	0.380452E+02	-0.145E+01	-0.379860E+01	0.462000E-01

\*\* RMSERR= 0.49634480E+01

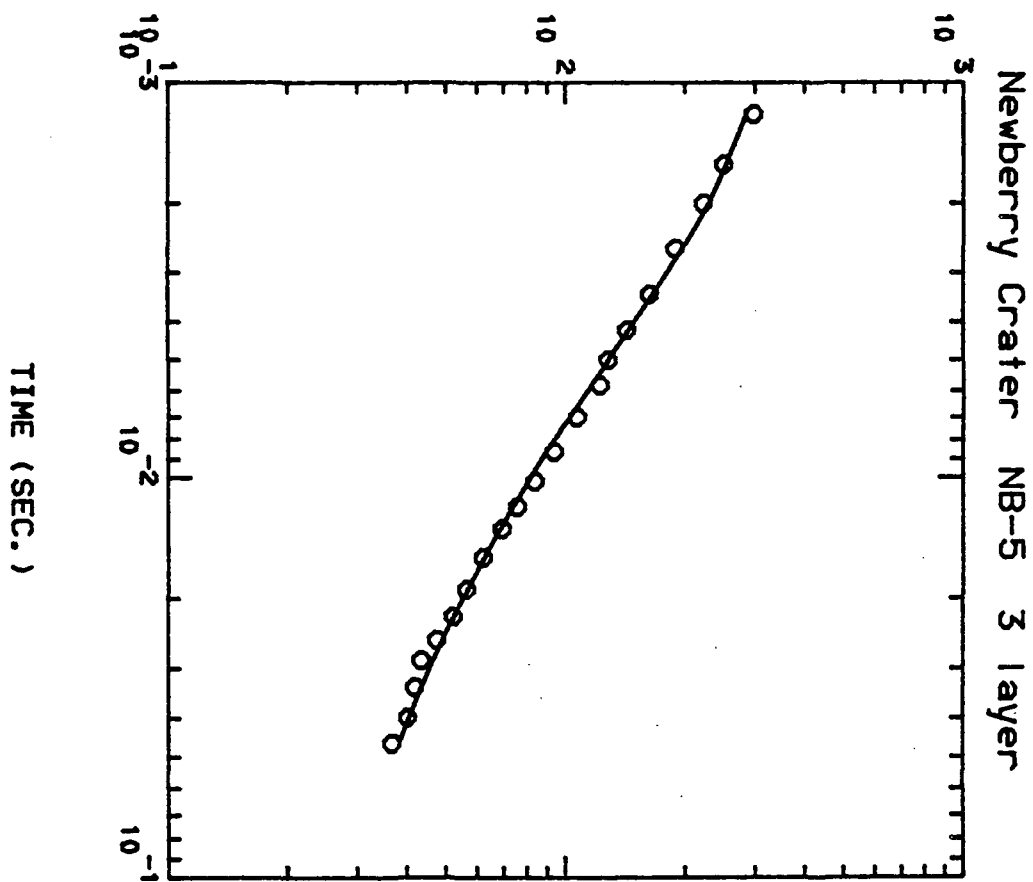
CORRELATION MATRIX

1	0.1000E+01				
2	0.2227E+00	0.1000E+01			
3	0.4656E+00	0.5078E+00	0.1000E+01		
4	0.4974E+00	0.8203E+00	0.5011E+00	0.1000E+01	
5	0.2213E+00	-0.1408E+00	0.3189E+00	-0.2769E+00	0.1000E+01

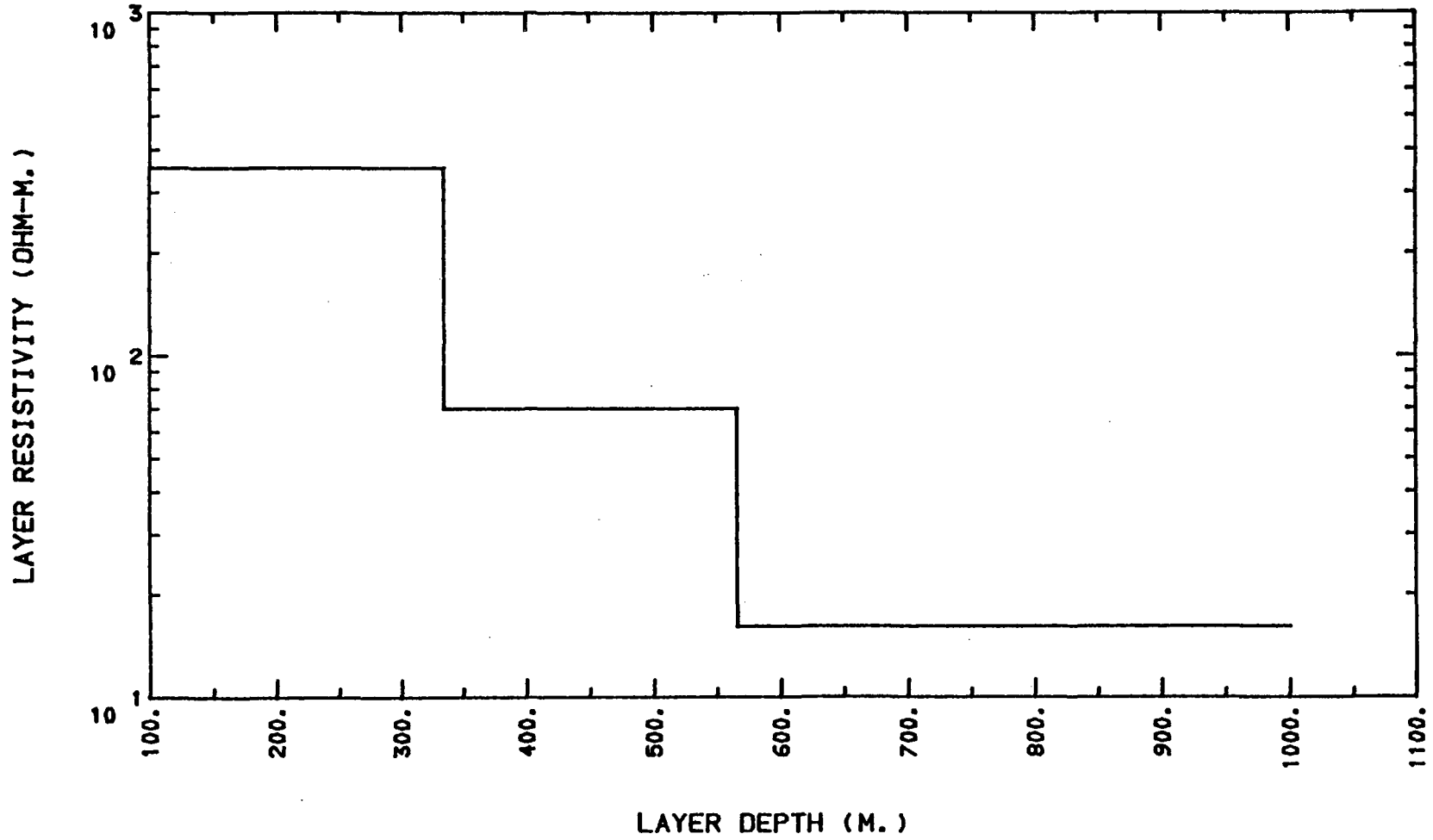
**PARAM_SOL.	STD_ERROR	REL_ERROR	% ERROR **
1	0.2826E-02	0.2385E-03	0.8440E-01
2	0.1430E-01	0.1086E-02	0.7597E-01
3	0.6202E-01	0.1689E-02	0.2723E-01
4	0.3344E+03	0.5220E-02	0.1561E-02
5	0.2313E+03	0.6684E-02	0.2890E-02

PARAMETER NAME	FINAL SOLUTION	RESISTIVITY	LAYER DEPTH
1 SIGMA( 1) =	0.28262159E-02	1 0.35383002E+03	
2 SIGMA( 2) =	0.14299732E-01	2 0.69931381E+02	
3 SIGMA( 3) =	0.62019791E-01	3 0.16123886E+02	
4 THICK( 1) =	0.33438226E+03		1 0.33438226E+03
5 THICK( 2) =	0.23125919E+03		2 0.56564148E+03
6 SHIFT =	0.10000000E+01		

APPARENT RESISTIVITY (OHM-M.)



Newberry Crater NB-5 3 layer



<NLSTCI2>: Newberry Crater NB-6 2 layer

A= 0.257900E+03

PARAMETERS HELD FIXED: IB= 4

\*\*\*\*\* X-CONVERGENCE \*\*\*\*\*

I	OBS.Y(I)	CAL	RES	%RES.ERR	X(I,1)
1	0.717000E+03	0.696352E+03	0.206E+02	0.296523E+01	0.120000E-02
2	0.576000E+03	0.587895E+03	-0.119E+02	-0.202332E+01	0.160000E-02
3	0.493000E+03	0.504980E+03	-0.120E+02	-0.237233E+01	0.200000E-02
4	0.414000E+03	0.425888E+03	-0.119E+02	-0.279132E+01	0.260000E-02
5	0.354000E+03	0.358043E+03	-0.404E+01	-0.112908E+01	0.340000E-02
6	0.320000E+03	0.313197E+03	0.680E+01	0.217227E+01	0.420000E-02
7	0.299000E+03	0.283220E+03	0.158E+02	0.557172E+01	0.500000E-02
8	0.275000E+03	0.260098E+03	0.149E+02	0.572957E+01	0.580000E-02
9	0.239000E+03	0.233931E+03	0.507E+01	0.216708E+01	0.700000E-02
10	0.209000E+03	0.210254E+03	-0.125E+01	-0.596204E+00	0.860000E-02
11	0.198000E+03	0.193326E+03	0.467E+01	0.241751E+01	0.102000E-01
12	0.177000E+03	0.180750E+03	-0.375E+01	-0.207490E+01	0.118000E-01
13	0.166000E+03	0.170953E+03	-0.495E+01	-0.289706E+01	0.134000E-01
14	0.153000E+03	0.159560E+03	-0.656E+01	-0.411132E+01	0.158000E-01

\*\* RMSERR= 0.11744075E+02

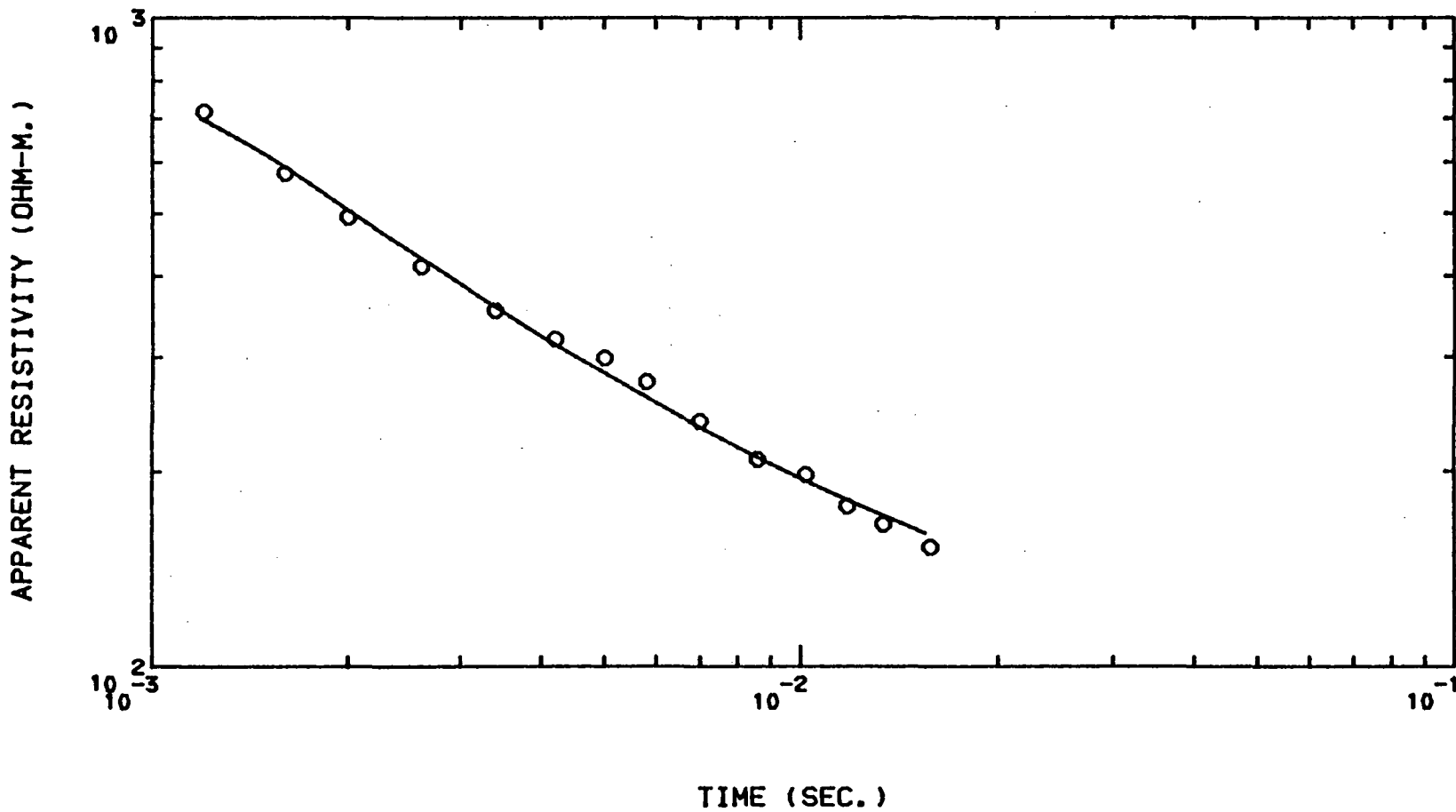
CORRELATION MATRIX

1	0.1000E+01		
2	-0.4264E+00	0.1000E+01	
3	-0.5542E+00	0.3028E+00	0.1000E+01

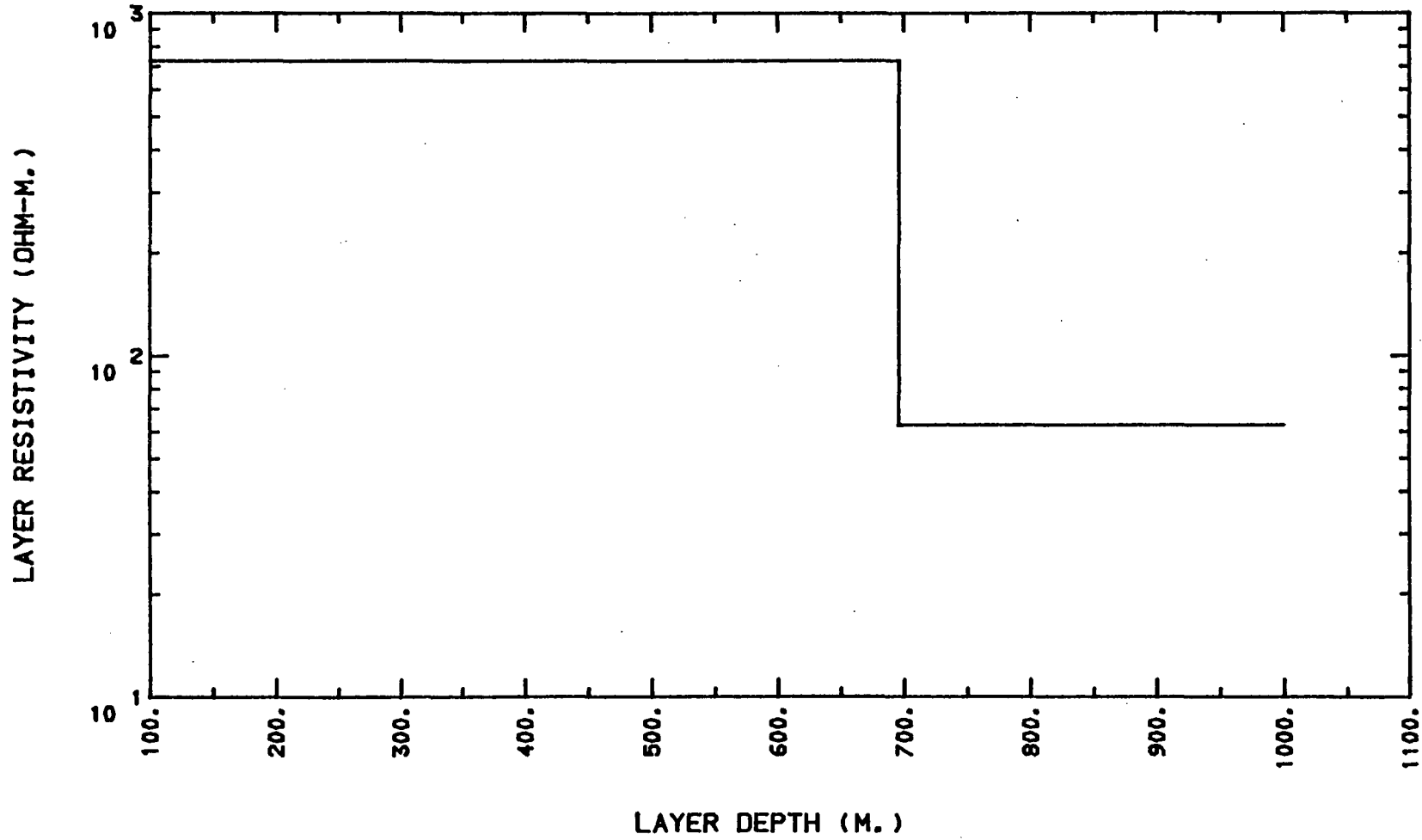
**PARAM_SOL.	STD_ERROR	REL_ERROR	% ERROR **
1	0.1377E-02	0.4998E-04	0.3630E-01
2	0.1601E-01	0.4325E-03	0.2702E-01
3	0.6964E+03	0.2608E-02	0.3745E-05

PARAMETER NAME	FINAL SOLUTION	RESISTIVITY	LAYER DEPTH
1 SIGMA( 1) =	0.13767633E-02	1 0.72634125E+03	
2 SIGMA( 2) =	0.16007731E-01	2 0.62469818E+02	
3 THICK( 1) =	0.69639349E+03		1 0.69639349E+03
4 SHIFT =	0.10000000E+01		

Newberry Crater NB-6 2 LAYER



Newberry Crater NB-6 2 LAYER



<NLSTCI2>: Newberry Crater NB-7 2 layer

A= 0.257900E+03

PARAMETERS HELD FIXED: IB= 4

\*\*\*\*\* X-CONVERGENCE \*\*\*\*\*

I	OBS.Y(I)	CAL	RES	%RES.ERR	X(I,1)
1	0.365000E+03	0.340598E+03	0.244E+02	0.716436E+01	0.120000E-02
2	0.317000E+03	0.322120E+03	-0.512E+01	-0.158943E+01	0.160000E-02
3	0.280000E+03	0.296954E+03	-0.170E+02	-0.570931E+01	0.200000E-02
4	0.245000E+03	0.257525E+03	-0.125E+02	-0.486360E+01	0.260000E-02
5	0.216000E+03	0.217986E+03	-0.199E+01	-0.910842E+00	0.340000E-02
6	0.193000E+03	0.190756E+03	0.224E+01	0.117613E+01	0.420000E-02
7	0.179000E+03	0.169297E+03	0.970E+01	0.573129E+01	0.500000E-02
8	0.161000E+03	0.153409E+03	0.759E+01	0.494834E+01	0.580000E-02
9	0.140000E+03	0.137047E+03	0.295E+01	0.215456E+01	0.700000E-02
10	0.124000E+03	0.120792E+03	0.321E+01	0.265570E+01	0.860000E-02
11	0.112000E+03	0.109103E+03	0.290E+01	0.265520E+01	0.102000E-01
12	0.103000E+03	0.100724E+03	0.228E+01	0.225954E+01	0.118000E-01
13	0.932000E+02	0.941709E+02	-0.971E+00	-0.103098E+01	0.134000E-01
14	0.825000E+02	0.863864E+02	-0.389E+01	-0.449882E+01	0.158000E-01
15	0.771000E+02	0.798546E+02	-0.175E+01	-0.222507E+01	0.190000E-01
16	0.727000E+02	0.733393E+02	-0.639E+00	-0.871760E+00	0.222000E-01
17	0.683000E+02	0.691490E+02	-0.849E+00	-0.122773E+01	0.254000E-01
18	0.623000E+02	0.658117E+02	-0.351E+01	-0.533605E+01	0.286000E-01

\*\* RMSERR= 0.92804003E+01

CORRELATION MATRIX

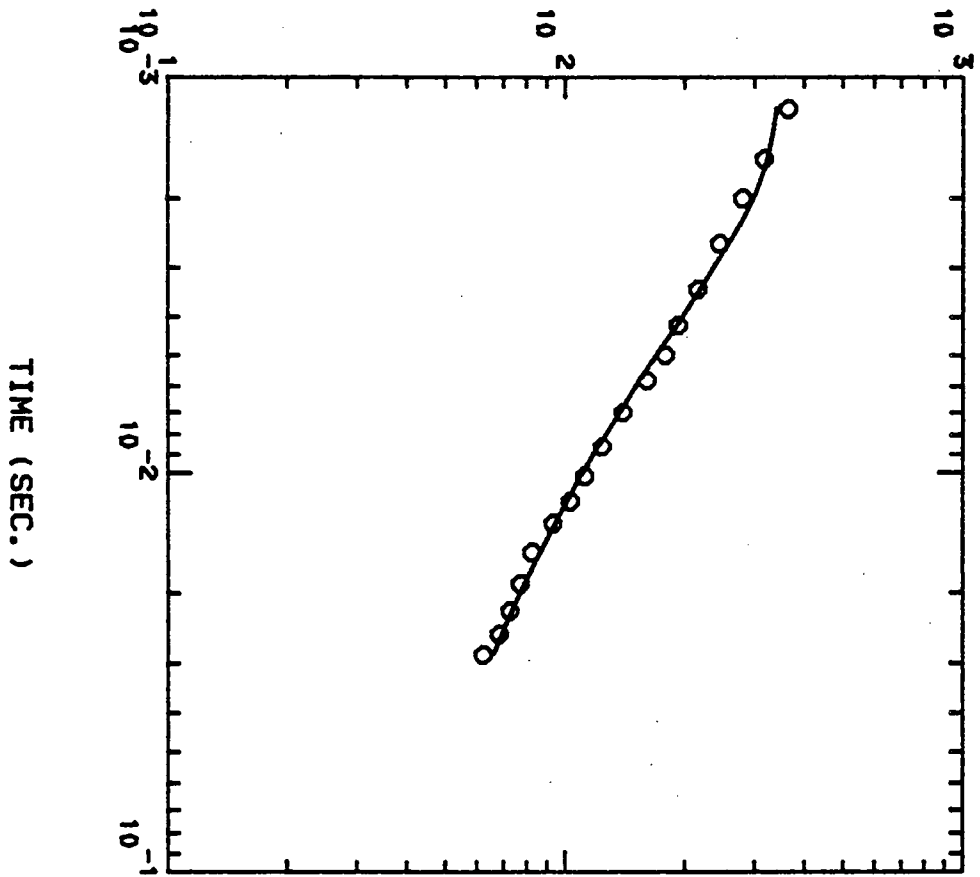
1	0.1000E+01		
2	-0.2126E+00	0.1000E+01	
3	-0.6523E-01	0.2364E+00	0.1000E+01

**PARAM_SOL.	STD_ERROR	REL_ERROR	% ERROR **
1	0.3494E-02	0.1181E-03	0.3381E-01
2	0.3908E-01	0.1251E-02	0.3200E-01
3	0.6062E+03	0.3365E-02	0.5551E-05

PARAMETER NAME	FINAL SOLUTION	RESISTIVITY	LAYER DEPTH
1 SIGMA( 1) =	0.34938017E-02	1 0.28622116E+03	
2 SIGMA( 2) =	0.39084874E-01	2 0.25585346E+02	
3 THICK( 1) =	0.60620282E+03		1 0.60620282E+03
4 SHIFT =	0.10000000E+01		

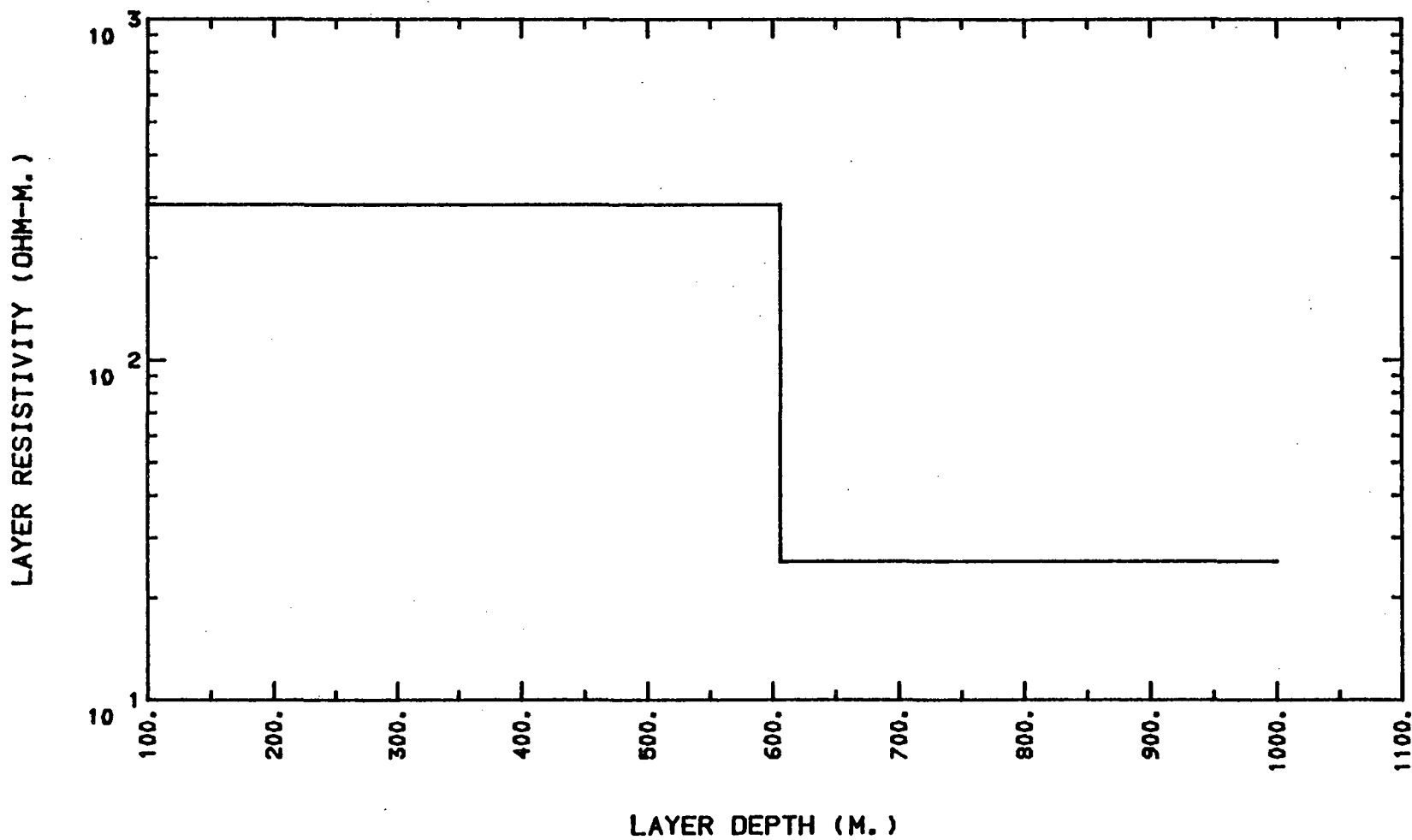
APPARENT RESISTIVITY (OHM-M.)

Newberry Crater NB-7 2 layer





Newberry Crater NB-7 2 layer



<NLSTCI2>: Newberry Crater NB-8 3 layer

A= 0.257900E+03

PARAMETERS HELD FIXED: IB= 6

\*\*\*\*\* X-CONVERGENCE \*\*\*\*\*

I	OBS.Y(I)	CAL	RES	%RES.ERR	X(I,1)
1	0.207000E+03	0.208521E+03	-0.152E+01	-0.729298E+00	0.120000E-02
2	0.195000E+03	0.195564E+03	-0.564E+00	-0.288635E+00	0.160000E-02
3	0.185000E+03	0.183844E+03	0.116E+01	0.628739E+00	0.200000E-02
4	0.170000E+03	0.169514E+03	0.486E+00	0.285526E+00	0.260000E-02
5	0.155000E+03	0.156531E+03	-0.153E+01	-0.978046E+00	0.340000E-02
6	0.141000E+03	0.143422E+03	-0.242E+01	-0.168875E+01	0.420000E-02
7	0.133000E+03	0.130678E+03	0.232E+01	0.177680E+01	0.500000E-02
8	0.122000E+03	0.120044E+03	0.196E+01	0.162948E+01	0.580000E-02
9	0.106000E+03	0.106303E+03	-0.303E+00	-0.285043E+00	0.700000E-02
10	0.904000E+02	0.916297E+02	-0.123E+01	-0.134203E+01	0.860000E-02
11	0.801000E+02	0.805847E+02	-0.485E+00	-0.601492E+00	0.102000E-01
12	0.721000E+02	0.719589E+02	0.141E+00	0.196135E+00	0.118000E-01
13	0.667000E+02	0.651686E+02	0.153E+01	0.234992E+01	0.134000E-01
14	0.576000E+02	0.574299E+02	0.170E+00	0.296109E+00	0.158000E-01
15	0.502000E+02	0.499901E+02	0.210E+00	0.419845E+00	0.190000E-01
16	0.455000E+02	0.445012E+02	0.999E+00	0.224438E+01	0.222000E-01
17	0.414000E+02	0.403118E+02	0.109E+01	0.269952E+01	0.254000E-01
18	0.374000E+02	0.370399E+02	0.360E+00	0.972163E+00	0.286000E-01
19	0.321000E+02	0.333070E+02	-0.121E+01	-0.362377E+01	0.334000E-01
20	0.286000E+02	0.296327E+02	-0.103E+01	-0.348509E+01	0.398000E-01

\*\* RMSERR= 0.14316093E+01

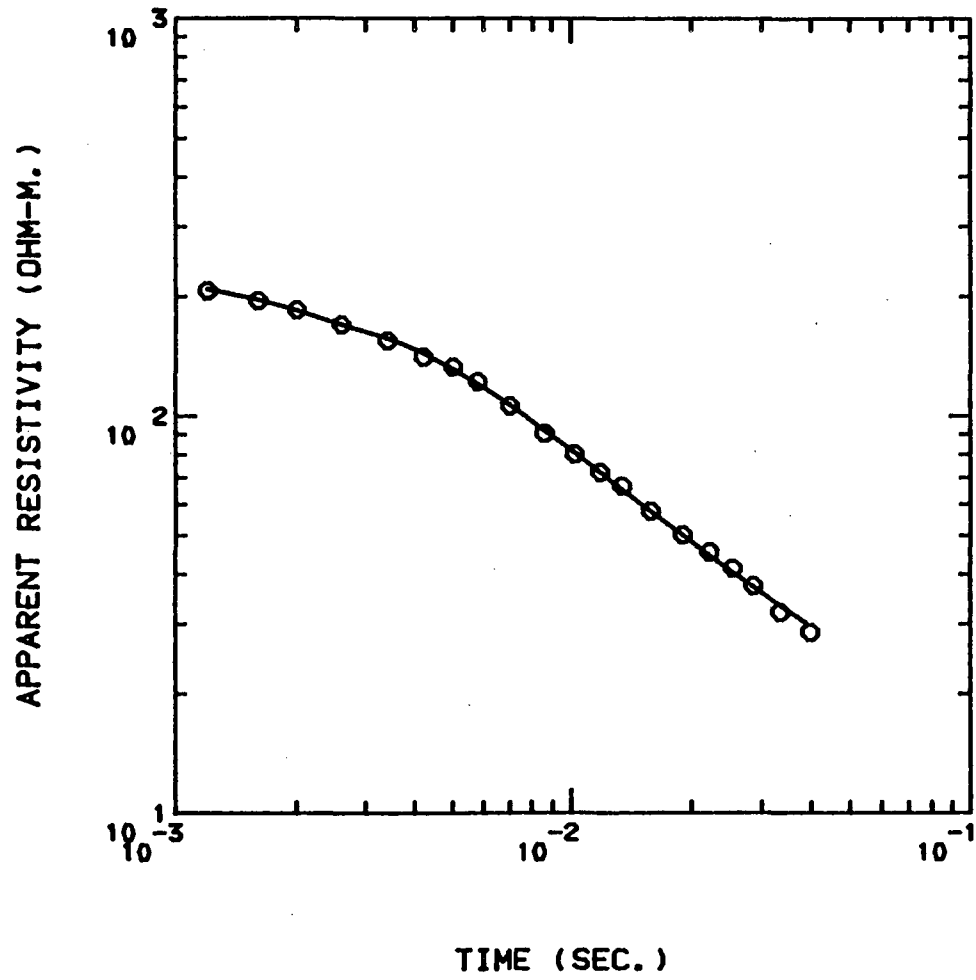
CORRELATION MATRIX

1	0.1000E+01				
2	0.8378E+00	0.1000E+01			
3	-0.1353E+00	-0.3102E+00	0.1000E+01		
4	0.8603E+00	0.9619E+00	-0.3672E+00	0.1000E+01	
5	-0.8210E+00	-0.8589E+00	0.2387E+00	-0.8981E+00	0.1000E+01

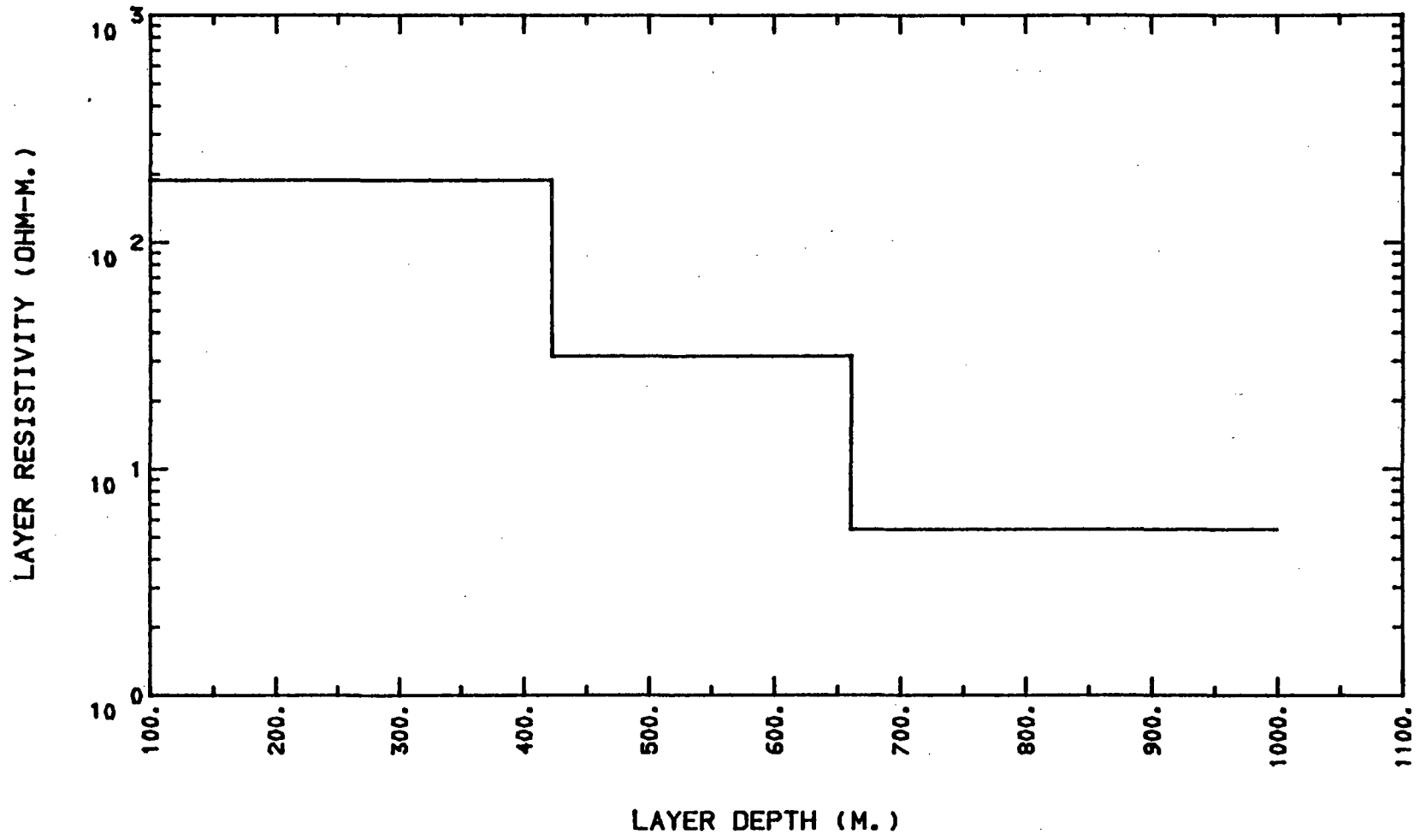
**PARAM_SOL.	STD_ERROR	REL_ERROR	% ERROR **
1	0.5327E-02	0.1623E-03	0.3046E-01
2	0.3183E-01	0.1355E-02	0.4256E-01
3	0.1853E+00	0.1662E-02	0.8974E+00
4	0.4222E+03	0.4436E-02	0.1051E-02
5	0.2387E+03	0.5186E-02	0.2173E-02

PARAMETER NAME	FINAL SOLUTION	RESISTIVITY	LAYER DEPTH
1 SIGMA( 1) =	0.53270226E-02	1 0.18772212E+03	
2 SIGMA( 2) =	0.31825010E-01	2 0.31421829E+02	
3 SIGMA( 3) =	0.18526085E+00	3 0.53977947E+01	
4 THICK( 1) =	0.42220587E+03		1 0.42220587E+03
5 THICK( 2) =	0.23867612E+03		2 0.66088202E+03
6 SHIFT =	0.10000000E+01		

Newberry Crater NB-8 3 layer



Newberry Crater NB-8 3 layer



<NLSTCI2>: Newberry Crater NB-9 3 layer

A= 0.257900E+03

PARAMETERS HELD FIXED: IB= 6

\*\*\*\*\* X-CONVERGENCE \*\*\*\*\*

I	OBS.Y(I)	CAL	RES	%RES.ERR	X(I,1)
1	0.331000E+03	0.328833E+03	0.217E+01	0.659051E+00	0.120000E-02
2	0.273000E+03	0.275666E+03	-0.267E+01	-0.967107E+00	0.160000E-02
3	0.241000E+03	0.242536E+03	-0.154E+01	-0.633244E+00	0.200000E-02
4	0.207000E+03	0.210931E+03	-0.393E+01	-0.186361E+01	0.260000E-02
5	0.185000E+03	0.184592E+03	0.408E+00	0.220757E+00	0.340000E-02
6	0.170000E+03	0.167674E+03	0.233E+01	0.138740E+01	0.420000E-02
7	0.161000E+03	0.155699E+03	0.530E+01	0.340489E+01	0.500000E-02
8	0.153000E+03	0.146641E+03	0.636E+01	0.433638E+01	0.580000E-02
9	0.134000E+03	0.136456E+03	-0.246E+01	-0.179961E+01	0.700000E-02
10	0.122000E+03	0.127028E+03	-0.503E+01	-0.395841E+01	0.860000E-02

\*\* RMSERR= 0.51970654E+01

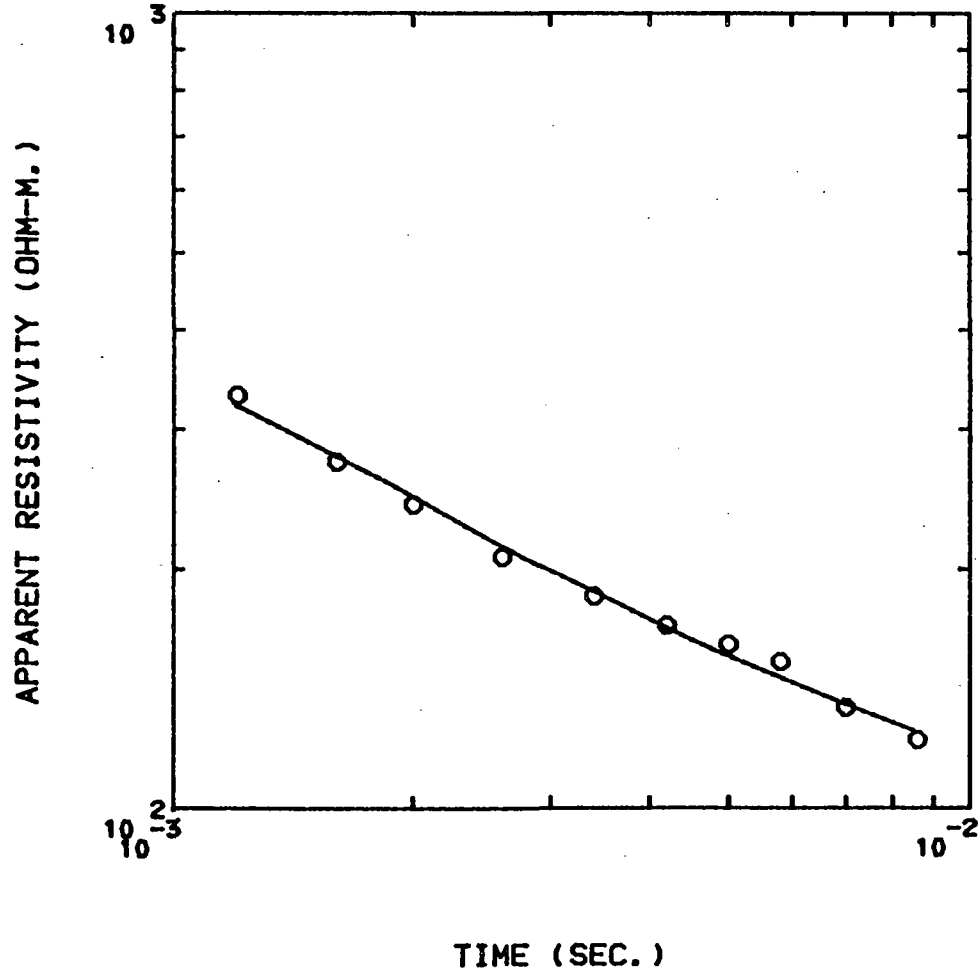
CORRELATION MATRIX

1	0.1000E+01				
2	-0.3382E+00	0.1000E+01			
3	-0.6829E+00	-0.2451E+00	0.1000E+01		
4	-0.2077E+00	0.4342E-02	0.3834E+00	0.1000E+01	
5	-0.2688E+00	0.3347E+00	0.6868E-01	-0.6915E+00	0.1000E+01

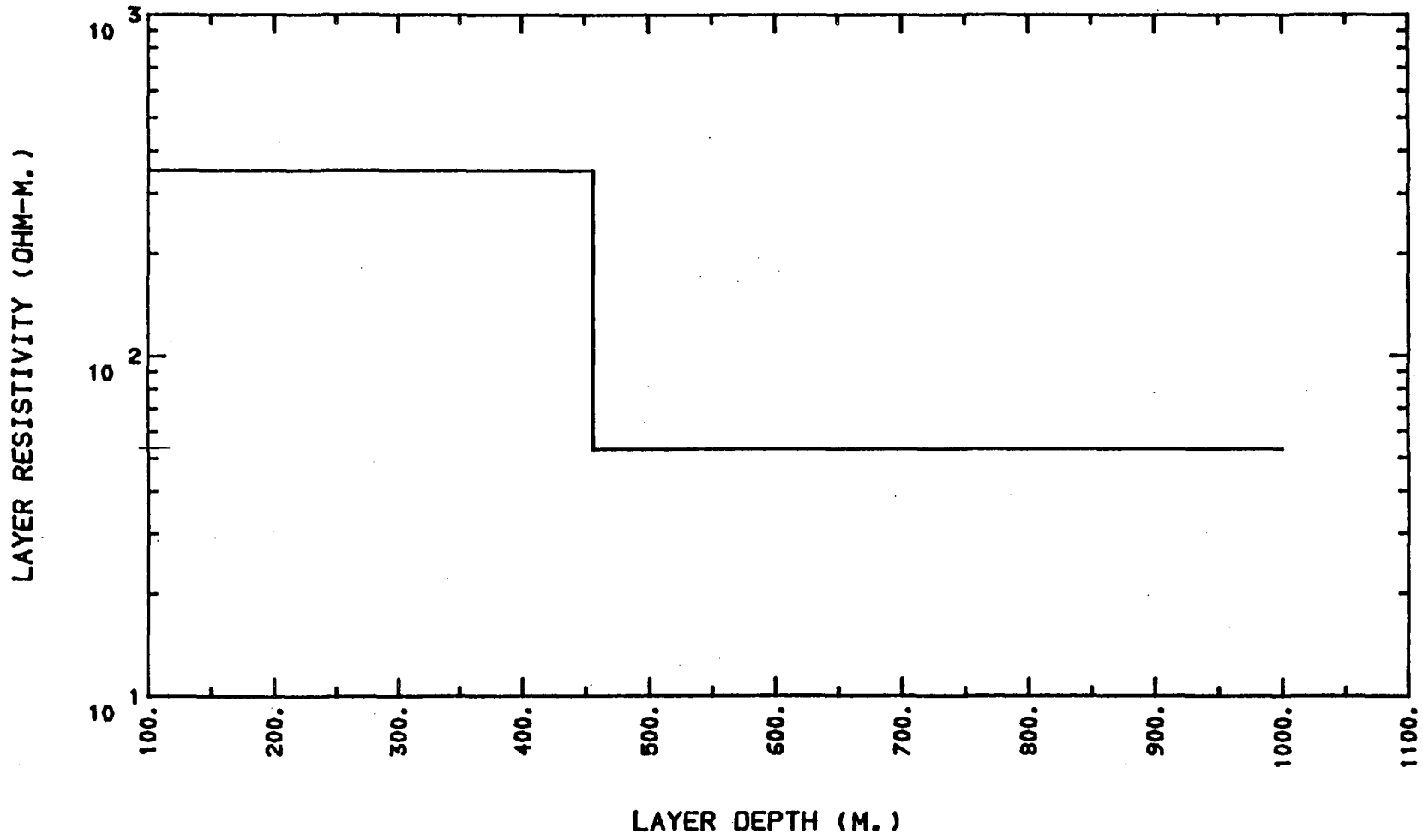
	**PARAM_SOL.	STD_ERROR	REL_ERROR	% ERROR **
1	0.1113E-02	0.5115E-03	0.4595E+00	0.4595E+02
2	0.5592E-02	0.1418E-02	0.2535E+00	0.2535E+02
3	0.1645E-01	0.1588E-02	0.9654E-01	0.9654E+01
4	0.2855E+03	0.5506E-02	0.1929E-04	0.1929E-02
5	0.1249E+03	0.1284E-01	0.1029E-03	0.1029E-01

PARAMETER NAME	FINAL SOLUTION	RESISTIVITY	LAYER DEPTH
1 SIGMA( 1) =	0.11131888E-02	1 0.89832019E+03	
2 SIGMA( 2) =	0.55924091E-02	2 0.17881381E+03	
3 SIGMA( 3) =	0.16453654E-01	3 0.60776775E+02	
4 THICK( 1) =	0.28549359E+03		1 0.28549359E+03
5 THICK( 2) =	0.12487097E+03		2 0.41036456E+03
6 SHIFT =	0.10000000E+01		

Newberry Crater NB-9 2 LAYER



Newberry Crater NB-9 2 LAYER



<NLSTCI2>: Newberry Crater NB-10 2 layer

A= 0.257900E+03

PARAMETERS HELD FIXED: IB= 4

\*\*\*\*\* VARIABILITY CONVERGENCE \*\*\*\*\*

I	OBS.Y(I)	CAL	RES	%RES.ERR	X(I,1)
1	0.539000E+03	0.523273E+03	0.157E+02	0.300541E+01	0.120000E-02
2	0.443000E+03	0.457858E+03	-0.149E+02	-0.324510E+01	0.160000E-02
3	0.381000E+03	0.393085E+03	-0.121E+02	-0.307434E+01	0.200000E-02
4	0.315000E+03	0.322468E+03	-0.747E+01	-0.231587E+01	0.260000E-02
5	0.262000E+03	0.256666E+03	0.533E+01	0.207836E+01	0.340000E-02
6	0.219000E+03	0.215065E+03	0.394E+01	0.182989E+01	0.420000E-02
7	0.191000E+03	0.187299E+03	0.370E+01	0.197580E+01	0.500000E-02
8	0.169000E+03	0.166005E+03	0.299E+01	0.180404E+01	0.580000E-02
9	0.148000E+03	0.142660E+03	0.534E+01	0.374319E+01	0.700000E-02
10	0.125000E+03	0.122390E+03	0.261E+01	0.213232E+01	0.860000E-02
11	0.107000E+03	0.108043E+03	-0.104E+01	-0.965572E+00	0.102000E-01
12	0.962000E+02	0.974934E+02	-0.129E+01	-0.132664E+01	0.118000E-01
13	0.902000E+02	0.894735E+02	0.726E+00	0.811957E+00	0.134000E-01
14	0.794000E+02	0.804204E+02	-0.102E+01	-0.126885E+01	0.158000E-01
15	0.704000E+02	0.717131E+02	-0.131E+01	-0.183098E+01	0.190000E-01
16	0.624000E+02	0.653913E+02	-0.299E+01	-0.457447E+01	0.222000E-01

\*\* RMSERR= 0.77798038E+01

CORRELATION MATRIX

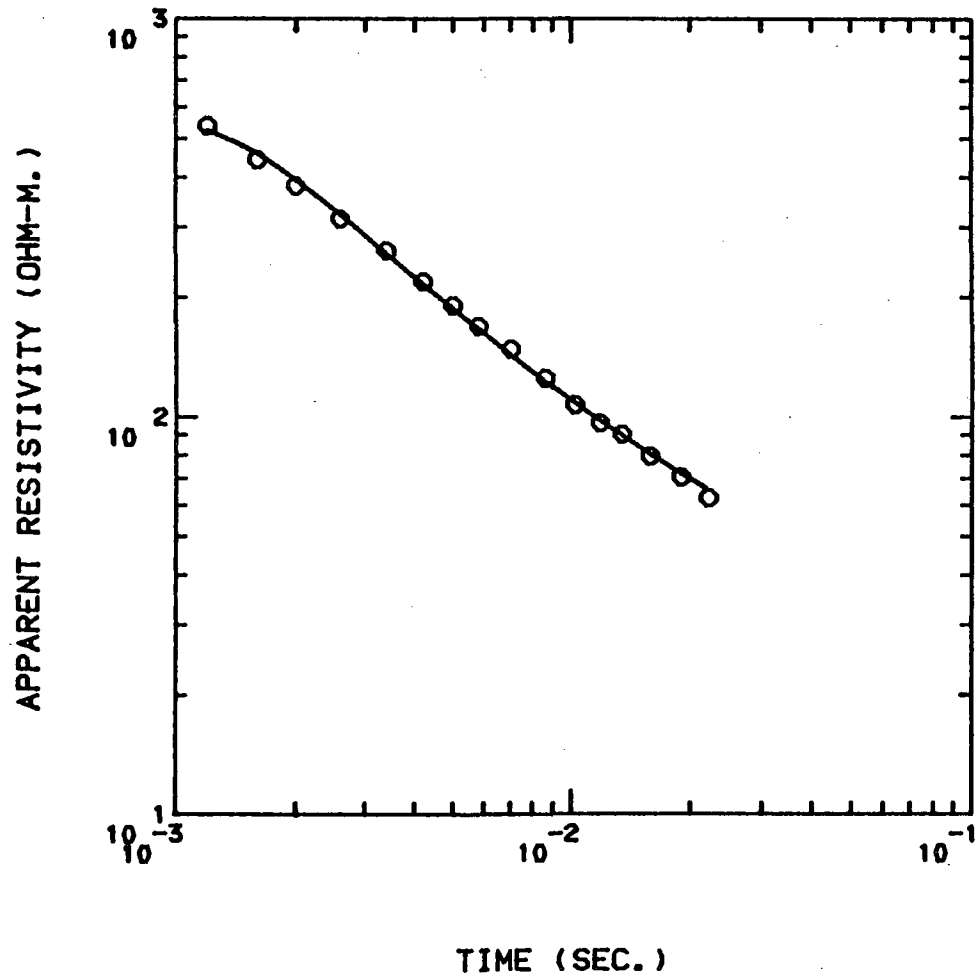
1	0.1000E+01		
2	-0.6231E-01	0.1000E+01	
3	0.1745E+00	-0.6711E-01	0.1000E+01

**PARAM_SOL.	STD_ERROR	REL_ERROR	% ERROR **
1	0.2416E-02	0.7581E-04	0.3138E-01
2	0.6271E-01	0.1437E-02	0.2292E-01
3	0.6375E+03	0.1853E-02	0.2907E-05

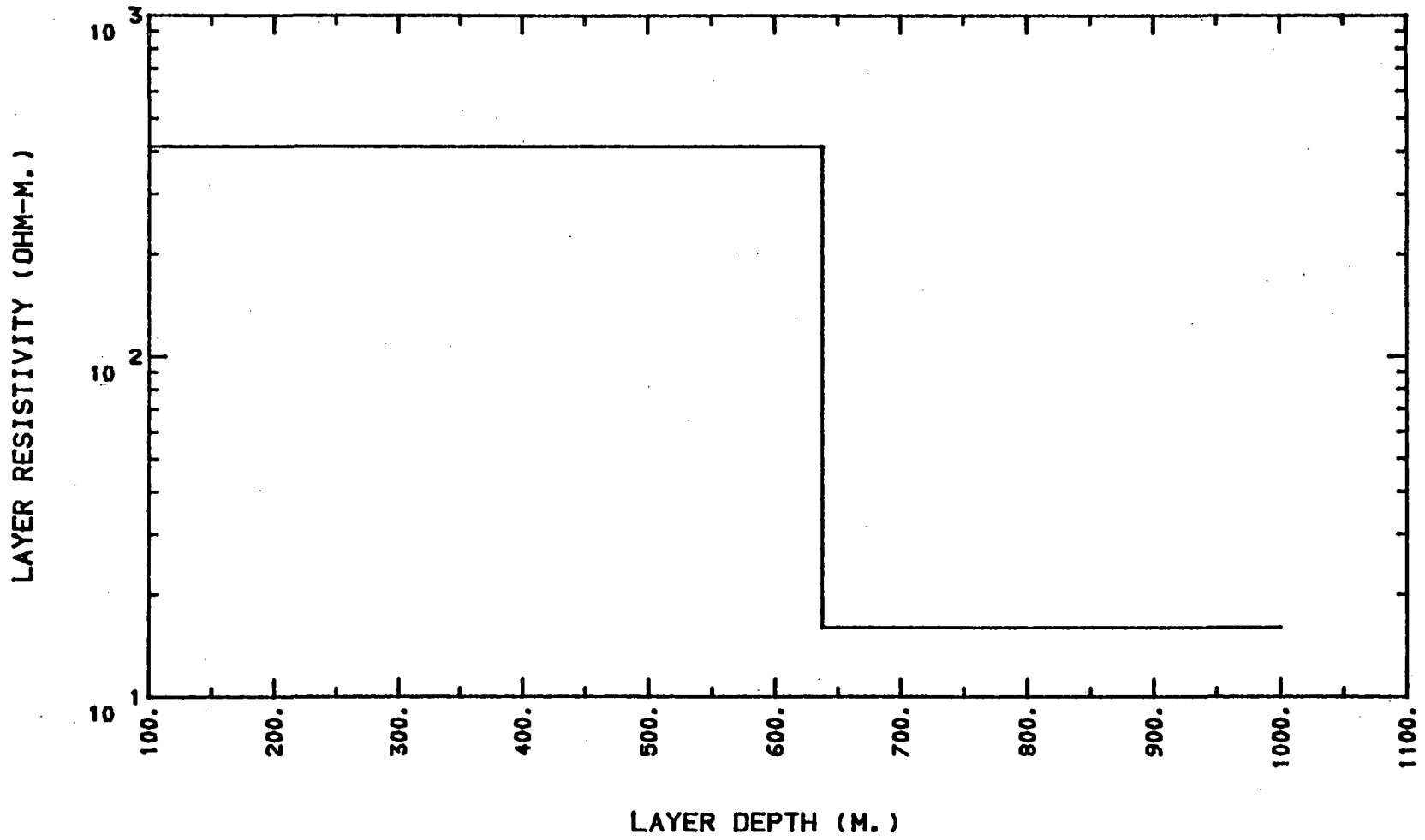
PARAMETER NAME	FINAL SOLUTION	RESISTIVITY	LAYER DEPTH
1 SIGMA( 1) =	0.24156065E-02	1 0.41397470E+03	
2 SIGMA( 2) =	0.62712103E-01	2 0.15945886E+02	
3 THICK( 1) =	0.63750897E+03		1 0.63750897E+03
4 SHIFT =	0.10000000E+01		



Newberry Crater NB-10 2 layer



Newberry Crater NB-10 2 layer



<NLSTCI2>: Newberry Crater NB-11 2 layer

A= 0.257900E+03

PARAMETERS HELD FIXED: IB= 4

\*\*\*\* X-CONVERGENCE \*\*\*\*

I	OBS.Y(I)	CAL	RES	%RES.ERR	X(I,1)
1	0.511000E+03	0.511044E+03	-0.441E-01	-0.863495E-02	0.120000E-02
2	0.398000E+03	0.400054E+03	-0.205E+01	-0.513450E+00	0.160000E-02
3	0.333000E+03	0.333795E+03	-0.795E+00	-0.238119E+00	0.200000E-02
4	0.270000E+03	0.273230E+03	-0.323E+01	-0.118199E+01	0.260000E-02
5	0.227000E+03	0.225479E+03	0.152E+01	0.674392E+00	0.340000E-02
6	0.194000E+03	0.195854E+03	-0.185E+01	-0.946533E+00	0.420000E-02
7	0.188000E+03	0.175486E+03	0.125E+02	0.713130E+01	0.500000E-02
8	0.165000E+03	0.160469E+03	0.453E+01	0.282360E+01	0.580000E-02
9	0.141000E+03	0.144145E+03	-0.315E+01	-0.218194E+01	0.700000E-02
10	0.127000E+03	0.129199E+03	-0.220E+01	-0.170174E+01	0.860000E-02
11	0.124000E+03	0.118645E+03	0.536E+01	0.451360E+01	0.102000E-01
12	0.107000E+03	0.110743E+03	-0.374E+01	-0.337975E+01	0.118000E-01
13	0.107000E+03	0.104595E+03	0.240E+01	0.229900E+01	0.134000E-01
14	0.101000E+03	0.975181E+02	0.348E+01	0.357051E+01	0.158000E-01
15	0.856000E+02	0.906268E+02	-0.503E+01	-0.554673E+01	0.190000E-01
16	0.822000E+02	0.854293E+02	-0.323E+01	-0.378006E+01	0.222000E-01

\*\* RMSERR= 0.48768506E+01

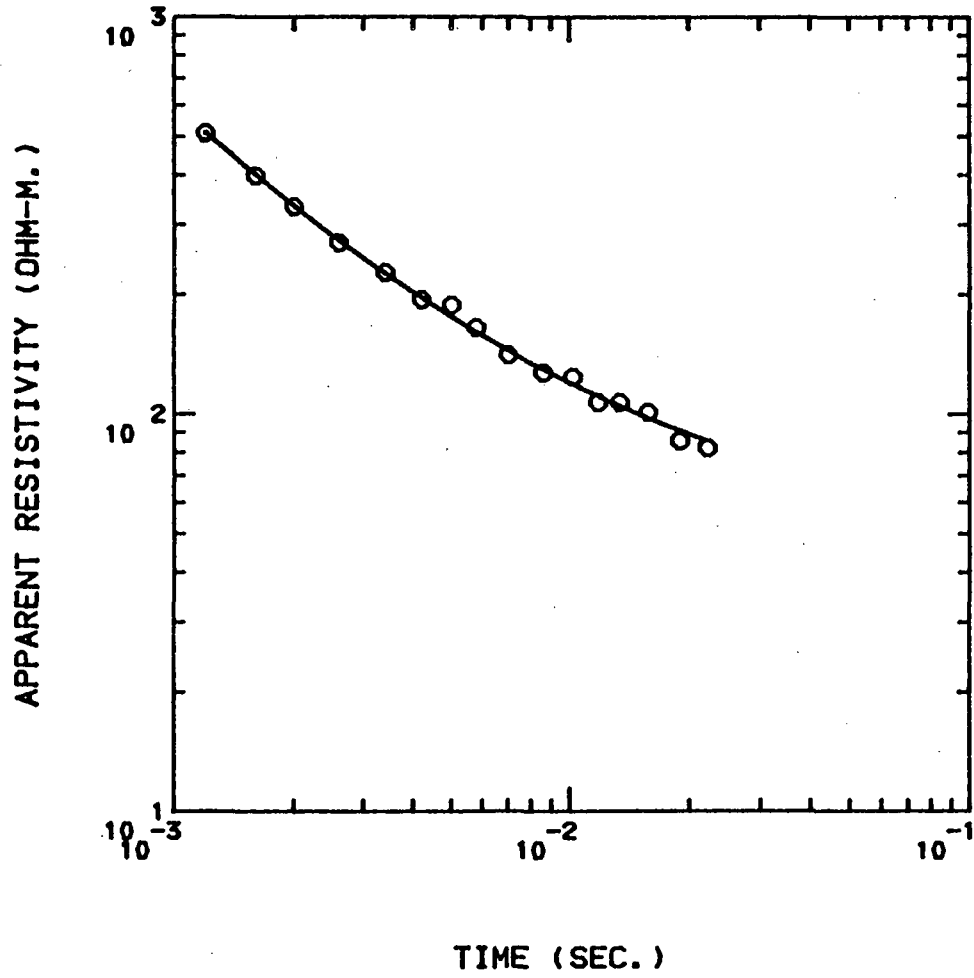
CORRELATION MATRIX

1	0.1000E+01		
2	0.1796E-01	0.1000E+01	
3	0.2936E+00	0.6251E+00	0.1000E+01

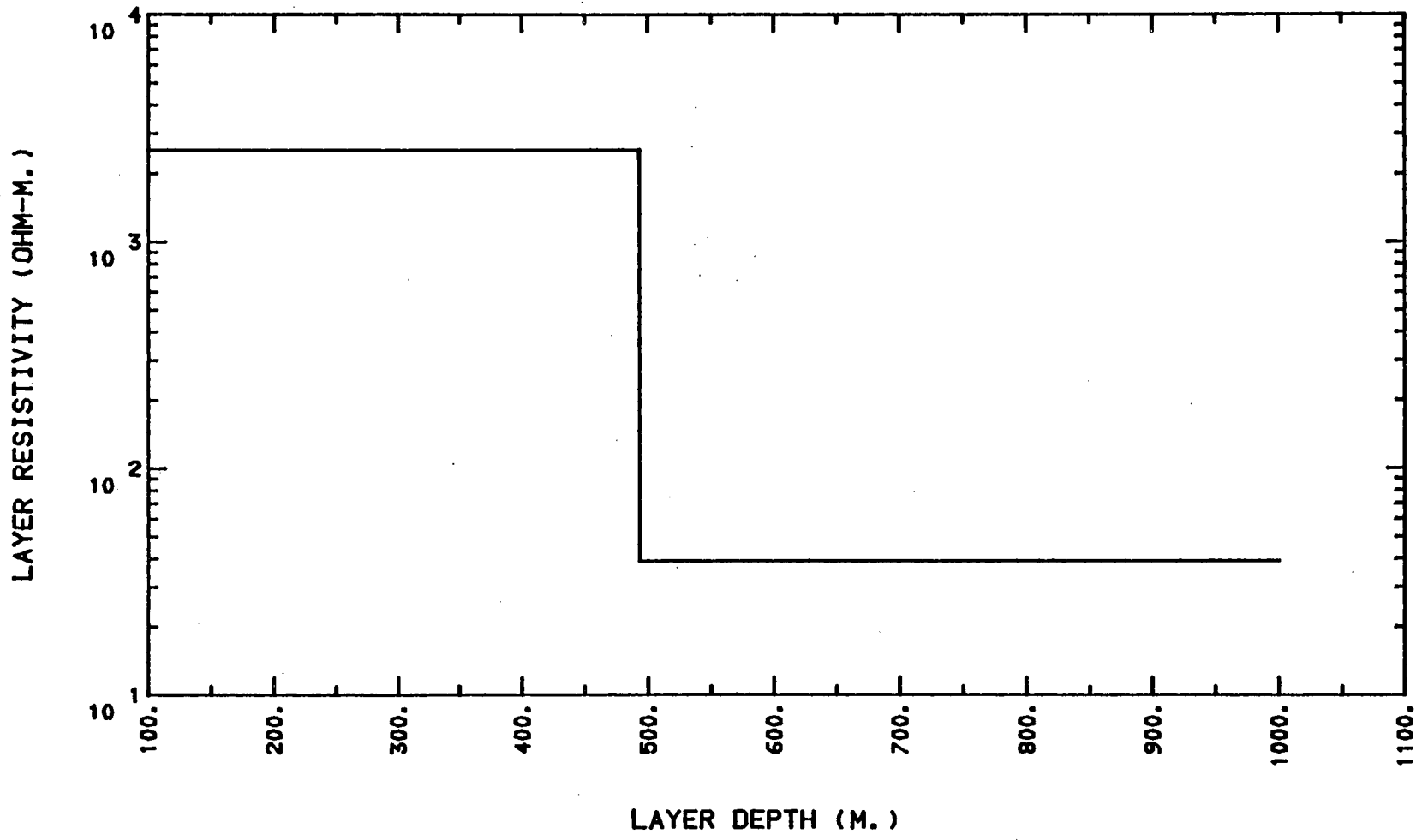
**PARAM_SOL.	STD_ERROR	REL_ERROR	% ERROR **
1	0.3953E-03	0.7494E-04	0.1896E+00
2	0.2566E-01	0.6324E-03	0.2464E-01
3	0.4935E+03	0.2192E-02	0.4441E-05

PARAMETER NAME	FINAL SOLUTION	RESISTIVITY	LAYER DEPTH
1 SIGMA( 1) =	0.39529626E-03	1 0.25297483E+04	
2 SIGMA( 2) =	0.25664145E-01	2 0.38964867E+02	
3 THICK( 1) =	0.49351880E+03		1 0.49351880E+03
4 SHIFT =	0.10000000E+01		

Newberry Crater NB-11 2 layer



Newberry Crater NB-11 2 layer



<NLSTCI2>: Newberry Crater NB-12 2 layer

A= 0.129000E+03

PARAMETERS HELD FIXED: IS= 4

\*\*\*\*\* X-CONVERGENCE \*\*\*\*\*

I	OBS.Y(I)	CAL	RES	%RES.ERR	X(I,1)
1	0.222000E+03	0.205097E+03	0.169E+02	0.824121E+01	0.120000E-02
2	0.185000E+03	0.183050E+03	0.195E+01	0.106537E+01	0.160000E-02
3	0.156000E+03	0.158874E+03	-0.287E+01	-0.180923E+01	0.200000E-02
4	0.127000E+03	0.131147E+03	-0.415E+01	-0.316236E+01	0.260000E-02
5	0.103000E+03	0.106417E+03	-0.342E+01	-0.321052E+01	0.340000E-02
6	0.879000E+02	0.893017E+02	-0.140E+01	-0.156963E+01	0.420000E-02
7	0.770000E+02	0.780401E+02	-0.104E+01	-0.133277E+01	0.500000E-02
8	0.690000E+02	0.698488E+02	-0.849E+00	-0.121518E+01	0.580000E-02
9	0.603000E+02	0.603924E+02	-0.924E-01	-0.152967E+00	0.700000E-02
10	0.525000E+02	0.520053E+02	0.495E+00	0.951281E+00	0.860000E-02
11	0.480000E+02	0.462502E+02	0.175E+01	0.378337E+01	0.102000E-01
12	0.432000E+02	0.419067E+02	0.129E+01	0.308620E+01	0.118000E-01
13	0.406000E+02	0.385644E+02	0.204E+01	0.527852E+01	0.134000E-01
14	0.369000E+02	0.348168E+02	0.208E+01	0.598340E+01	0.158000E-01
15	0.323000E+02	0.312262E+02	0.107E+01	0.343866E+01	0.190000E-01

\*\* RMSERR= 0.53620958E+01

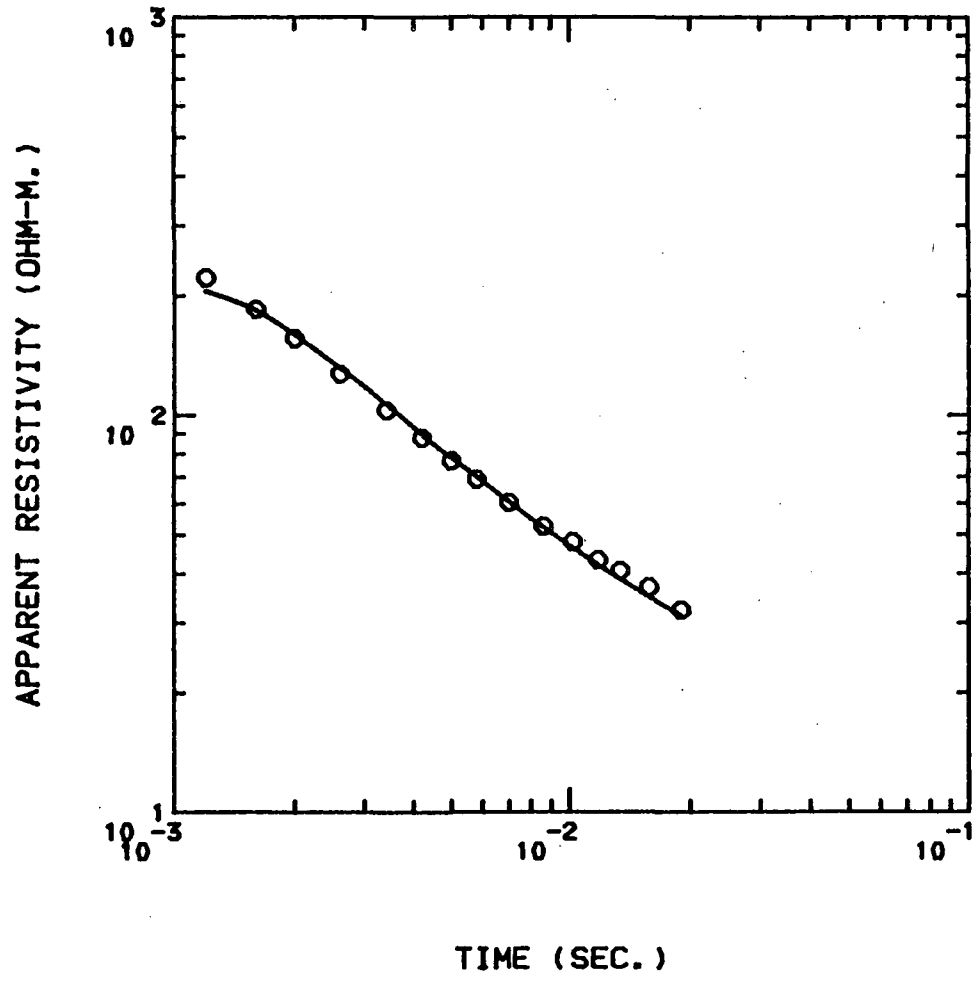
CORRELATION MATRIX

1	0.1000E+01		
2	0.2146E+00	0.1000E+01	
3	-0.6170E+00	0.9738E-01	0.1000E+01

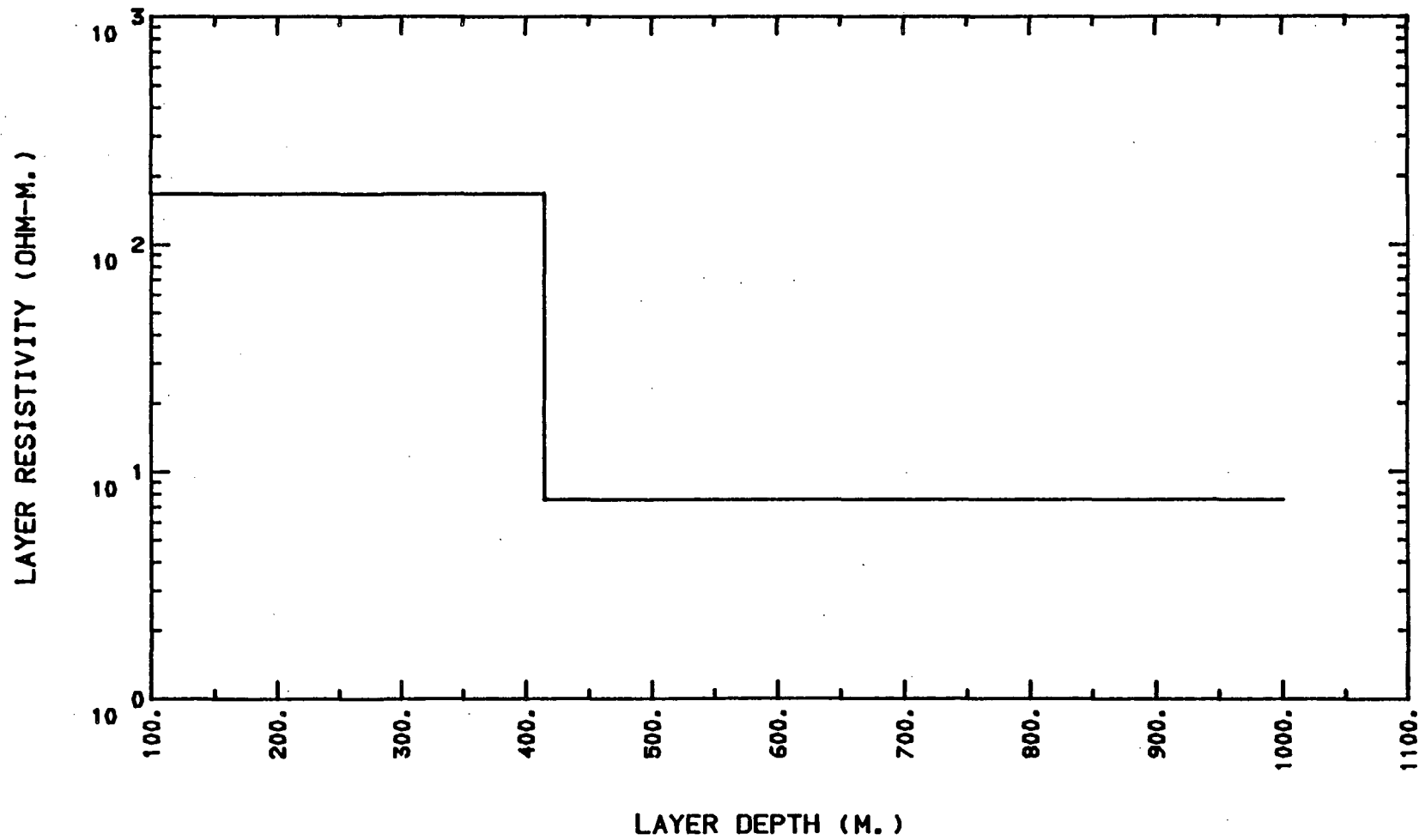
**PARAM_SOL.	STD_ERROR	REL_ERROR	% ERROR **
1	0.6000E-02	0.1981E-03	0.3302E-01
2	0.1330E+00	0.3297E-02	0.2478E-01
3	0.4147E+03	0.2822E-02	0.6807E-05

PARAMETER NAME	FINAL SOLUTION	RESISTIVITY	LAYER DEPTH
1 SIGMA( 1) =	0.59996559E-02	1 0.16667622E+03	
2 SIGMA( 2) =	0.13302813E+00	2 0.75172067E+01	
3 THICK( 1) =	0.41465356E+03		1 0.41465356E+03
4 SHIFT =	0.10000000E+01		

Newberry Crater NB-12 2 layer



Newberry Crater NB-12 2 layer





<NLSTCI2>: Newberry Crater NB-13 3 layer

A= 0.129000E+03

PARAMETERS HELD FIXED: IB= 6

\*\*\*\*\* X-CONVERGENCE \*\*\*\*\*

I	OBS.Y(I)	CAL	RES	%RES.ERR	X(I,1)
1	0.145000E+03	0.145252E+03	-0.252E+00	-0.173659E+00	0.120000E-02
2	0.133000E+03	0.132123E+03	0.877E+00	0.663670E+00	0.160000E-02
3	0.124000E+03	0.122460E+03	0.154E+01	0.125743E+01	0.200000E-02
4	0.110000E+03	0.111647E+03	-0.165E+01	-0.147520E+01	0.260000E-02
5	0.992000E+02	0.100071E+03	-0.871E+00	-0.870052E+00	0.340000E-02
6	0.894000E+02	0.907704E+02	-0.137E+01	-0.150974E+01	0.420000E-02
7	0.840000E+02	0.837284E+02	0.272E+00	0.324390E+00	0.500000E-02
8	0.761000E+02	0.779535E+02	-0.185E+01	-0.237766E+01	0.580000E-02
9	0.695000E+02	0.708854E+02	-0.139E+01	-0.195437E+01	0.700000E-02
10	0.623000E+02	0.638322E+02	-0.153E+01	-0.240033E+01	0.860000E-02
11	0.603000E+02	0.585505E+02	0.175E+01	0.298807E+01	0.102000E-01
12	0.558000E+02	0.543315E+02	0.147E+01	0.270278E+01	0.118000E-01
13	0.549000E+02	0.508654E+02	0.403E+01	0.793187E+01	0.134000E-01
14	0.479000E+02	0.465727E+02	0.133E+01	0.284992E+01	0.158000E-01
15	0.433000E+02	0.420429E+02	0.126E+01	0.299014E+01	0.190000E-01
16	0.367000E+02	0.386602E+02	-0.196E+01	-0.507042E+01	0.222000E-01

\*\* RMSERR= 0.20227797E+01

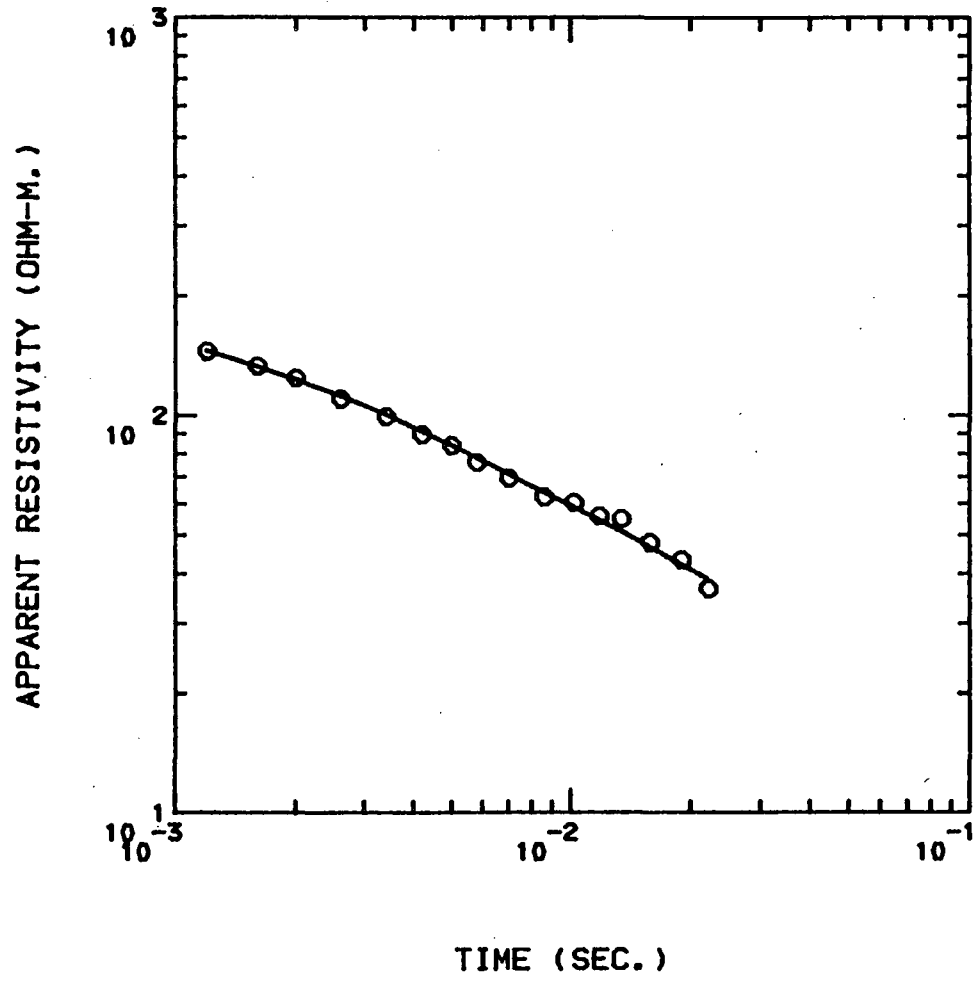
CORRELATION MATRIX

1	0.1000E+01				
2	-0.6194E+00	0.1000E+01			
3	-0.1043E+00	-0.4634E+00	0.1000E+01		
4	-0.5828E+00	0.9288E+00	-0.5044E+00	0.1000E+01	
5	0.5709E+00	-0.8789E+00	0.1984E+00	-0.8589E+00	0.1000E+01

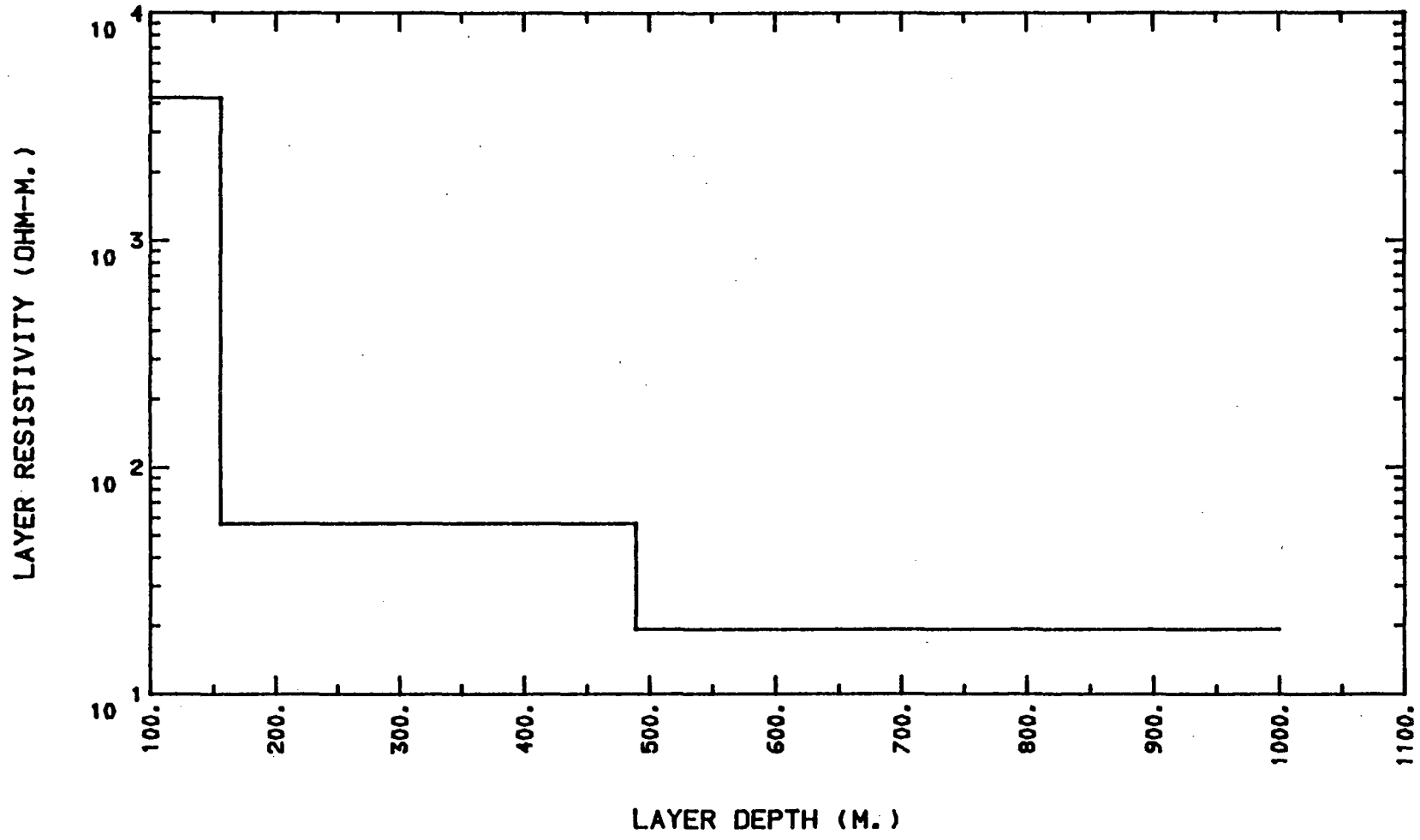
**	PARAM_SOL.	STD_ERROR	REL_ERROR	% ERROR	**
1	0.2360E-03	0.6390E-04	0.2707E+00	0.2707E+02	
2	0.1770E-01	0.6303E-03	0.3560E-01	0.3560E+01	
3	0.5187E-01	0.1506E-02	0.2904E-01	0.2904E+01	
4	0.1557E+03	0.5029E-02	0.3229E-04	0.3229E-02	
5	0.3333E+03	0.1019E-01	0.3056E-04	0.3056E-02	

PARAMETER NAME	FINAL SOLUTION	RESISTIVITY	LAYER DEPTH
1 SIGMA( 1) =	0.23603022E-03	1 0.42367456E+04	
2 SIGMA( 2) =	0.17703634E-01	2 0.56485580E+02	
3 SIGMA( 3) =	0.51869310E-01	3 0.19279222E+02	
4 THICK( 1) =	0.15571378E+03		1 0.15571378E+03
5 THICK( 2) =	0.33328336E+03		2 0.48899713E+03
6 SHIFT =	0.10000000E+01		

Newberry Crater NB-13 3 layer



Newberry Crater NB-13 3 layer



<NLSTCI2>: Newberry Crater NB-14 3 layer

A= 0.129000E+03

PARAMETERS HELD FIXED: IB= 6

\*\*\*\*\* X-CONVERGENCE \*\*\*\*\*

I	OBS.Y(I)	CAL	RES	%RES.ERR	X(I,1)
1	0.199000E+03	0.187446E+03	0.116E+02	0.616379E+01	0.120000E-02
2	0.165000E+03	0.166806E+03	-0.181E+01	-0.108241E+01	0.160000E-02
3	0.144000E+03	0.149318E+03	-0.532E+01	-0.356172E+01	0.200000E-02
4	0.124000E+03	0.129179E+03	-0.518E+01	-0.400936E+01	0.260000E-02
5	0.109000E+03	0.110290E+03	-0.129E+01	-0.116925E+01	0.340000E-02
6	0.981000E+02	0.981234E+02	-0.234E-01	-0.238080E-01	0.420000E-02
7	0.908000E+02	0.890088E+02	0.179E+01	0.201238E+01	0.500000E-02
8	0.848000E+02	0.818478E+02	0.295E+01	0.360688E+01	0.580000E-02
9	0.761000E+02	0.741803E+02	0.192E+01	0.258784E+01	0.700000E-02
10	0.680000E+02	0.670097E+02	0.990E+00	0.147782E+01	0.860000E-02
11	0.618000E+02	0.617188E+02	0.812E-01	0.131502E+00	0.102000E-01
12	0.592000E+02	0.577922E+02	0.141E+01	0.243600E+01	0.118000E-01
13	0.553000E+02	0.547372E+02	0.563E+00	0.102815E+01	0.134000E-01
14	0.506000E+02	0.511800E+02	-0.580E+00	-0.113323E+01	0.158000E-01
15	0.472000E+02	0.477131E+02	-0.513E+00	-0.107538E+01	0.190000E-01

\*\* RMSERR= 0.46153741E+01

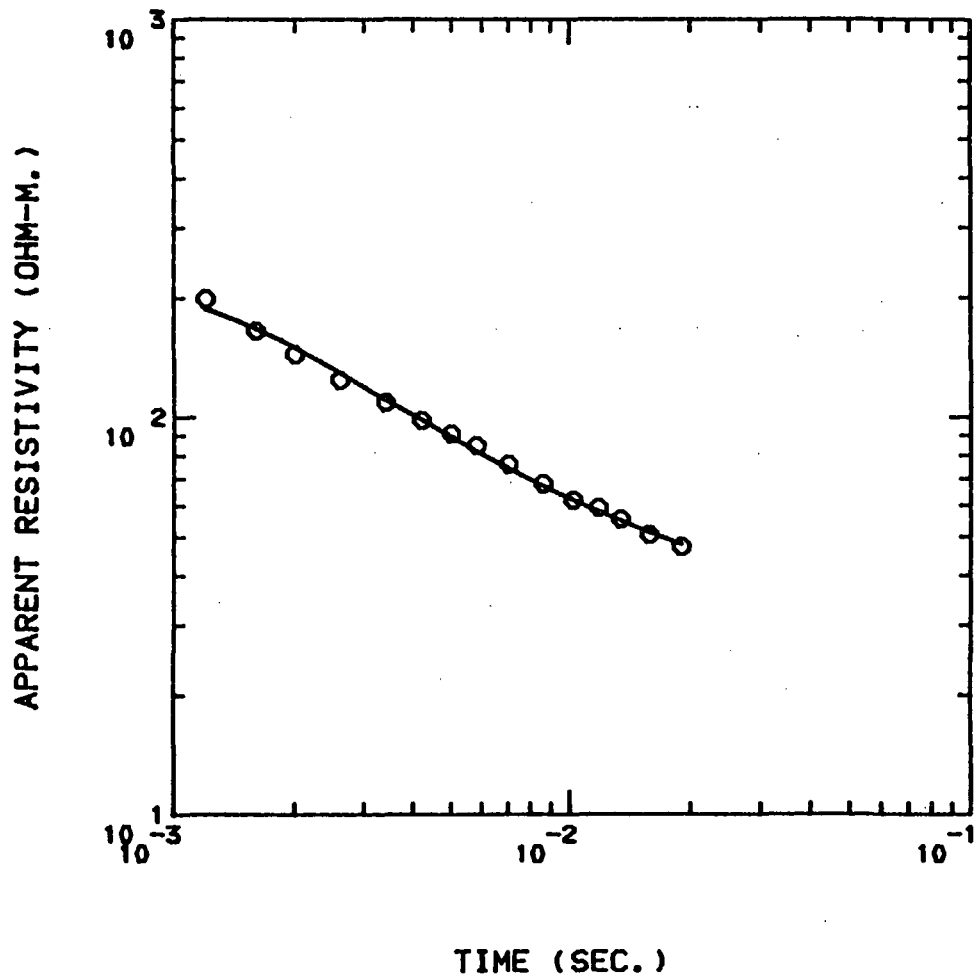
CORRELATION MATRIX

1	0.1000E+01				
2	0.1015E-01	0.1000E+01			
3	-0.1733E+00	-0.5940E+00	0.1000E+01		
4	-0.1797E-01	0.3896E+00	-0.2776E+00	0.1000E+01	
5	0.6491E-01	-0.5181E+00	0.2617E+00	-0.8175E+00	0.1000E+01

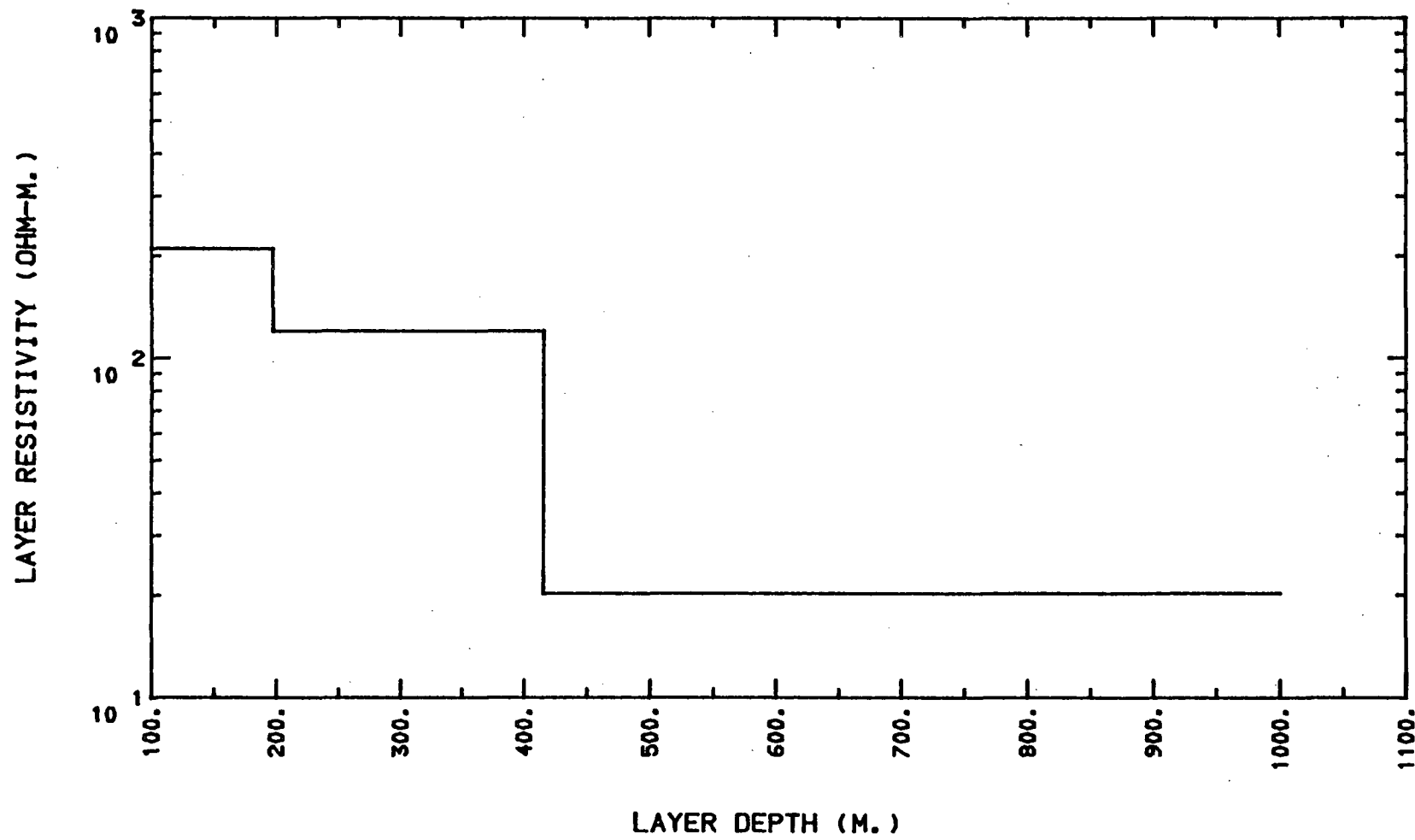
**	PARAM_SQL.	STD_ERROR	REL_ERROR	% ERROR **
1	0.4759E-02	0.9058E-04	0.1903E-01	0.1903E+01
2	0.8331E-02	0.4777E-03	0.5735E-01	0.5735E+01
3	0.4932E-01	0.9405E-03	0.1907E-01	0.1907E+01
4	0.1971E+03	0.3820E-02	0.1938E-04	0.1938E-02
5	0.2184E+03	0.4690E-02	0.2147E-04	0.2147E-02

PARAMETER NAME	FINAL SOLUTION	RESISTIVITY	LAYER DEPTH
1 SIGMA( 1) =	0.47591785E-02	1 0.21012030E+03	
2 SIGMA( 2) =	0.83308360E-02	2 0.12003597E+03	
3 SIGMA( 3) =	0.49321495E-01	3 0.20275135E+02	
4 THICK( 1) =	0.19714076E+03		1 0.19714076E+03
5 THICK( 2) =	0.21840993E+03		2 0.41555069E+03
6 SHIFT =	0.10000000E+01		

Newberry Crater NB-14 3 layer



Newberry Crater NB-14 3 layer



<NLSTCI2>: Newberry Crater NB-15 2 layer

A= 0.129000E+03

PARAMETERS HELD FIXED: IB= 4

\*\*\*\*\* X-CONVERGENCE \*\*\*\*\*

I	OBS.Y(I)	CAL	RES	%RES.ERR	X(I,1)
1	0.330000E+03	0.286423E+03	0.436E+02	0.152142E+02	0.120000E-02
2	0.275000E+03	0.278239E+03	-0.324E+01	-0.116421E+01	0.160000E-02
3	0.240000E+03	0.258164E+03	-0.182E+02	-0.703567E+01	0.200000E-02
4	0.204000E+03	0.221843E+03	-0.178E+02	-0.804305E+01	0.260000E-02
5	0.177000E+03	0.184055E+03	-0.706E+01	-0.383316E+01	0.340000E-02
6	0.161000E+03	0.157122E+03	0.388E+01	0.246810E+01	0.420000E-02
7	0.141000E+03	0.136316E+03	0.468E+01	0.343587E+01	0.500000E-02
8	0.123000E+03	0.121359E+03	0.164E+01	0.135216E+01	0.580000E-02
9	0.111000E+03	0.105800E+03	0.520E+01	0.491459E+01	0.700000E-02
10	0.897000E+02	0.905564E+02	-0.856E+00	-0.945700E+00	0.860000E-02
11	0.824000E+02	0.799727E+02	0.243E+01	0.303516E+01	0.102000E-01
12	0.722000E+02	0.724338E+02	-0.234E+00	-0.322792E+00	0.118000E-01
13	0.693000E+02	0.665638E+02	0.274E+01	0.411068E+01	0.134000E-01
14	0.630000E+02	0.597228E+02	0.328E+01	0.548733E+01	0.158000E-01
15	0.563000E+02	0.532646E+02	0.304E+01	0.569878E+01	0.190000E-01

\*\* RMSERR= 0.15023120E+02

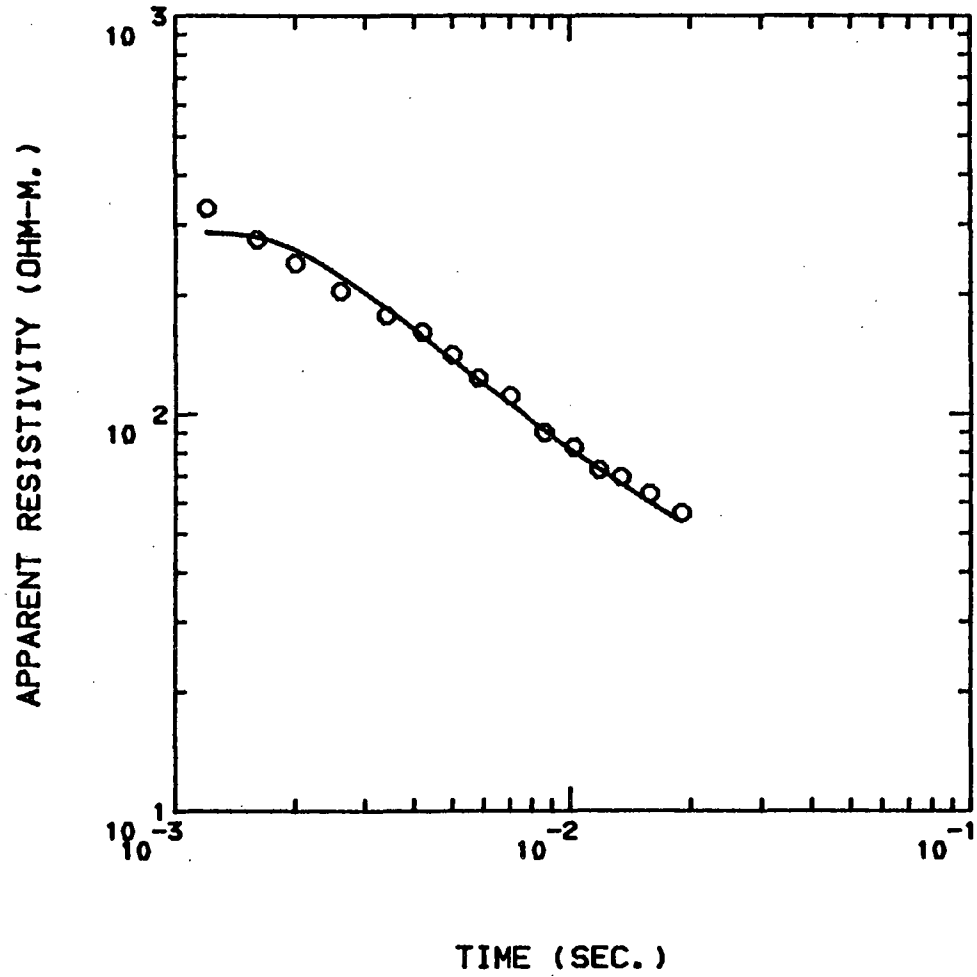
CORRELATION MATRIX

1	0.1000E+01		
2	-0.1627E+00	0.1000E+01	
3	0.1351E+00	-0.8361E-01	0.1000E+01

**PARAM_SOL.	STD_ERROR	REL_ERROR	% ERROR **
1	0.4304E-02	0.1858E-03	0.4317E-01
2	0.8631E-01	0.2860E-02	0.3314E-01
3	0.5672E+03	0.3545E-02	0.6250E-05

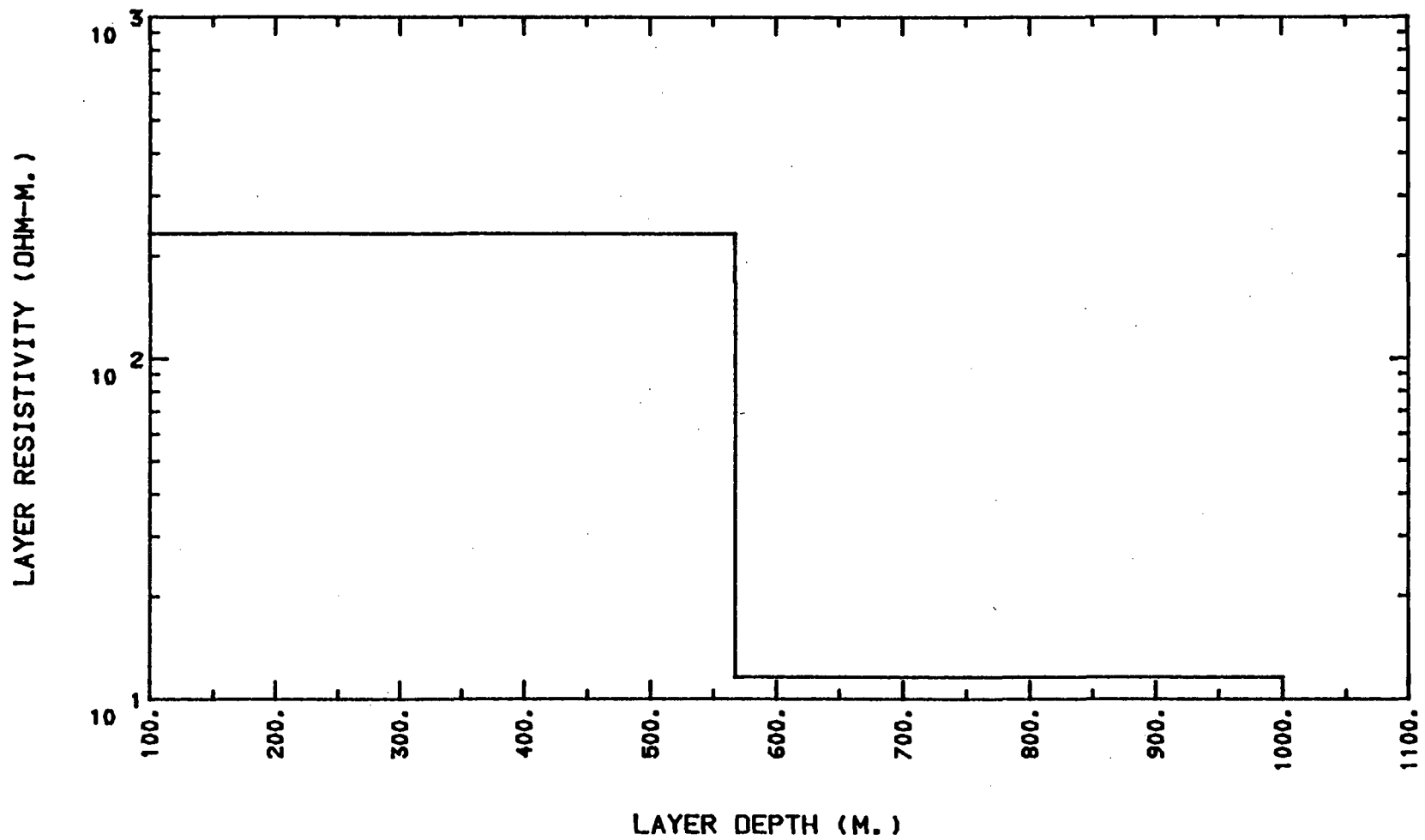
PARAMETER NAME	FINAL SOLUTION	RESISTIVITY	LAYER DEPTH
1 SIGMA( 1) =	0.43036090E-02	1 0.23236311E+03	
2 SIGMA( 2) =	0.86310074E-01	2 0.11586133E+02	
3 THICK( 1) =	0.56717145E+03		1 0.56717145E+03
4 SHIFT =	0.10000000E+01		

Newberry Crater NB-15 2 layer





Newberry Crater NB-15 2 layer



<NLSTCI2>: Newberry Crater NB-16 3 layer

A= 0.129000E+03

PARAMETERS HELD FIXED: IB= 6

\*\*\*\*\* X-CONVERGENCE \*\*\*\*\*

I	OBS.Y(I)	CAL	RES	%RES.ERR	X(I,1)
1	0.487000E+03	0.475804E+03	0.112E+02	0.235300E+01	0.120000E-02
2	0.404000E+03	0.399945E+03	0.405E+01	0.101380E+01	0.160000E-02
3	0.353000E+03	0.353157E+03	-0.157E+00	-0.443302E-01	0.200000E-02
4	0.294000E+03	0.303925E+03	-0.992E+01	-0.326556E+01	0.260000E-02
5	0.245000E+03	0.255699E+03	-0.107E+02	-0.418405E+01	0.340000E-02
6	0.215000E+03	0.220194E+03	-0.519E+01	-0.235905E+01	0.420000E-02
7	0.191000E+03	0.193154E+03	-0.215E+01	-0.111529E+01	0.500000E-02
8	0.170000E+03	0.171463E+03	-0.146E+01	-0.853279E+00	0.580000E-02
9	0.144000E+03	0.146226E+03	-0.223E+01	-0.152241E+01	0.700000E-02
10	0.124000E+03	0.122622E+03	0.138E+01	0.112376E+01	0.860000E-02
11	0.109000E+03	0.105664E+03	0.334E+01	0.315670E+01	0.102000E-01
12	0.973000E+02	0.927126E+02	0.459E+01	0.494793E+01	0.118000E-01
13	0.888000E+02	0.827934E+02	0.601E+01	0.725497E+01	0.134000E-01
14	0.764000E+02	0.714898E+02	0.491E+01	0.686846E+01	0.158000E-01

\*\* RMSERR= 0.73616719E+01

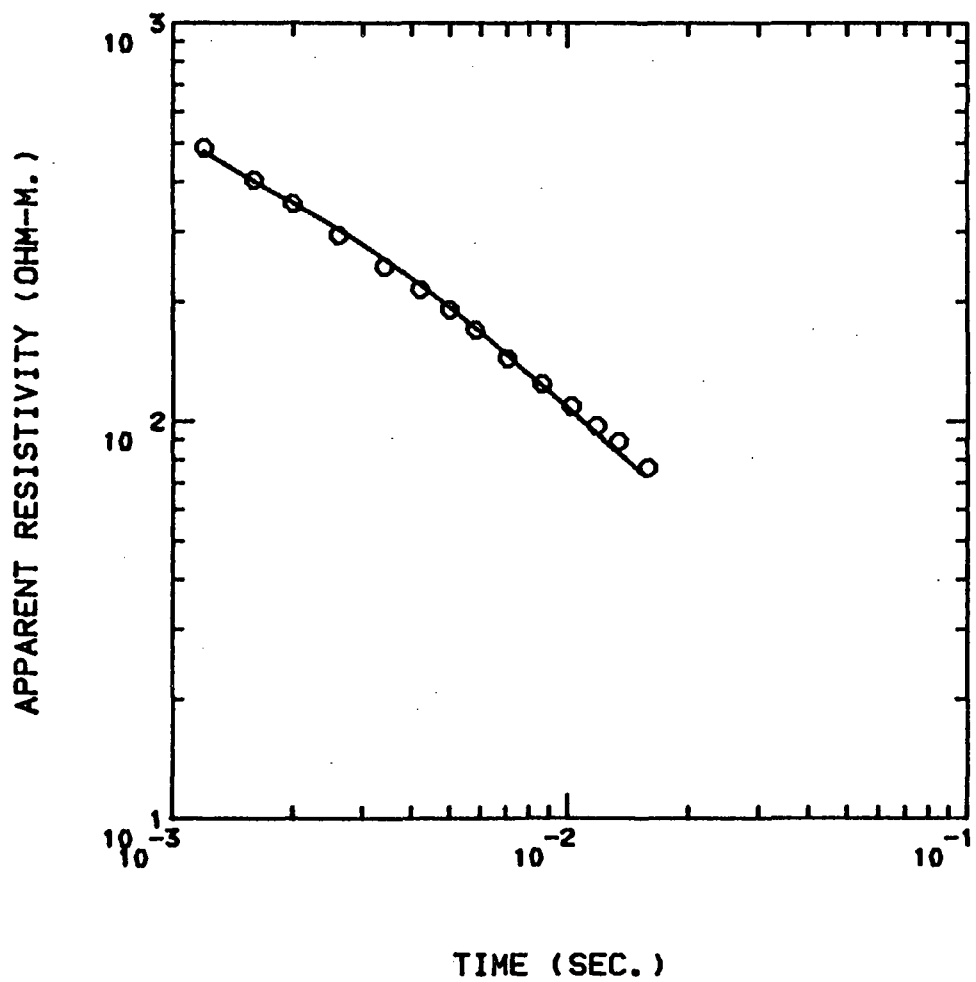
CORRELATION MATRIX

1	0.1000E+01				
2	-0.7277E+00	0.1000E+01			
3	-0.8195E+00	0.5012E+00	0.1000E+01		
4	-0.2315E+00	0.5397E+00	-0.1860E-01	0.1000E+01	
5	0.2992E+00	-0.6481E+00	-0.1194E+00	-0.6639E+00	0.1000E+01

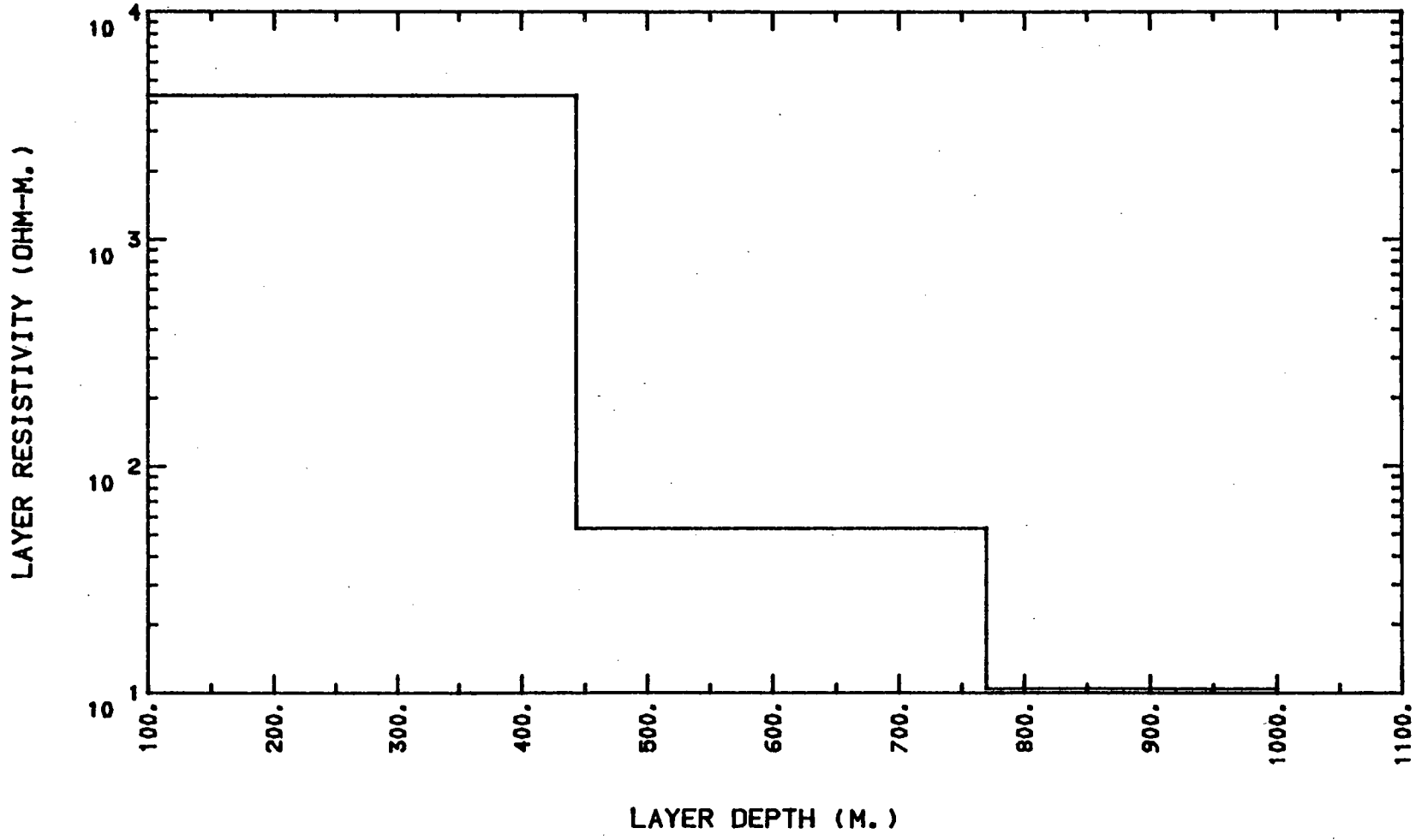
**	PARAM_SOL.	STD_ERROR	REL_ERROR	% ERROR	**
1	0.2334E-03	0.3555E-04	0.1523E+00	0.1523E+02	
2	0.1881E-01	0.5441E-03	0.2893E-01	0.2893E+01	
3	0.9594E-01	0.1294E-02	0.1348E-01	0.1348E+01	
4	0.4431E+03	0.2345E-02	0.5293E-05	0.5293E-03	
5	0.3264E+03	0.3344E-02	0.1025E-04	0.1025E-02	

PARAMETER NAME	FINAL SOLUTION	RESISTIVITY	LAYER DEPTH
1 SIGMA( 1) =	0.23338229E-03	1 0.42848154E+04	
2 SIGMA( 2) =	0.18810613E-01	2 0.53161480E+02	
3 SIGMA( 3) =	0.95942847E-01	3 0.10422872E+02	
4 THICK( 1) =	0.44313925E+03		1 0.44313925E+03
5 THICK( 2) =	0.32636188E+03		2 0.76950116E+03
6 SHIFT =	0.10000000E+01		

Newberry Crater NB-16 3 layer



Newberry Crater NB-16 3 layer



<NLSTCI2>: Newberry Crater NB-17 3 layer

A= 0.129000E+03

PARAMETERS HELD FIXED: IB= 6

\*\*\*\*\* VARIABILITY CONVERGENCE \*\*\*\*\*

I	OBS.Y(I)	CAL	RES	%RES.ERR	X(I,1)
1	0.100000E+03	0.100371E+03	-0.371E+00	-0.370017E+00	0.120000E-02
2	0.983000E+02	0.964696E+02	0.183E+01	0.189740E+01	0.160000E-02
3	0.979000E+02	0.942440E+02	0.366E+01	0.387925E+01	0.200000E-02
4	0.965000E+02	0.945513E+02	0.195E+01	0.206099E+01	0.260000E-02
5	0.987000E+02	0.958641E+02	0.284E+01	0.295824E+01	0.340000E-02
6	0.947000E+02	0.949352E+02	-0.235E+00	-0.247699E+00	0.420000E-02
7	0.880000E+02	0.933353E+02	-0.534E+01	-0.571623E+01	0.500000E-02
8	0.856000E+02	0.902201E+02	-0.462E+01	-0.512091E+01	0.580000E-02
9	0.783000E+02	0.834095E+02	-0.511E+01	-0.612585E+01	0.700000E-02
10	0.748000E+02	0.733851E+02	0.141E+01	0.192805E+01	0.860000E-02
11	0.661000E+02	0.644609E+02	0.164E+01	0.254271E+01	0.102000E-01
12	0.600000E+02	0.573557E+02	0.264E+01	0.461030E+01	0.118000E-01

\*\* RMSERR= 0.40768962E+01

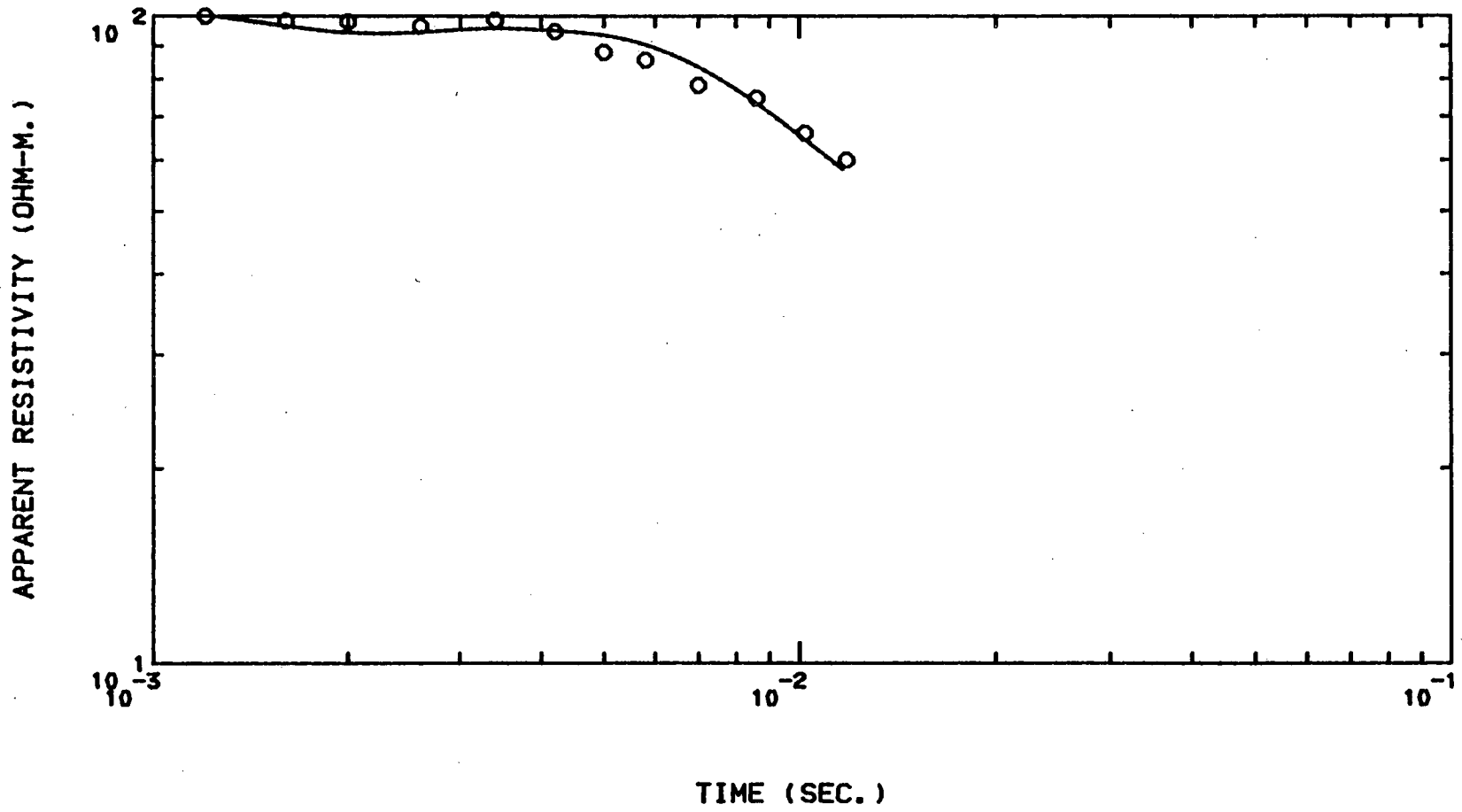
CORRELATION MATRIX

1	0.1000E+01				
2	0.5903E+00	0.1000E+01			
3	0.4247E+00	0.7590E-01	0.1000E+01		
4	0.6423E+00	0.6753E+00	0.3354E+00	0.1000E+01	
5	0.3025E+00	-0.2995E+00	0.5040E+00	0.2862E+00	0.1000E+01

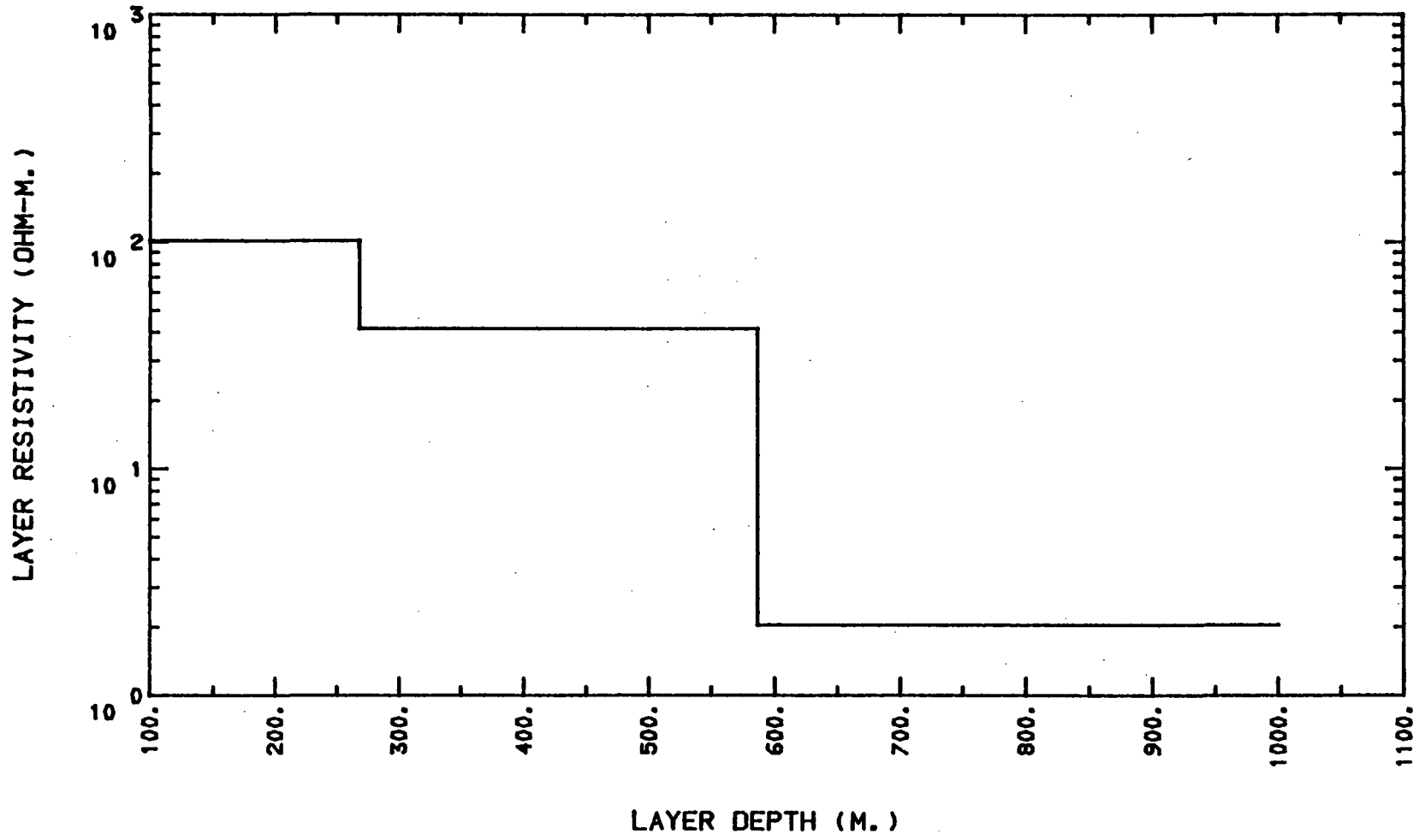
**PARM_SOL.	STD_ERROR	REL_ERROR	% ERROR **	
1	0.9863E-02	0.2772E-03	0.2811E-01	0.2811E+01
2	0.2414E-01	0.1447E-02	0.5996E-01	0.5996E+01
3	0.4898E+00	0.8245E-02	0.1683E-01	0.1683E+01
4	0.2679E+03	0.9751E-02	0.3640E-04	0.3640E-02
5	0.3185E+03	0.9323E-02	0.2927E-04	0.2927E-02

PARAMETER NAME	FINAL SOLUTION	RESISTIVITY	LAYER DEPTH
1 SIGMA( 1) =	0.98628579E-02	1 0.10139049E+03	
2 SIGMA( 2) =	0.24136271E-01	2 0.41431419E+02	
3 SIGMA( 3) =	0.48984161E+00	3 0.20414762E+01	
4 THICK( 1) =	0.26787317E+03		1 0.26787317E+03
5 THICK( 2) =	0.31850494E+03		2 0.58637811E+03
6 SHIFT =	0.10000000E+01		

Newberry Crater NB-17 3 layer



Newberry Crater NB-17 3 layer



<NLSTCI2>: Newberry Crater NB-18 2 layer

A= 0.860000E+02

PARAMETERS HELD FIXED: IB= 4

\*\*\*\*\* X-CONVERGENCE \*\*\*\*\*

I	OBS.Y(I)	CAL	RES	%RES.ERR	X(I,1)
1	0.408000E+03	0.438315E+03	-0.303E+02	-0.691621E+01	0.120000E-02
2	0.335000E+03	0.353527E+03	-0.185E+02	-0.524060E+01	0.160000E-02
3	0.290000E+03	0.296412E+03	-0.641E+01	-0.216309E+01	0.200000E-02
4	0.239000E+03	0.245090E+03	-0.609E+01	-0.248474E+01	0.260000E-02
5	0.206000E+03	0.199036E+03	0.696E+01	0.349862E+01	0.340000E-02
6	0.180000E+03	0.169992E+03	0.100E+02	0.588740E+01	0.420000E-02
7	0.159000E+03	0.150416E+03	0.858E+01	0.570653E+01	0.500000E-02
8	0.144000E+03	0.135808E+03	0.819E+01	0.603215E+01	0.580000E-02
9	0.125000E+03	0.120438E+03	0.456E+01	0.378774E+01	0.700000E-02
10	0.114000E+03	0.106171E+03	0.783E+01	0.737443E+01	0.860000E-02
11	0.954000E+02	0.959114E+02	-0.511E+00	-0.533230E+00	0.102000E-01
12	0.879000E+02	0.882818E+02	-0.382E+00	-0.432450E+00	0.118000E-01

\*\* RMSERR= 0.13793665E+02

CORRELATION MATRIX

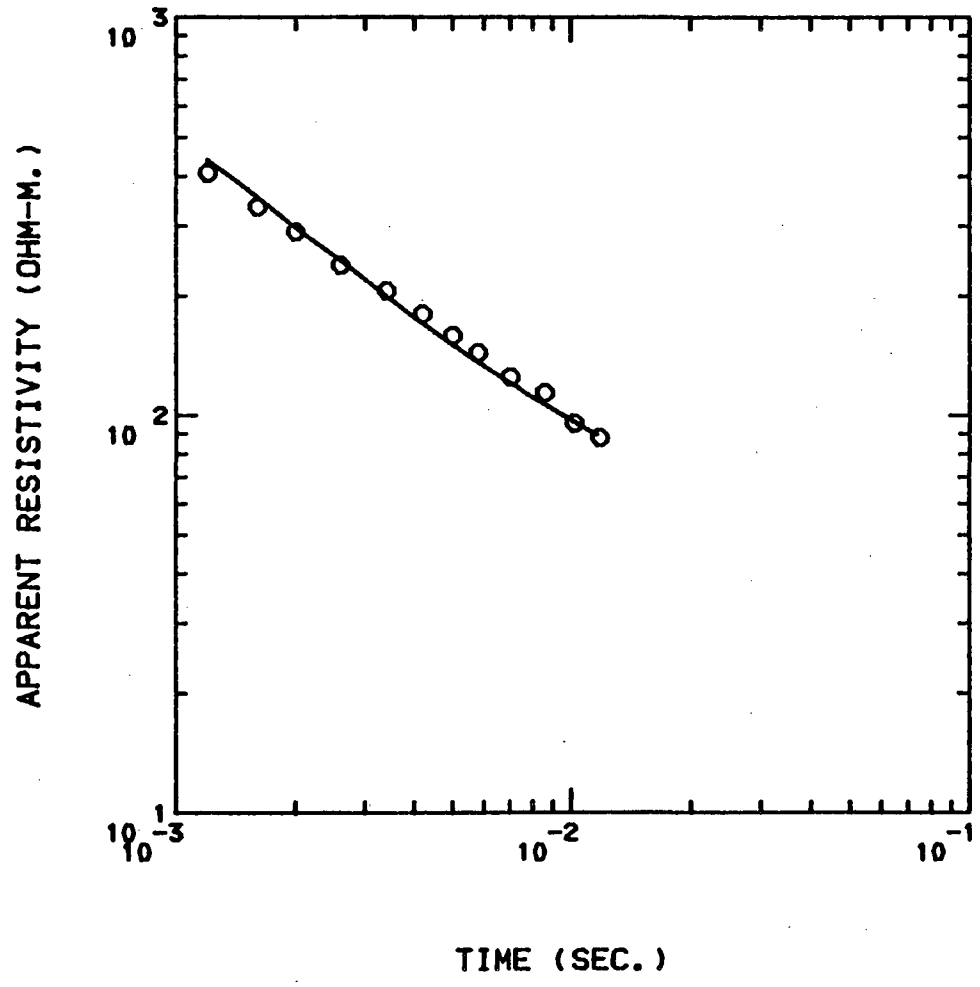
1	0.1000E+01		
2	0.9710E-02	0.1000E+01	
3	-0.4974E+00	0.3889E+00	0.1000E+01

**PARAM_SOL.	STD_ERROR	REL_ERROR	% ERROR **
1	0.2060E-02	0.1934E-04	0.9391E-02
2	0.4233E-01	0.9932E-03	0.2346E-01
3	0.5350E+03	0.1765E-02	0.3300E-03

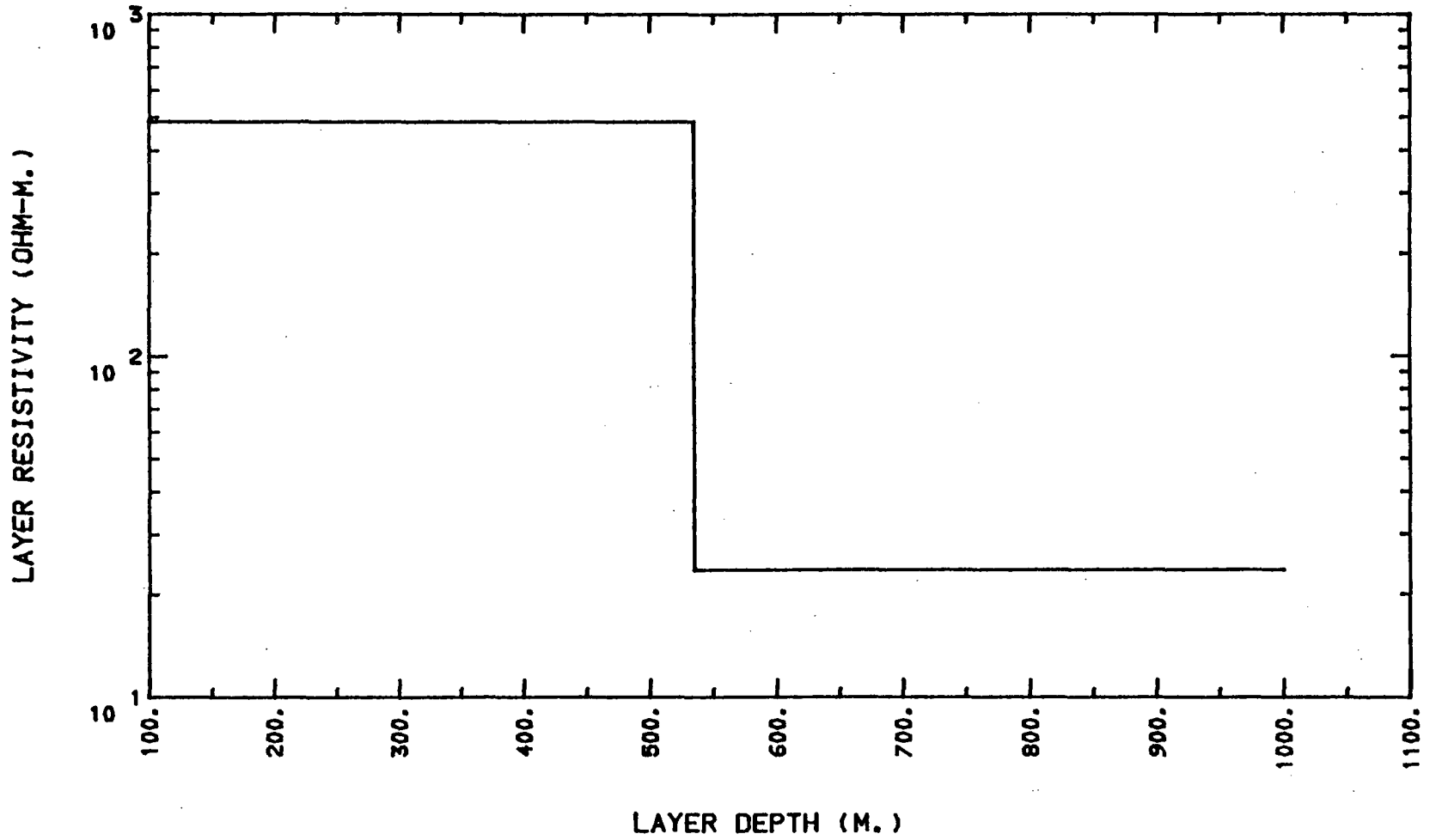
PARAMETER NAME	FINAL SOLUTION	RESISTIVITY	LAYER DEPTH
1 SIGMA( 1) =	0.20598779E-02	1 0.48546567E+03	
2 SIGMA( 2) =	0.42326998E-01	2 0.23625584E+02	
3 THICK( 1) =	0.53501312E+03		1 0.53501312E+03
4 SHIFT =	0.10000000E+01		



Newberry Crater NB-18 2 layer



Newberry Crater NB-18 2 layer



UNITED STATES DEPARTMENT OF THE INTERIOR

GEOLOGICAL SURVEY

More Time-Domain Electromagnetic Soundings of Newberry Volcano,  
Deschutes County, Oregon

by

David V. Fitterman, Deborah K. Neev, Jerry A. Bradley, and Clark T. Grose

Open-File Report 85-451

29 July 1985

This report is preliminary and has not been reviewed for conformity with U.S. Geological Survey editorial standards. Any use of trade names is for descriptive purposes only and does not imply endorsement by the U.S. Geological Survey.

## Introduction

This report describes the results of a time-domain electromagnetic (TDEM) survey of Newberry Volcano, Deschutes County, Oregon, which was performed during July 1984 to determine the geoelectrical structure of the volcano. Twenty-three TDEM soundings were made using a central induction loop configuration. This was our second field season at Newberry Volcano. During the previous field season 18 soundings were made (Fitterman, 1983). Figure 1 shows the locations of the 1983 and 1984 soundings.

This research project was funded by the Department of Energy in conjunction with the USGS Geothermal Program.

## Field Procedure and Equipment

TDEM measurements were made using a SIROTEM II system (Buselli and O'Neill, 1977). The SIROTEM system injects a bipolar, square-wave current into a transmitter loop. When the current is turned off, the voltage induced in a receiving coil located at the center of the transmitter loop is recorded. The SIROTEM system records and stacks the transients from a large number of current turn-offs, and reports the averaged voltage-current ratios.

Square transmitter loops 305 m on a side were used. The receiver coil was an eight turn 38 m x 38 m loop (receiver coil moment  $M_r = 11,613 \text{ turn-m}^2$ ) situated at the center of the transmitter loop. Four to six runs, consisting of 2,048 transients per run, were made at each site. The polarity of the receiver coil was reversed on alternate runs to reduce instrumental noise.

At all 1984 locations except NB-41, an external transmitter built by the USGS was used to increase transmitter current to about 20 amperes. The higher current made it possible to obtain useful signals at later times, thereby collecting information from greater depths. At NB-41 a single loop (L=305 m) was used for the transmitter and receiver with the lower power internal SIROTEM transmitter.

At most locations VLF resistivity data were collected at 25 m intervals along one leg of the transmitter loop using a Geonics EM16R. This information was used to determine near surface resistivities for use in inversion of the TDEM sounding. The geometric mean of thirteen measurements from each site are given in Table 1.

## Data Preparation

The recorded voltage-current ratios were converted to late stage apparent resistivity (Kaufmann and Keller, 1983, p. 457) using the formula

$$\rho = \frac{\mu_0}{4\pi t} \left( \frac{2\mu_0 L^2 M_r}{5t V/I} \right)^{2/3}$$

where  $\mu_0$  is the free space permeability, L is the length of a side of the transmitter loop,  $M_r$  is the receiver loop moment, t is time since current shutoff, and V/I is the voltage-current ratio (all in SI units). Data from

Table 1. VLF apparent resistivities from transient sounding sites. The data were obtained using the 24.8 kHz VLF station at Jim Creek, WA. The results are the geometric mean of 13 data points spaced along a 300 m long line.

<u>Station</u>	<u>Apparent Resistivity (ohm-m)</u>
NB-19	1700
NB-20	1500
NB-21	1200
NB-22	2800
NB-25	1400
NB-26	2200
NB-27	1400
NB-28	1200
NB-29	560
NB-30	930
NB-31	1000
NB-32	880
NB-33	2600
NB-34	780
NB-35	1200
NB-36	1700
NB-37	2600
NB-38	900
NB-39	1600
NB-40	4700
NB-41	1600

several runs were averaged and converted to apparent resistivity. Data from the first two SIROTEM channels were not used because they appeared to be noisy. Late-time data were rejected when the data appeared to be noisy and the apparent resistivity curves no longer behaved smoothly. Data obtained using the external transmitter were combined with data from the internal transmitter to obtain longer data records with less noise.

### Inversion of Soundings

Initial models for the data were obtained by curve matching using a catalog of two-layer models (Kaufmann and Keller, 1983). These models served as starting points for a non-linear least squares inversion by computer (Anderson, 1982). Best-fit two and three layer models were found for each sounding. If the three layer model did not provide a significantly better fit than the two-layer model, then the three-layer model was rejected. Initial estimates of first layer resistivity were made using the VLF apparent resistivities. The first layer thickness was taken as the VLF skin depth. The first layer parameters were usually held fixed. If an acceptable fit was not obtained with these values, the first layer parameters were allowed to vary.

### Results

Results of the inversions are presented in Figures 2 through 24. Figures 2a through 24a contain the output from the inversion program. This consists of the name of the inversion program used, the sounding title, and the effective transmitter loop radius ( $A = \pi^{-1/2} L$ ).

The first table contains the observation time (seconds), the observed apparent resistivity (ohm-m), the estimated standard deviation in the observation, the computed model resistivity, and the percent error in the fit. The estimated standard deviation is based upon the statistics of several runs. Following these data are the RMS error in the fit and the convergence criterion which terminated the inversion. See Dennis et al. (1981) for a discussion of the convergence criteria.

The next table gives the parameter correlation matrix for the unconstrained parameters. This provides a measure of the interdependence of the model parameter estimates. A high correlation between parameters indicates that only their ratio can be determined, while a high inverse correlation between parameters means that only their product can be resolved. Only the lower half of the symmetric correlation matrix is shown. The column integers at the left gives the parameter number. These numbers are seen to the left of the third table and under the "P" heading in the "FINAL INVERSION MODEL" table. As an example, the second entry in the first column of any correlation matrix will be the correlation between the second and first unconstrained model parameters.

The third table gives the unconstrained model parameter estimates, the standard deviation in the parameter estimates, the relative error (the standard deviation divided by the model parameter), and the percentage relative error in the parameter estimates. This information is provided for the unconstrained parameters. The parameter error estimates are based on nonlinear statistics, and as such cannot be taken as actual parameter

uncertainties. It is necessary to do a sensitivity analysis to determine the actual bounds on allowable models.

The last table gives the resistivity, conductivity, thickness, and depth to the top of each layer. The column marked "p" gives the model parameter number. An asterisks under the column marked "F" indicates that the model parameter was fixed in the inversion.

Figures 2b through 24b contain the apparent resistivity sounding curve (circles) plotted as a function of  $(2\pi t)^{1/2}$ . The data error estimates are indicated by vertical bars on the data points. The solid line is the calculated sounding curve based upon the final inversion model.

The final inversion model is shown in Figures 2c through 24c. The interpreted layer resistivities are plotted as a function of depth. Solid lines represent layer resistivities and thicknesses which were allowed to vary during inversion. Dashed lines represent model parameters which were constrained during inversion.

### Discussion

The data are similar in nature to the previous survey results (Fitterman, 1983). The geoelectrical section is resistive near the surface, becoming conductive with depth. All soundings described in this report were made outside the caldera rim. The first layer resistivities range from 370 ohm-m to 2800 ohm-m. These values are often not well determined. Some values were constrained based upon the VLF resistivity data. The basement resistivities ranged from 19 ohm-m to 73 ohm-m. A second layer of intermediate resistivity was required for most interpretations.

Figure 25 shows a contour map of depth to the conductive basement based upon all soundings made to date. Depth to the conductive basement ranges from 370 m to 810 m. After the intra-caldera region, the shallowest conductive zones lie to the west of the caldera where depths as shallow as 410 m are seen. This region has been the focus of commercial drilling activity.

Inside the caldera, the conductor is associated with high-temperature fluids as confirmed by drilling. The cause of the conductor outside the caldera is not as clear. The conductor could be due to conductive rocks that predate Newberry such as Tertiary ash flows or sedimentary rocks. Pre-Newberry rocks would be expected at an elevation of below 1280 m (N.S. MacCleod, personal communication, 1985). The elevation of the conductor varies from 640 m to 1580 m, and is lower away from the caldera. Thus, in some regions the pre-Newberry rock hypothesis is supported, whereas in others it is contradicted. The conductor could also be due to the water table. Dry, near surface, Newberry rocks are exceedingly resistive. Saturating these same rocks should significantly reduce their resistivity. The deepening of the conductor away from the volcano is in accord with the idea of ground water flowing downward and outward from the caldera. Increased saturation of Newberry, or possibly pre-Newberry, rocks with depth could account for the conductive layer we have detected. There are no publically available well data in the vicinity of the volcano to unambiguously unravel the cause of the conductor, however, the regional water table elevations are about 1280 m (Black, 1983). We suspect that the conductor is caused by increased saturation with depth, and that in places the conductor may be pre-Newberry rocks.

### Acknowledgements

This work was funded by the Department of Energy under Interagency Agreement DE-AI01-79RA50294. Permission to conduct the field work was granted by the Deschutes National Forest, Bend, Oregon.

### References

- Anderson, W. L., 1982, Nonlinear least-squares inversion of transient soundings for a central induction loop system (Program NLSTCI): U.S. Geological Survey Open-File Report 82-1129, 85 p.
- Black, Gerald L., 1983, Newberry hydrology, in Priest, G. R., Voyt, B. F., and Black, G. L., editors, Survey of potential geothermal exploration sites of Newberry Volcano, Deschutes County, Oregon: Oregon Department of Geology and Mineral Industries, Open-File Report O-83-3, p. 28-44.
- Buselli, G., and O'Neill, G., 1977, SIROTEM--a new portable instrument for multichannel electromagnetic measurements: Bull. Aust. Soc. Expl. Geophys., 8, 82-87.
- Dennis, J. E., Gay, D. M., and Welsch, R. E., 1981, An adaptive nonlinear least-squares algorithm: ACM Trans. Math. Software, 7, 348-368.
- Fitterman, D. V., 1983, Time-domain electromagnetic soundings of Newberry Volcano, Deschutes County, Oregon: U.S. Geological Survey Open-File Report 83-832, 57 p.
- Kaufman, A. A., and Keller, G. R., 1983, Frequency and Transient Sounding: Amsterdam, Elsevier, 687 p.



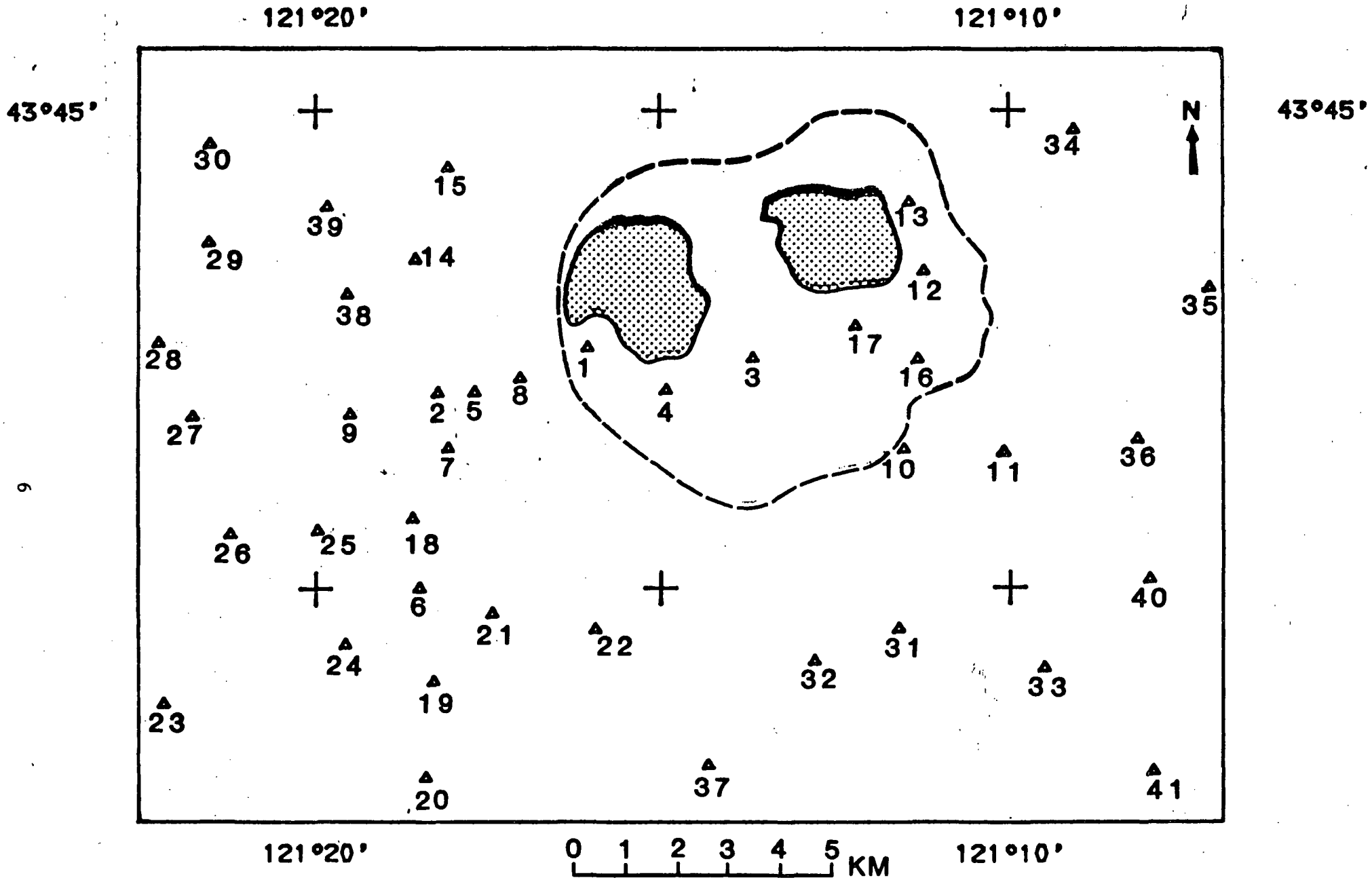


Figure 1

Figure 2a

<NLSTCI>: Newberry Volcano NBE-19  
 LOOP RADIUS= 172.0

I	TIME(s)	OBSERVED RESISTIVITY	STANDARD DEVIATION	COMPUTED RESISTIVITY	PERCENT ERROR
1	0.0016000	450.4	6.6	450.3	0.0
2	0.0020000	382.6	9.2	382.3	0.1
3	0.0026000	315.0	7.4	316.9	-0.6
4	0.0034000	265.6	6.3	265.0	0.2
5	0.0042000	232.4	9.0	230.3	0.9
6	0.0050000	209.8	8.9	207.0	1.4
7	0.0058000	191.3	11.3	189.7	0.8
8	0.0070000	168.9	10.8	170.4	-0.9
9	0.0086000	147.3	8.9	152.4	-3.4
10	0.0102000	135.9	5.7	139.8	-2.8
11	0.0118000	127.7	3.9	130.3	-2.0
12	0.0134000	129.5	6.2	123.0	5.3
13	0.0158000	115.9	12.7	114.3	1.4
14	0.0190000	104.1	10.1	105.9	-1.7
15	0.0222000	94.0	17.6	99.6	-5.6
16	0.0254000	95.4	23.7	94.6	0.9
17	0.0286000	93.6	29.1	90.4	3.5
18	0.0334000	80.1	26.1	85.6	-6.5
19	0.0398000	87.7	43.2	80.9	8.4

RMS ERROR= 3.841 X-CONVERGENCE

CORRELATION MATRIX

	2	3	5
2	1.000		
3	-0.208	1.000	
5	0.502	0.418	1.000

	PARAMETER ESTIMATE	STANDARD ERROR	RELATIVE ERROR	PERCENT ERROR
2	0.1966E-02	0.6308E-04	0.3209E-01	3.2
3	0.2299E-01	0.1920E-03	0.8353E-02	0.8
5	0.4657E+03	0.1465E-02	0.3145E-05	0.0

FINAL INVERSION MODEL

LAYER	RESISTIVITY	P F	CONDUCTIVITY	P F	THICKNESS	DEPTH
1	1652.9	1 *	0.60500001E-03	4 *	130.0	0.0
2	508.7	2	0.19659291E-02	5	465.7	130.0
3	43.5	3	0.22991039E-01			595.7

P - parameter number  
 F - \* indicates fixed parameter

Figure 2b

Newberry Volcano NBE-19

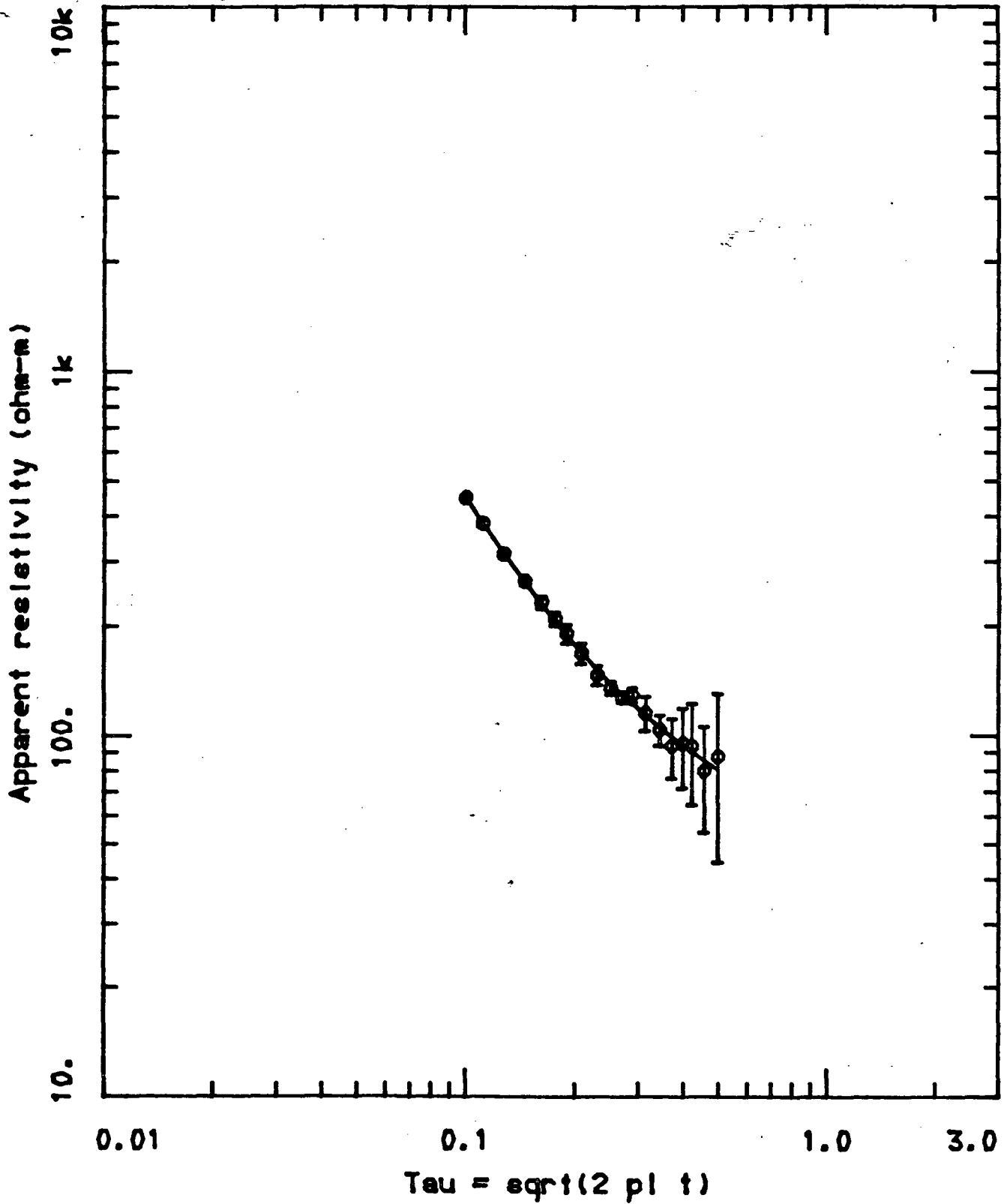


Figure 2c

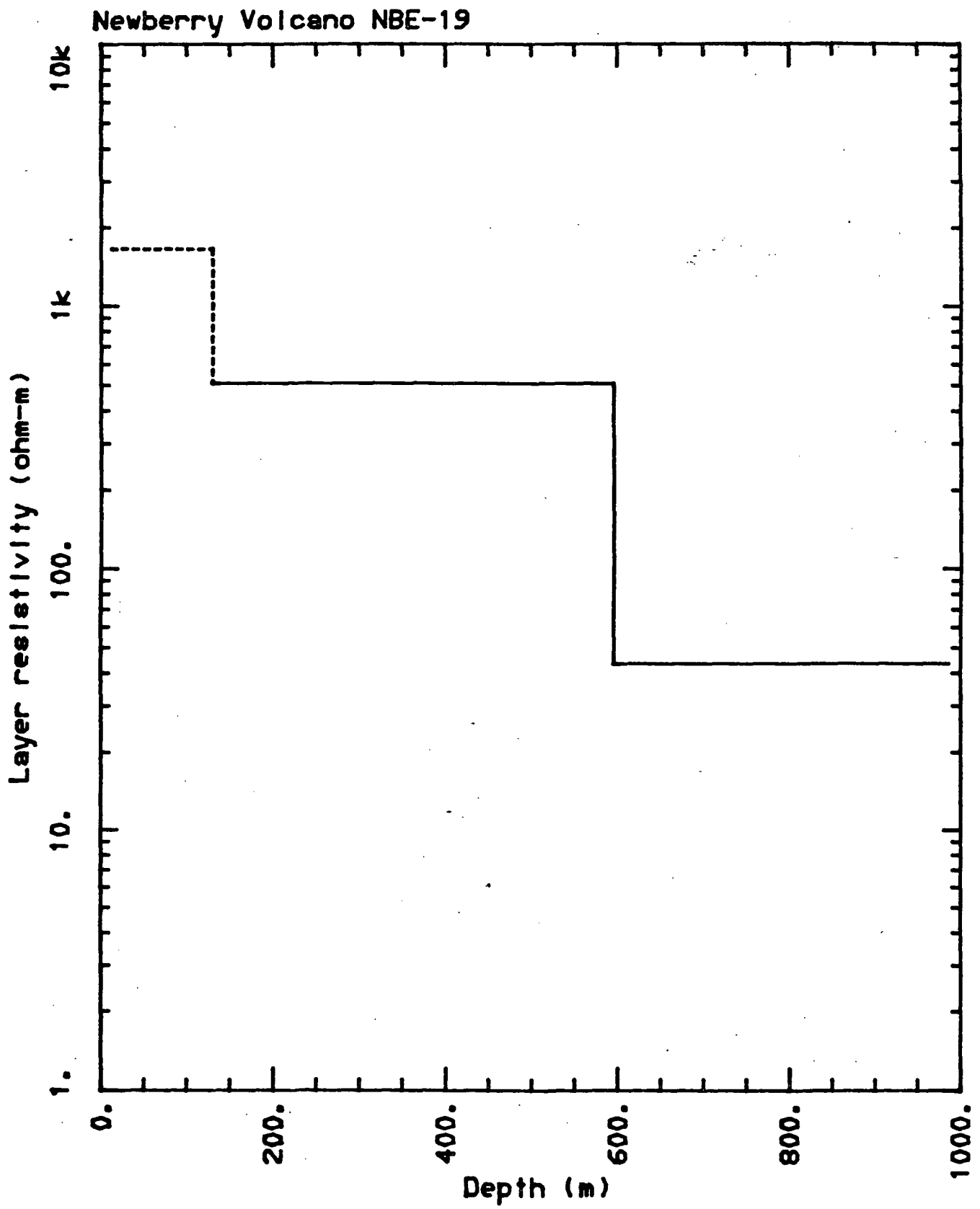


Figure 3a

<NLSTCI>: Newberry Volcano NBE-20  
 LOOP RADIUS= 172.0

I	TIME(s)	OBSERVED RESISTIVITY	STANDARD DEVIATION	COMPUTED RESISTIVITY	PERCENT ERROR
1	0.0016000	530.7	2.6	501.5	5.8
2	0.0020000	456.5	3.2	456.9	-0.1
3	0.0026000	386.9	1.7	398.4	-2.9
4	0.0034000	329.6	2.1	334.0	-1.3
5	0.0042000	287.9	2.0	285.7	0.8
6	0.0050000	258.6	5.4	251.4	2.9
7	0.0058000	237.3	8.7	226.6	4.7
8	0.0070000	204.8	3.8	198.0	3.4
9	0.0086000	193.3	9.6	171.0	13.0
10	0.0102000	175.4	7.1	152.8	14.8
11	0.0118000	169.5	11.3	139.2	21.8
12	0.0134000	151.3	4.9	128.3	17.9
13	0.0158000	136.0	11.3	116.1	17.1
14	0.0190000	108.7	4.3	104.5	4.0
15	0.0222000	100.0	5.9	95.9	4.3
16	0.0254000	91.9	4.8	89.2	3.0
17	0.0286000	84.9	4.8	84.1	1.0
18	0.0334000	74.4	3.3	78.0	-4.6
19	0.0398000	72.6	5.2	71.9	1.0

RMS ERROR= 17.17 X-CONVERGENCE

CORRELATION MATRIX

	1	2	3	4	5
1	1.000				
2	-0.422	1.000			
3	-0.326	0.450	1.000		
4	-0.264	-0.417	0.030	1.000	
5	-0.301	0.627	0.064	-0.764	1.000

	PARAMETER ESTIMATE	STANDARD ERROR	RELATIVE ERROR	PERCENT ERROR
1	0.1179E-02	0.1011E-03	0.8575E-01	8.6
2	0.2801E-02	0.2381E-03	0.8500E-01	8.5
3	0.3832E-01	0.1289E-02	0.3363E-01	3.4
4	0.1325E+03	0.6219E-02	0.4693E-04	0.0
5	0.6392E+03	0.9625E-02	0.1506E-04	0.0

FINAL INVERSION MODEL

LAYER	RESISTIVITY	P	F	CONDUCTIVITY	P	F	THICKNESS	DEPTH
1	848.2	1		0.11789675E-02	4		132.5	0.0
2	357.0	2		0.28009799E-02	5		639.2	132.5
3	26.1	3		0.38316090E-01				771.8

P - parameter number  
 F - \* indicates fixed parameter

Figure 3b

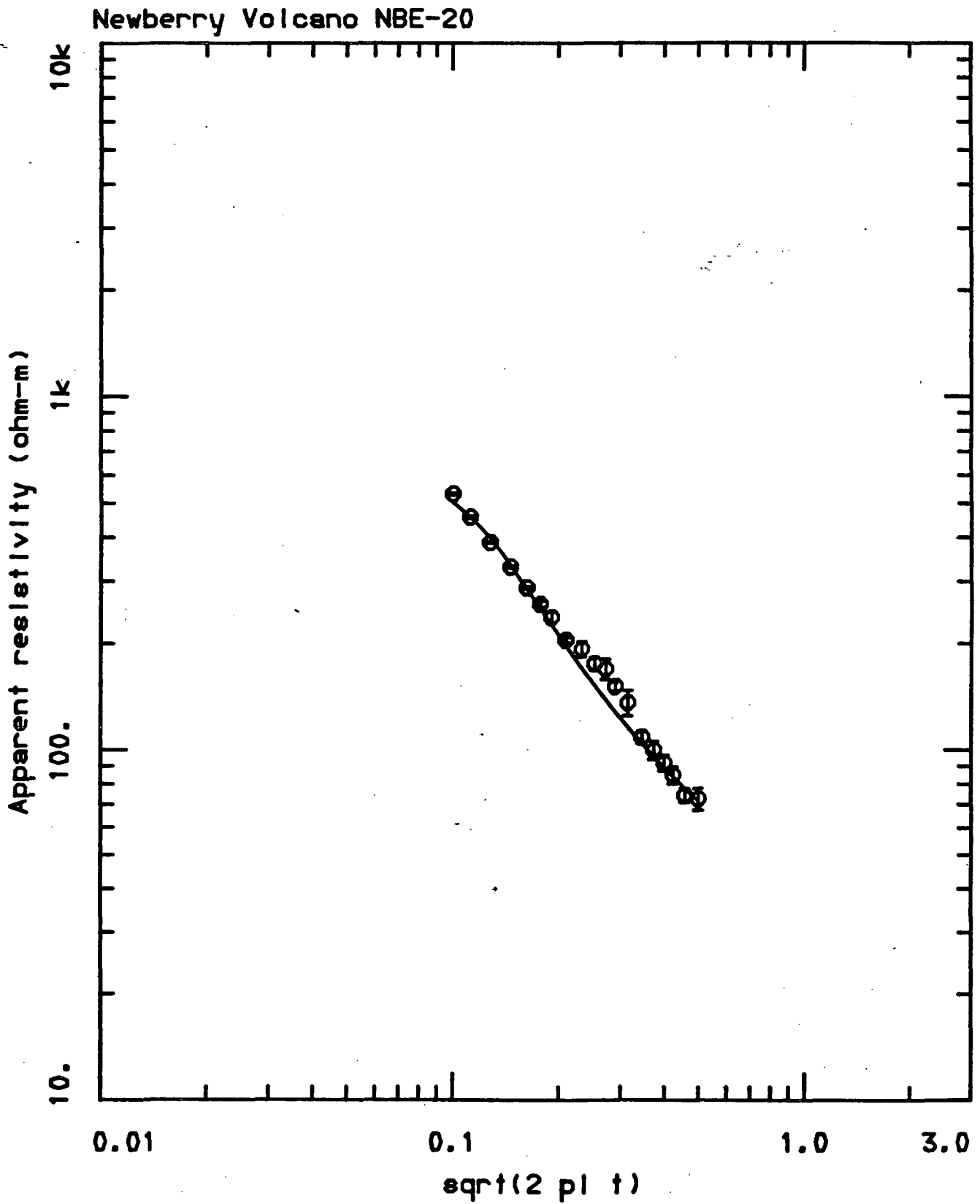


Figure 3c

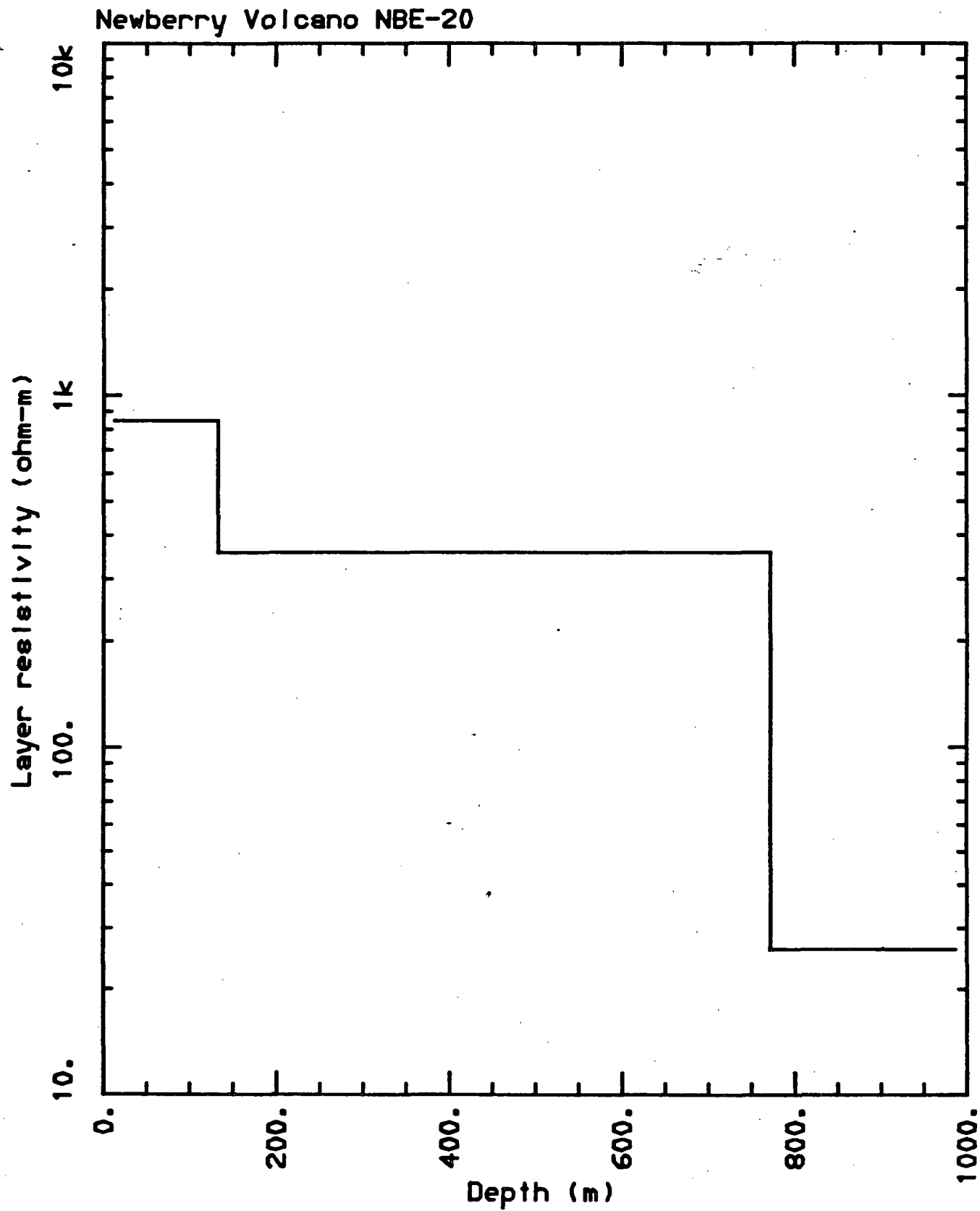


Figure 4a

<NLSTCI>: Newberry Volcano NBE-21  
 LOOP RADIUS= 172.0

I	TIME(s)	OBSERVED RESISTIVITY	STANDARD DEVIATION	COMPUTED RESISTIVITY	PERCENT ERROR
1	0.0016000	474.7	1.8	461.7	2.8
2	0.0020000	399.5	3.0	399.6	0.0
3	0.0026000	328.5	1.6	336.3	-2.3
4	0.0034000	274.6	0.7	279.1	-1.6
5	0.0042000	244.2	3.5	240.3	1.6
6	0.0050000	216.6	28.9	213.5	1.5
7	0.0058000	205.0	3.2	193.8	5.8
8	0.0070000	180.2	1.3	171.3	5.2
9	0.0086000	155.2	1.3	150.2	3.3
10	0.0102000	139.6	1.2	135.4	3.1
11	0.0118000	128.3	1.9	124.1	3.4
12	0.0134000	115.6	3.1	115.1	0.4
13	0.0158000	106.8	1.7	104.5	2.2
14	0.0190000	95.1	2.3	93.9	1.3
15	0.0222000	91.9	4.9	85.7	7.2
16	0.0254000	82.5	5.6	79.1	4.3
17	0.0286000	75.8	2.2	73.8	2.7
18	0.0334000	69.8	2.6	67.2	3.8
19	0.0398000	61.8	4.4	60.8	1.7

RMS ERROR= 6.592 X-CONVERGENCE

CORRELATION MATRIX

	1	2	3	4	5
1	1.000				
2	-0.383	1.000			
3	-0.303	0.122	1.000		
4	0.002	0.173	-0.474	1.000	
5	-0.470	0.265	0.434	-0.740	1.000

	PARAMETER ESTIMATE	STANDARD ERROR	RELATIVE ERROR	PERCENT ERROR
1	0.2003E-03	0.4305E-04	0.2149E+00	21.5
2	0.3324E-02	0.2112E-03	0.6354E-01	6.4
3	0.2943E-01	0.4798E-03	0.1630E-01	1.6
4	0.1692E+03	0.4116E-02	0.2433E-04	0.0
5	0.5045E+03	0.3917E-02	0.7765E-05	0.0

FINAL INVERSION MODEL

LAYER	RESISTIVITY	P	F	CONDUCTIVITY	P	F	THICKNESS	DEPTH
1	4992.2	1		0.20031395E-03	4		169.2	0.0
2	300.8	2		0.33240221E-02	5		504.5	169.2
3	34.0	3		0.29433116E-01				673.7

P - parameter number  
 F - \* indicates fixed parameter



Figure 4b

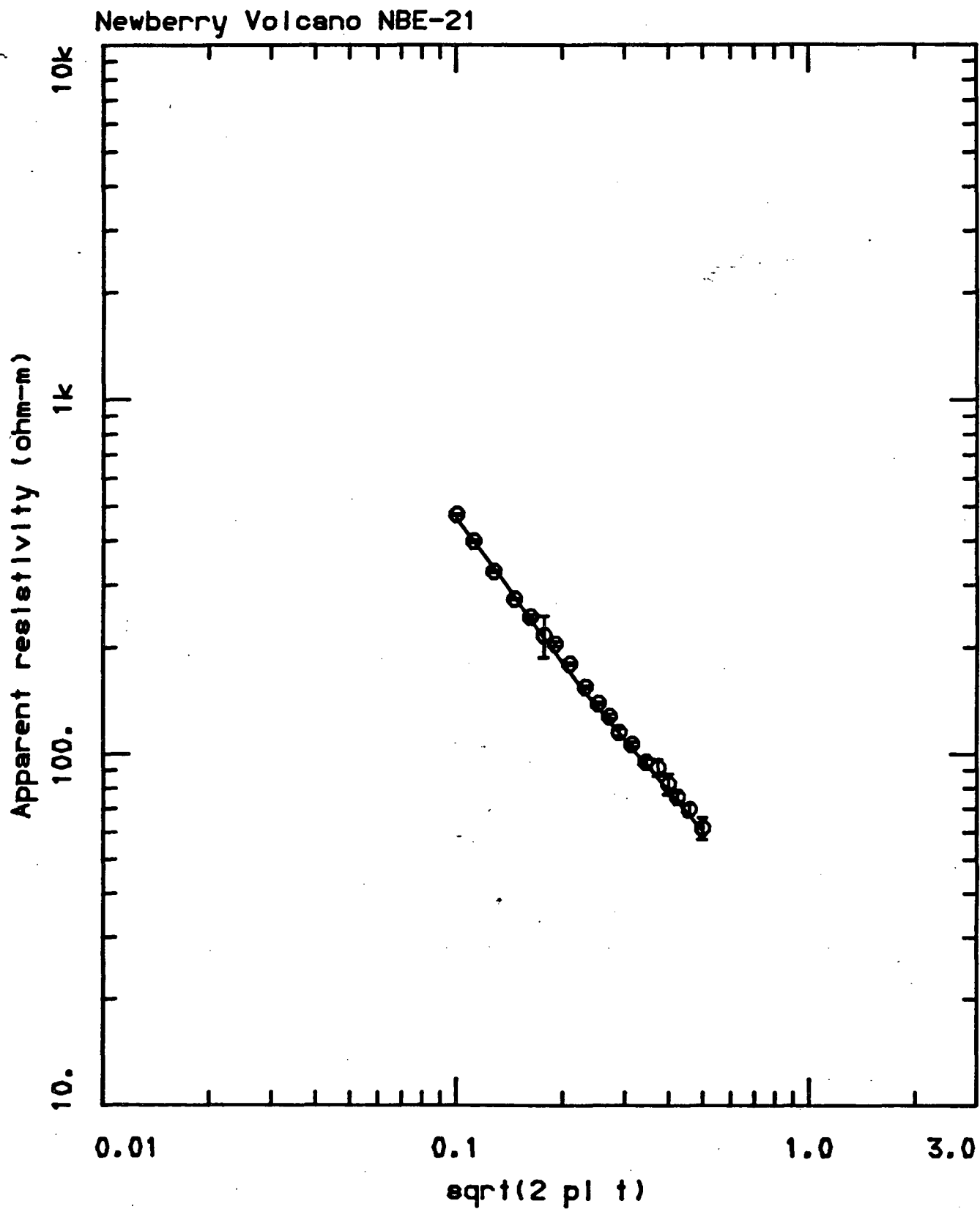


Figure 4c

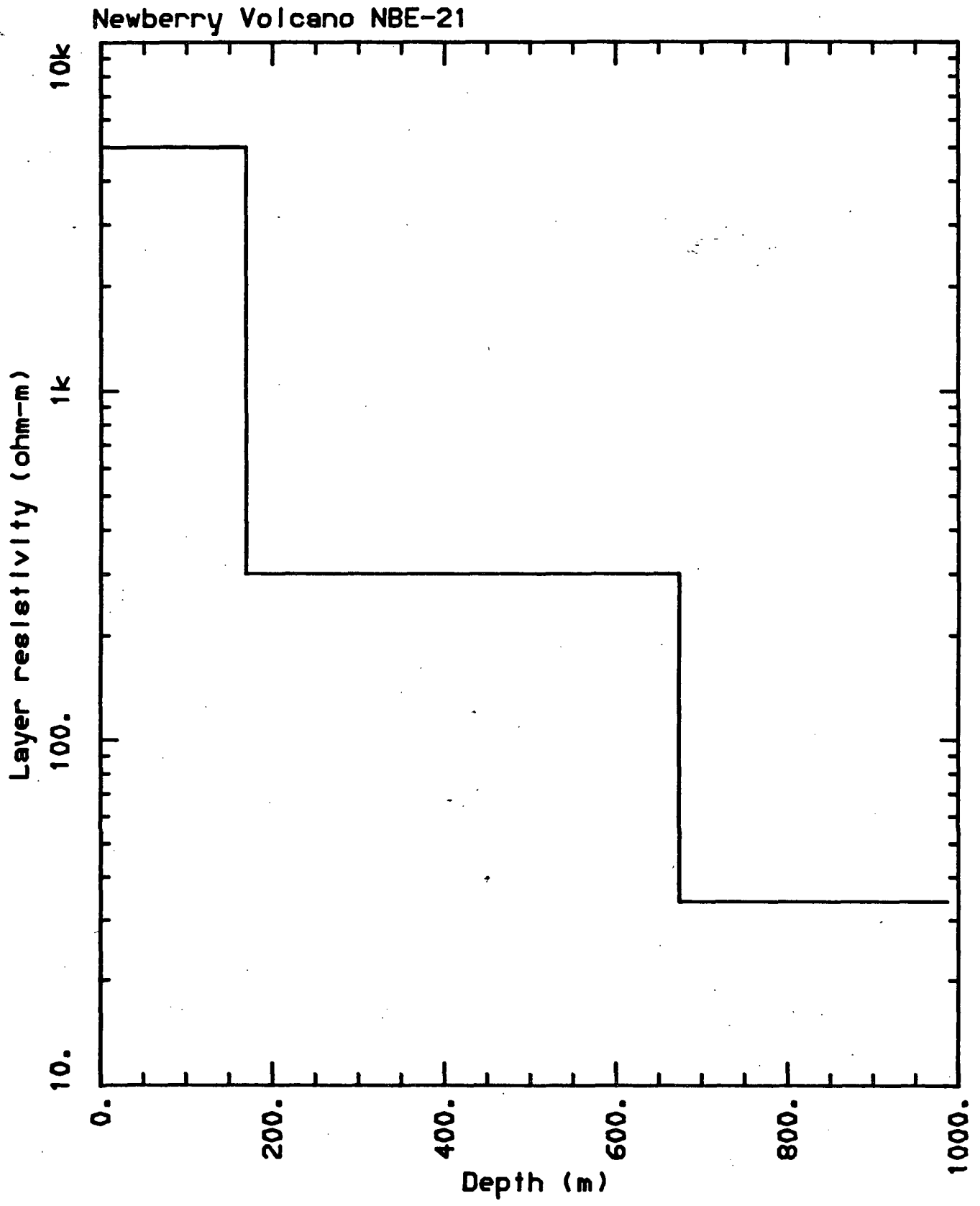


Figure 5a

<NLSTCI>: Newberry Volcano NBE-22  
 LOOP RADIUS= 172.0

I	TIME(s)	OBSERVED RESISTIVITY	STANDARD DEVIATION	COMPUTED RESISTIVITY	PERCENT ERROR
1	0.0016000	550.3	4.3	536.9	2.5
2	0.0020000	458.6	2.5	464.7	-1.3
3	0.0026000	377.2	3.4	388.1	-2.8
4	0.0034000	315.2	2.0	317.0	-0.6
5	0.0042000	270.5	2.4	269.9	0.2
6	0.0050000	242.3	2.6	238.2	1.7
7	0.0058000	218.2	3.7	214.3	1.8
8	0.0070000	193.5	1.6	187.2	3.4
9	0.0086000	165.3	3.7	162.8	1.5
10	0.0102000	144.1	5.6	145.9	-1.2
11	0.0118000	127.6	3.9	133.1	-4.1
12	0.0134000	117.0	6.3	123.2	-5.1
13	0.0158000	106.8	4.8	112.1	-4.7
14	0.0190000	99.8	3.0	101.2	-1.4
15	0.0222000	92.2	6.1	93.2	-1.1
16	0.0254000	87.4	4.9	86.9	0.5
17	0.0286000	80.3	3.0	82.0	-2.0
18	0.0334000	72.7	3.2	76.1	-4.5
19	0.0398000	64.3	3.7	70.2	-8.3

RMS ERROR= 6.360 X-CONVERGENCE

CORRELATION MATRIX

	1	2	3	4	5
1	1.000				
2	-0.790	1.000			
3	0.520	-0.378	1.000		
4	0.544	-0.657	0.188	1.000	
5	-0.716	0.805	-0.266	-0.902	1.000

	PARAMETER ESTIMATE	STANDARD ERROR	RELATIVE ERROR	PERCENT ERROR
1	0.5920E-03	0.2397E-04	0.4049E-01	4.0
2	0.2707E-02	0.1511E-03	0.5581E-01	5.6
3	0.3538E-01	0.4582E-03	0.1295E-01	1.3
4	0.1657E+03	0.3282E-02	0.1980E-04	0.0
5	0.5588E+03	0.4209E-02	0.7532E-05	0.0

FINAL INVERSION MODEL

LAYER	RESISTIVITY	P	F	CONDUCTIVITY	P	F	THICKNESS	DEPTH
1	1689.1	1		0.59203734E-03	4		165.7	0.0
2	369.4	2		0.27069722E-02	5		558.8	165.7
3	28.3	3		0.35377163E-01				724.5

P - parameter number  
 F - \* indicates fixed parameter

Figure 5b

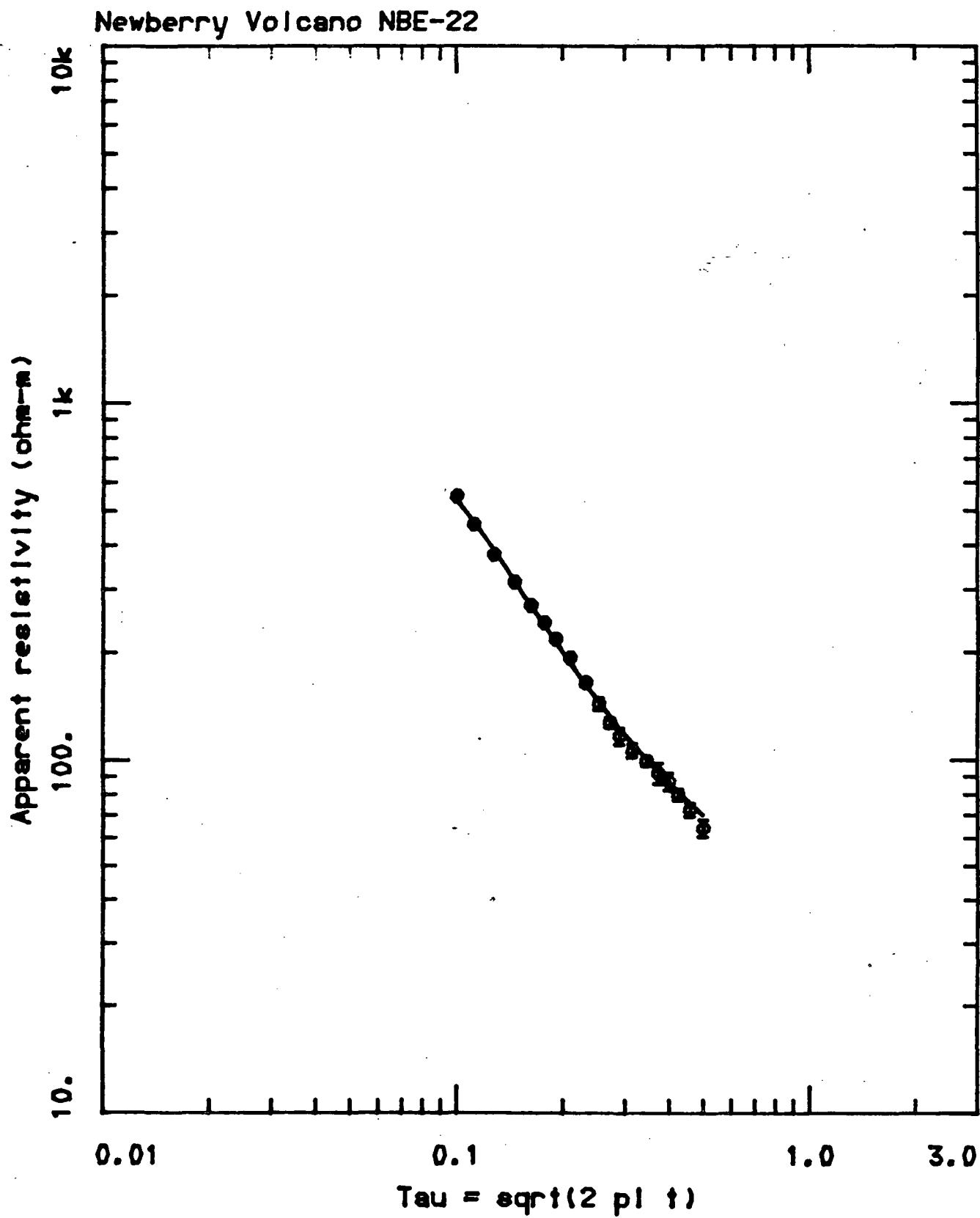


Figure 5c

Newberry Volcano NBE-22

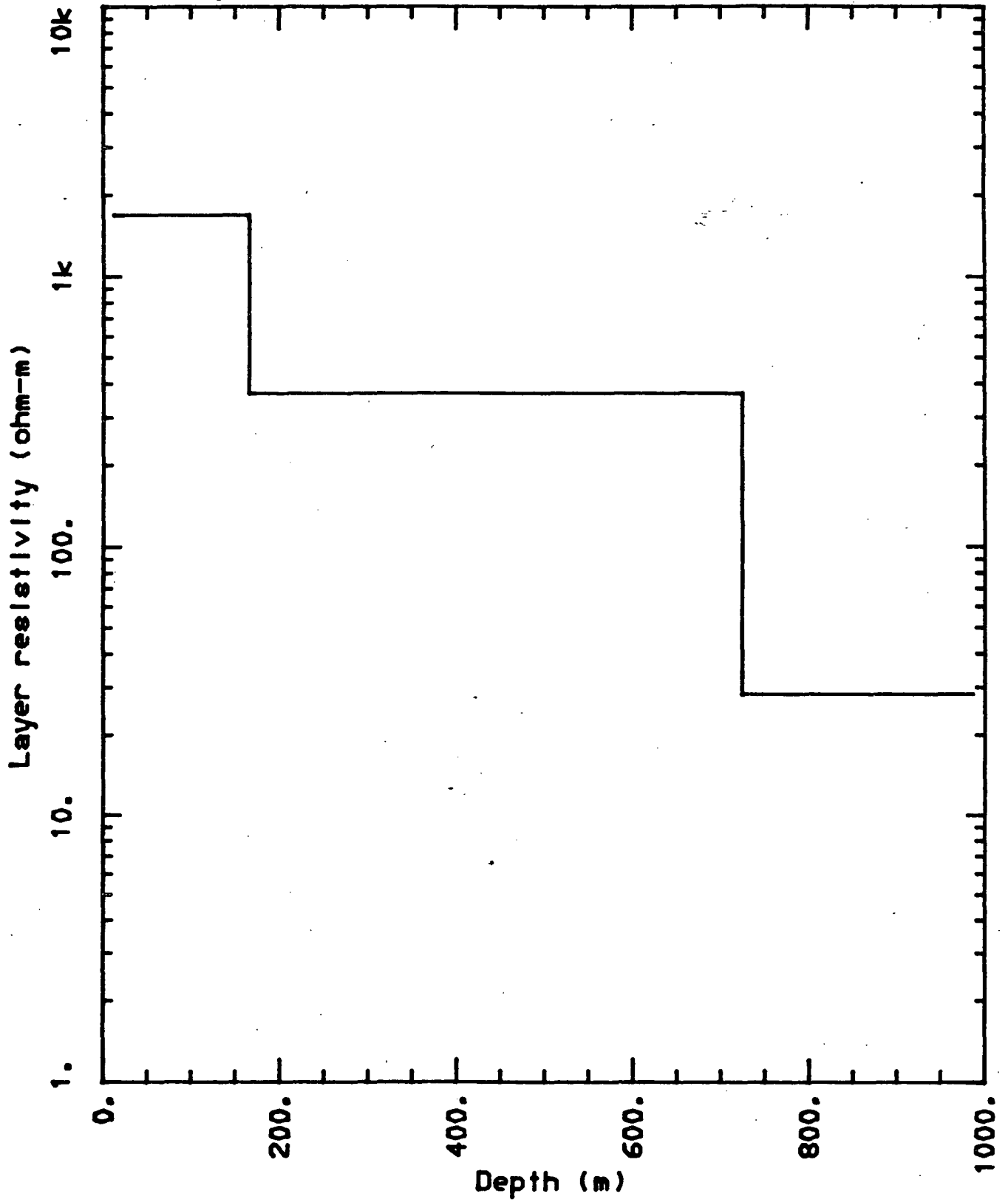


Figure 6a

<NLSTCI>: Newberry Volcano NBE-23  
 LOOP RADIUS= 172.0

I	TIME(s)	OBSERVED RESISTIVITY	STANDARD DEVIATION	COMPUTED RESISTIVITY	PERCENT ERROR
1	0.0016000	803.5	9.4	789.2	1.8
2	0.0020000	676.0	4.3	665.8	1.5
3	0.0026000	546.2	3.5	545.6	0.1
4	0.0034000	443.2	4.4	448.5	-1.2
5	0.0042000	379.4	8.3	383.9	-1.2
6	0.0050000	339.8	24.4	341.3	-0.4
7	0.0058000	300.7	11.6	309.3	-2.8
8	0.0070000	268.4	5.0	273.5	-1.9
9	0.0086000	234.4	6.1	241.0	-2.7
10	0.0102000	218.4	7.3	218.2	0.1
11	0.0118000	198.6	6.2	201.3	-1.4
12	0.0134000	181.5	11.1	188.5	-3.7
13	0.0158000	163.5	6.8	173.2	-5.6
14	0.0190000	148.0	2.1	158.3	-6.5
15	0.0222000	133.0	13.5	147.4	-9.8
16	0.0254000	118.3	11.9	138.8	-14.8
17	0.0286000	126.3	8.7	132.0	-4.3

RMS ERROR= 10.06 X-CONVERGENCE

CORRELATION MATRIX

	1	2	3
1	1.000		
2	0.061	1.000	
3	-0.124	-0.065	1.000

	PARAMETER ESTIMATE	STANDARD ERROR	RELATIVE ERROR	PERCENT ERROR
1	0.1049E-02	0.7331E-05	0.6992E-02	0.7
2	0.1867E-01	0.1478E-03	0.7913E-02	0.8
3	0.8130E+03	0.1248E-02	0.1535E-05	0.0

FINAL INVERSION MODEL

LAYER	RESISTIVITY	P	F	CONDUCTIVITY	P	F	THICKNESS	DEPTH
1	953.7	1		0.10485020E-02	3		813.0	0.0
2	53.6	2		0.18673740E-01				813.0

P - parameter number  
 F - \* indicates fixed parameter

Figure 6b

Newberry Volcano NBE-23

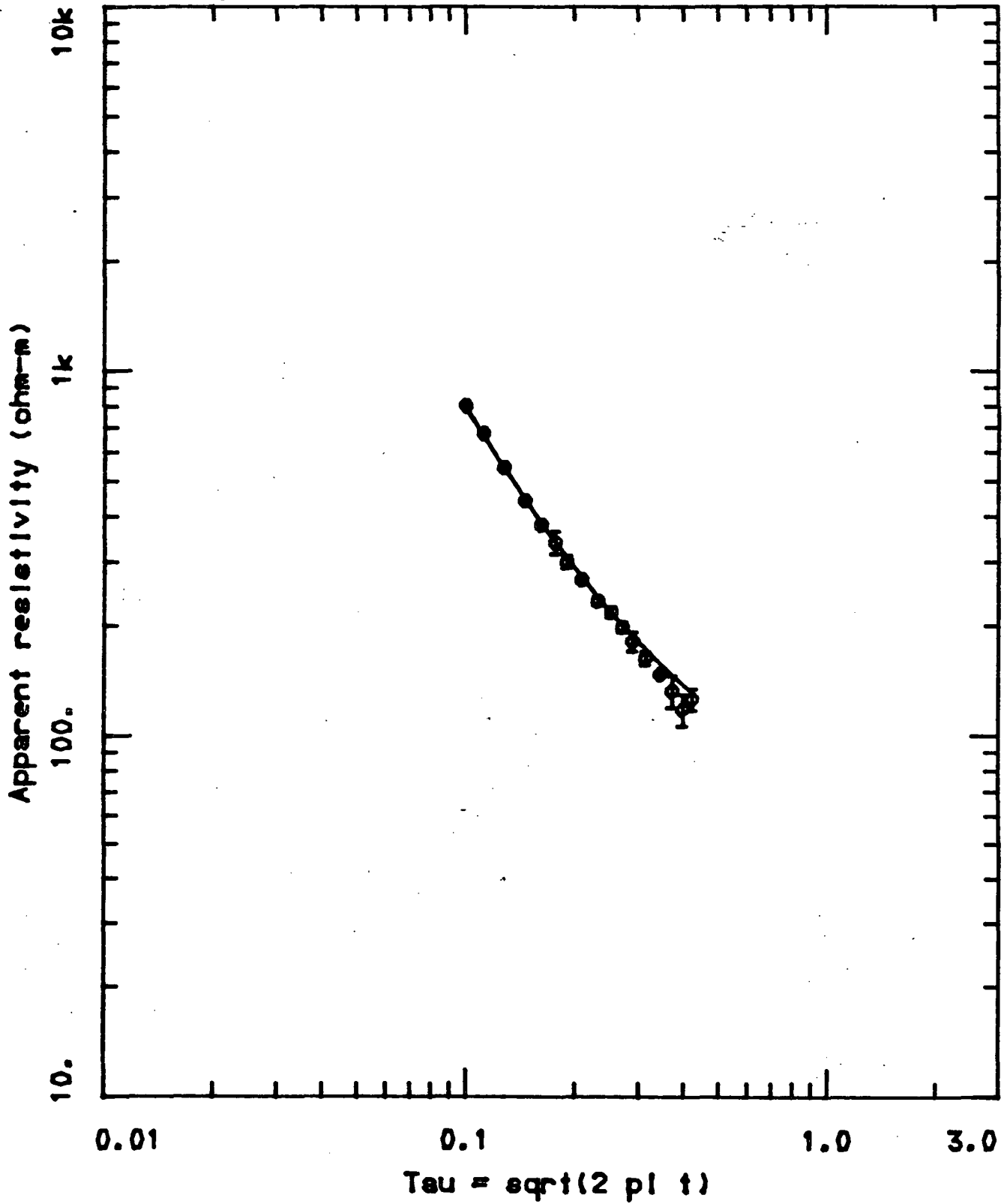


Figure 6c

Newberry Volcano NBE-23

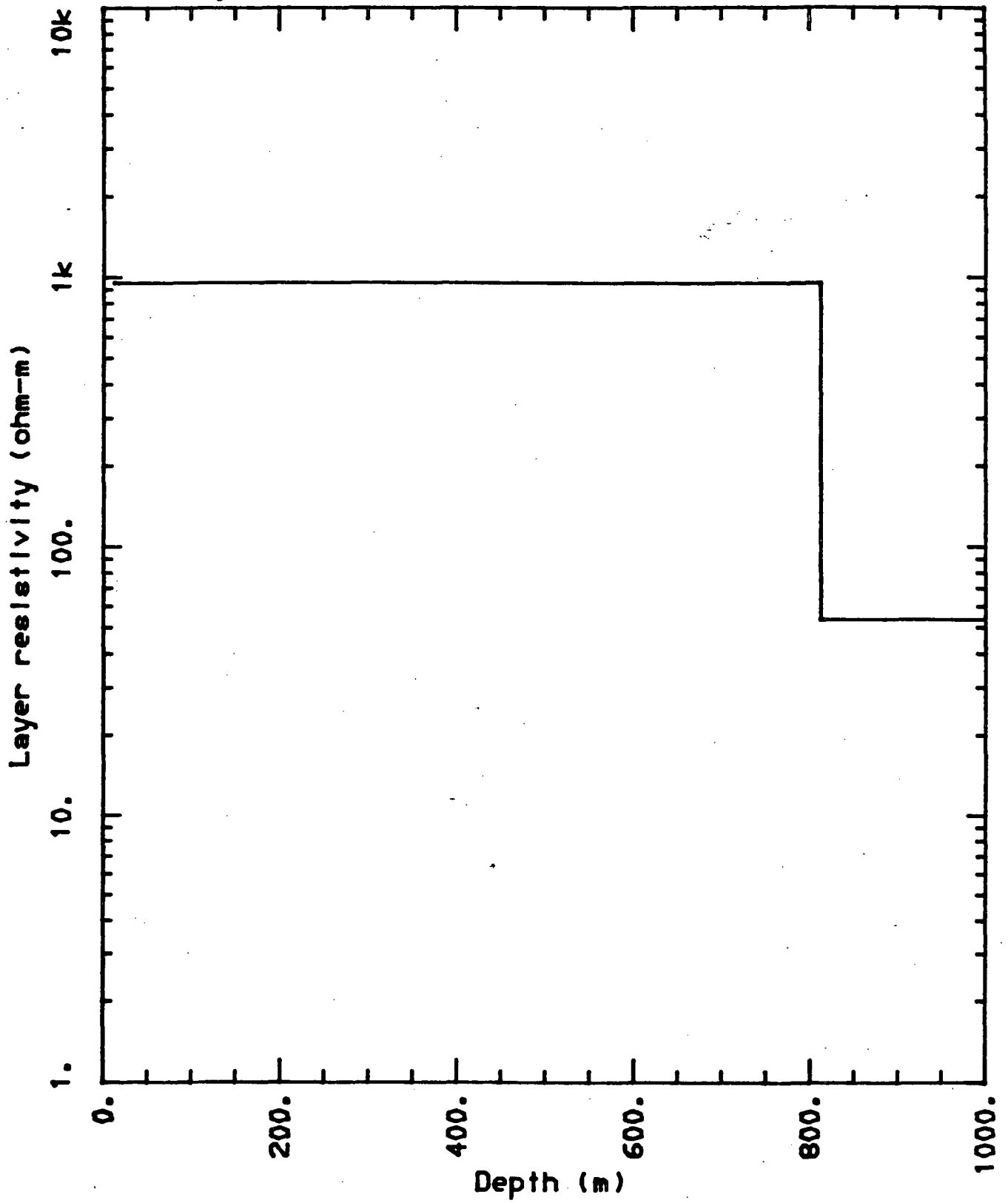




Figure 7a

<NLSTCI>: Newberry Volcano NBE-24  
 LOOP RADIUS= 172.0

I	TIME(s)	OBSERVED RESISTIVITY	STANDARD DEVIATION	COMPUTED RESISTIVITY	PERCENT ERROR
1	0.0016000	494.7	7.2	509.8	-3.0
2	0.0020000	445.0	7.3	460.0	-3.3
3	0.0026000	376.3	5.7	394.7	-4.7
4	0.0034000	327.1	2.1	335.5	-2.5
5	0.0042000	296.3	4.5	291.7	1.6
6	0.0050000	263.3	39.1	261.4	0.7
7	0.0058000	246.4	1.0	240.2	2.6
8	0.0070000	220.4	5.2	215.2	2.4
9	0.0086000	196.6	3.4	190.9	3.0
10	0.0102000	165.0	4.2	174.3	-5.3
11	0.0118000	152.0	6.9	161.6	-5.9
12	0.0134000	136.6	3.7	151.3	-9.7
13	0.0158000	139.1	4.8	139.6	-0.4
14	0.0190000	122.2	5.8	128.4	-4.8
15	0.0222000	133.9	18.9	120.1	11.5
16	0.0254000	132.1	24.8	113.8	16.1
17	0.0286000	104.2	11.3	108.8	-4.2

RMS ERROR= 11.84 X-CONVERGENCE

CORRELATION MATRIX

	1	2	3
1	1.000		
2	0.270	1.000	
3	-0.929	-0.253	1.000

	PARAMETER ESTIMATE	STANDARD ERROR	RELATIVE ERROR	PERCENT ERROR
1	0.2069E-02	0.4261E-04	0.2059E-01	2.1
2	0.2177E-01	0.4253E-03	0.1954E-01	2.0
3	0.7416E+03	0.2596E-02	0.3500E-05	0.0

FINAL INVERSION MODEL

LAYER	RESISTIVITY	P F	CONDUCTIVITY	P F	THICKNESS	DEPTH
1	483.3	1	0.20692274E-02	3	741.6	0.0
2	45.9	2	0.21765832E-01			741.6

P - parameter number  
 F - \* indicates fixed parameter

Figure 7b

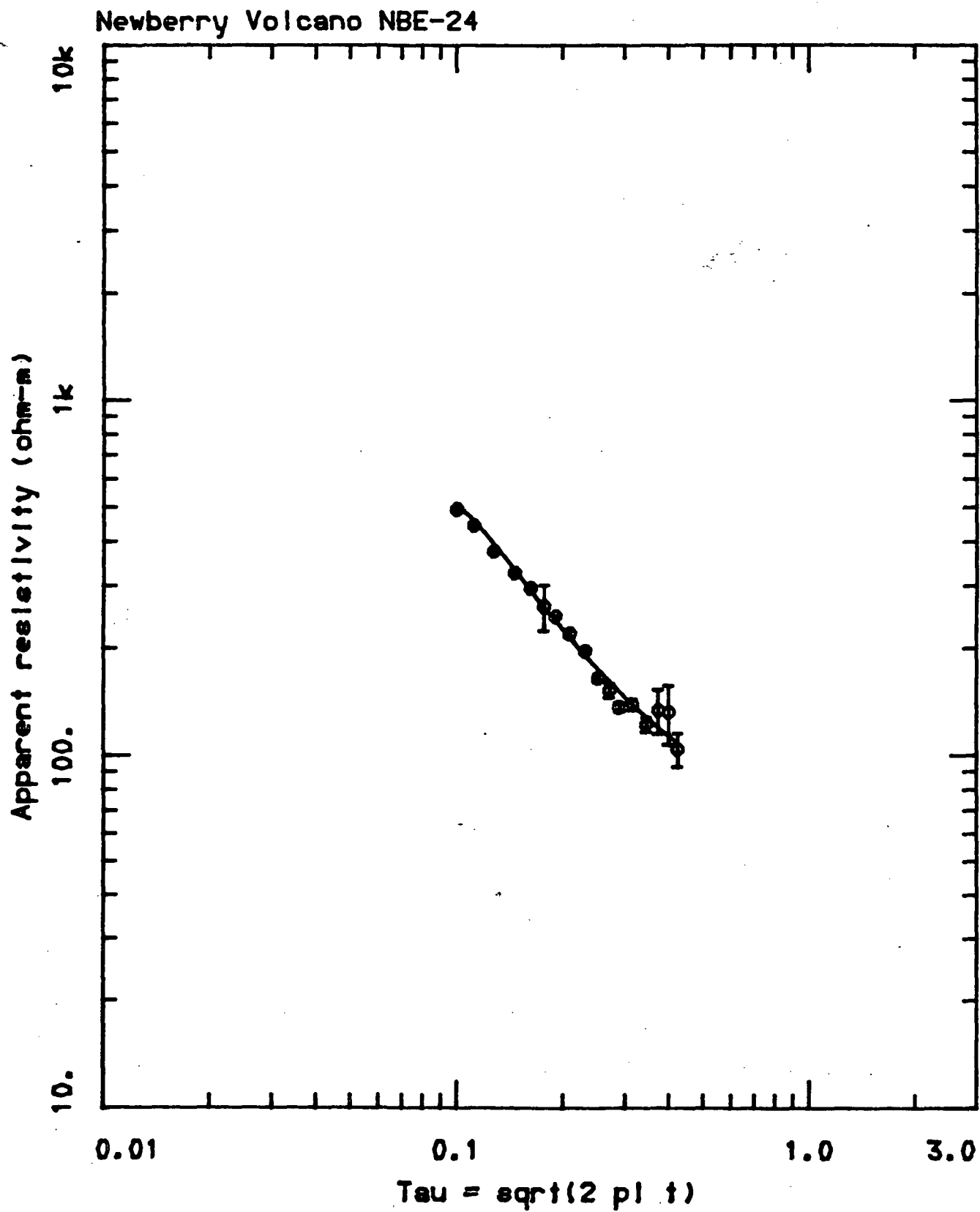


Figure 7c

Newberry Volcano NBE-24

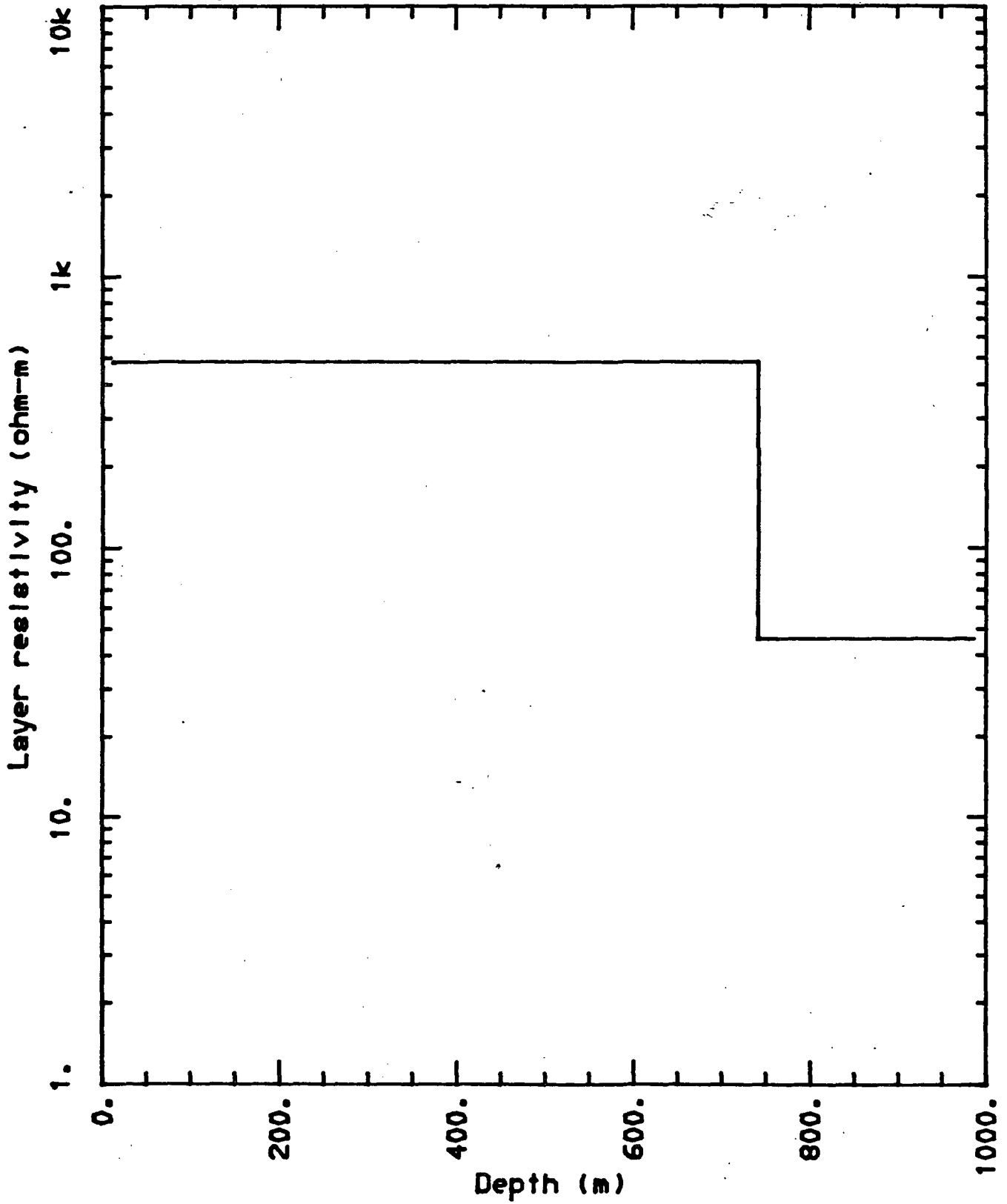


Figure 8a

<NLSTCI>: Newberry Volcano NBE-25  
 LOOP RADIUS= 172.0

I	TIME(s)	OBSERVED RESISTIVITY	STANDARD DEVIATION	COMPUTED RESISTIVITY	PERCENT ERROR
1	0.0016000	418.7	0.9	417.9	0.2
2	0.0020000	379.4	0.7	379.4	0.0
3	0.0026000	323.5	2.6	332.4	-2.7
4	0.0034000	279.4	1.7	280.7	-0.5
5	0.0042000	242.6	1.7	243.1	-0.2
6	0.0050000	217.0	1.6	216.5	0.2
7	0.0058000	199.6	3.4	196.7	1.5
8	0.0070000	175.1	2.6	173.6	0.8
9	0.0086000	156.6	3.9	152.1	3.0
10	0.0102000	137.9	3.9	137.3	0.5
11	0.0118000	128.6	1.9	125.9	2.1
12	0.0134000	119.6	5.0	116.7	2.5
13	0.0158000	107.0	4.1	106.3	0.6
14	0.0190000	97.2	2.7	96.2	1.0
15	0.0222000	94.0	5.4	88.6	6.0
16	0.0254000	83.1	3.8	82.6	0.6
17	0.0286000	77.2	3.5	77.6	-0.6
18	0.0334000	69.1	4.3	71.7	-3.6
19	0.0398000	62.8	0.8	65.4	-3.9

RMS ERROR= 3.261 X-CONVERGENCE

CORRELATION MATRIX

	2	3	5
2	1.000		
3	-0.719	1.000	
5	-0.055	-0.034	1.000

	PARAMETER ESTIMATE	STANDARD ERROR	RELATIVE ERROR	PERCENT ERROR
2	0.3576E-02	0.3268E-04	0.9138E-02	0.9
3	0.3362E-01	0.3090E-03	0.9194E-02	0.9
5	0.5893E+03	0.7973E-03	0.1353E-05	0.0

FINAL INVERSION MODEL

LAYER	RESISTIVITY	P	F	CONDUCTIVITY	P	F	THICKNESS	DEPTH
1	2770.1	1	*	0.36100001E-03	4	*	120.0	0.0
2	279.6	2		0.35759581E-02	5		589.3	120.0
3	29.7	3		0.33615280E-01				709.3

P - parameter number  
 F - \* indicates fixed parameter

Figure 8b

Newberry Volcano NBE-25

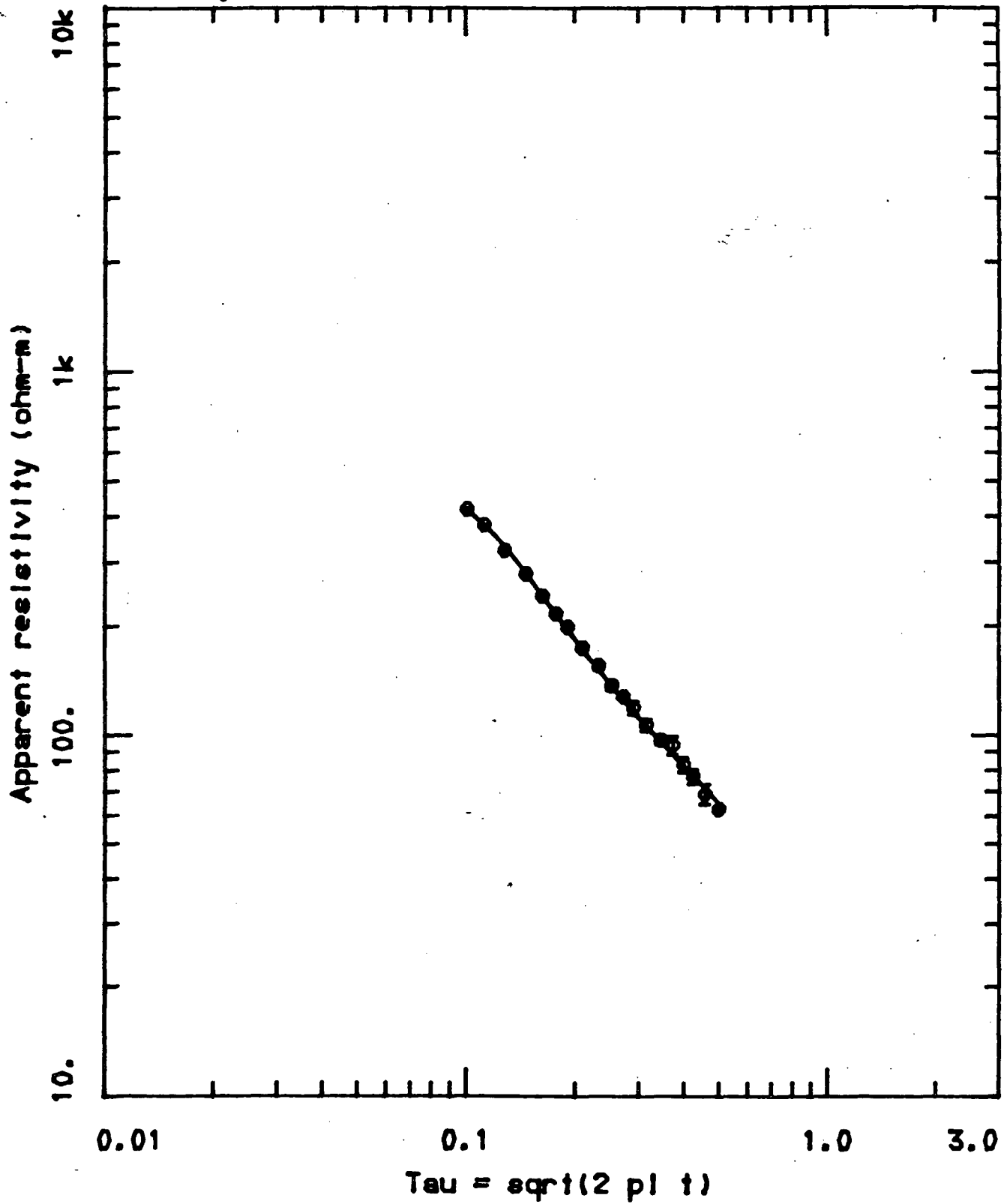


Figure 8c

Newberry Volcano NBE-25

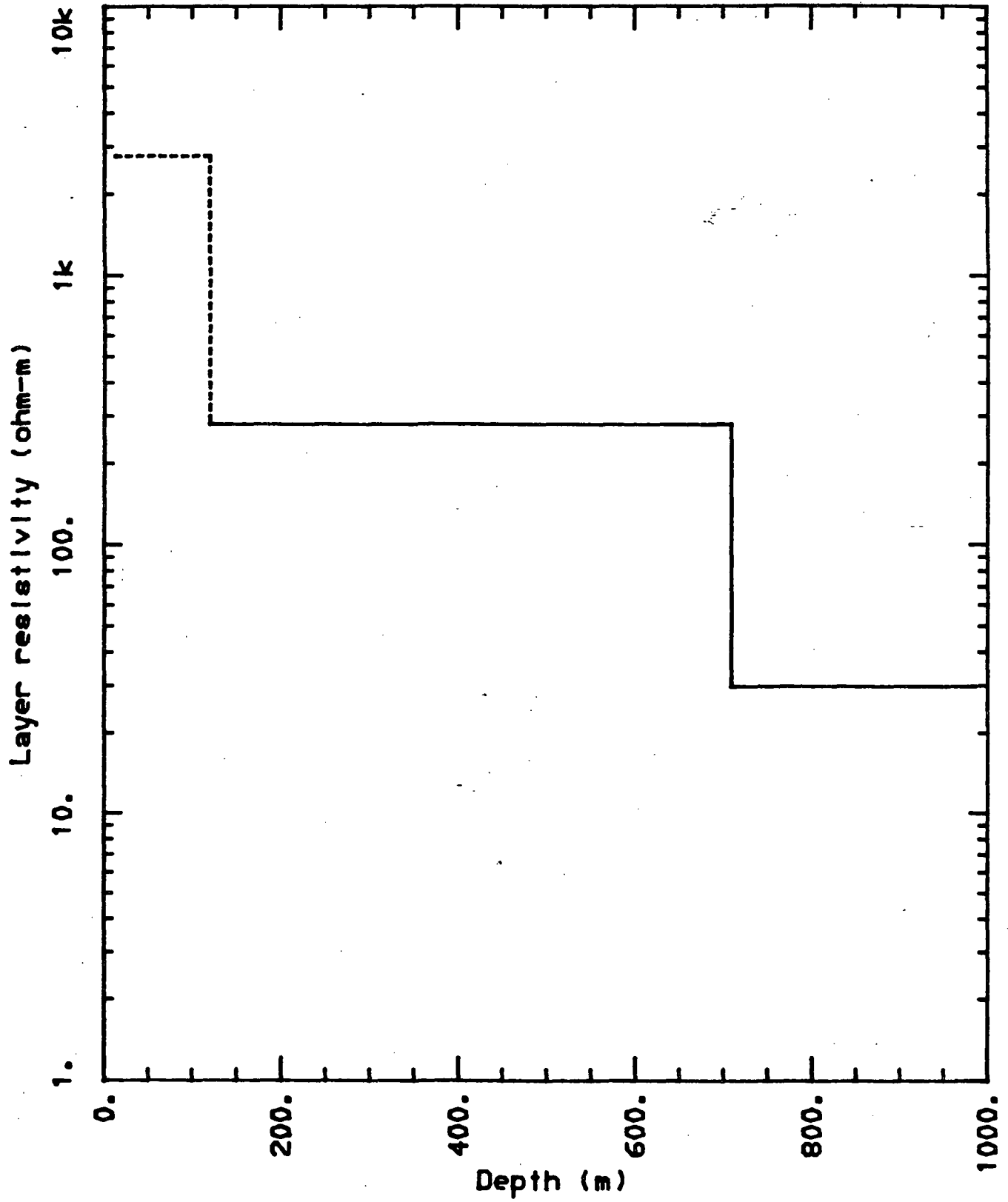


Figure 9a

<NLSTCI>: Newberry Volcano NBE-26  
 LOOP RADIUS= 172.0

I	TIME(s)	OBSERVED RESISTIVITY	STANDARD DEVIATION	COMPUTED RESISTIVITY	PERCENT ERROR
1	0.0016000	569.5	1.1	568.4	0.2
2	0.0020000	493.4	5.0	506.0	-2.5
3	0.0026000	418.7	5.8	425.9	-1.7
4	0.0034000	348.7	5.4	352.8	-1.2
5	0.0042000	307.4	3.5	303.6	1.2
6	0.0050000	258.7	48.0	267.0	-3.1
7	0.0058000	244.6	11.2	239.9	2.0
8	0.0070000	212.5	3.9	211.2	0.6
9	0.0086000	184.9	3.1	184.1	0.4
10	0.0102000	173.2	2.7	164.7	5.2
11	0.0118000	155.3	5.5	150.6	3.2
12	0.0134000	142.8	6.2	139.5	2.3
13	0.0158000	127.1	2.1	126.6	0.4
14	0.0190000	112.9	3.9	113.9	-0.9
15	0.0222000	102.5	1.4	104.7	-2.1
16	0.0254000	95.0	1.8	97.5	-2.6
17	0.0286000	100.7	11.2	91.7	9.8
18	0.0334000	84.8	4.5	84.8	0.0
19	0.0398000	68.7	5.2	77.8	-11.7

RMS ERROR= 6.208 X-CONVERGENCE

CORRELATION MATRIX

	2	3	5
2	1.000		
3	0.069	1.000	
5	-0.910	0.050	1.000

	PARAMETER ESTIMATE	STANDARD ERROR	RELATIVE ERROR	PERCENT ERROR
2	0.2575E-02	0.4734E-04	0.1839E-01	1.8
3	0.3062E-01	0.1544E-03	0.5044E-02	0.5
5	0.6267E+03	0.1218E-02	0.1944E-05	0.0

FINAL INVERSION MODEL

LAYER	RESISTIVITY	P F	CONDUCTIVITY	P F	THICKNESS	DEPTH
1	2232.1	1 *	0.44800001E-03	4 *	150.0	0.0
2	388.4	2	0.25747700E-02	5	626.7	150.0
3	32.7	3	0.30615348E-01			776.7

P - parameter number  
 F - \* indicates fixed parameter

Figure 9b

Newberry Volcano NBE-26

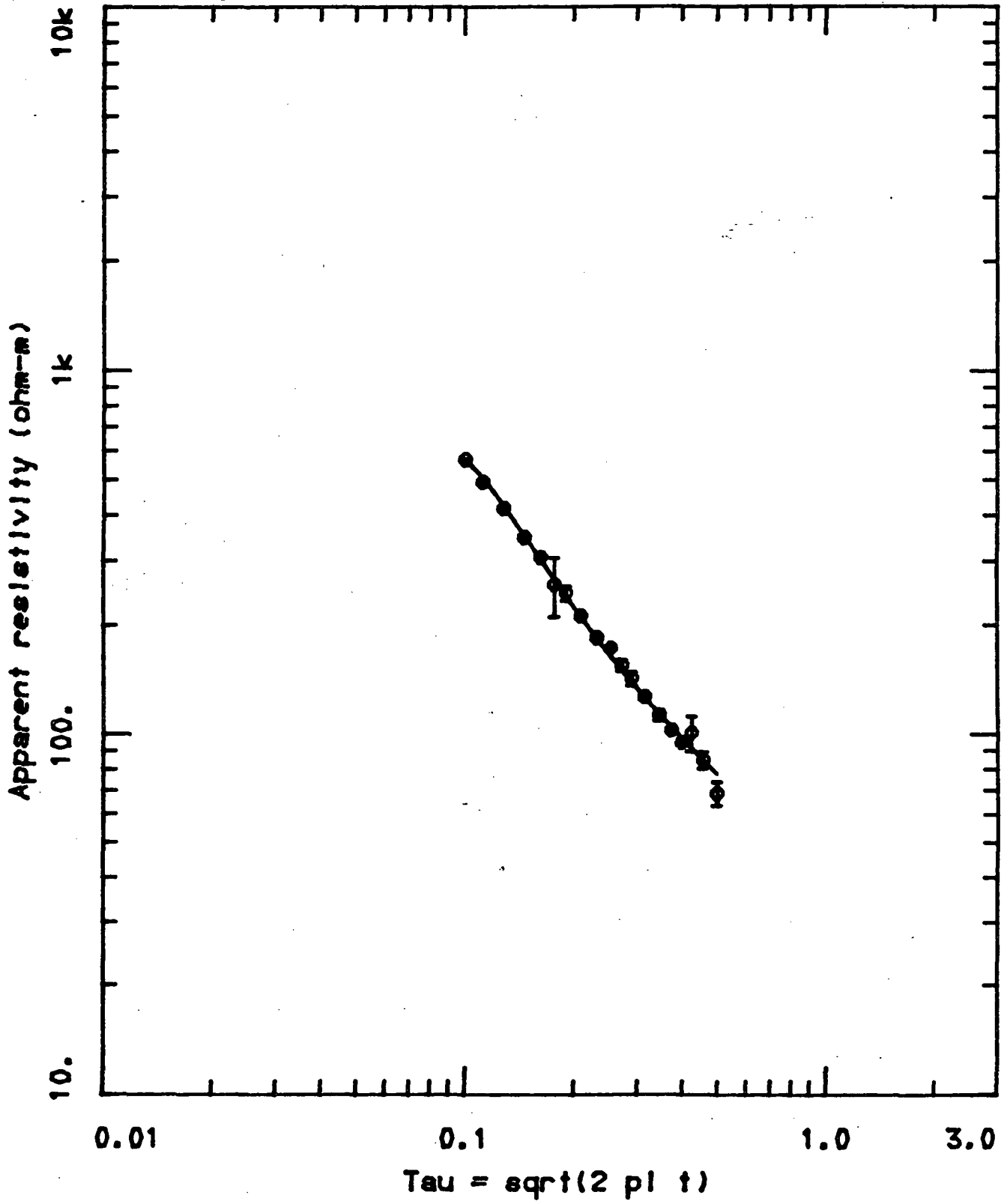




Figure 9c

Newberry Volcano NBE-26

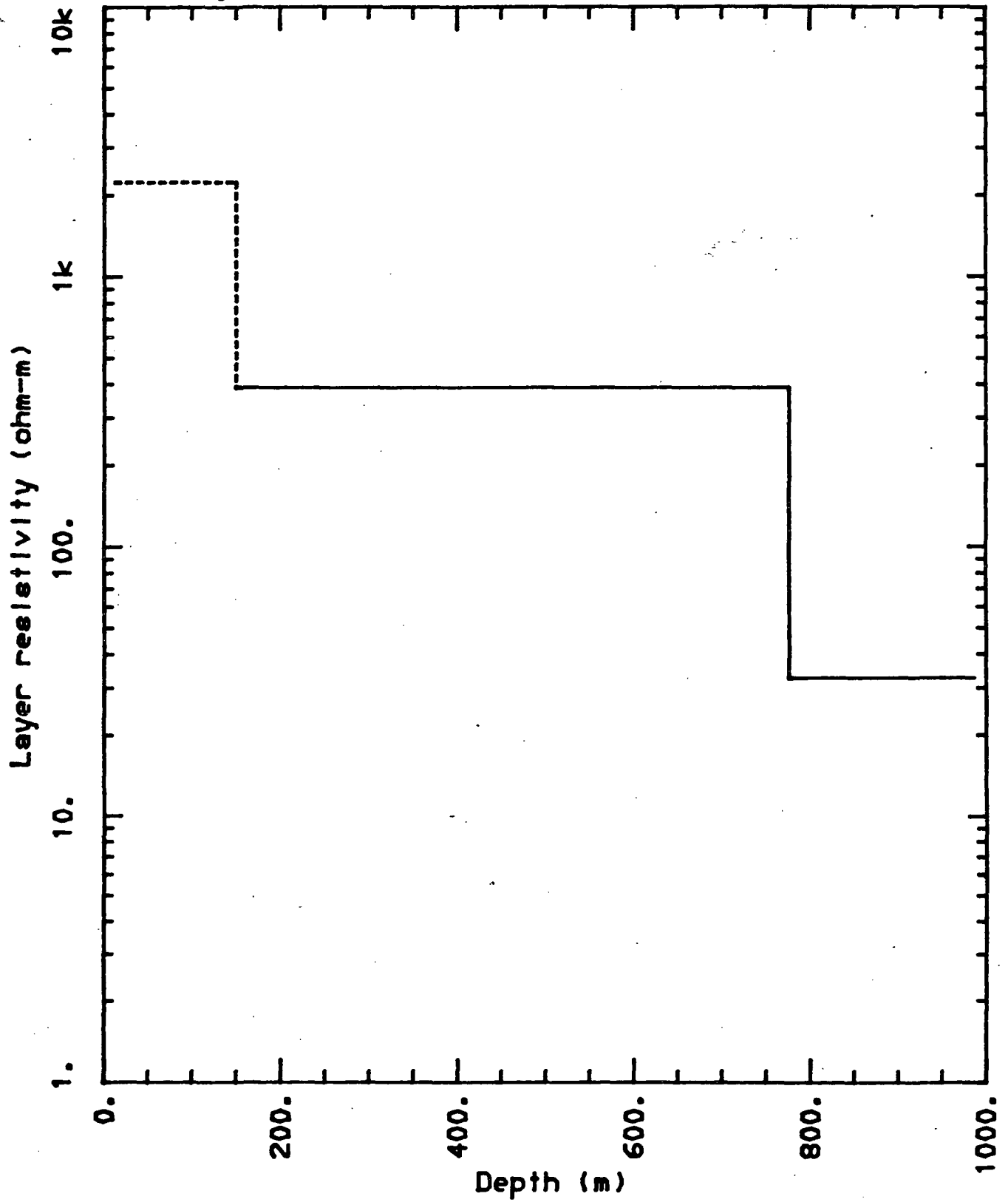


Figure 10a

<NLSTCI>: Newberry Volcano NBE-27  
 LOOP RADIUS= 172.0

I	TIME(s)	OBSERVED RESISTIVITY	STANDARD DEVIATION	COMPUTED RESISTIVITY	PERCENT ERROR
1	0.0016000	343.8	0.3	339.8	-1.2
2	0.0020000	313.0	0.5	324.2	-3.5
3	0.0026000	280.6	1.7	294.8	-4.8
4	0.0034000	255.2	0.9	257.0	-0.7
5	0.0042000	233.7	1.3	227.5	2.7
6	0.0050000	207.6	18.2	203.9	1.8
7	0.0058000	196.0	16.9	185.1	5.9
8	0.0070000	181.1	10.0	164.0	10.4
9	0.0086000	155.8	0.8	144.8	7.6
10	0.0102000	139.2	0.7	130.4	6.7
11	0.0118000	128.8	2.0	119.3	8.0
12	0.0134000	117.0	3.2	110.7	5.7
13	0.0158000	101.8	0.5	101.1	0.7
14	0.0190000	87.5	1.2	91.5	-4.4
15	0.0222000	82.5	1.9	84.4	-2.2
16	0.0254000	82.5	4.0	78.9	4.6
17	0.0286000	73.7	7.0	74.4	-0.9
18	0.0334000	63.9	1.1	69.1	-7.5
19	0.0398000	58.8	2.8	63.6	-7.5

RMS ERROR= 9.332 X-CONVERGENCE

CORRELATION MATRIX

	1	2	3	4	5
1	1.000				
2	-0.850	1.000			
3	0.392	-0.512	1.000		
4	-0.762	0.882	-0.326	1.000	
5	0.457	-0.586	-0.160	-0.786	1.000

	PARAMETER ESTIMATE	STANDARD ERROR	RELATIVE ERROR	PERCENT ERROR
1	0.5405E-03	0.8094E-04	0.1498E+00	15.0
2	0.4576E-02	0.2847E-03	0.6221E-01	6.2
3	0.3784E-01	0.1361E-02	0.3597E-01	3.6
4	0.1223E+03	0.5348E-02	0.4372E-04	0.0
5	0.5957E+03	0.7033E-02	0.1181E-04	0.0

FINAL INVERSION MODEL

LAYER	RESISTIVITY	P F	CONDUCTIVITY	P F	THICKNESS	DEPTH
1	1850.2	1	0.54047536E-03	4	122.3	0.0
2	218.5	2	0.45763673E-02	5	595.7	122.3
3	26.4	3	0.37836563E-01			718.1

P - parameter number  
 F - \* indicates fixed parameter

Figure 10b

Newberry Volcano NBE-27

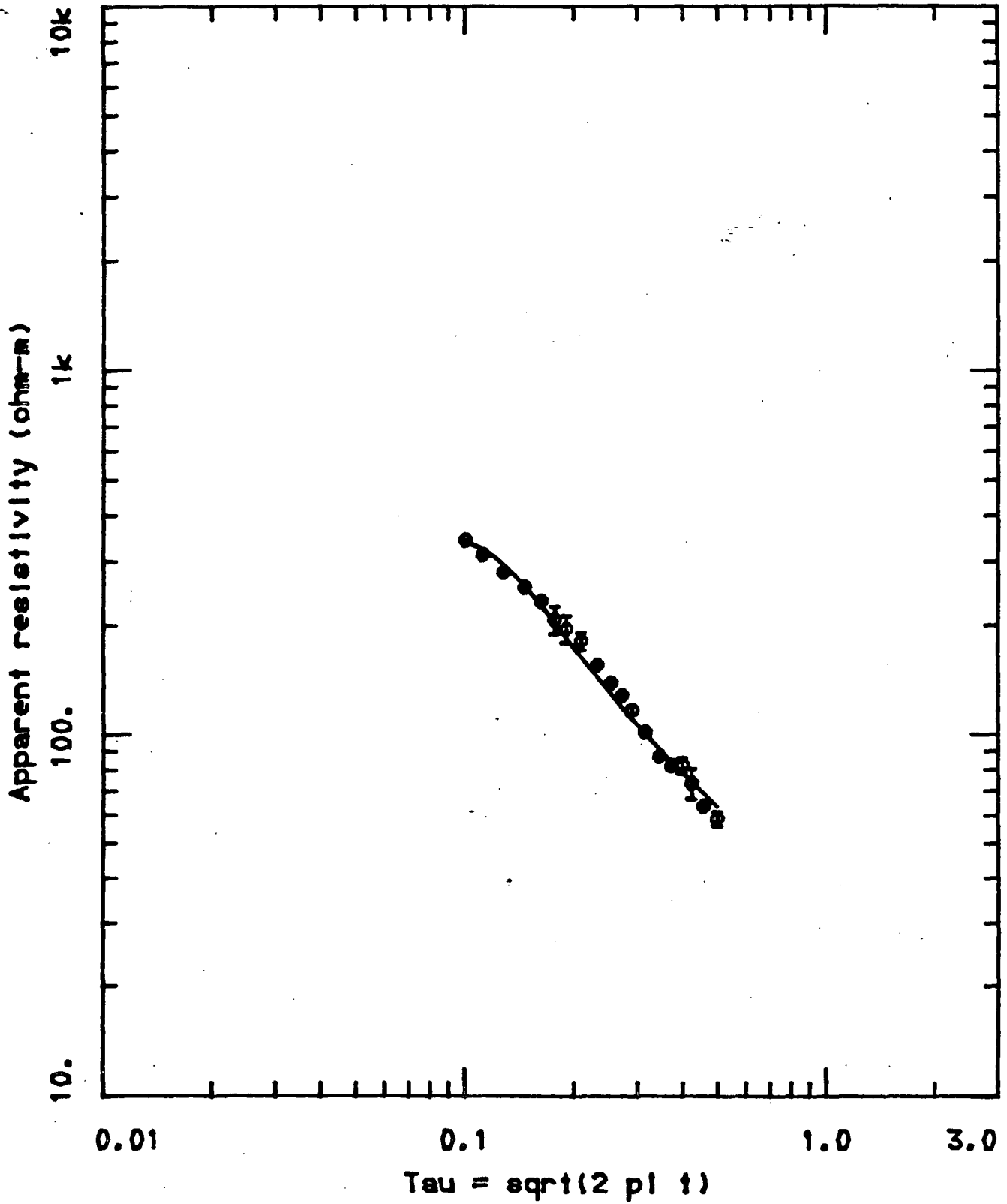


Figure 10c

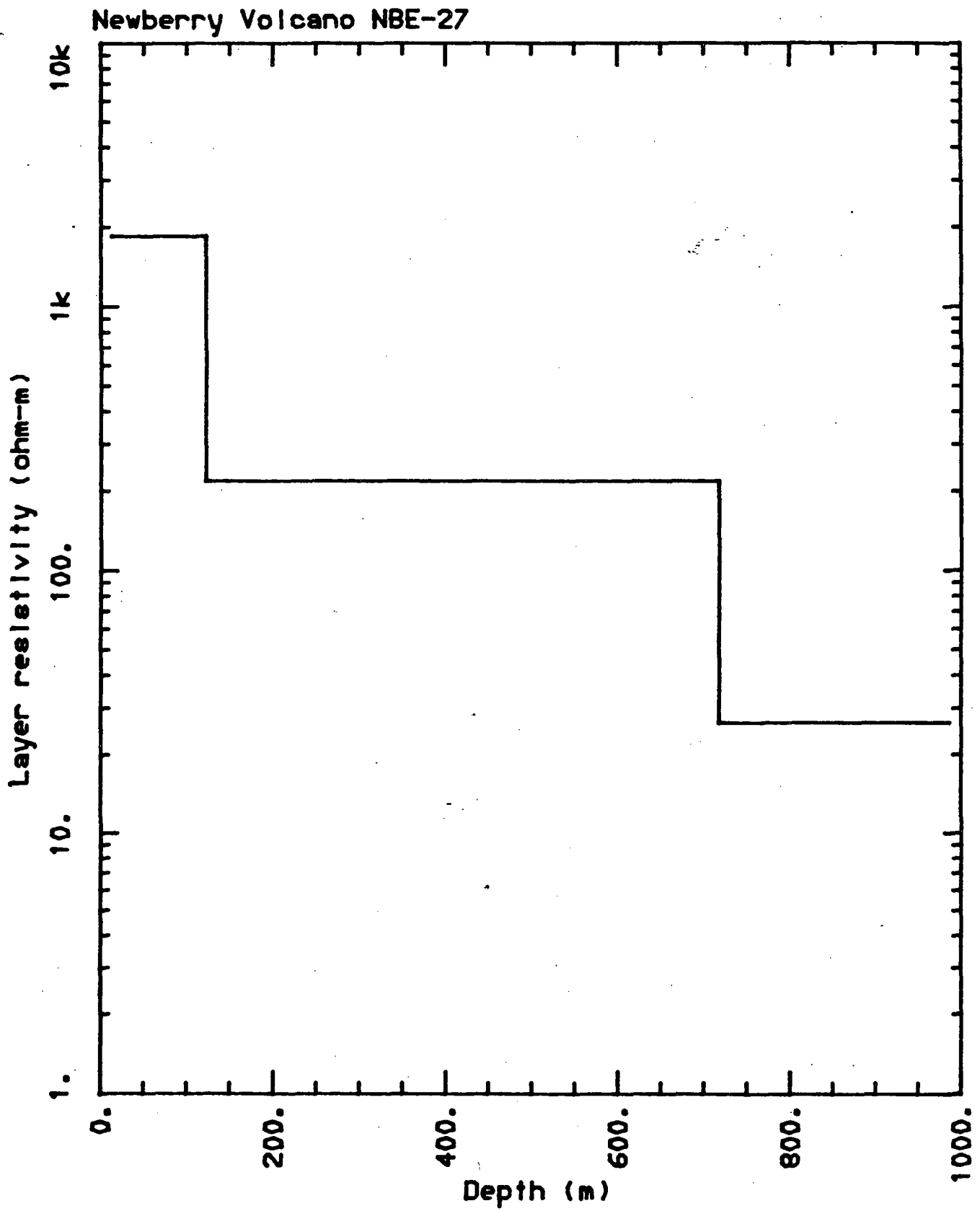


Figure 11a

<NLSTCI>: Newberry Volcano NBE-28  
 LOOP RADIUS= 172.0

I	TIME(s)	OBSERVED RESISTIVITY	STANDARD DEVIATION	COMPUTED RESISTIVITY	PERCENT ERROR
1	0.0016000	429.5	11.1	412.6	4.1
2	0.0020000	389.6	7.7	391.5	-0.5
3	0.0026000	343.2	3.4	352.7	-2.7
4	0.0034000	292.6	12.3	304.4	-3.9
5	0.0042000	267.5	8.4	263.3	1.6
6	0.0050000	253.7	15.9	231.7	9.5
7	0.0058000	195.6	49.5	208.0	-6.0
8	0.0070000	159.5	61.3	182.0	-12.4
9	0.0086000	177.7	7.8	156.6	13.4
10	0.0102000	160.7	18.2	138.9	15.7
11	0.0118000	156.9	11.6	126.1	24.5
12	0.0134000	138.8	16.9	116.0	19.7
13	0.0158000	163.0	40.7	104.2	56.4
14	0.0190000	167.9	81.1	92.8	80.8
15	0.0222000	121.1	65.5	84.7	43.0

RMS ERROR= 38.07 X-CONVERGENCE

CORRELATION MATRIX

	1	2	3	4	5
1	1.000				
2	-0.824	1.000			
3	0.514	-0.296	1.000		
4	-0.913	0.970	-0.299	1.000	
5	0.453	-0.795	-0.142	-0.708	1.000

	PARAMETER ESTIMATE	STANDARD ERROR	RELATIVE ERROR	PERCENT ERROR
1	0.7732E-03	0.3808E-03	0.4925E+00	49.3
2	0.3727E-02	0.1125E-02	0.3018E+00	30.2
3	0.4854E-01	0.2960E-02	0.6097E-01	6.1
4	0.1197E+03	0.1992E-01	0.1664E-03	0.0
5	0.6447E+03	0.1234E-01	0.1914E-04	0.0

FINAL INVERSION MODEL

LAYER	RESISTIVITY	P F	CONDUCTIVITY	P F	THICKNESS	DEPTH
1	1293.3	1	0.77318924E-03	4	119.7	0.0
2	268.3	2	0.37266919E-02	5	644.7	119.7
3	20.6	3	0.48544604E-01			764.4

P - parameter number  
 F - \* indicates fixed parameter

Figure 11b

Newberry Volcano NBE-28

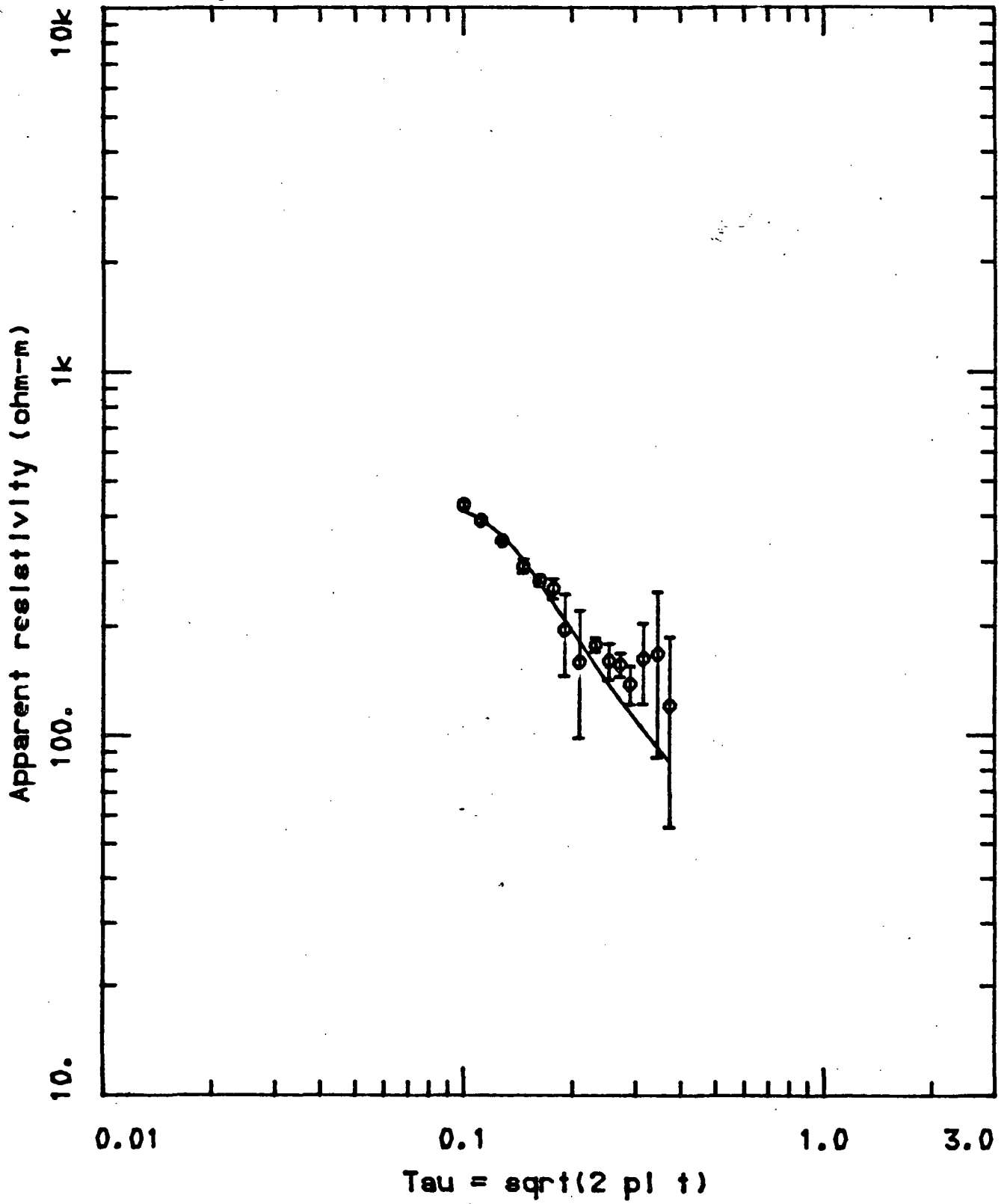


Figure 11c

Newberry Volcano NBE-28

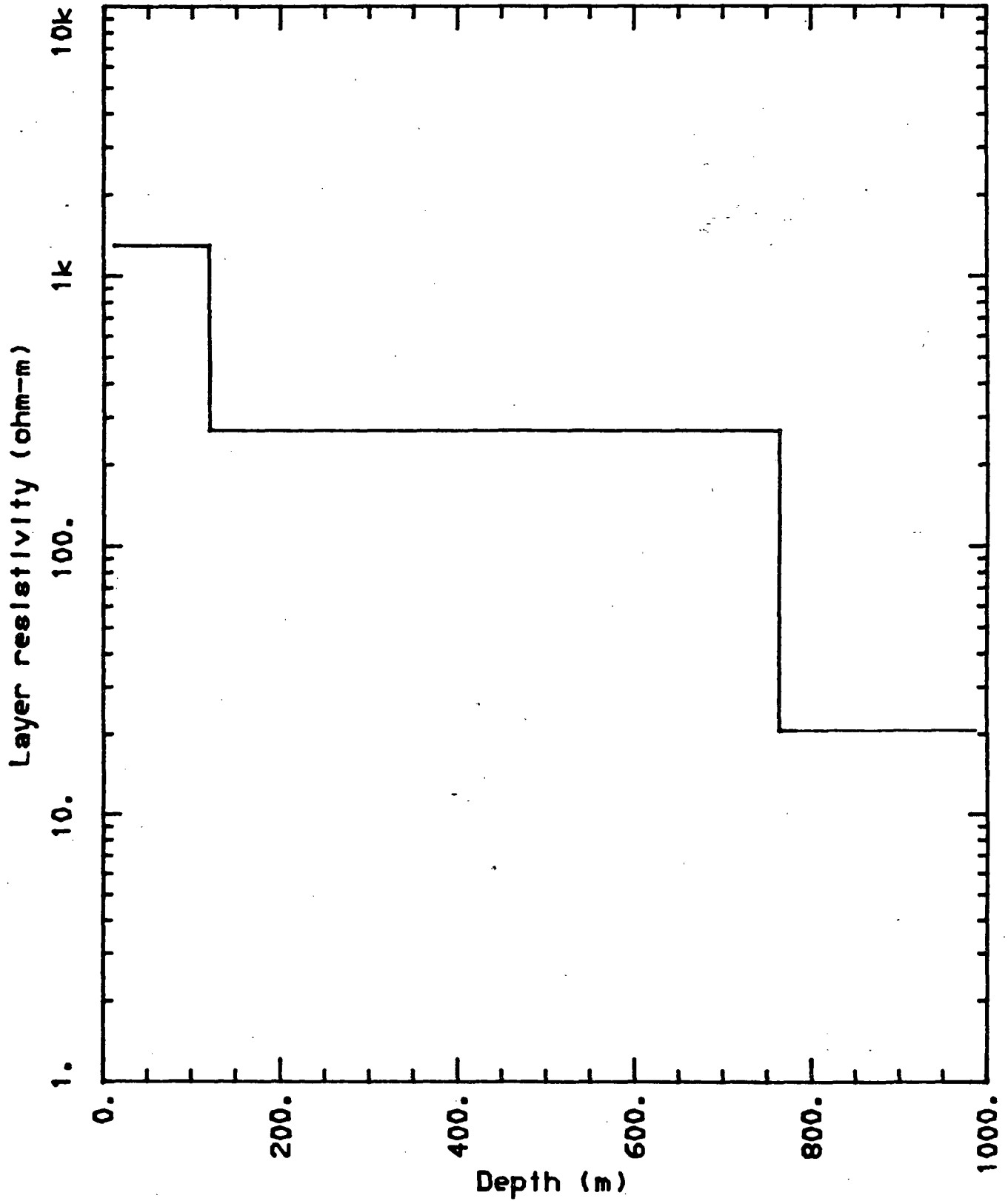


Figure 12a

<NLSTCI>: Newberry Volcano NBE-29  
 LOOP RADIUS= 172.0

I	TIME(s)	OBSERVED RESISTIVITY	STANDARD DEVIATION	COMPUTED RESISTIVITY	PERCENT ERROR
1	0.0016000	520.8	7.1	498.9	4.4
2	0.0020000	461.7	5.1	468.5	-1.4
3	0.0026000	396.5	3.0	412.6	-3.9
4	0.0034000	343.1	4.5	347.9	-1.4
5	0.0042000	305.3	4.8	298.7	2.2
6	0.0050000	285.3	144.6	260.5	9.5
7	0.0058000	232.0	22.8	232.8	-0.4
8	0.0070000	239.2	33.0	203.2	17.7
9	0.0086000	192.7	4.2	174.5	10.4
10	0.0102000	171.5	5.5	154.3	11.1
11	0.0118000	153.2	9.3	139.9	9.5
12	0.0134000	142.9	12.3	128.7	11.1
13	0.0158000	130.8	9.8	115.7	13.1
14	0.0190000	116.7	4.3	103.3	13.0
15	0.0222000	108.0	4.9	94.4	14.4
16	0.0254000	93.9	6.4	87.6	7.2
17	0.0286000	87.2	4.3	82.2	6.1

RMS ERROR= 17.79 X-CONVERGENCE

CORRELATION MATRIX

	1	2	3
1	1.000		
2	-0.050	1.000	
3	-0.254	0.112	1.000

	PARAMETER ESTIMATE	STANDARD ERROR	RELATIVE ERROR	PERCENT ERROR
1	0.2418E-02	0.5334E-04	0.2205E-01	2.2
2	0.4384E-01	0.8804E-03	0.2008E-01	2.0
3	0.7916E+03	0.4801E-02	0.6065E-05	0.0

FINAL INVERSION MODEL

LAYER	RESISTIVITY	P F	CONDUCTIVITY	P F	THICKNESS	DEPTH
1	413.5	1	0.24184240E-02	3	791.6	0.0
2	22.8	2	0.43841951E-01			791.6

P - parameter number  
 F - \* indicates fixed parameter



Figure 12b

Newberry Volcano NBE-29

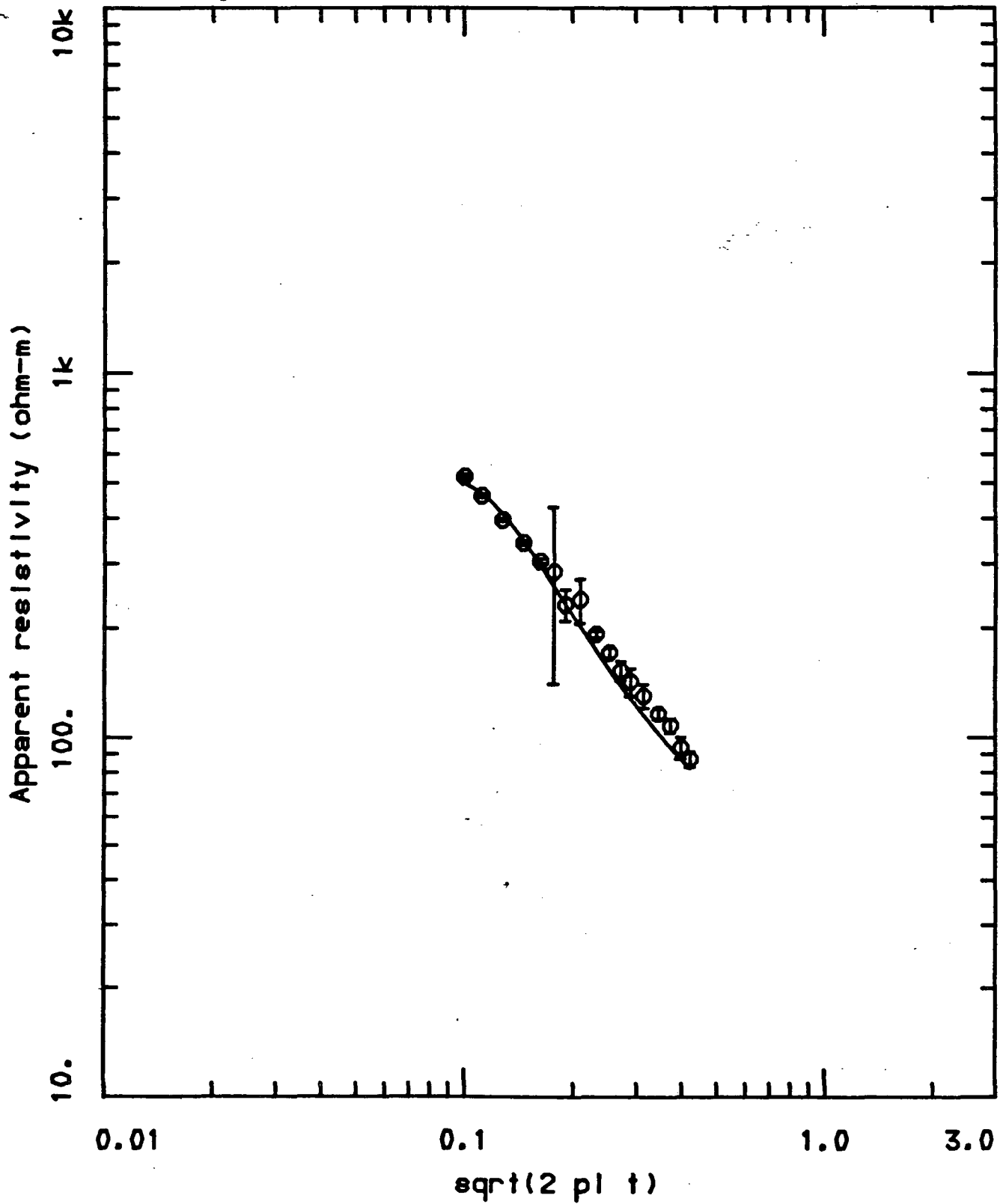


Figure 12c

Newberry Volcano NBE-29

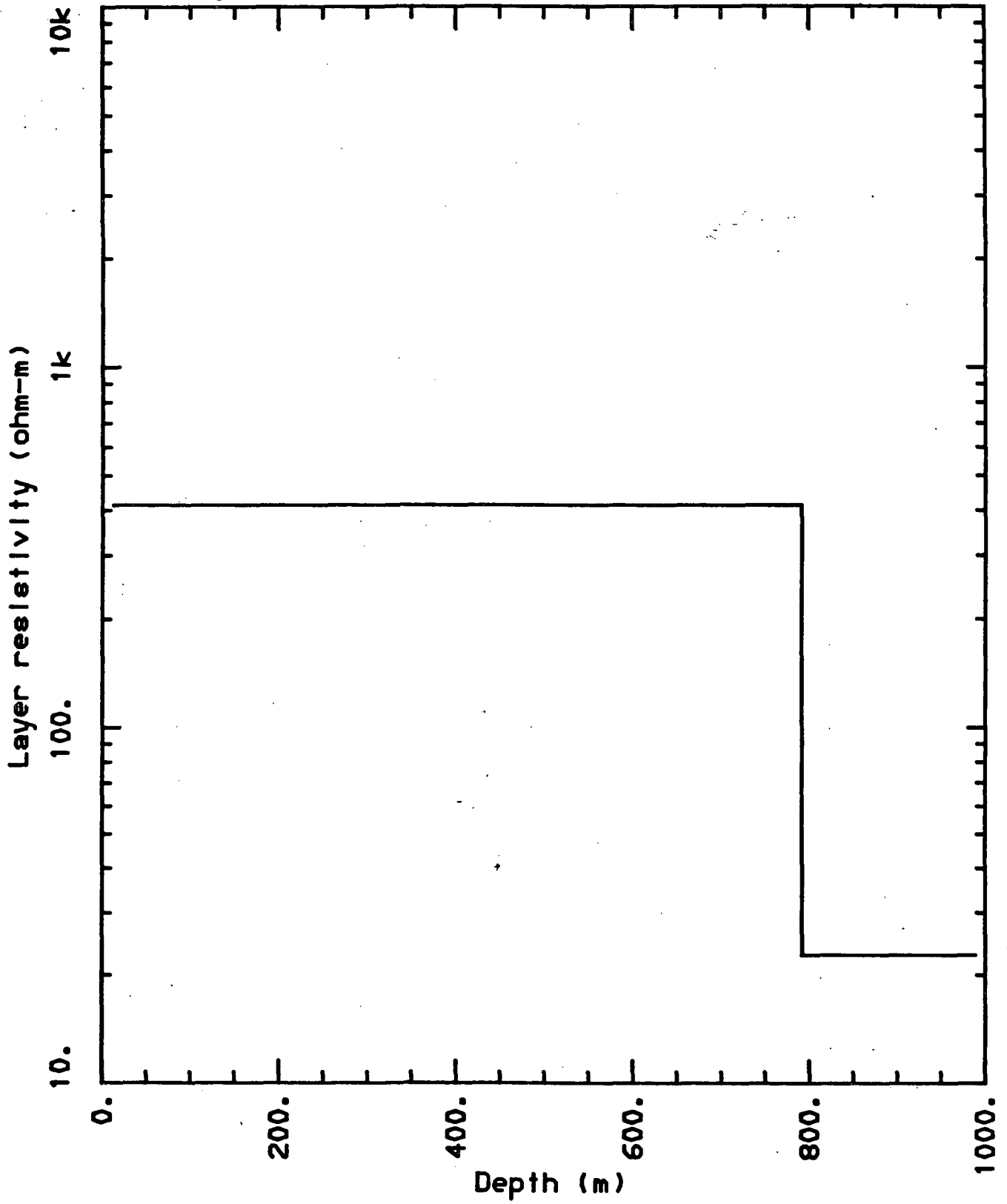


Figure 13a

<NLSTCI>: Newberry Volcano NBE-30  
 LOOP RADIUS= 172.0

I	TIME(s)	OBSERVED RESISTIVITY	STANDARD DEVIATION	COMPUTED RESISTIVITY	PERCENT ERROR
1	0.0016000	476.1	2.0	437.8	8.8
2	0.0020000	433.5	4.6	432.2	0.3
3	0.0026000	384.1	4.8	411.5	-6.7
4	0.0034000	340.3	4.2	365.8	-7.0
5	0.0042000	304.4	3.3	324.4	-6.2
6	0.0050000	278.9	26.9	288.2	-3.2
7	0.0058000	254.7	14.9	259.3	-1.8
8	0.0070000	223.0	5.8	228.7	-2.5
9	0.0086000	201.8	5.9	199.0	1.4
10	0.0102000	179.4	5.7	176.7	1.5
11	0.0118000	167.2	4.4	160.6	4.1
12	0.0134000	155.9	7.4	148.6	4.9
13	0.0158000	143.0	6.1	134.1	6.6
14	0.0190000	125.4	4.3	119.7	4.8
15	0.0222000	115.9	9.0	109.3	6.0
16	0.0254000	98.0	0.6	101.5	-3.4
17	0.0286000	96.3	1.9	95.3	1.1

RMS ERROR= 16.25 X-CONVERGENCE

CORRELATION MATRIX

	1	2	3
1	1.000		
2	0.281	1.000	
3	0.162	0.476	1.000

PARAMETER ESTIMATE	STANDARD ERRDR	RELATIVE ERROR	PERCENT ERROR
1 0.2704E-02	0.5341E-04	0.1975E-01	2.0
2 0.3716E-01	0.8861E-03	0.2385E-01	2.4
3 0.8678E+03	0.7882E-02	0.9083E-05	0.0

FINAL INVERSION MODEL

LAYER	RESISTIVITY	P F	CONDUCTIVITY	P F	THICKNESS	DEPTH
1	369.8	1	0.27038516E-02	3	867.8	0.0
2	26.9	2	0.37156533E-01			867.8

P - parameter number  
 F - \* indicates fixed parameter

Figure 13b

Newberry Volcano NBE-30

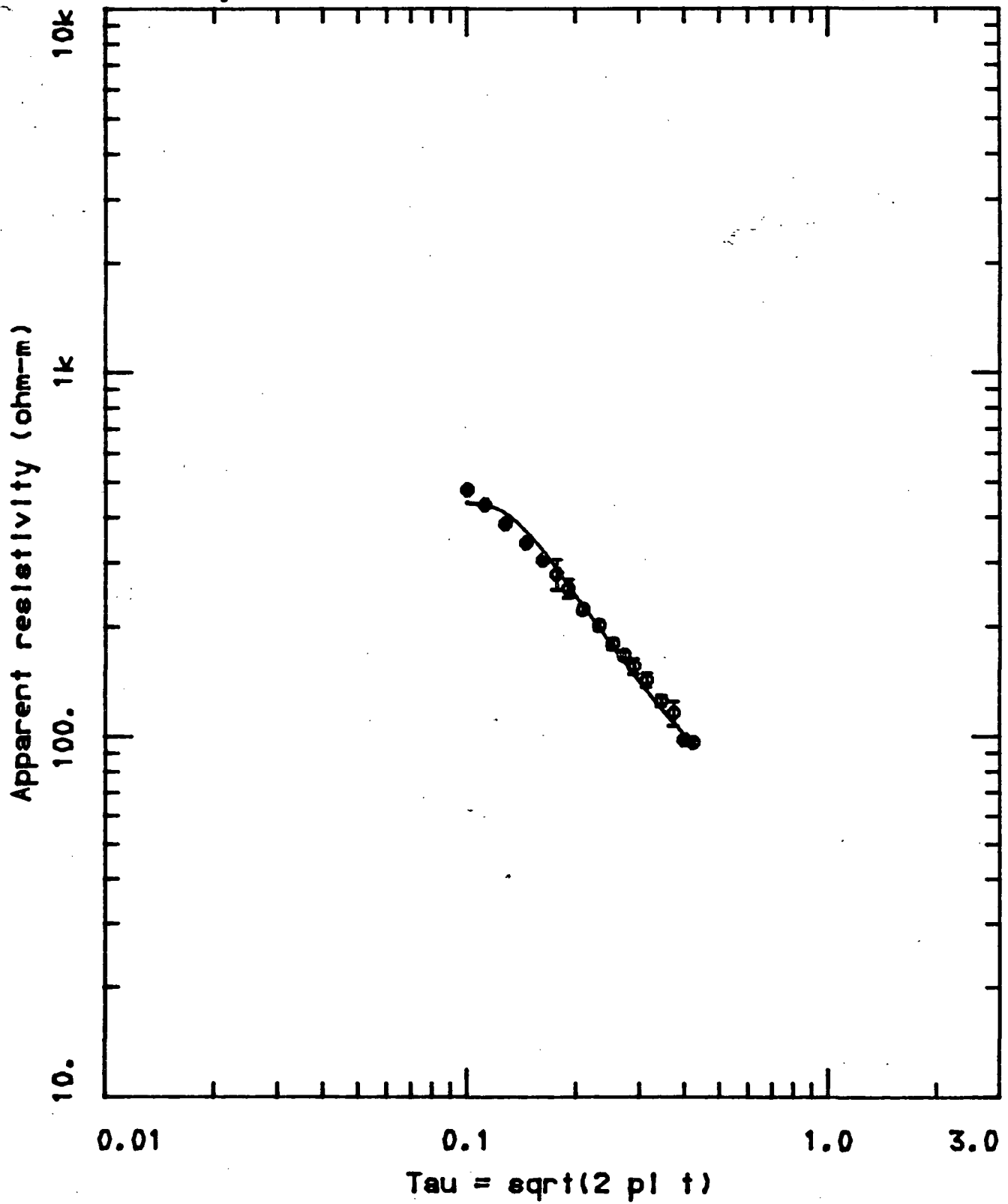


Figure 13c

Newberry Volcano NBE-30

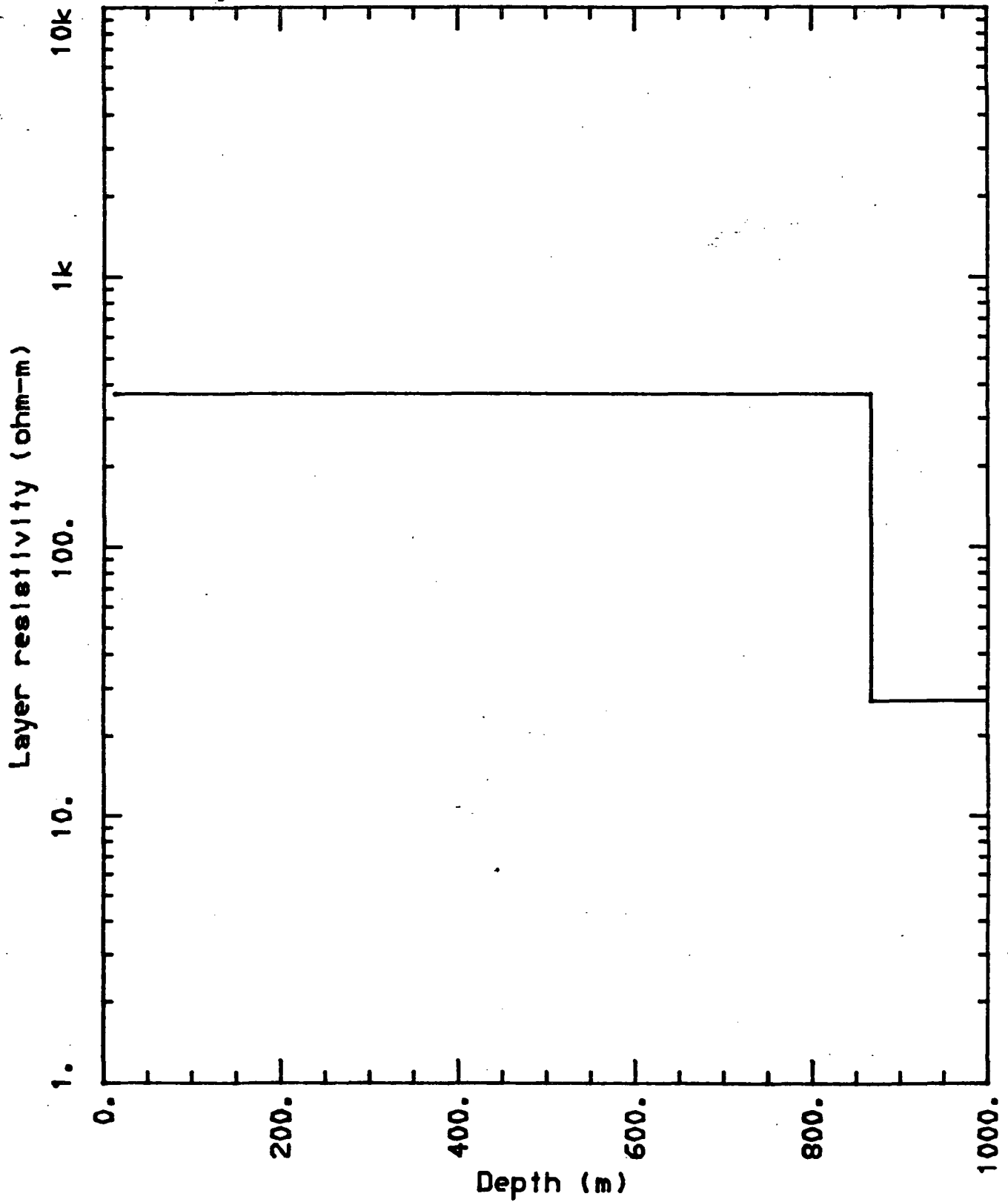


Figure 14a

<NLSTC1>: Newberry Volcano NBE-31  
 LOOP RADIUS= 172.0

I	TIME(s)	OBSERVED RESISTIVITY	STANDARD DEVIATION	COMPUTED RESISTIVITY	PERCENT ERROR
1	0.0016000	426.3	1.4	420.5	1.4
2	0.0020000	373.0	1.9	370.0	0.8
3	0.0026000	318.8	0.6	319.8	-0.3
4	0.0034000	276.6	1.8	273.8	1.0
5	0.0042000	246.0	2.7	242.8	1.3
6	0.0050000	229.2	28.0	222.2	3.2
7	0.0058000	201.2	14.5	205.7	-2.2
8	0.0070000	184.3	2.1	186.8	-1.4
9	0.0086000	167.6	2.2	169.7	-1.2
10	0.0102000	155.4	3.3	157.4	-1.3
11	0.0118000	153.0	5.3	148.0	3.4
12	0.0134000	145.6	1.7	140.6	3.5
13	0.0158000	129.5	3.0	132.1	-2.0
14	0.0190000	113.8	3.8	123.8	-8.1
15	0.0222000	100.1	5.4	117.6	-14.9
16	0.0254000	92.5	5.9	112.5	-17.8
17	0.0286000	96.0	5.2	108.4	-11.4

RMS ERROR= 9.113 X-CONVERGENCE

CORRELATION MATRIX

	2	3	5
2	1.000		
3	-0.209	1.000	
5	0.342	-0.301	1.000

	PARAMETER ESTIMATE	STANDARD ERROR	RELATIVE ERROR	PERCENT ERROR
2	0.2482E-02	0.8234E-04	0.3317E-01	3.3
3	0.1757E-01	0.2441E-03	0.1390E-01	1.4
5	0.5207E+03	0.9011E-03	0.1730E-05	0.0

FINAL INVERSION MODEL

LAYER	RESISTIVITY	P	F	CONDUCTIVITY	P	F	THICKNESS	DEPTH
1	1015.2	1	*	0.98500005E-03	4	*	100.0	0.0
2	402.9	2		0.24823032E-02	5		520.7	100.0
3	56.9	3		0.17567847E-01				620.7

P - parameter number  
 F - \* indicates fixed parameter

Figure 14b

Newberry Volcano NBE-31

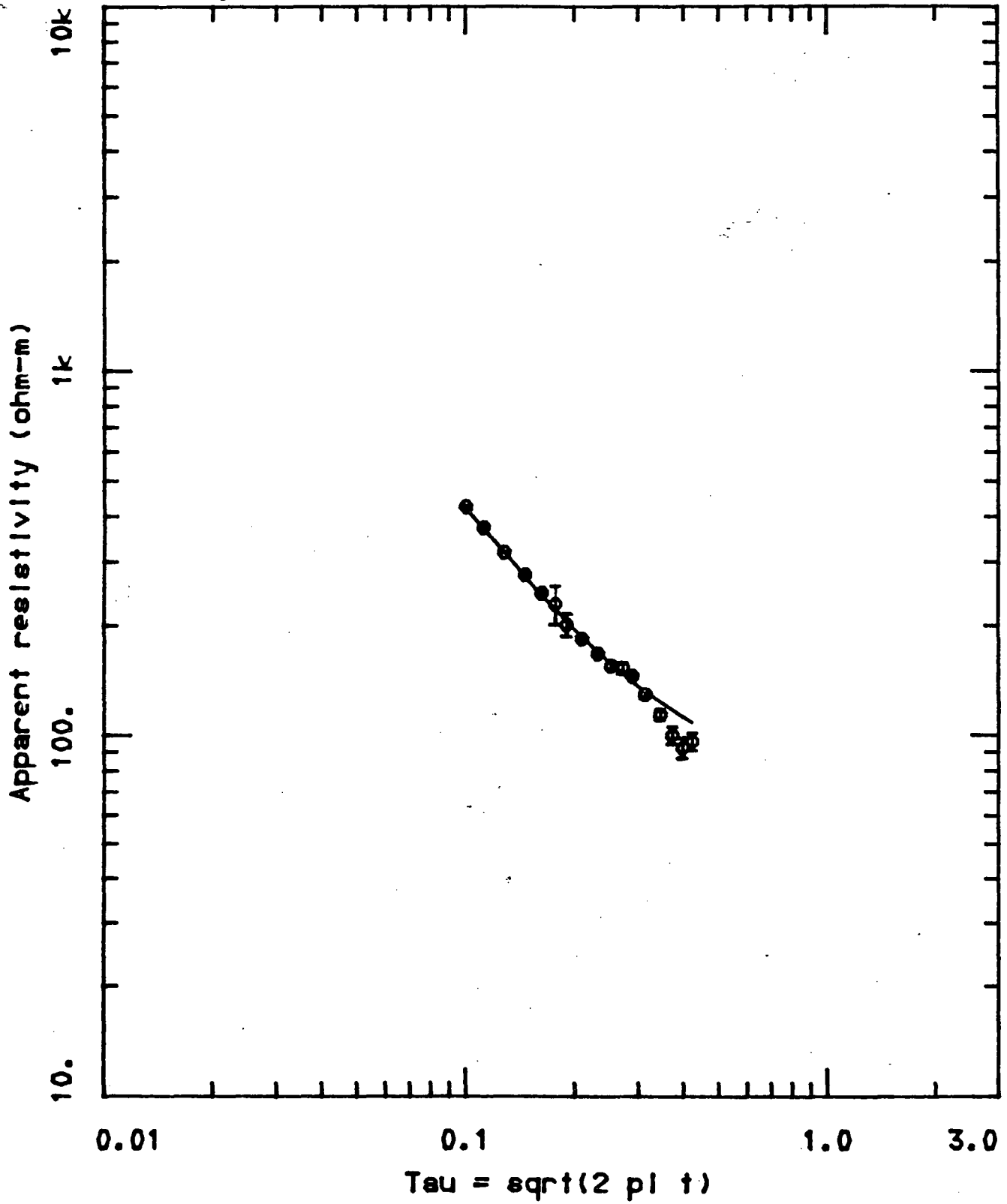


Figure 14c

Newberry Volcano NBE-31

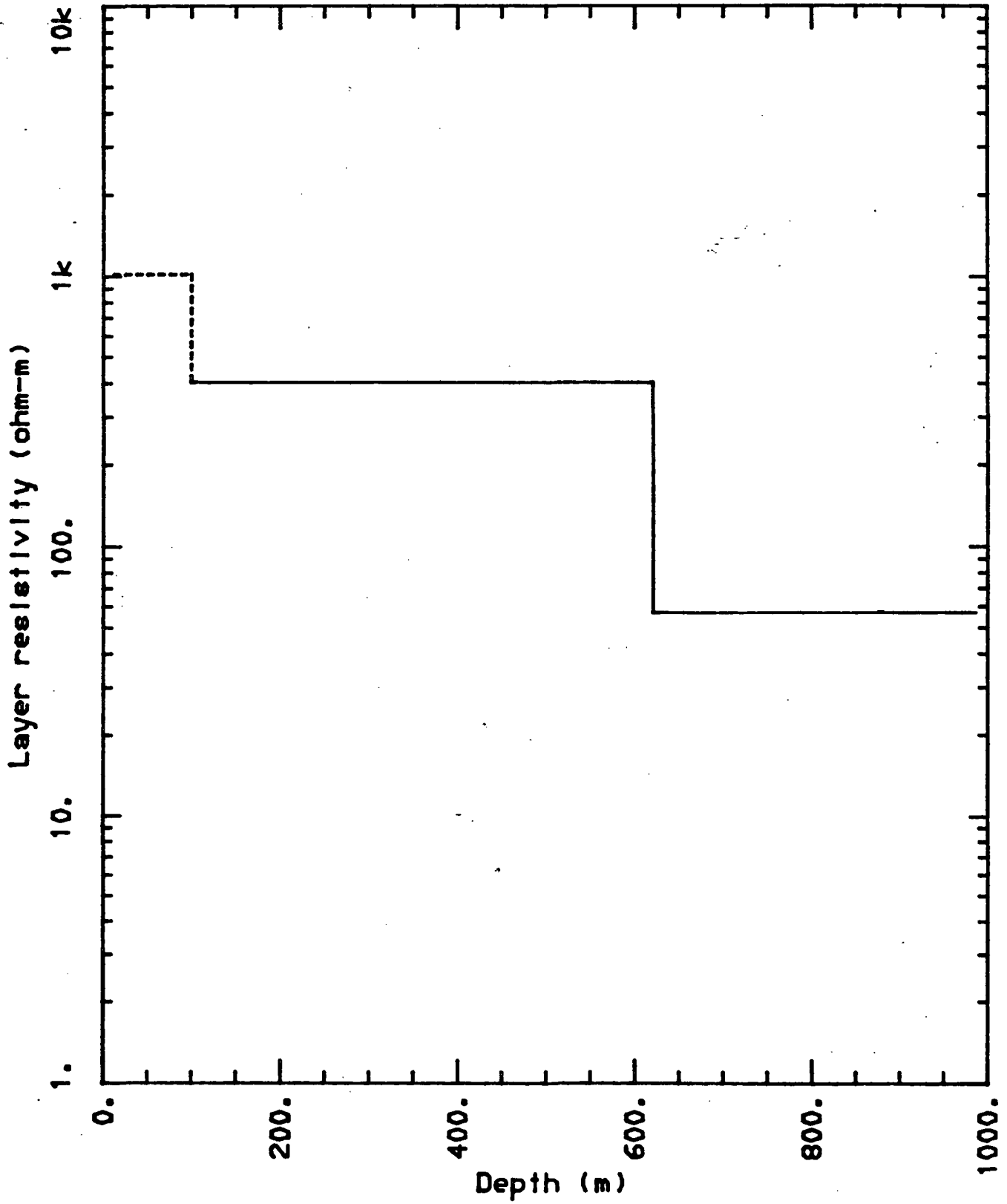




Figure 15a

<NLSTCI>: Newberry Volcano NBE-32  
 LOOP RADIUS= 172.0

I	TIME(s)	OBSERVED RESISTIVITY	STANDARD DEVIATION	COMPUTED RESISTIVITY	PERCENT ERROR
1	0.0016000	523.9	3.4	513.2	2.1
2	0.0020000	466.0	7.4	476.0	-2.1
3	0.0026000	399.0	6.9	417.3	-4.4
4	0.0034000	346.4	5.4	357.3	-3.0
5	0.0042000	308.2	10.3	310.3	-0.7
6	0.0050000	278.1	35.7	275.8	0.8
7	0.0058000	259.3	10.6	251.7	3.0
8	0.0070000	226.8	9.2	223.8	1.3
9	0.0086000	201.6	10.1	196.3	2.7
10	0.0102000	178.9	9.9	177.7	0.7
11	0.0118000	165.1	12.9	163.9	0.7
12	0.0134000	151.3	11.8	152.6	-0.9
13	0.0158000	134.5	8.7	139.8	-3.8
14	0.0190000	121.3	4.8	127.4	-4.8
15	0.0222000	115.0	9.6	118.4	-2.8
16	0.0254000	112.7	9.3	111.3	1.2
17	0.0286000	106.1	14.6	105.8	0.2

RMS ERROR= 7.813 X-CONVERGENCE

CORRELATION MATRIX

	1	2	3
1	1.000		
2	0.616	1.000	
3	0.379	0.733	1.000

	PARAMETER ESTIMATE	STANDARD ERROR	RELATIVE ERROR	PERCENT ERROR
1	0.2192E-02	0.3582E-04	0.1634E-01	1.6
2	0.2526E-01	0.6069E-03	0.2403E-01	2.4
3	0.7932E+03	0.6278E-02	0.7915E-05	0.0

FINAL INVERSION MODEL

LAYER	RESISTIVITY	P	F	CONDUCTIVITY	P	F	THICKNESS	DEPTH
1	456.2	1		0.21921159E-02	3		793.2	0.0
2	39.6	2		0.25256963E-01				793.2

P - parameter number.  
 F - \* indicates fixed parameter

Figure 15b

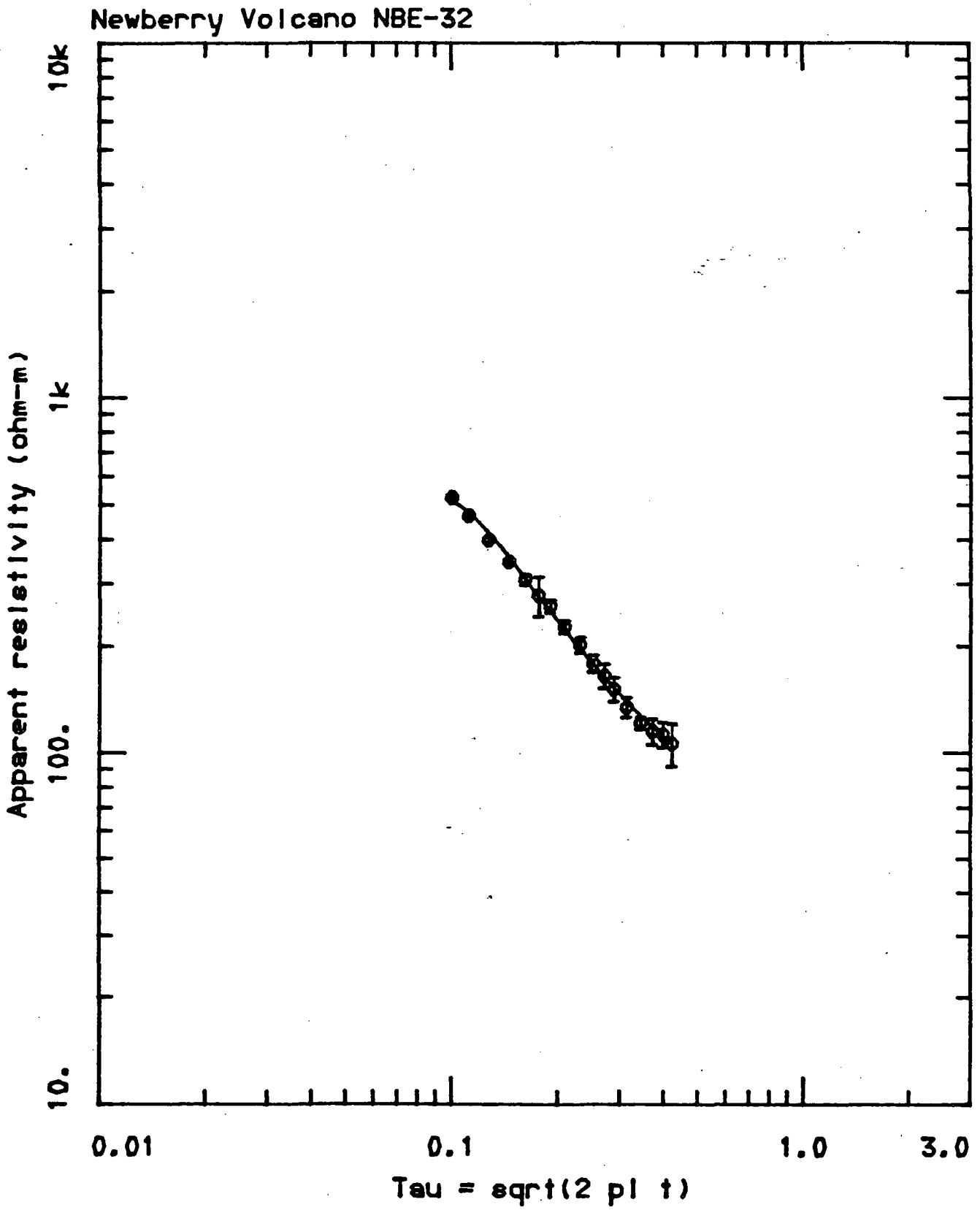


Figure 15c

Newberry Volcano NBE-32

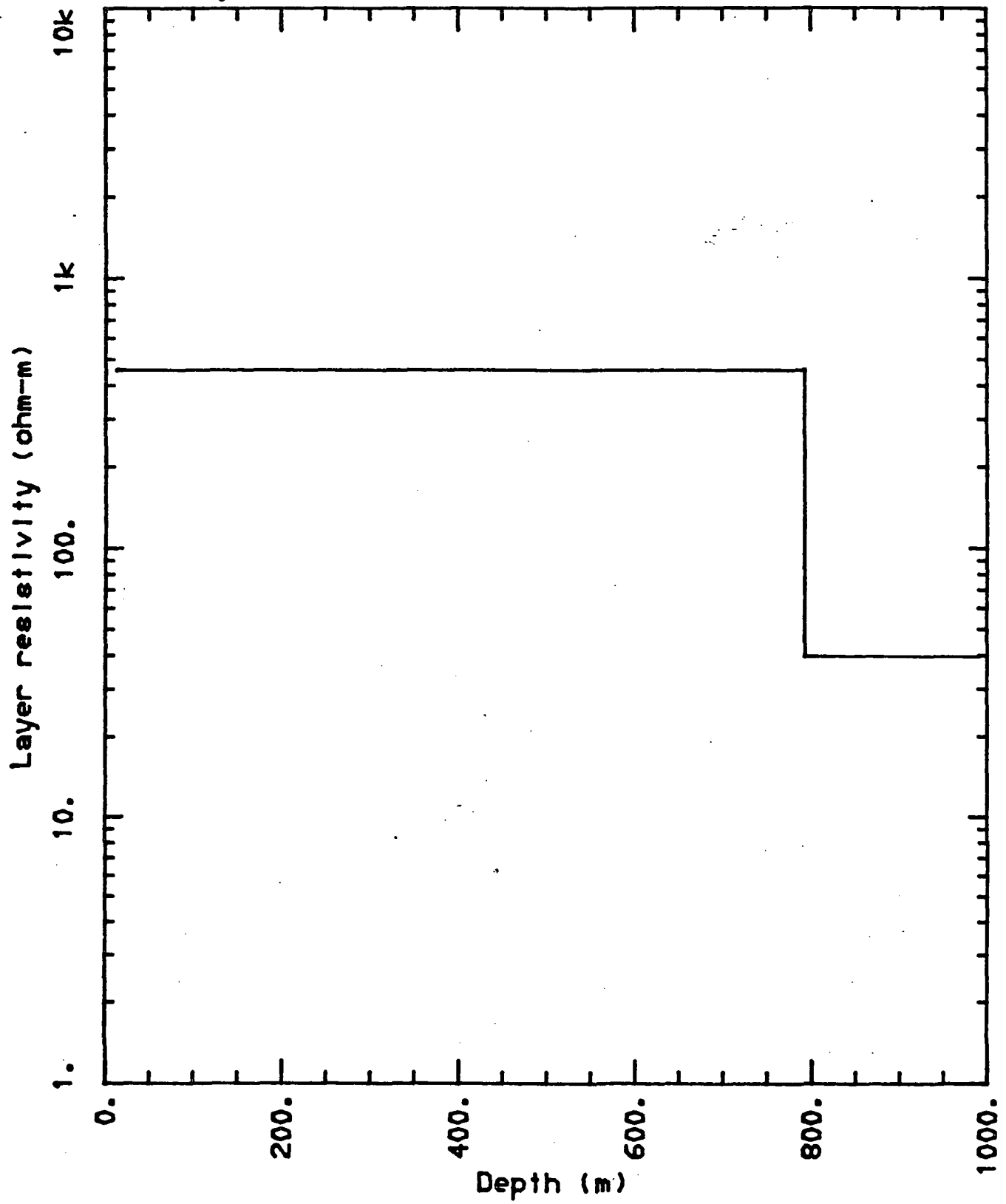


Figure 16a

<NLSTCI>: Newberry Volcano NBE-33  
 LOOP RADIUS= 172.0

I	TIME(S)	OBSERVED RESISTIVITY	STANDARD DEVIATION	COMPUTED RESISTIVITY	PERCENT ERROR
1	0.0016000	588.1	2.8	594.4	-1.1
2	0.0020000	497.3	3.6	499.5	-0.4
3	0.0026000	412.7	1.5	410.0	0.6
4	0.0034000	342.1	1.7	338.5	1.1
5	0.0042000	298.6	1.7	293.7	1.7
6	0.0050000	266.8	5.9	262.5	1.7
7	0.0058000	240.7	4.9	239.5	0.5
8	0.0070000	209.9	2.4	214.4	-2.1
9	0.0086000	191.6	2.0	191.6	0.0
10	0.0102000	174.3	6.6	175.4	-0.6
11	0.0118000	173.4	6.9	163.3	6.2
12	0.0134000	158.1	10.4	153.8	2.8
13	0.0158000	141.2	3.8	142.9	-1.2
14	0.0190000	125.6	4.0	131.9	-4.8
15	0.0222000	108.5	3.8	124.1	-12.6
16	0.0254000	103.8	5.6	118.1	-12.1
17	0.0286000	107.4	11.1	113.2	-5.1

RMS ERROR= 7.445

VARIABILITY CONVERGENCE

CORRELATION MATRIX

	1	2	3
1	1.000		
2	-0.029	1.000	
3	-0.216	-0.228	1.000

	PARAMETER ESTIMATE	STANDARD ERROR	RELATIVE ERROR	PERCENT ERROR
1	0.7330E-03	0.9701E-05	0.1324E-01	1.3
2	0.1871E-01	0.3472E-03	0.1856E-01	1.9
3	0.6481E+03	0.6665E-03	0.1028E-05	0.0

FINAL INVERSION MODEL

LAYER	RESISTIVITY	P F	CONDUCTIVITY	P F	THICKNESS	DEPTH
1	1364.3	1	0.73295023E-03	3	648.1	0.0
2	53.4	2	0.18710205E-01			648.1

P - parameter number

F - \* indicates fixed parameter

Figure 16b

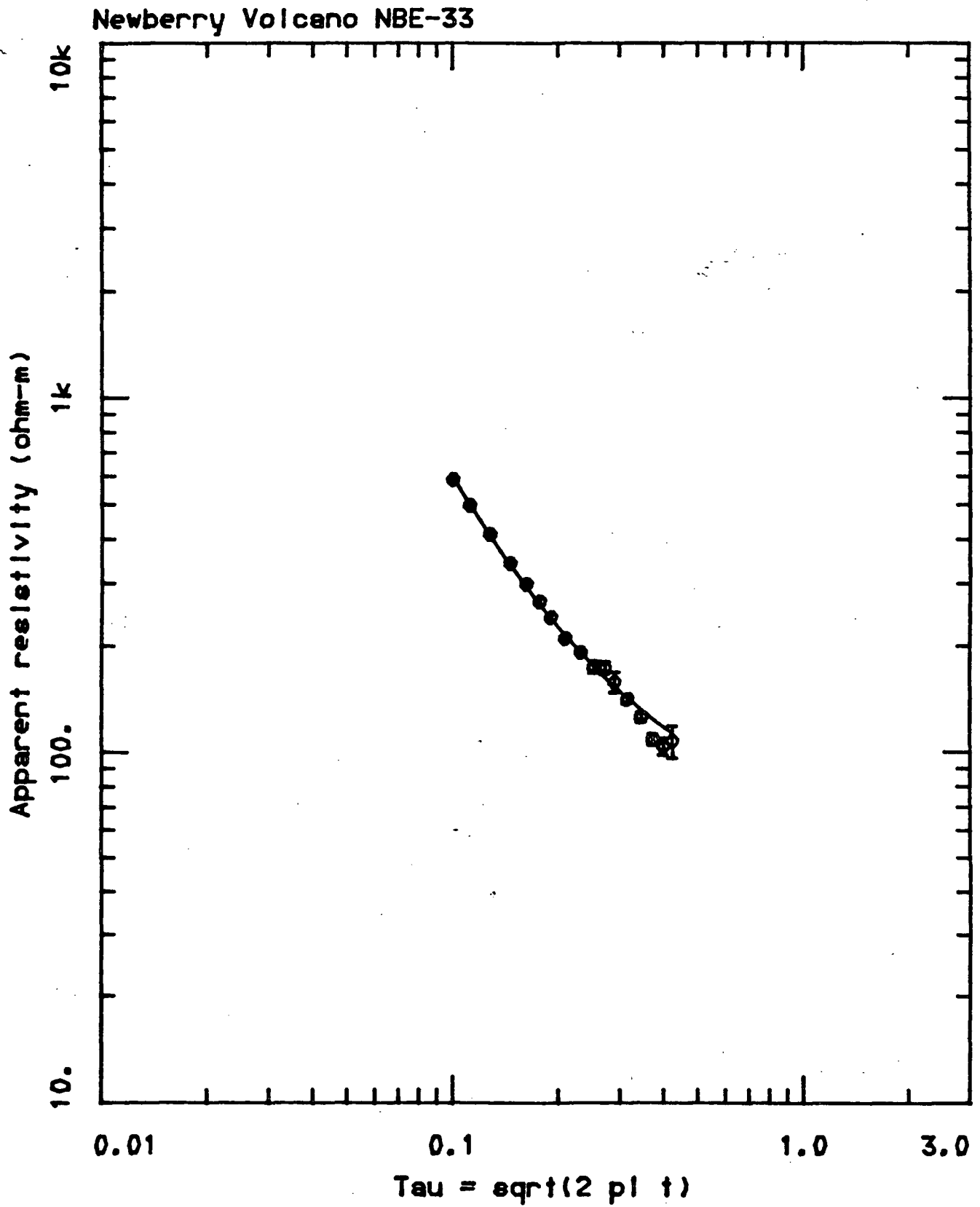


Figure 16c

Newberry Volcano NBE-33

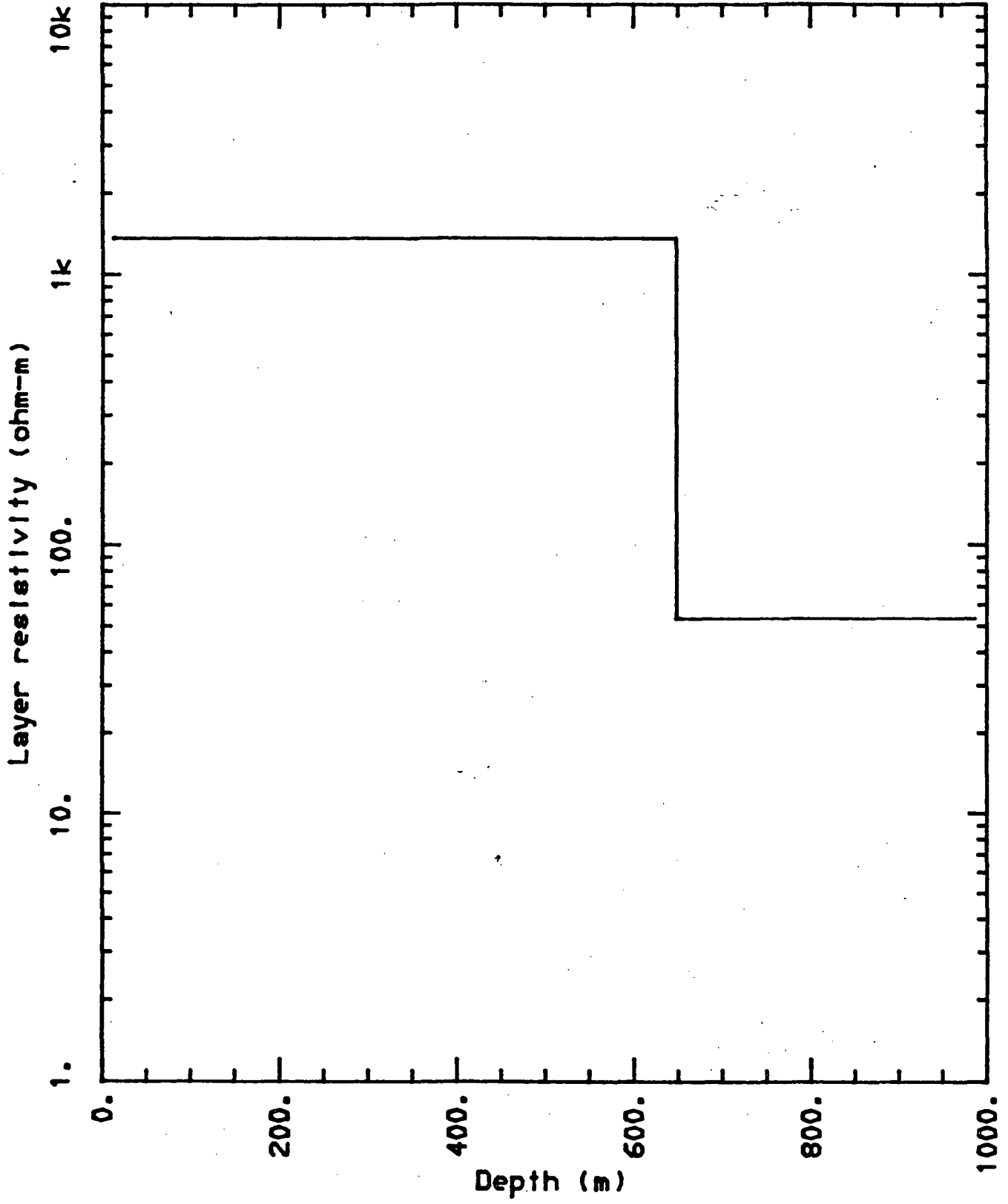


Figure 17a

<NLSTCI>: Newberry Volcano NBE-34  
 LOOP RADIUS= 172.0

	TIME(s)	OBSERVED RESISTIVITY	STANDARD DEVIATION	COMPUTED RESISTIVITY	PERCENT ERROR
1	0.0016000	347.7	1.2	345.3	0.7
2	0.0020000	307.1	1.9	309.7	-0.9
3	0.0026000	265.1	1.1	267.5	-0.9
4	0.0034000	228.6	1.0	229.9	-0.5
5	0.0042000	205.5	0.8	203.2	1.1
6	0.0050000	188.5	12.7	183.1	3.0
7	0.0058000	172.4	5.9	168.8	2.1
8	0.0070000	154.2	2.7	152.9	0.9
9	0.0086000	138.0	4.7	137.2	0.6
10	0.0102000	126.6	4.3	126.1	0.4
11	0.0118000	113.1	3.1	117.9	-4.1
12	0.0134000	105.5	2.4	111.3	-5.2
13	0.0158000	98.8	2.0	103.8	-4.8
14	0.0190000	90.4	3.3	96.3	-6.1
15	0.0222000	85.5	5.6	90.8	-5.8
16	0.0254000	84.8	6.7	86.5	-2.0
17	0.0286000	79.3	2.0	83.0	-4.5

RMS ERROR= 4.052 X-CONVERGENCE

CORRELATION MATRIX

	2	3	5
2	1.000		
3	0.385	1.000	
5	0.481	0.717	1.000

PARAMETER ESTIMATE	STANDARD ERROR	RELATIVE ERROR	PERCENT ERROR
2	0.3430E-02	0.8874E-04	0.2587E-01
3	0.2546E-01	0.3837E-03	0.1507E-01
5	0.5133E+03	0.1213E-02	0.2363E-05

FINAL INVERSION MODEL

LAYER	RESISTIVITY	P F	CONDUCTIVITY	P F	THICKNESS	DEPTH
1	775.2	1 *	0.12900000E-02	4 *	90.0	0.0
2	291.5	2	0.34304564E-02	5	513.3	90.0
3	39.3	3	0.25457317E-01			603.3

P - parameter number  
 F - \* indicates fixed parameter

Figure 17b

Newberry Volcano NBE-34

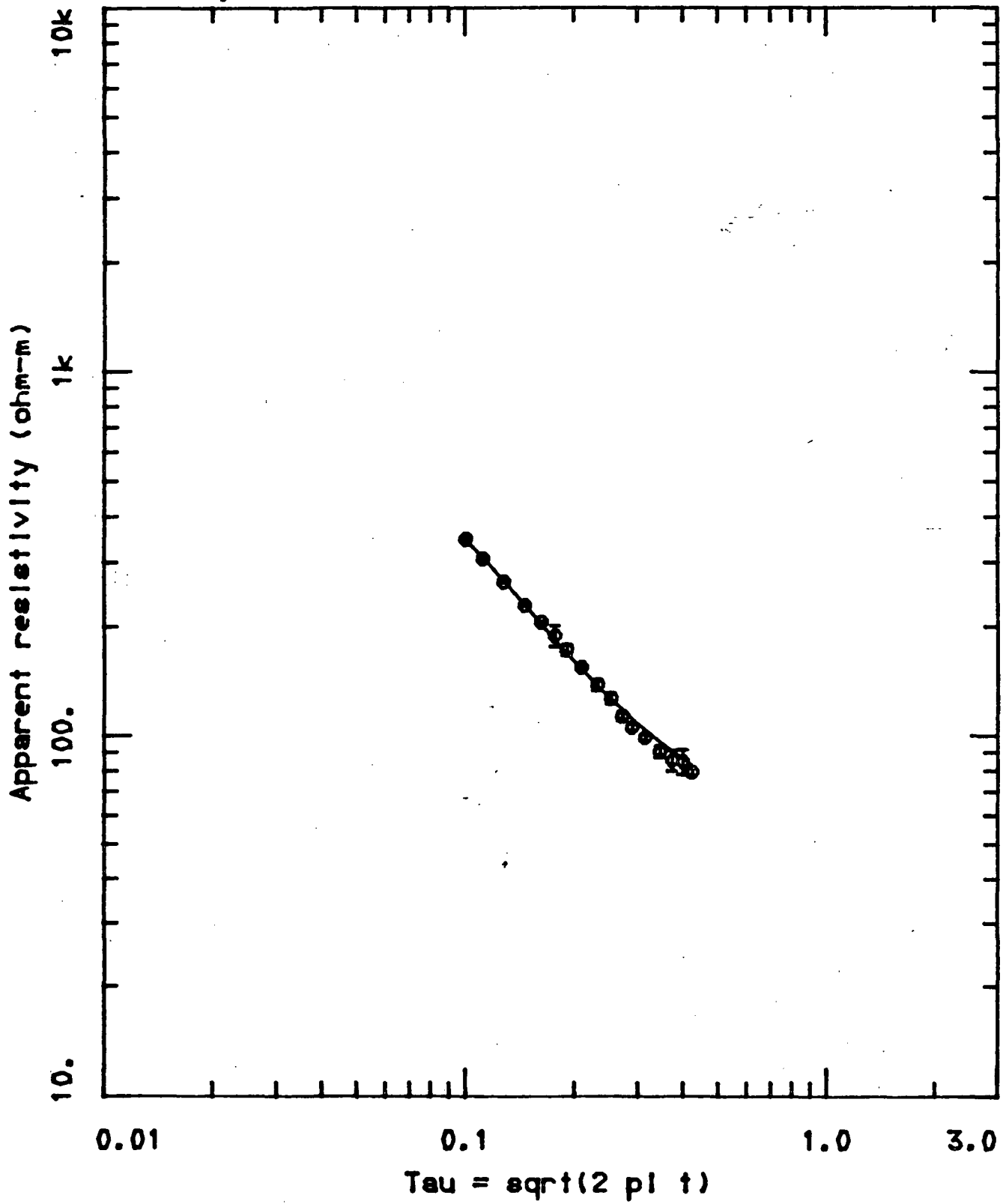




Figure 17c

Newberry Volcano NBE-34

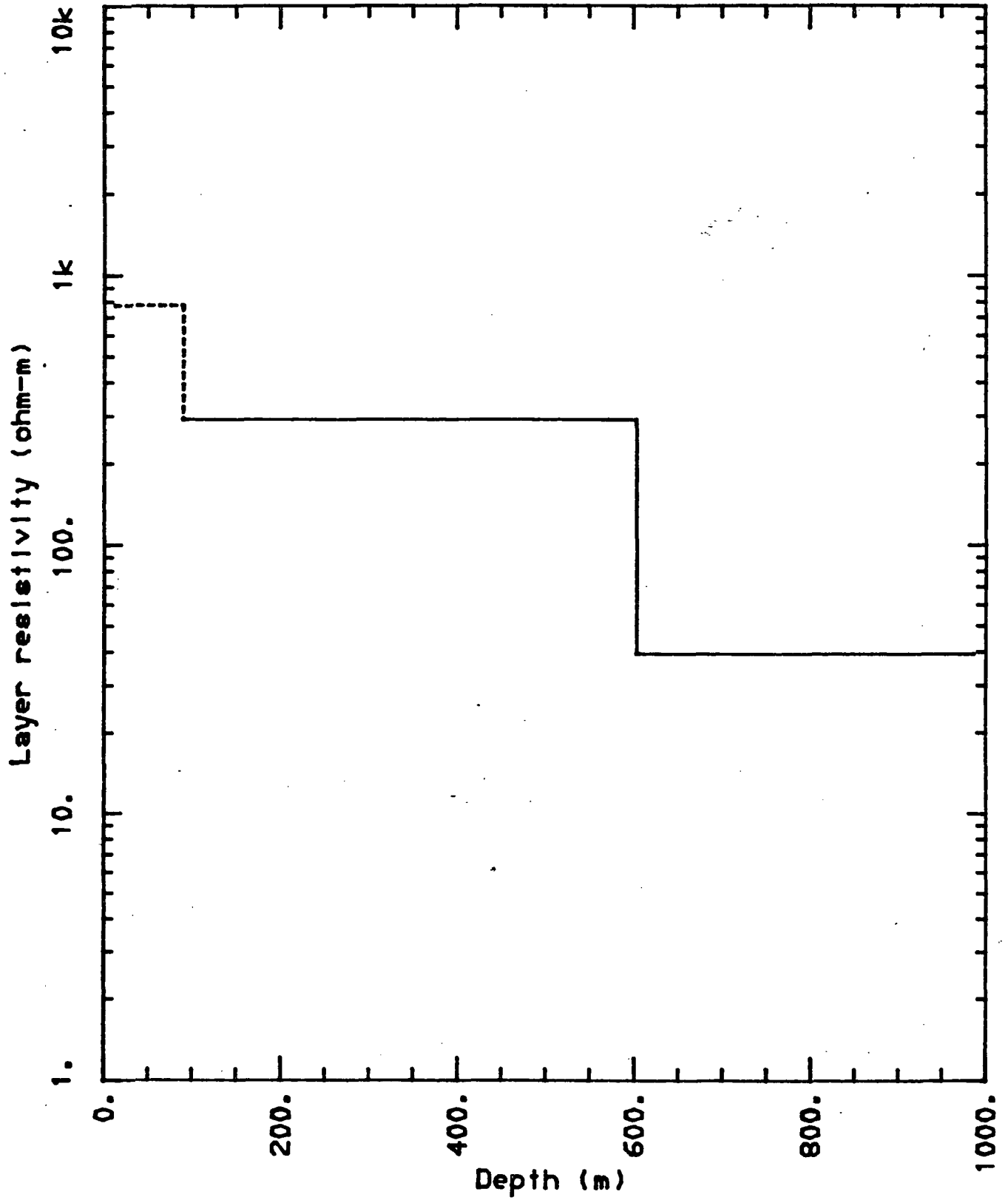


Figure 18a

<NLSTCI>: Newberry Volcano NBE-35  
 LOOP RADIUS= 172.0

I	TIME(s)	OBSERVED RESISTIVITY	STANDARD DEVIATION	COMPUTED RESISTIVITY	PERCENT ERROR
1	0.0016000	604.5	1.8	617.1	-2.0
2	0.0020000	518.0	4.3	524.1	-1.2
3	0.0026000	433.2	1.4	434.3	-0.3
4	0.0034000	373.9	2.7	362.8	3.1
5	0.0042000	330.1	5.2	317.4	4.0
6	0.0050000	301.6	23.2	285.7	5.6
7	0.0058000	285.5	11.7	262.2	8.9
8	0.0070000	254.4	11.7	236.8	7.4
9	0.0086000	230.3	5.7	213.2	8.0
10	0.0102000	211.8	1.8	196.4	7.8
11	0.0118000	207.9	17.3	183.9	13.1
12	0.0134000	192.6	14.7	174.1	10.6
13	0.0158000	174.9	8.2	162.8	7.5
14	0.0190000	160.1	5.9	151.1	5.9
15	0.0222000	137.0	8.7	142.6	-4.0
16	0.0254000	130.1	10.4	136.2	-4.5
17	0.0286000	120.4	10.6	130.8	-8.0

RMS ERROR= 15.68                      VARIABILITY CONVERGENCE

CORRELATION MATRIX

	1	2	3
1	1.000		
2	-0.533	1.000	
3	-0.727	0.603	1.000

	PARAMETER ESTIMATE	STANDARD ERROR	RELATIVE ERROR	PERCENT ERROR
1	0.7022E-03	0.8988E-04	0.1280E+00	12.8
2	0.1499E-01	0.4855E-03	0.3238E-01	3.2
3	0.6537E+03	0.2675E-02	0.4092E-05	0.0

FINAL INVERSION MODEL

LAYER	RESISTIVITY	P F	CONDUCTIVITY	P F	THICKNESS	DEPTH
1	1424.1	1	0.70220424E-03	3	653.7	0.0
2	66.7	2	0.14993451E-01			653.7

P - parameter number  
 F - \* indicates fixed parameter

Figure 18b

Newberry Volcano NBE-35

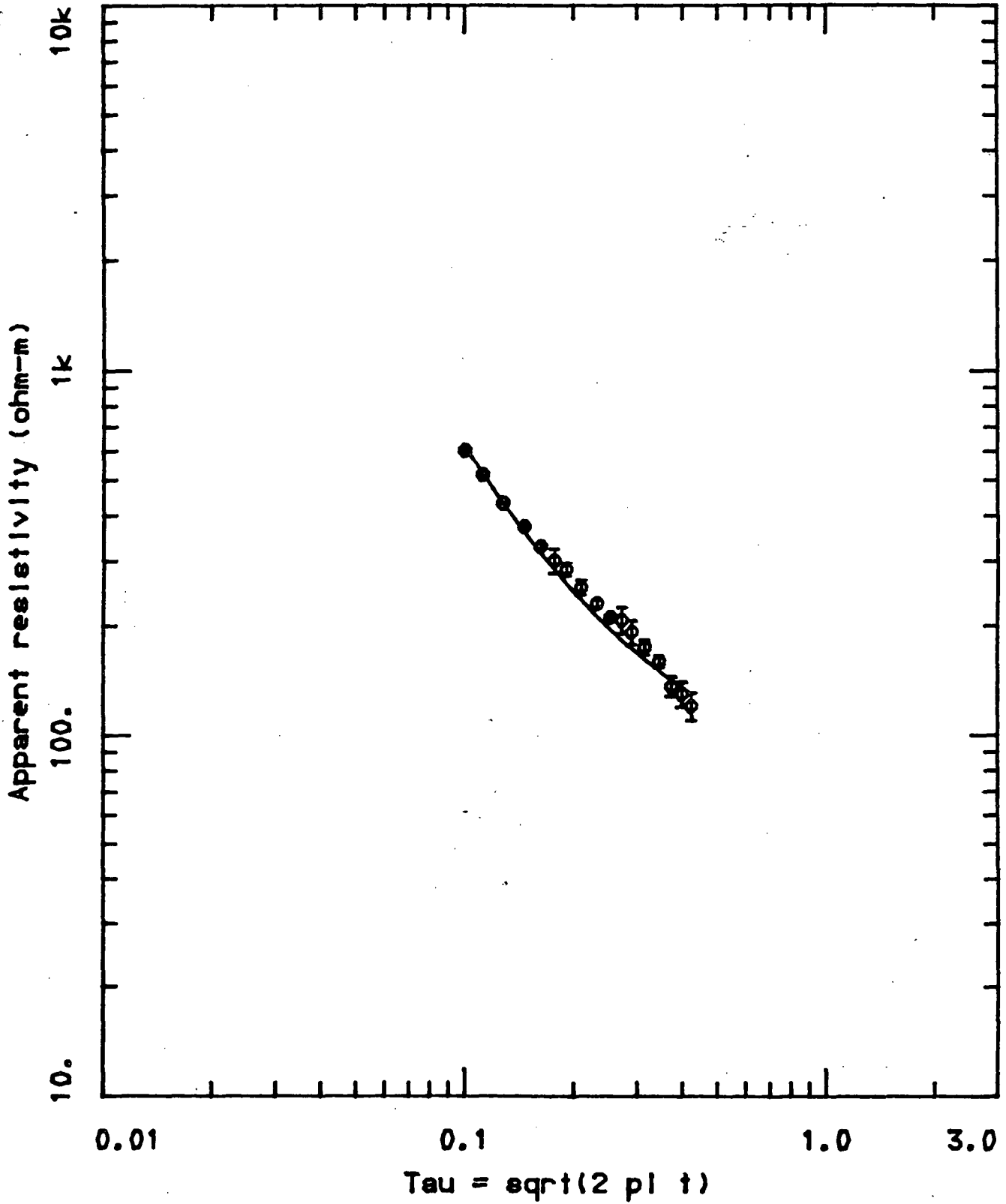


Figure 18c

Newberry Volcano NBE-35

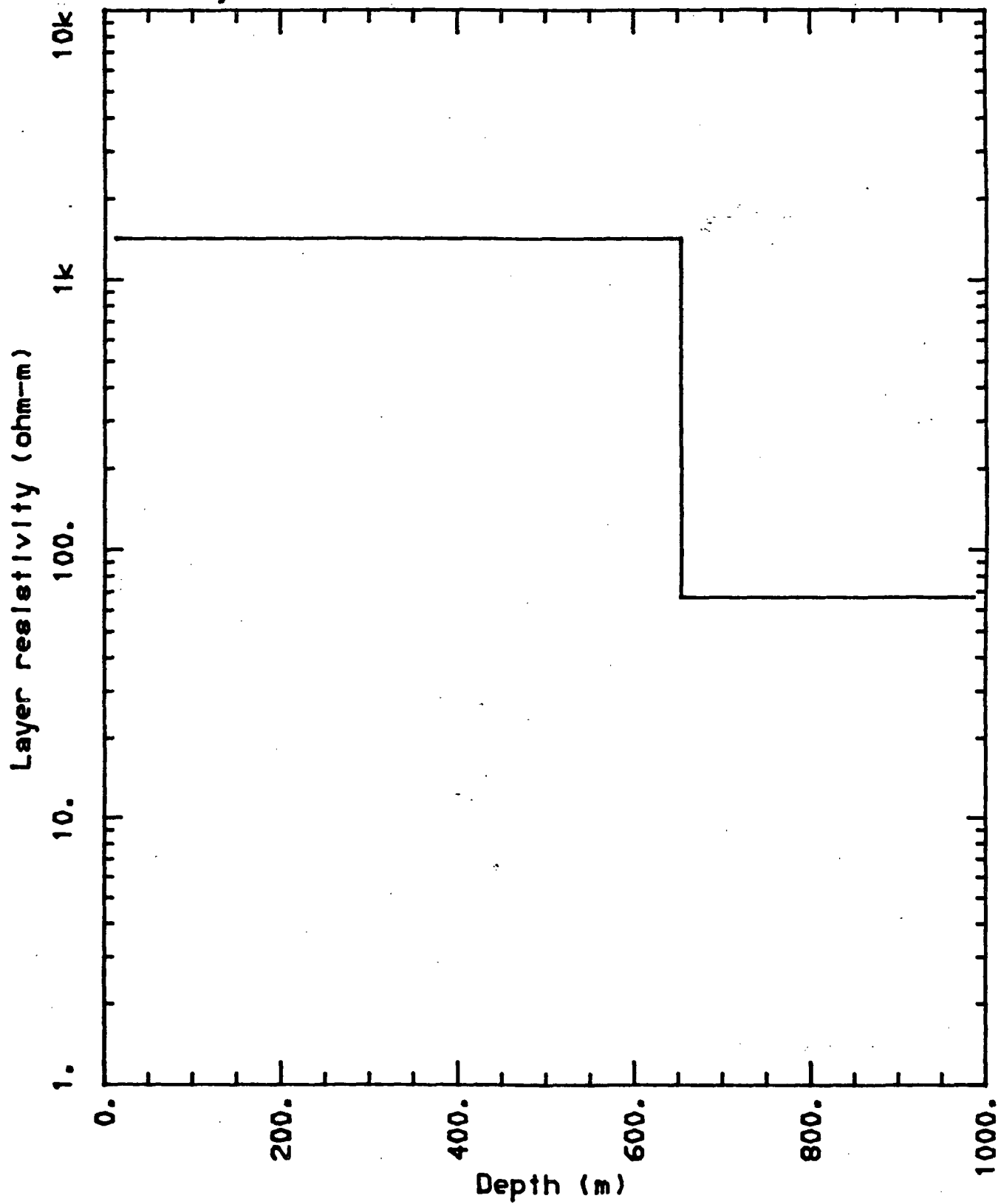


Figure 19a

<NLSTICI>: Newberry Volcano NBE-36  
 LOOP RADIUS= 172.0

I	TIME(s)	OBSERVED RESISTIVITY	STANDARD DEVIATION	COMPUTED RESISTIVITY	PERCENT ERROR
1	0.0016000	667.0	9.7	697.9	-4.4
2	0.0020000	564.6	2.9	576.7	-2.1
3	0.0026000	456.8	2.4	466.6	-2.1
4	0.0034000	381.4	3.9	379.8	0.4
5	0.0042000	333.5	20.0	326.2	2.2
6	0.0050000	290.2	21.1	289.0	0.4
7	0.0058000	273.1	4.8	262.1	4.2
8	0.0070000	234.2	1.3	232.9	0.6
9	0.0086000	213.6	2.2	206.0	3.7
10	0.0102000	198.8	4.8	187.2	6.2
11	0.0118000	186.4	1.1	173.1	7.7
12	0.0134000	177.0	5.1	162.1	9.2
13	0.0158000	152.2	2.4	149.4	1.9
14	0.0190000	135.2	0.6	136.9	-1.2
15	0.0222000	120.9	2.2	127.6	-5.2
16	0.0254000	109.0	2.6	120.3	-9.4
17	0.0286000	110.9	6.7	114.4	-3.1

RMS ERROR= 12.44 X-CONVERGENCE

CORRELATION MATRIX

	1	2	3
1	1.000		
2	-0.145	1.000	
3	0.250	-0.349	1.000

	PARAMETER ESTIMATE	STANDARD ERROR	RELATIVE ERROR	PERCENT ERROR
1	0.4449E-03	0.3395E-04	0.7632E-01	7.6
2	0.1950E-01	0.3188E-03	0.1635E-01	1.6
3	0.6921E+03	0.1692E-02	0.2445E-05	0.0

FINAL INVERSION MODEL

LAYER	RESISTIVITY	P F	CONDUCTIVITY	P F	THICKNESS	DEPTH
1	2247.8	1	0.44488852E-03	3	692.1	0.0
2	51.3	2	0.19498365E-01			692.1

P - parameter number  
 F - \* indicates fixed parameter

Figure 19b

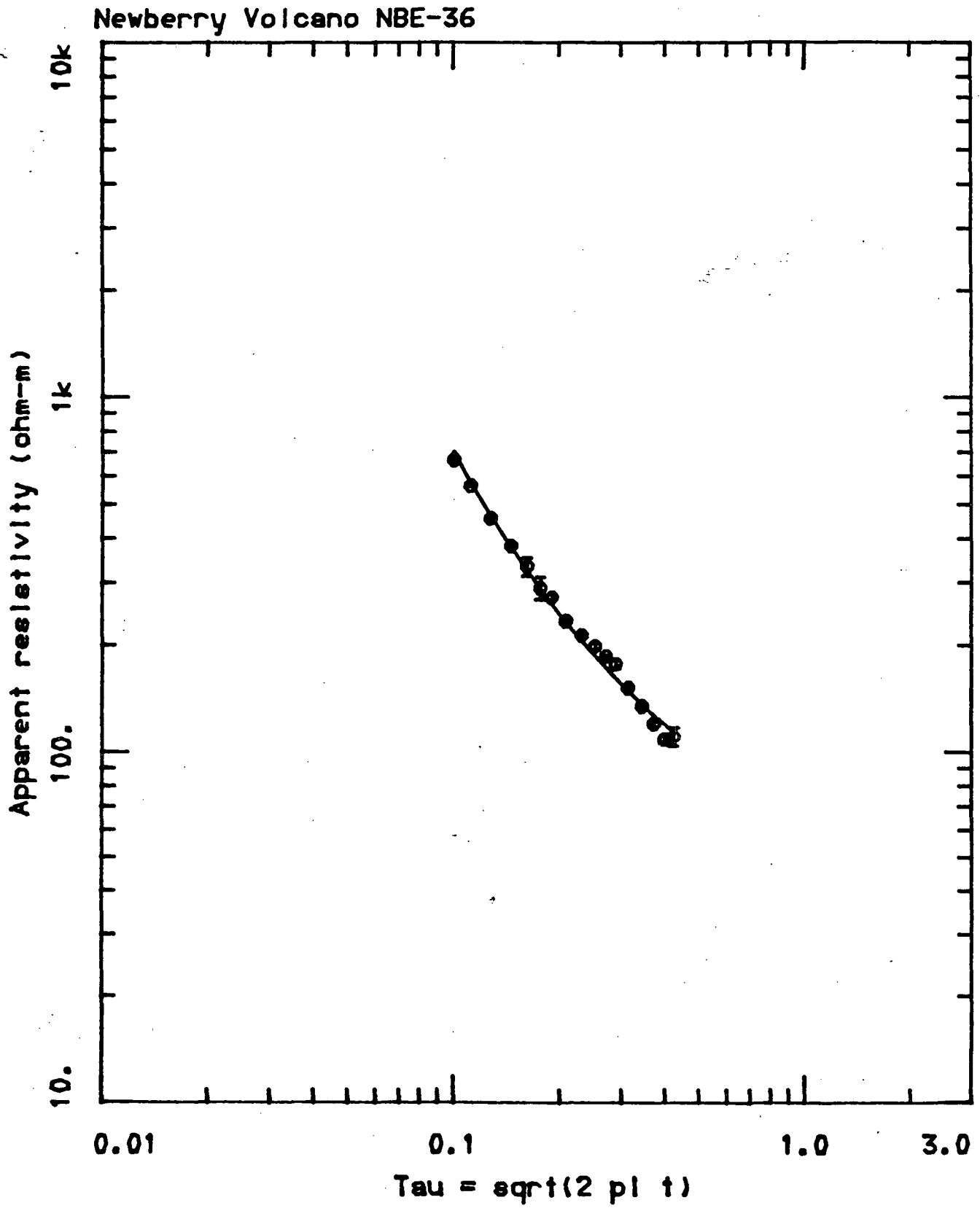


Figure 19c

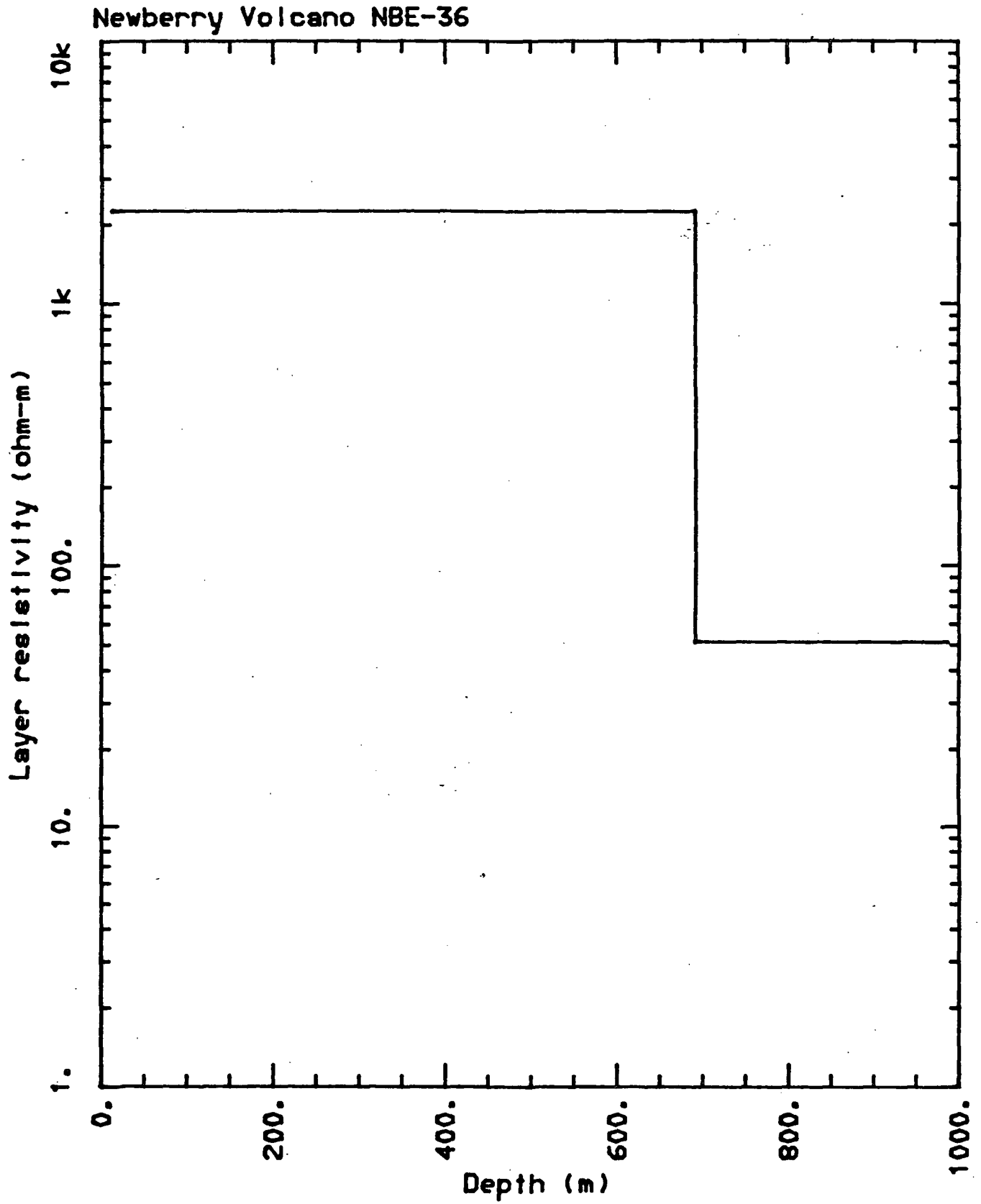


Figure 20a

<NLSTCI>: Newberry Volcano NBE-37  
 LOOP RADIUS= 172.0

I	TIME(s)	OBSERVED RESISTIVITY	STANDARD DEVIATION	COMPUTED RESISTIVITY	PERCENT ERROR
1	0.0016000	738.9	6.9	767.0	-3.7
2	0.0020000	606.1	4.1	616.9	-1.8
3	0.0026000	472.4	2.8	479.9	-1.6
4	0.0034000	379.9	5.0	375.6	1.1
5	0.0042000	318.0	10.0	312.0	1.9
6	0.0050000	279.1	8.4	269.3	3.6
7	0.0058000	246.0	1.7	238.5	3.2
8	0.0070000	217.0	1.8	205.4	5.6
9	0.0086000	183.2	5.4	175.7	4.3
10	0.0102000	163.4	7.6	155.3	5.2
11	0.0118000	150.2	9.3	140.2	7.1
12	0.0134000	136.8	11.0	128.6	6.4
13	0.0158000	122.9	3.2	115.5	6.4
14	0.0190000	109.8	5.4	102.9	6.8
15	0.0222000	103.2	7.5	93.5	10.3
16	0.0254000	94.9	2.9	86.3	10.0
17	0.0286000	83.4	5.4	80.4	3.8
18	0.0334000	76.2	8.3	73.4	3.8
19	0.0398000	70.1	10.1	66.2	5.9

RMS ERROR= 10.89 X-CONVERGENCE

CORRELATION MATRIX

	1	2	3
1	1.000		
2	0.090	1.000	
3	-0.829	-0.167	1.000

	PARAMETER ESTIMATE	STANDARD ERROR	RELATIVE ERROR	PERCENT ERROR
1	0.3674E-03	0.1351E-04	0.3678E-01	3.7
2	0.3824E-01	0.5269E-03	0.1378E-01	1.4
3	0.7260E+03	0.2827E-02	0.3894E-05	0.0

FINAL INVERSION MODEL

LAYER	RESISTIVITY	P	F	CONDUCTIVITY	P	F	THICKNESS	DEPTH
1	2721.9	1		0.36739412E-03	3		726.0	0.0
2	26.2	2		0.38237121E-01				726.0

P - parameter number  
 F - \* indicates fixed parameter



Figure 20b

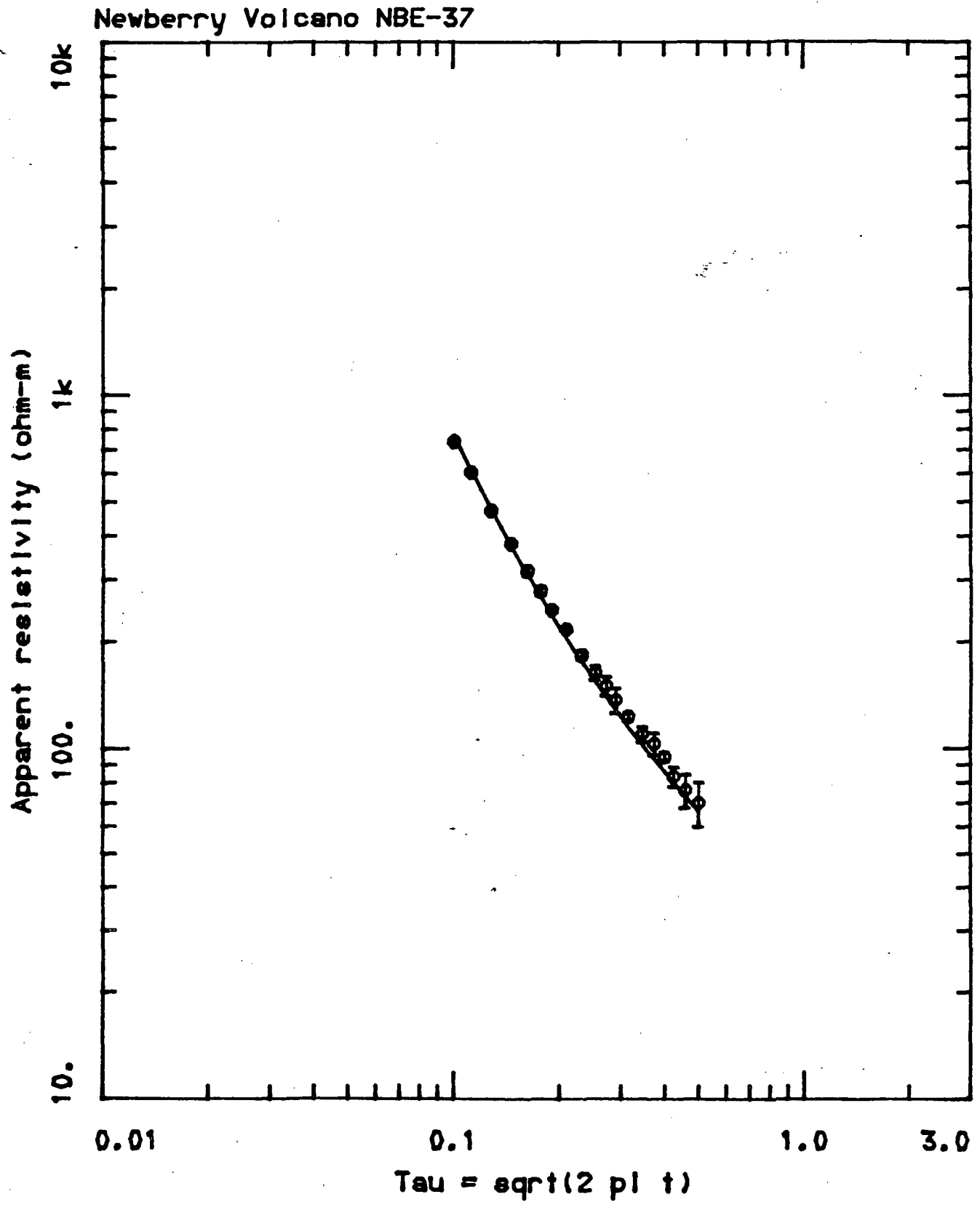


Figure 20c

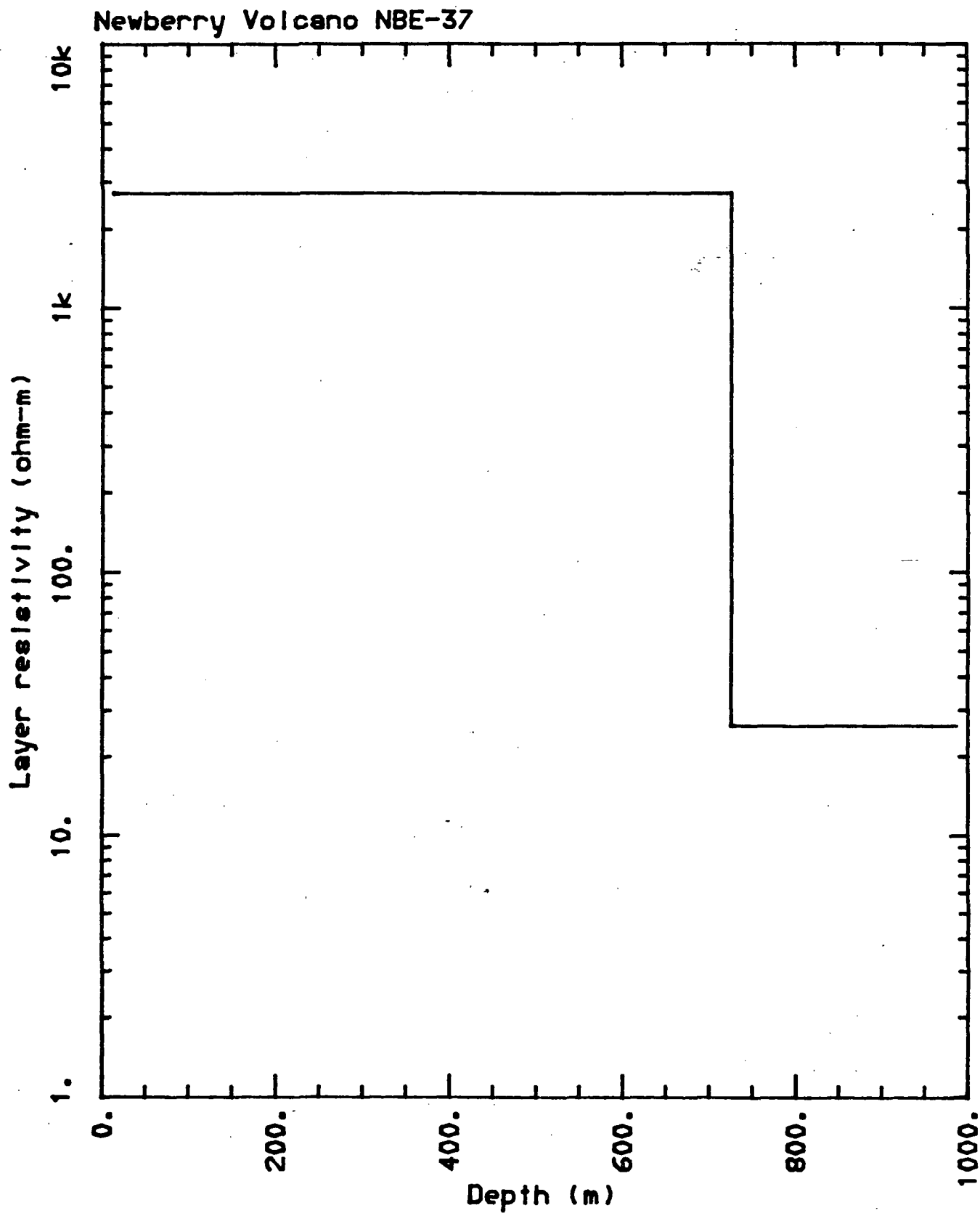


Figure 21a

<NLSTCI>: Newberry Volcano NBE-38  
 LOOP RADIUS= 172.0

I	TIME(s)	OBSERVED RESISTIVITY	STANDARD DEVIATION	COMPUTED RESISTIVITY	PERCENT ERROR
1	0.0016000	318.5	1.7	315.0	1.1
2	0.0020000	291.0	2.0	294.4	-1.2
3	0.0026000	251.5	2.5	264.0	-4.7
4	0.0034000	214.2	2.0	224.8	-4.7
5	0.0042000	189.4	2.5	195.4	-3.1
6	0.0050000	170.4	11.1	174.3	-2.2
7	0.0058000	147.2	8.4	157.9	-6.8
8	0.0070000	150.2	14.6	138.6	8.4
9	0.0086000	124.8	1.5	120.9	3.2
10	0.0102000	112.6	1.6	108.7	3.5
11	0.0118000	105.6	3.2	99.4	6.3
12	0.0134000	99.2	1.7	91.9	7.9
13	0.0158000	92.4	1.1	83.7	10.4
14	0.0190000	82.0	2.6	75.7	8.3
15	0.0222000	73.2	5.6	69.8	4.9
16	0.0254000	65.1	6.5	65.2	-0.2
17	0.0286000	64.5	8.6	61.6	4.8

RMS ERROR= 7.802 X-CONVERGENCE

CORRELATION MATRIX

	2	3	5
2	1.000		
3	-0.164	1.000	
5	0.240	0.049	1.000

	PARAMETER ESTIMATE	STANDARD ERROR	RELATIVE ERROR	PERCENT ERROR
2	0.4634E-02	0.1662E-03	0.3586E-01	3.6
3	0.4895E-01	0.1039E-02	0.2122E-01	2.1
5	0.5499E+03	0.3706E-02	0.6739E-05	0.0

FINAL INVERSION MODEL

LAYER	RESISTIVITY	P F	CONDUCTIVITY	P F	THICKNESS	DEPTH
1	909.1	1 *	0.11000000E-02	4 *	100.0	0.0
2	215.8	2	0.46335631E-02	5	549.9	100.0
3	20.4	3	0.48954826E-01			649.9

P - parameter number  
 F - \* indicates fixed parameter

Figure 21b

Newberry Volcano NBE-38

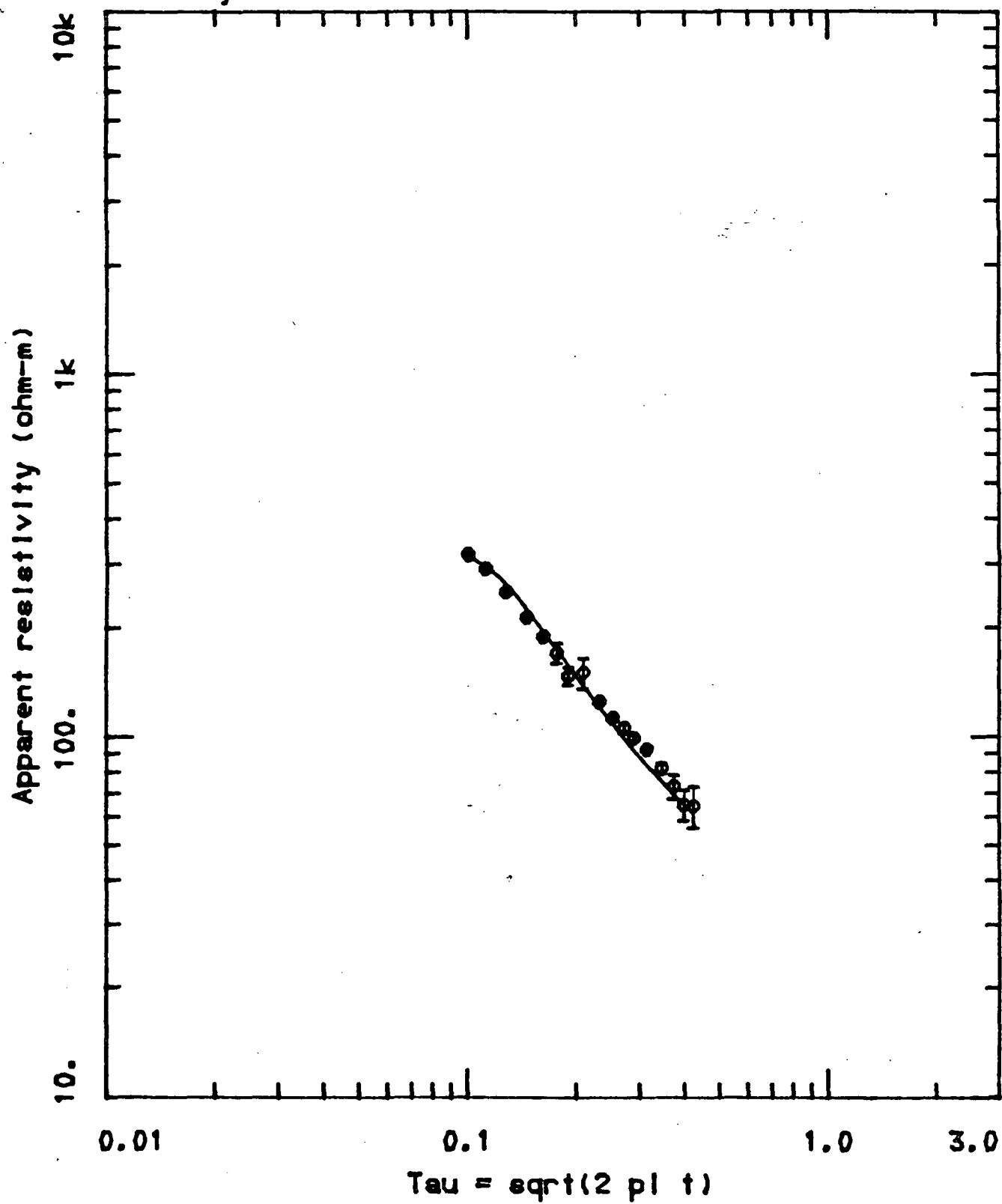


Figure 21c

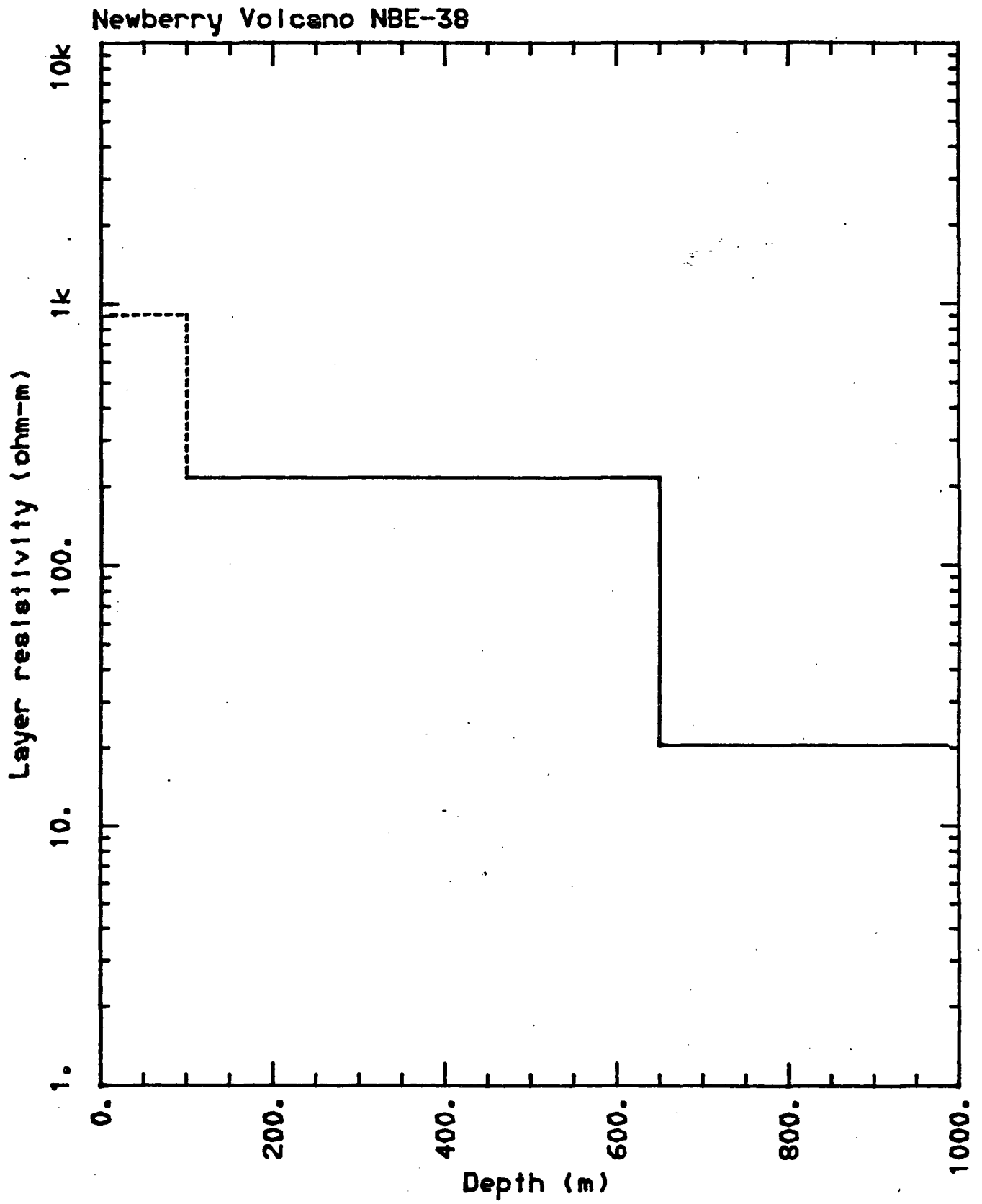


Figure 22a

<NLSTCI>: Newberry Volcano NBE-39  
 LOOP RADIUS= 172.0

		OBSERVED	STANDARD	COMPUTED	PERCENT
1	TIME(s)	RESISTIVITY	DEVIATION	RESISTIVITY	ERROR
1	0.0016000	429.4	1.1	427.9	0.4
2	0.0020000	376.0	2.1	380.0	-1.0
3	0.0026000	316.5	1.6	325.3	-2.7
4	0.0034000	268.1	2.0	270.1	-0.7
5	0.0042000	234.5	2.2	231.4	1.4
6	0.0050000	208.3	10.7	204.5	1.8
7	0.0058000	199.3	11.7	184.8	7.8
8	0.0070000	162.9	4.0	162.1	0.5
9	0.0086000	146.4	1.3	141.3	3.6
10	0.0102000	130.9	1.6	127.0	3.1
11	0.0118000	117.9	1.5	116.1	1.5
12	0.0134000	109.7	3.3	107.6	2.0
13	0.0158000	97.4	2.6	97.9	-0.5
14	0.0190000	84.7	2.0	88.5	-4.3
15	0.0222000	79.8	1.5	81.6	-2.3
16	0.0254000	74.6	1.7	76.3	-2.2
17	0.0286000	68.4	2.6	72.0	-4.9

RMS ERROR= 5.465 X-CONVERGENCE

CORRELATION MATRIX

	2	3	5
2	1.000		
3	-0.576	1.000	
5	0.552	-0.645	1.000

	PARAMETER ESTIMATE	STANDARD ERROR	RELATIVE ERROR	PERCENT ERROR
2	0.3456E-02	0.1456E-03	0.4213E-01	4.2
3	0.3974E-01	0.2940E-03	0.7398E-02	0.7
5	0.5514E+03	0.1842E-02	0.3341E-05	0.0

FINAL INVERSION MODEL

LAYER	RESISTIVITY	P F	CONDUCTIVITY	P F	THICKNESS	DEPTH
1	1589.6	1 *	0.62900002E-03	4 *	130.0	0.0
2	289.4	2	0.34558526E-02	5	551.4	130.0
3	25.2	3	0.39743692E-01			681.4

P - parameter number  
 F - \* indicates fixed parameter

Figure 22b

Newberry Volcano NBE-39

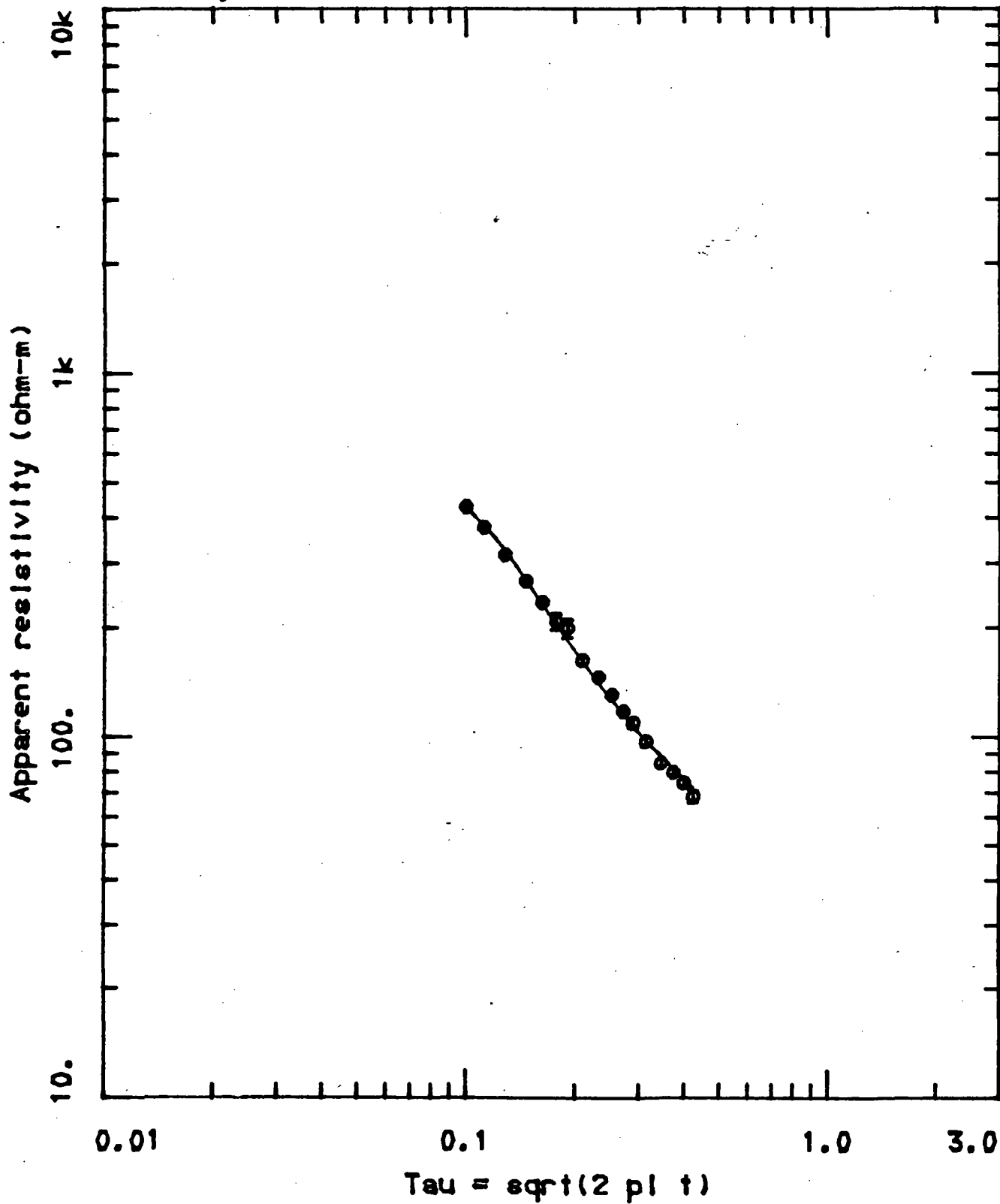


Figure 22c

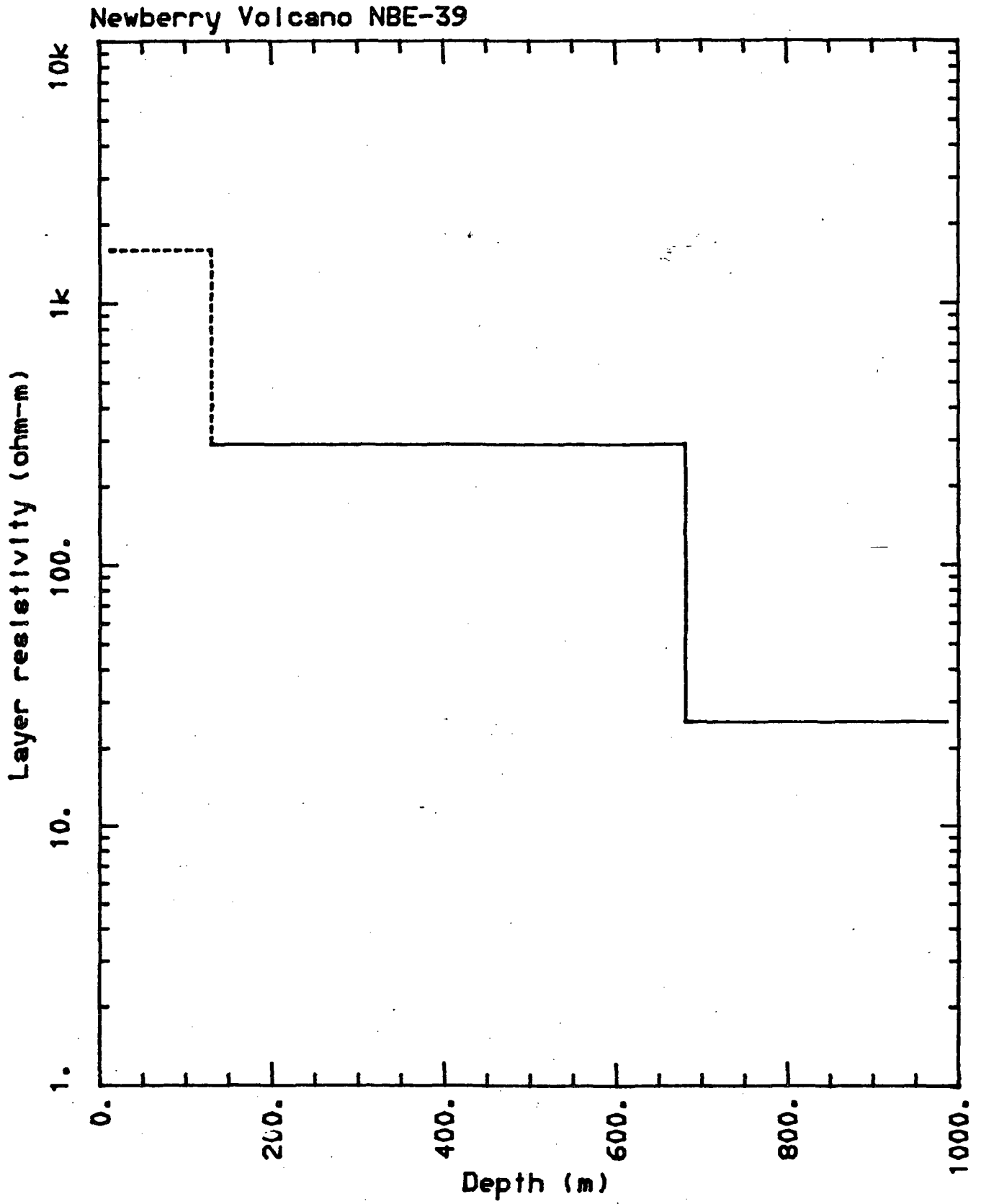




Figure 23a

<NLSTCI>: Newberry Volcano NBE-40  
 LOOP RADIUS= 172.0

I	TIME(s)	OBSERVED RESISTIVITY	STANDARD DEVIATION	COMPUTED RESISTIVITY	PERCENT ERROR
1	0.0016000	677.5	2.9	679.1	-0.2
2	0.0020000	573.9	4.1	571.4	0.4
3	0.0026000	474.6	2.8	474.1	0.1
4	0.0034000	395.9	2.7	395.2	0.2
5	0.0042000	348.0	2.5	345.3	0.8
6	0.0050000	311.2	21.9	310.6	0.2
7	0.0058000	287.3	8.1	285.2	0.7
8	0.0070000	251.8	10.1	257.3	-2.1
9	0.0086000	227.8	6.1	231.6	-1.7
10	0.0102000	209.1	2.4	213.5	-2.1
11	0.0118000	195.5	6.4	199.7	-2.1
12	0.0134000	186.0	4.3	188.9	-1.5
13	0.0158000	166.5	12.2	176.3	-5.6
14	0.0190000	151.3	24.9	164.1	-7.8
15	0.0222000	147.3	35.0	155.0	-4.9

RMS ERROR= 5.773 X-CONVERGENCE

CORRELATION MATRIX

	2	3
2	1.000	
3	-0.185	1.000

	PARAMETER ESTIMATE	STANDARD ERROR	RELATIVE ERROR	PERCENT ERROR
2	0.1373E-01	0.3015E-04	0.2196E-02	0.2
3	0.6727E+03	0.3161E-03	0.4700E-06	0.0

FINAL INVERSION MODEL

LAYER	RESISTIVITY	P F	CONDUCTIVITY	P F	THICKNESS	DEPTH
1	1956.2	1 *	0.51119964E-03	3	672.7	0.0
2	72.8	2	0.13732332E-01			672.7

P - parameter number  
 F - \* indicates fixed parameter

Figure 23b

Newberry Volcano NBE-40

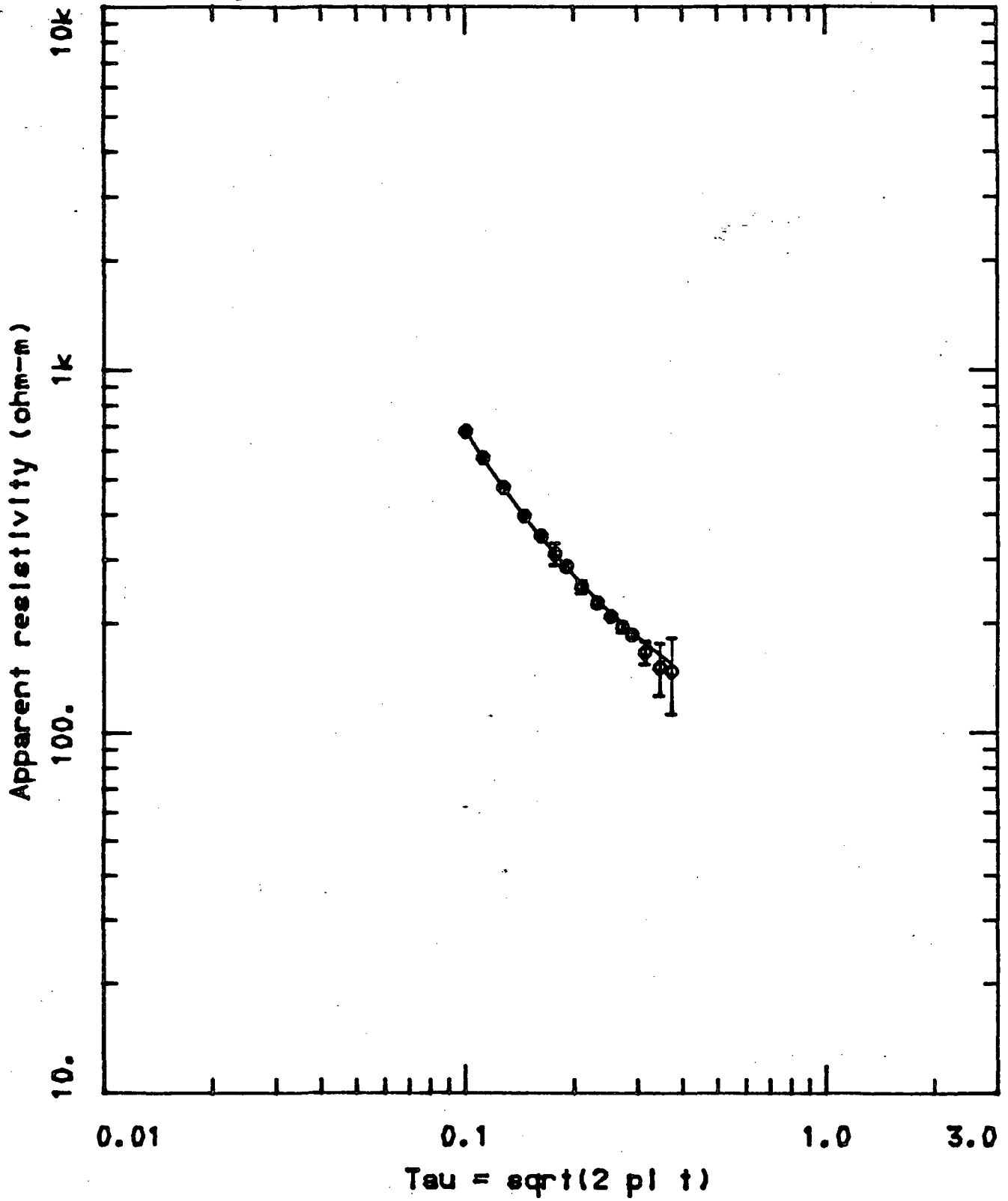


Figure 23c

Newberry Volcano NBE-40

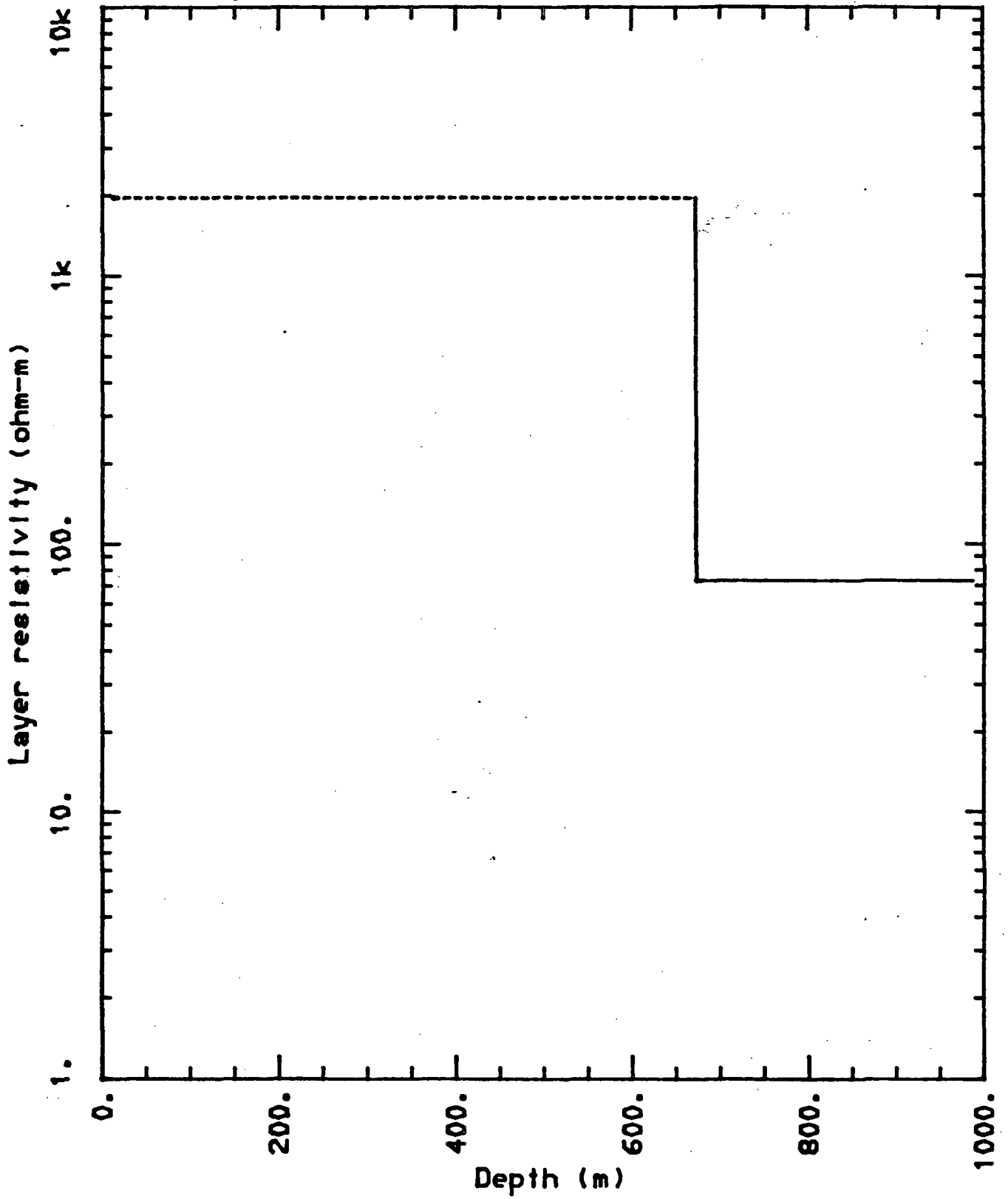


Figure 24a

<NLSTCI>: Newberry Volcano NBS-41  
 LOOP RADIUS= 172.0

I	TIME(s)	OBSERVED RESISTIVITY	STANDARD DEVIATION	COMPUTED RESISTIVITY	PERCENT ERROR
1	0.0012000	646.0	7.5	648.2	-0.3
2	0.0016000	523.3	9.9	521.0	0.4
3	0.0020000	451.6	8.5	446.0	1.3
4	0.0026000	377.5	11.3	374.2	0.9
5	0.0034000	313.0	7.6	316.2	-1.0
6	0.0042000	273.2	7.2	279.6	-2.3
7	0.0050000	257.1	15.3	254.2	1.2
8	0.0058000	236.2	16.3	235.2	0.4
9	0.0070000	210.7	12.8	214.4	-1.7
10	0.0086000	192.7	34.3	195.1	-1.2
11	0.0102000	172.9	18.0	181.1	-4.5
12	0.0118000	163.6	24.1	170.3	-4.0
13	0.0134000	149.3	62.9	162.1	-7.9
14	0.0158000	129.0	14.6	152.7	-15.5
15	0.0190000	144.8	93.6	143.1	1.2
16	0.0222000	112.6	53.1	135.9	-17.2

RMS ERROR= 10.80 X-CONVERGENCE

CORRELATION MATRIX

	1	2	3
1	1.000		
2	-0.030	1.000	
3	0.288	0.422	1.000

	PARAMETER ESTIMATE	STANDARD ERROR	RELATIVE ERROR	PERCENT ERROR
1	0.7312E-03	0.1473E-04	0.2014E-01	2.0
2	0.1439E-01	0.1651E-03	0.1147E-01	1.1
3	0.5817E+03	0.1251E-02	0.2151E-05	0.0

FINAL INVERSION MODEL

LAYER	RESISTIVITY	P	F	CONDUCTIVITY	P	F	THICKNESS	DEPTH
1	1367.6	1		0.73121284E-03	3		581.7	0.0
2	69.5	2		0.14385572E-01				581.7

P - parameter number  
 F - \* indicates fixed parameter

Figure 24b

Newberry Volcano NBS-41

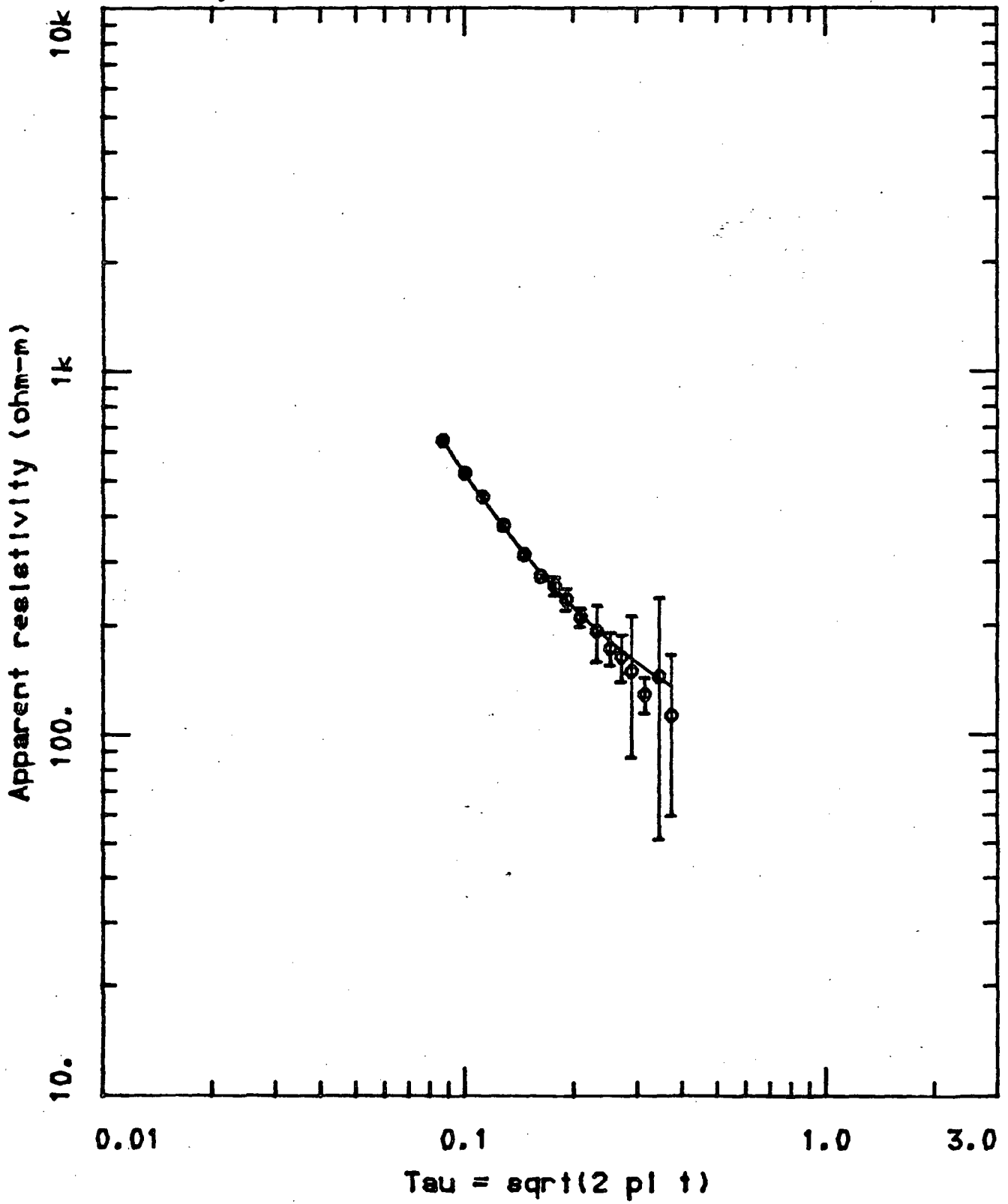
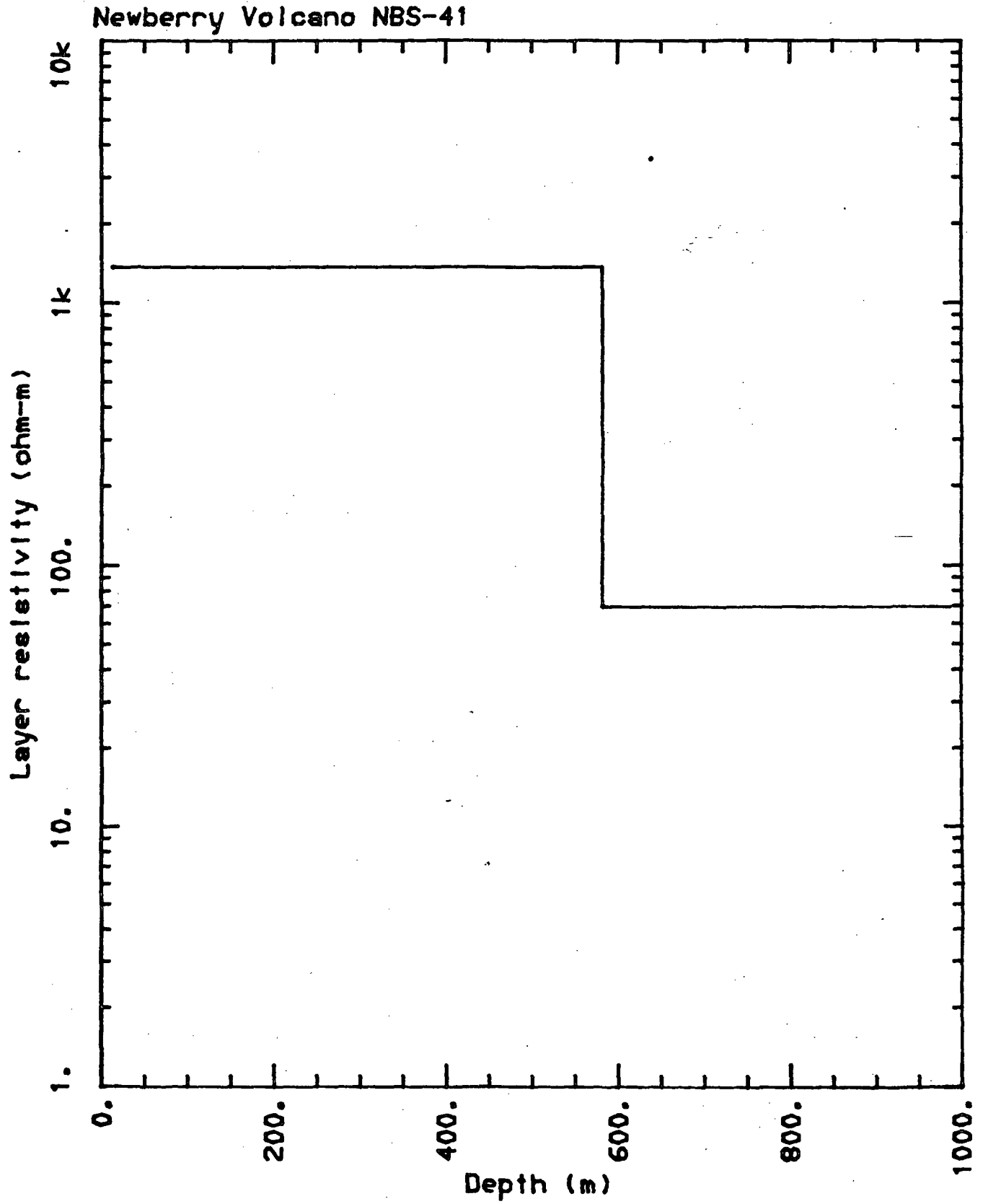


Figure 24c



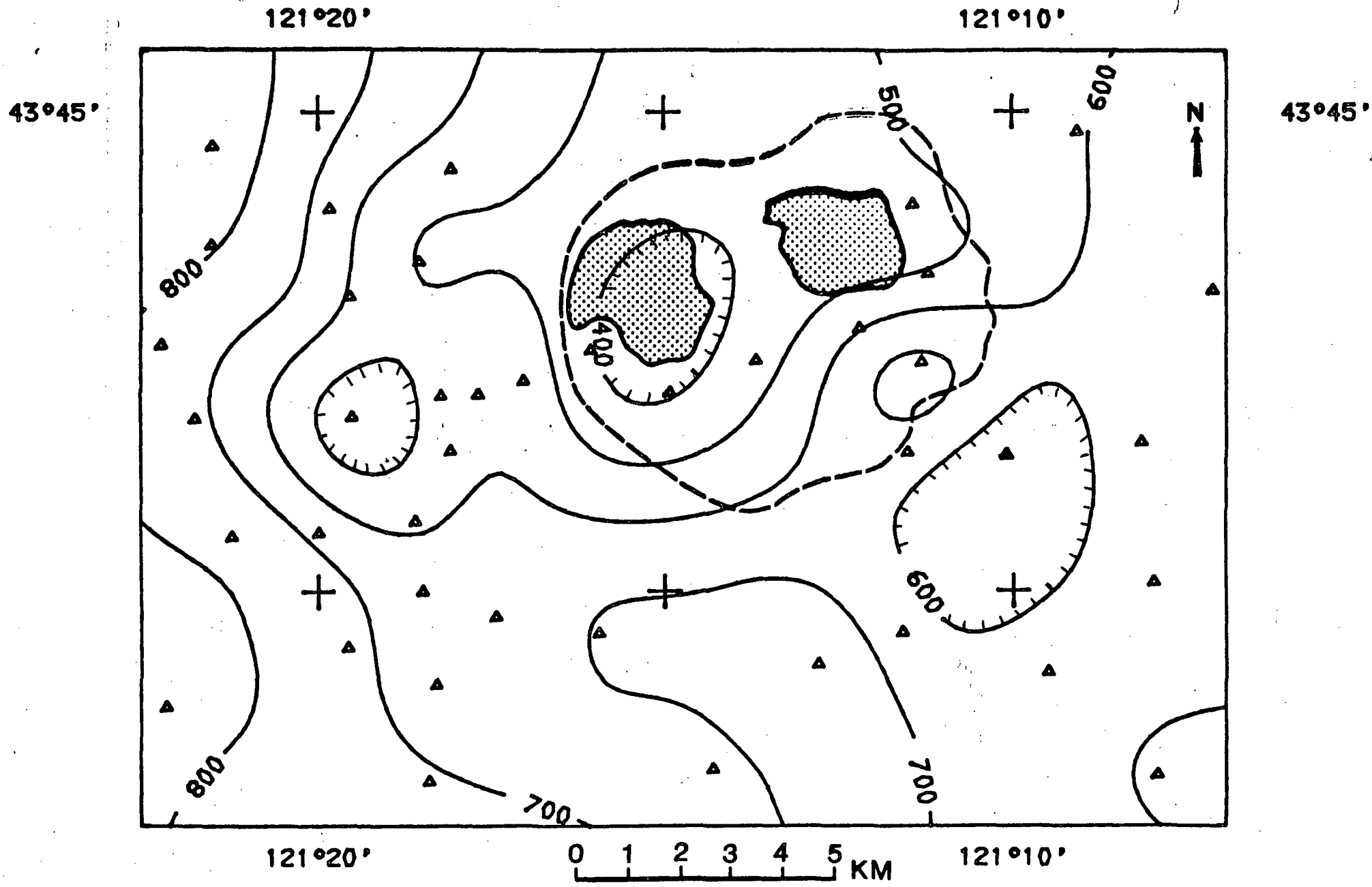


Figure 25